

# **Investigating the Impact of Flavonoid Metabolites on Endothelial Function and Vascular Inflammation**

**Emily Francesca Warner, BSc. (Hons)**

A Thesis Presented to the University of East Anglia in accordance with the requirements for the Degree of Doctor of Philosophy

Norwich Medical School

May 2016

This copy of the thesis has been supplied on condition that anyone who consults it is understood to recognise that its copyright rests with the author and that use of any information derived there from must be in accordance with current UK Copyright Law.

In addition, any quotation or extract must include full attribution.

## Acknowledgements

I would firstly like to thank my supervisors, Dr. Colin Kay and Dr. Maria O'Connell, for the opportunity to undertake this PhD, and for their invaluable support throughout the process. I am infinitely thankful to you both for the skills and confidence I have gained, which have allowed me to develop as a researcher. Particular thanks to Colin- your excellent mentorship has been equalled only by your marvellous taste in beer and music.

I also would like to thank past and present members of the Kay lab and the Department of Nutrition, especially Dr. Jessica di Gesso and Mike Smith, and many thanks to the Faculty of Medicine & Health Sciences at the University of East Anglia for their funding and provision of facilities to carry out this research.

I would like to thank my much loved family and friends for their kindness and support, especially my parents, Philip & Susan Warner, for a lifetime of opportunities and happiness- you are my role models and words cannot begin to express how thankful I am for everything you have ever given me. To the best of all the friends, Dr. Matthew Yates, many thanks for the beer, hugs, road trips, and Fleetwood Mac fangirling. To all members of Norfolk's greatest rock/pop coverband, Stone Soda- you guys literally rock! It has been (and continues to be) a limitless joy and honour to be part of the group. Finally, to my partner in crime, Dr. Helena Louise Dare-Edwards, I have learnt so much from your awe-inspiring strength, determination, and love. Aposiopsis.

## Abstract

The consumption of dietary flavonoids has been associated with reduced cardiovascular disease risk, however, many *in vitro* studies have demonstrated effects using supraphysiological concentrations of flavonoids, overlooking the potential bioactivity of flavonoid metabolites and additive effects in combination.

This thesis investigated metabolite activity relative to their unmetabolised precursors, their additive activities, and mechanisms of action, on vascular and inflammatory biomarkers of endothelial dysfunction.

20 flavonoids and metabolites were screened for their effects on endothelial nitric oxide synthase (eNOS), haem oxygenase-1 (HO-1/Hmox-1), and vascular cell adhesion molecule-1 (sVCAM-1) in endothelial and smooth muscle cells. Active treatments were further explored for effect of concentration, mRNA response, and mechanisms of action (e.g. Nrf2 and NFκB). Additionally, up to 25 combinations of flavonoids and metabolites were explored, reflecting 3 unique serum profiles of cyanidin-3-glucoside (C3G) metabolites observed *in vivo* post-consumption.

HO-1 was increased >20 % in response to quercetin and 2 phenolic acids, of which only quercetin increased Nrf2 activation (3 fold), suggesting metabolites act on alternative pathways to their precursors. 4 combinations of protocatechuic acid (PCA) and PCA-conjugates significantly increased Hmox-1 (8.7-15.7 %), signifying additive effects. sVCAM-1 secretion was inhibited in response to 4 phenolic metabolites (10.1-17.2 %) but not their precursor structures, suggesting that metabolites are more active than their precursors in inflammatory mechanisms of action. sVCAM-1 was also inhibited in response a C3G metabolite profile reflecting 24 h (27.84 %) post-bolos sampling, but not at 1 h, indicating that anti-inflammatory activities of flavonoid metabolites are modulated by metabolites of microbial action which appear many hours post-consumption.

Data herein suggest multiple mechanisms are modulated by flavonoid metabolites which contributes to our understanding of how flavonoids influence physiological responses, and therefore the associations between diet and health.

# Table of Contents

ACKNOWLEDGEMENTS.....	II
ABSTRACT.....	III
TABLE OF CONTENTS.....	IV
LIST OF TABLES.....	VI
LIST OF FIGURES.....	VII
LIST OF ABBREVIATIONS.....	IX
CHAPTER 1. FLAVONOIDS AND CARDIOVASCULAR DISEASE: A REVIEW OF CURRENT LITERATURE. ....	1
1.1. Introduction.....	1
1.2. Flavonoids .....	2
1.3. Flavonoids and Cardiovascular Disease.....	8
1.4. Hypotheses, Rationale, & Aims .....	23
CHAPTER 2. METHODS & MATERIALS .....	26
2.1. General Materials and Equipment .....	26
2.2. General Reagents and Buffers.....	26
2.3. Treatment Solutions.....	27
2.4. Cell Culture Techniques.....	28
2.5. Biochemical Techniques .....	30
2.6. Statistical analysis.....	38
CHAPTER 3. EFFECT OF FLAVONOIDS AND THEIR METABOLITES ON THE BASAL EXPRESSION OF VASCULAR BIOMARKERS IN ENDOTHELIAL CELLS.....	39
3.1. Introduction.....	39
3.2. Methods .....	42
3.3 Results .....	45
3.4. Discussion.....	53
CHAPTER 4. EFFECT OF FLAVONOIDS AND THEIR METABOLITES ON THE BASAL EXPRESSION OF HAEM OXYGENASE-1 IN VASCULAR SMOOTH MUSCLE CELLS.....	59
4.1. Introduction.....	59
4.2. Methods .....	61
4.3. Results .....	64
4.4. Discussion.....	68

CHAPTER 5. THE EFFECT OF FLAVONOIDS AND THEIR METABOLITES ON INFLAMMATORY MECHANISMS IN HUMAN ENDOTHELIAL CELLS.....	73
5.1. Introduction.....	73
5.2. Methods .....	75
5.3. Results .....	78
5.4. Discussion.....	88
CHAPTER 6. EFFECTS OF PEAK SERUM ANTHOCYANIN METABOLITE PROFILES ON INFLAMMATORY MECHANISMS IN HUMAN CORONARY ARTERY ENDOTHELIAL CELLS.....	94
6.1. Introduction.....	94
6.2. Methods .....	97
6.3. Results .....	100
6.4. Discussion.....	107
CHAPTER 7. GENERAL DISCUSSION & FUTURE PERSPECTIVES.....	114
7.1. General Discussion .....	114
7.2. Future perspectives.....	119
CHAPTER 8. REFERENCES.....	123
CHAPTER 9. APPENDICES.....	146
9.1. Appendices for Chapter 3.....	146
9.2. Appendices for Chapter 4.....	146
9.3. Appendices for Chapter 5.....	148
9.4. Appendices for Chapter 6.....	153

## List of tables

Table 1.1. Dietary sources of flavonoids .....	1
Table 1.2. Structures of common subclasses of flavonoids.. .....	3
Table 1.3. Kinetic data for example flavonoids .....	7
Table 2.1. Fibronectin coating solution for cell culture plates .....	28
Table 2.2. Primers of target genes for RT-qPCR .....	33
Table 2.3. Reference genes from geNORM kit description .....	34
Table 2.4. Primary and secondary antibodies used in Western blotting assays .....	38
Table 3.1. Structures of flavonoids and metabolites included in treatments. ....	41
Table 3.2. Effects on cell viability .....	64
Table 6.1. Serum profile mixture constituents and concentrations.....	97
Table 6.2. Effect of peak metabolite profiles on endothelial cell viability .....	100

## List of figures

Figure 1.1. Flavalium backbone .....	2
Figure 1.2. Proposed mechanisms of flavonoid absorption and metabolism.....	4
Figure 1.3. Pathogenesis of atherosclerosis.....	10
Figure 1.4.Characteristics of the healthy and dysfunctional endothelium..	11
Figure 1.5. Functional and dysfunctional eNOS activity. ....	12
Figure 1.6. Degradation of Haem by Haem oxygenase-1 (HO-1) .....	14
Figure 1.7. Cell adhesion and roles of adhesion molecules during early stages of atherosclerosis.....	16
Figure 1.8. Regulation of the Nrf2-mediated transcription pathway.....	19
Figure 1.9. TNF- $\alpha$ activated NF $\kappa$ B transcription factor and signalling kinase cascades..	21
Figure 3.1. Method optimisation experiments for Chapter 3.....	44
Figure 3.2. Effect of flavonoids and metabolites on eNOS protein .....	46
Figure 3.3. Effect of flavonoids and metabolites on HO-1 protein .....	47
Figure 3.4. Effect of mixtures of flavonoids and metabolites on HO-1 protein..	48
Figure 3.5. Effect of dose of quercetin and 2 phenolic metabolites on HO-1 protein .....	49
Figure 3.6. Effect of quercetin, 4-hydroxybenzoic acid, and PCA-4-sulfate on HO-1 mRNA expression.....	50
Figure 3.7. Effect of inhibitors of Akt1 and ERK1/2 on quercetin and 4-hydroxybenzoic acid induced total Nrf2 protein expression..	51
Figure 3.8. Effect of quercetin, 4-hydroxybenzoic acid and protocatechuic acid-4-sulfate on Akt1 and ERK1/2 phosphorylation..	52
Figure 4.1. Method optimisation experiments for Chapter 4.....	63
Figure 4.2. Effect of flavonoids and their metabolites on Hmox-1 protein. ....	65
Figure 4.3. Effect of mixtures of flavonoids and metabolites on Hmox-1 protein.....	66
Figure 4.4. Effect of quercetin, peonidin-3-glucoside, and PCA on Hmox-1 mRNA.....	67
Figure 5.1. Method optimisation experiments for Chapter 5.....	77
Figure 5.2. Effect of flavonoids and phenolic acid metabolites on TNF- $\alpha$ stimulated sVCAM-1 protein secretion .....	79
Figure 5.3. Effect of mixtures of flavonoids and phenolic acid metabolites on TNF- $\alpha$ stimulated sVCAM-1 protein secretion. ....	80

Figure 5.4. Effect of concentration of phenolic acid metabolites on TNF- $\alpha$ stimulated sVCAM-1 protein secretion. ....	82
Figure 5.5. Effect of concentration of phenolic acid metabolites on TNF- $\alpha$ stimulated sIL-6 protein secretion. ....	83
Figure 5.6. Effect of concentration of phenolic acid metabolites on TNF- $\alpha$ stimulated VCAM-1 mRNA expression by HUVECs. ....	85
Figure 5.7. Concentration response of PCA on NF $\kappa$ B p65 phosphorylation. ....	86
Figure 5.8. Concentration response of PCA on signalling kinase phosphorylation. ....	87
Figure 5.9. Relative inhibition of sVCAM-1 in response to PCA, PCA3S, PCA4S, IVA, and IVA3G, at 10 $\mu$ M. ....	90
Figure 6.1. Serum pharmacokinetic profiles of C3G and its metabolites in humans after the consumption of 500 mg $^{13}$ C <sub>5</sub> -C3G in eight healthy male participants. ....	95
Figure 6.2. Method optimisation experiments for Chapter 6. ....	99
Figure 6.3. Effect of peak metabolite profiles on sVCAM-1 protein expression. ....	101
Figure 6.4. Effect of peak metabolite profiles on VCAM-1 mRNA expression. ....	102
Figure 6.5. Effect of peak metabolite profiles on sIL-6 protein expression. ....	103
Figure 6.6. Effect of peak metabolite profiles on IL-6 mRNA expression. ....	104
Figure 6.7. Effect of peak metabolite profiles on phosphorylated NF $\kappa$ B p65 expression. ....	105
Figure 6.8. Effect of peak metabolite profiles on phosphorylation of p38 and JNK MAP kinases. ....	106
Figure 7.1. Experiment and treatment schematic. ....	115

## List of abbreviations

ANOVA	Analysis of variance
ARE	Antioxidant response element
BA4G	Benzoic acid-4-glucuronide
BA4S	Benzoic acid-4-sulfate
C3G	Cyanidin-3-glucoside
C $\beta$ G	Cytosolic- $\beta$ -glucosidase
CD40	Cluster of differentiation 40
CHD	Coronary heart disease
COMT	Catechol-O-methyltransferase
CVD	Cardiovascular disease
DMSO	Dimethyl sulfoxide
ELISA	Enzyme-linked immunosorbent assay
eNOS	Endothelial nitric oxide synthase
ERK	Extracellular-signal-related kinase
FCS	Foetal calf serum
FMD	Flow mediated dilation
GAPDH	Glyceraldehyde 3-phosphate dehydrogenase
GCL	Gamma-glutamylcysteine synthetase
4HBA	4-Hydroxybenzoic acid
HCAEC	Human coronary artery endothelial cells
HO-1	Haem oxygenase-1
HUVEC	Human umbilical vascular endothelial cells
ICAM-1	Intracellular adhesion molecule-1
I $\kappa$ B	Inhibitors of $\kappa$ B
IKK	I $\kappa$ B kinase
IL-6	Interleukin 6
IVA	Isovanillic acid
IVA3G	Isovanillic acid-3-glucuronide
IVA3S	Isovanillic acid-3-sulfate

JNK, c-Jun N-terminal kinase

Keap1 Kelch-like ECH associated protein 1

LPH Lactase phlorizin hydrolase

LPS Lipopolysaccharide

LSD Least significant difference

MMP Matrix metalloproteinases

MRP Multidrug resistance protein

NADPH Nicotinamide adenine dinucleotide phosphate

NQO1 Nicotinamide adenine dinucleotide phosphate: quinone oxidoreductase-1

NF- $\kappa$ B Nuclear factor kappa light chain enhancer of activated B-cells

NO Nitric oxide

Nrf2 Nuclear factor-erythroid 2-related factor 2

OxLDL Oxidised low density lipoproteins

p38, mitogen-activated protein kinase

P3G Peonidin-3-glucoside

PBS Phosphate buffered saline

PCA Protocatechuic acid

PCA3G Protocatechuic acid-3-glucuronide

PCA4G Protocatechuic acid-4-glucuronide

PCA3S Protocatechuic acid-3-sulfate

PCA4S Protocatechuic acid-4-sulfate

PI3K, phosphoinositide 3-kinase;

RASMC Rat aortic smooth muscle cell

RCT Randomised controlled trial

ROS Reactive oxygen species

RT-qPCR Quantitative reverse transcription polymerase chain reaction

SDS Sodium dodecyl sulfate

SGLT-1 Sodium-dependant glucose transporter

SULT Sulfotransferase

TAB1-2, TAK1 binding protein

TACE Tumour necrosis factor-alpha converting enzyme

TAK1, TGF $\beta$ -activated kinase 1  
TNF- $\alpha$  Tumour necrosis factor-alpha  
TNFR1 Tumour necrosis factor-alpha receptor  
TRADD, TNFR1-associated DEATH domain  
UDP-GT UDP-glucuronosyltransferase  
UK United Kingdom  
VA Vanillic acid  
VA4G Vanillic acid-4-glucuronide  
VA4S Vanillic acid-4-sulfate  
VCAM-1 Vascular cell adhesion molecule-1  
VSMC Vascular smooth muscle cell

# Chapter 1. Flavonoids and Cardiovascular Disease: A Review of Current Literature.

## 1.1. Introduction

Flavonoids are a class of polyphenolic compounds present as secondary metabolites in many plants and fruit and are consumed in varied amounts in our diet; common sources are tea, berries and red wine (**Table 1.1**; Spencer, 2012). Flavonoids are considered non-essential nutrients as their intake is not considered essential to growth and development (Birt and Jeffery, 2013), however, there is a mounting epidemiological evidence suggesting that long-term consumption of flavonoid-rich foods reduces the occurrence of a number of chronic disorders, such as atherosclerosis (Faridi et al., 2008, Lekakis et al., 2005, Oyama et al., 2010, Yang and Zhao, 2012), cancer (Su et al., 2012, Adebamowo et al., 2005, Cutler et al., 2008, Theodoratou et al., 2007) and neurodegeneration (Spencer, 2009).

**Table 1.1. Dietary sources of flavonoids**

Sub-class name	Example dietary flavonoid in this subclass	Example dietary sources (approx. serving size)	Approximate polyphenol content per serving size (mg)
Flavan-3-ols (Flavanols)	(+)-Catechin	Chocolate (50 g)	23–30
	(-)-Epicatechin	Green tea (200 mL)	20–160
	(-)-Epicatechin-3-O-gallate	Black tea (200 mL)	12–100
Flavanones	Naringenin	Orange juice (200 mL)	40–140
	Hesperetin	Grapefruit juice (200 mL)	20–130
	Eriodictyol	Lemon juice (200 mL)	10–60
Flavones	Apigenin	Parsley (5 g)	1.2–9.2
	Luteolin	Celery (200 g)	4–28
		Capsicum pepper (100 g)	0.5–1
Flavonols	Quercetin	Yellow onion (100 g)	35–120
	Kaempferol	Curly kale (200 g)	60–120
	Myricetin	Leek (200 g)	6–45
Anthocyanins	Cyanidin	Blueberry (100 g)	25–500
	Peonidin	Black grape (200 g)	60–1500
	Malvidin	Red wine (100 mL)	20–35

Adapted from (Manach et al., 2004) and Phenol Explorer (Rothwell et al., 2013).

Cardiovascular-related disorders are the most prevalent causes of death in the Western world (Mendis et al., 2015). The total cost of cardiovascular disease care in the UK exceeded £15.4 billion in 2014 with a predicted increase to £18 billion by 2020 (Tofield, 2013). Prevention of chronic disease by means of diet is therefore of great interest to the fields of nutrition and medicine.

Protective effects of dietary flavonoids against cardiovascular-related disorders have been observed in numerous randomised-control trials (Barona et al., 2012, Weseler et al., 2011, Bondonno et al., 2012, Curtis et al., 2009, Faridi et al., 2008), animal feeding (Bornhoeft et al., 2012, Gandhi et al., 2009, Heeba et al., 2012, Loke et al., 2010, Nabavi et al., 2012, Sheng et al., 2009) and *in vitro* studies (Kawai et al., 2008, Tu et al., 2007, Yamagata et al., 2010). Unfortunately, the underlying mechanisms of flavonoids cardiovascular bioactivity have yet to be elucidated and it has been proposed that their bioactivity is mediated through their lesser studied metabolic degradants (Kay et al., 2009). Most previous *in vitro* studies have been conducted using supraphysiological concentrations of single flavonoids, overlooking appropriate dose, the potential bioactivity of flavonoid metabolites, and additive effects metabolites may have in combination. Additionally, the study of metabolite bioactivity is restricted by the limited availability of pure metabolite standards (Rodriguez-Mateos et al., 2014b, Kay, 2010). Elucidating the cellular effects of flavonoid metabolites at concentrations obtainable through diet, is therefore essential to our understanding of flavonoids 'true' cardiovascular bioactivity.

## 1.2. Flavonoids

### 1.2.1. Structures and Functions in Nature.

Flavonoids are a family of phytochemicals that share a common flavalium backbone (**Figure 1.1**). Antioxidant activities have been attributed to the multiple hydroxyl groups, common to all flavonoid structures, coupled with conjugated double-bonds and carbonyl groups allowing for stable electron delocalisation (Corcoran et al., 2012). These compounds act as scavengers of reactive oxygen species (ROS) in plants, preventing cells from intracellular

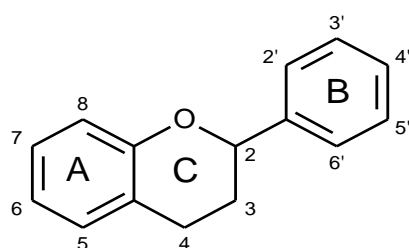


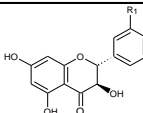
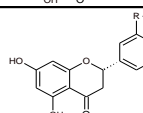
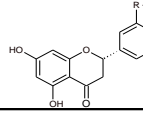
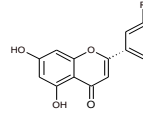
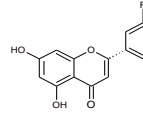
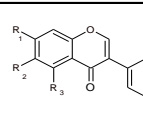
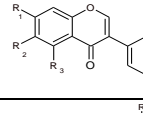
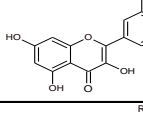
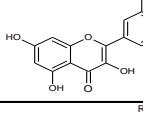
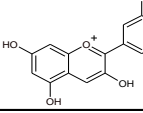
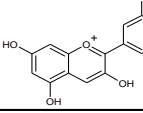
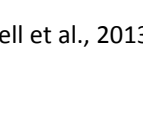
**Figure 1.1. Flavalium backbone**

damage resulting from ultraviolet (UV) light exposure (Agati et al., 2013), amongst other activities (anti-fungal, anti-microbial etc.; Corcoran et al., 2012).

Initial research into flavonoid bioactivity was focused on extrapolating this plant cell antioxidant activity to analogous functions in humans and animal systems (Robak and Gryglewski, 1988), however, such activity in humans did not account for systemic, tissue, and cell concentrations of scavenging substrates/flavonoids, where most tissue levels *in vivo* are too low to act as effective radical scavengers (Brunetti et al., 2013). The need for an alternative hypothesis of flavonoid activity has therefore led to a focus on regulation of protein and enzyme systems (Kay, 2015).

Flavonoids are characterised into six chemical sub-classes, based on their structural characteristics (**Table 1.2**). Subclasses of flavonoids share a common C6-C3-C6 structure and are further sub-classified by their functional groups (Birt and Jeffery, 2013). Over five thousand structurally distinct flavonoids have been identified and characterised, although the exact number varies in the literature (Beecher, 2003, Corcoran et al., 2012).

**Table 1.2. Structures of common subclasses of flavonoids.**

Sub-class name	Example dietary flavonoids in this subclass <sup>1</sup>	Common structure	Substituent(s)		
			R <sub>1</sub>	R <sub>2</sub>	R <sub>3</sub>
Flavan-3-ols (Flavanols)	(+)-Catechin		OH	OH	H
	(-)-Epicatechin		OH	OH	H
Flavanones	Naringenin		H	OH	H
	Hesperetin		OH	OCH <sub>3</sub>	H
Flavones	Apigenin		H	OH	H
	Luteolin		OH	OH	H
Isoflavones	Daidzein		OH	H	H
	Genistein		OH	H	OH
Flavonols	Quercetin		OH	OH	H
	Kaempferol		H	OH	H
Anthocyanins	Cyanidin		OH	OH	H
	Peonidin		OCH <sub>3</sub>	OH	H

<sup>1</sup>Derived from Phenol Explorer (Rothwell et al., 2013).

### 1.2.2. Metabolism and Absorption

Many flavonoids found in nature are conjugated to sugar moieties, such as  $\beta$ -glycoside (e.g. cyanidin-3-glucoside). Consequently, due to their high polarity and occurrence in larger, more complex structures, many flavonoids were initially thought to be non-absorbable following oral consumption (Bravo, 1998), though postulated to be hydrolysed by intestinal bacteria and partially absorbed (Bokkenheuser et al., 1987). There is now evidence to suggest that flavonoids are absorbed into the intestinal enterocytes of the small intestine by a number of reported mechanisms (Walle, 2004; **Figure 1.2**).

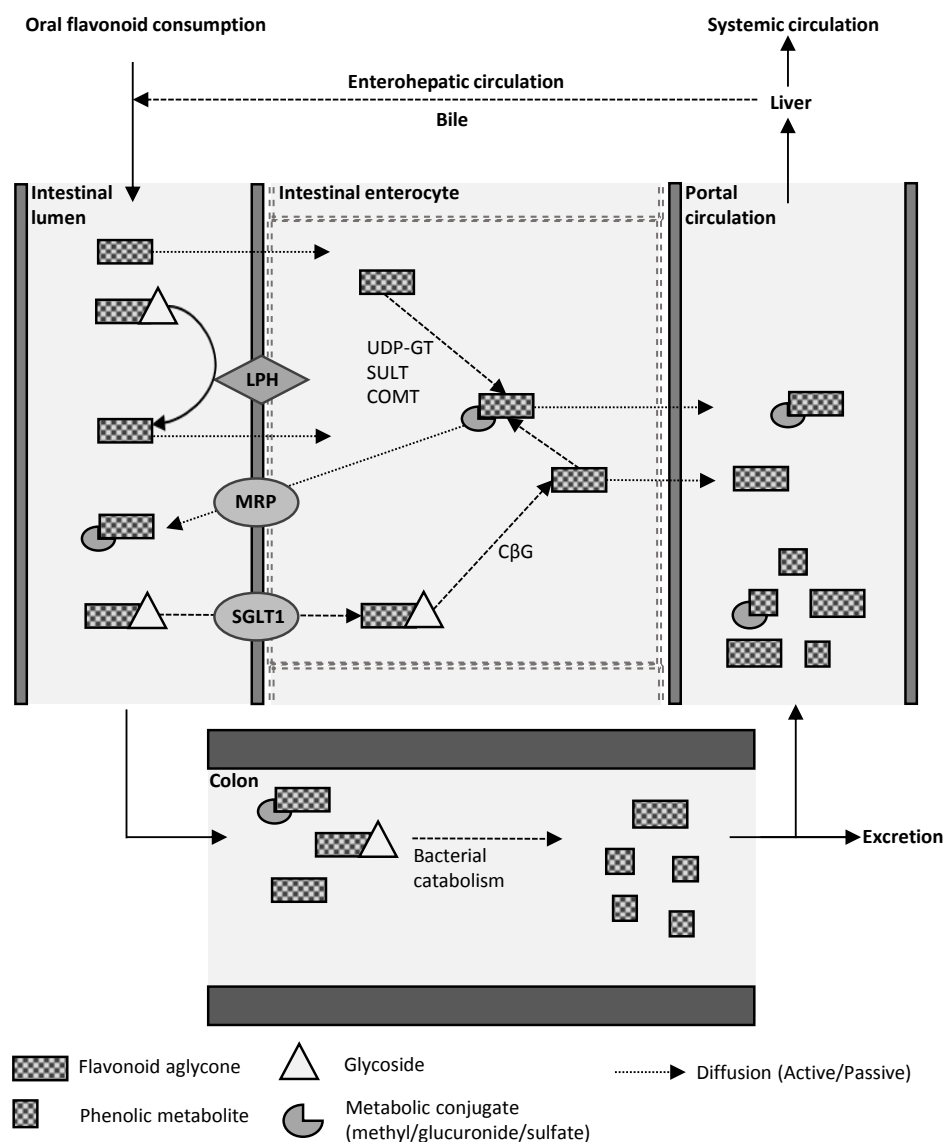


**Figure 1.2. Proposed mechanisms of flavonoid absorption and metabolism.** Abbreviations: C $\beta$ G, cytosolic- $\beta$ -glucosidase; COMT, catechol-O-methyltransferase; LPH, lactase phloridzin hydrolase; MRP, multidrug resistance protein; SGLT-1, sodium-dependant glucose transporter; SULT, sulfotransferase; UDP-GT, UDP-glucuronosyltransferase. Adapted from Serra et al., 2012 and Kay, 2006.

Flavonoid glycosides may be deconjugated by lactase phlorizin hydrolase (LPH) located on the brush border of the small intestine (Day et al., 2003). Aglycones, being less hydrophilic than glycoside conjugates, are readily absorbed by intestinal enterocytes. It is believed that the uptake process for glycosides is facilitated by the use of an active transport mechanism via sodium-dependent glucose transporter-1 (SGLT-1). Hydrolysis of the glycoside may then occur intracellularly by cytosolic- $\beta$ -glucosidase (CBG), and the aglycones may then diffuse into the hepatic portal vein by passive diffusion (Day et al., 2003) or be further conjugated by phase II enzymes.

Within the intestinal enterocytes, flavonoid aglycones are subjected to the activity of phase II metabolic enzymes; UDP-glucuronosyltransferase (UDP-GT), sulfotransferase (SULT) and catechol-O-methyltransferase (COMT; Murota and Terao, 2003), responsible for the conjugation to glucuronide, sulfate and methyl moieties, respectively (Singh et al., 2008). The resulting products are transported to the liver through the portal vein and may further undergo glucuronidation or sulfation and/or methylation within hepatocytes in the liver (Singh et al., 2008, Perez-Vizcaino et al., 2012) before entering the systemic circulation and ultimately being distributed to the tissues of the body or eliminated via the kidneys (urinary excretion; Perez-Vizcaino et al., 2012). Similarly, conjugates may re-enter the small intestinal lumen through the enterohepatic circulatory system through bile acids; ultimately these compounds are transported to the colon (Serra et al., 2012), where ring fission of flavonoids occurs through the action of microbial catabolism (Kumar and Pandey, 2013).

Colonic microbiota contain a number of metabolic enzymes, such as dehydroxylases, decarboxylases, glucosidases, demethylases and esterases (Serra et al., 2012). The process of fermentation produces a number of smaller compounds, such as phenolic acids, cinnamic acids, phenylacetic acids, phenylpropionic acids and valerolactones (Serra et al., 2012, Stalmach et al., 2013). Products of fermentation may then be absorbed, re-absorbed and circulate to the liver through the portal vein (resulting in further phase II metabolism) and distributed to the tissues, or can be excreted in faeces (Monagas et al., 2010).

A large proportion of degradants originating from the B-ring of flavonoids appear to circulate as phenolic metabolites (Vitaglione et al., 2007, Pimpão et al., 2015). Common phenolic metabolites of flavonoids, such as phenolic acids have been detected following the consumption of berry anthocyanins (de Ferrars et al., 2014a), cocoa and tea (Clifford et al., 2013), and citrus fruits (Schar et al., 2015, Pereira-Caro et al., 2014). It has been proposed that the flavonoid A-ring is metabolised to oxaloacetate, which is then degraded to CO<sub>2</sub> via

the citric acid cycle (Walle et al., 2001b), resulting in eventual excretion by exhalation from the lungs (Czank et al., 2013).

Many previous *in vitro* studies have focused on the bioactivity of flavonoid aglycones, which are extensively metabolised, as described above. It has been suggested that the beneficial effects of flavonoids are most likely the result of their more abundant bacterial catabolites and phase II metabolites (Kay et al., 2009), which are present in the circulation for extended periods of time. The study of the bioactivity of these phenolic metabolites is relatively contemporary (Heleno et al., 2015, Edwards et al., 2015, di Gesso et al., 2015) and therefore are the focus of the present thesis. Additionally, *in vitro* studies treating with precursor/un-metabolised structures in isolation do not take into account the additive, antagonistic, or synergistic effects that these metabolites may have in combination (Kerimi and Williamson, 2016). To address this issue, studies presented in this thesis also explored potential additive effects of flavonoid metabolites as mixtures or complex profiles.

### **1.2.3. Bioavailability**

Bioavailability is defined as the available fraction of a substance available to the tissues for physiological function and/or storage (Bohn, 2014). The bioavailability of flavonoids is generally measured based on approximations derived from plasma concentration ( $C_{max}$ ) of a given compound and the time at which this concentration is achieved ( $t_{max}$ ; **Table 1.3**). A possible reason for the low recovery of flavonoids, particularly anthocyanins, may be that the majority of bioavailability studies conducted to date have generally attempted to detect aglycones, or intact or conjugated flavonoid structures (Felgines et al., 2005, Kay et al., 2005) and have not identified lower molecular weight metabolites, such as phenolic acids. Additionally, the majority of *in vivo* absorption and metabolism studies have utilised flavonoid-rich extracts from fruits, which may have an influence on absorption, and production of degradants and metabolites in the body due to the complex mixture of various molecules present (Crozier et al., 2009). Bioavailability data are important in the design of both *in vivo* and *in vitro* studies, as utilised concentrations or doses used should ideally reflect physiologically achievable concentrations of flavonoids post-consumption.

**Table 1.3. Kinetic data for example flavonoids**

Flavonoid	Source	Dose (mg)	t <sub>max</sub> (h)	C <sub>max</sub> (μM)
Quercetin	Pure compound	4000	1.3-1.9	<0.33
	Onion	68	0.7	0.74
(+)-Catechin	Pure compound	2000	0.5	2.8-5.9
(-)-Epicatechin	Green tea infusion	32	3-6	0.27
	Chocolate	220	2	4.77
Naringenin	Grapefruit juice	199	4.8	5.99
Hesperetin	Orange juice	126	5.4	2.2
Cyanidin-3-glucoside	Pure ( <sup>13</sup> C) compound	500	1.8	0.14

Data derived from (Manach et al., 2005, Manach et al., 2004, de Ferrars et al., 2014b). Abbreviations:

t<sub>max</sub>, time to reach maximum plasma concentration; C<sub>max</sub>, plasma concentration at t<sub>max</sub>

As previously mentioned, the bioavailability of parent flavonoids, particularly anthocyanins, is low, but more recent evidence has suggested that flavonoids largely circulate as their chemical degradation products or bacterial catabolites (Kay et al., 2005). A pertinent example of this is a study providing a regular dose of orange juice vs. control drink (Schar et al., 2015), where the recovered concentration of the total (8) flavanones was 1.75 μM at 5 h post-consumption, compared to 13.3 μM of total phenolic intermediates/metabolites at the same time point. Likewise, following ingestion of 500 mg <sup>13</sup>C-labelled cyanidin-3-glucoside (C3G), our group reported a C<sub>max</sub> of 0.14 μM C3G at 1.8 h (Czank et al., 2013), whereas peak phenolic metabolites were reported between 2 and 30 h at 10 - 2000 nM (de Ferrars et al., 2014b). Therefore, while there is little scope to explore flavonoid *in vitro* activity at concentrations >1 μM, there is scope to explore metabolite mixtures at concentrations reflective of physiological conditions >10 μM. Additionally, following an initial 0.5-1 h spike/peak in concentration in plasma following consumption of a cocoa polyphenol extract (Vitaglione et al., 2013) and <sup>13</sup>C-labelled cyanidin-3-glucoside (de Ferrars et al., 2014b), phenolic metabolites again peaked at 6 h (2.2 μM) and 24 h (4.39 μM). Given that these phenolics circulate at higher concentrations for longer periods of time than their precursors, there is necessity to investigate whether it is the collective activity of the phenolic metabolites which are responsible for the long-term health benefits of flavonoids and prevention of cardiovascular disease.

### **1.3. Flavonoids and Cardiovascular Disease**

#### **1.3.1. Cardiovascular disease**

Cardiovascular disease (CVD) is a global term for a number of diseases relating to the cardiovascular system. Common types of CVD include coronary heart disease (CHD; also known as ischemic heart disease), peripheral arterial disease, aortic disease (such as aortic aneurysm) and stroke (WHO, 2014). The projected number of deaths between 2014 and 2020 is an estimated 1,422,968 people across six major EU countries, including the UK (Cebr, 2014). Certain types of CVD (such as atherosclerosis) may be undiagnosed for many years prior to a medical event, such as myocardial infarction (McGill et al., 2008). Therefore, long-term prevention of chronic diseases through the management of diet has become an important factor in reducing the risk of CVD (NICE, 2014).

Epidemiological evidence suggests that the increased consumption of flavonoid-rich foods is associated with the reduced risk of CVD (Wang et al., 2014, Mink et al., 2007) though not all studies support these associations (Wang et al., 2012, Vogiatzoglou et al., 2015). A prospective study involving 156,957 participants from the Nurse's Health Society and Health Professionals Study identified a reduction in the relative risk (8 %) of hypertension in the highest quintile of anthocyanin consumption compared to the lowest (Cassidy et al., 2011). The Iowa Women's Health Study identified evidence linking individuals that consumed the highest quantities of flavonoid-rich foods to a lower incidence of fatal CVD over a 16 year period (Mink et al., 2007). In a cohort of 93,600 healthy women (24- 45 y) there was a 32 % reduced risk of myocardial infarction (MI) amongst the highest consumers of anthocyanins over 18 y (Cassidy et al., 2013). Multiple classes of flavonoids, such as anthocyanins (Dell'Agli et al., 2004), flavan-3-ols (Arts et al., 2001, Geleijnse et al., 2002), flavonols and flavones (Knekt et al., 2002), and phenolic acids (Tresserra-Rimbau et al., 2014) are also positively associated with the reduced risk of CVD-related death/disorders amongst the highest consumers.

Recommendations for the consumption of flavonoid-rich foods in particular are largely based on observations from epidemiological studies (Rangel-Huerta et al., 2015), though evidence from meta-analyses of randomised control trials (RCTs) vary in conclusions regarding impact on specific factors of cardiovascular disease (Desch et al., 2010, Knekt et al., 2002, Wang et al., 2012), potentially due to the lack of consistency between studies (e.g. the given dose, length of study, statistical methods utilised, and a lack of biomarkers of flavonoid intake; Wallace et al., 2016, Kay et al., 2012, Feliciano et al., 2015). Investigations into the potential mechanisms of action of flavonoids *in vitro* may therefore aid in the design

of future, targeted RCTs, which together may forward our understanding of flavonoids cardiovascular bioactivity.

### **1.3.2. Atherosclerosis**

Atherosclerosis, a common pathology of coronary heart disease (CHD), is characterised as an accumulation of plaque in the arterial wall. The condition originates in the intimal layer of the vascular wall, where macrophages develop into foam cells; an inflammatory process driven by endothelial cell dysfunction in the layer surrounding the vascular lumen (Sitia et al., 2010). Endothelial dysfunction is defined as the modulation of cell phenotype in response to a non-adaptive functional state (Sitia et al., 2010). The presence of pro-inflammatory factors (such as TNF- $\alpha$ , high levels of oxidised-low density lipoprotein (oxLDL), bacterial toxins or viral infection) activates inflammatory cell signalling cascades in endothelial cells, such as NF $\kappa$ B, which upregulates the transcription and expression of adhesion molecules, such as VCAM-1 and E-selectin (**Figure 1.3**). E-selectins mediate a loose rolling interaction that slows passing leukocytes at the surface of activated endothelial cells and facilitates high affinity binding to the endothelium which is mediated by the action of VCAM-1 (Hopkins, 2013). Chemokines, such as the monocyte chemoattractant protein-1 (MCP-1) present in the developing atheroma, stimulate circulating leukocytes to migrate into the tunica intima of the blood vessels and proliferate. MCP-1 stimulated endocytosis of modified lipoproteins by macrophages leads to the formation of foam cells, further upregulating the production of pro-inflammatory molecules, such as TNF- $\alpha$ , interleukin-1 beta (IL-1 $\beta$ ), tissue factor and matrix metalloproteinases (MMPs; Ramji and Davies, 2015). The subsequent recruitment of inflammatory T cells, and further release of cytokines and growth factors from leukocytes and endothelial cells, leads to the migration and proliferation of smooth muscle cells, which then stimulate the degradation of elastin and collagen (Frostedgard, 2013). Severe build-up of an atheroma eventually leads to the blockage of the artery, or rupture of the lesion, resulting in infarction and death. Multiple animal studies utilising flavonoids have reported reductions in atheroma size, or slowed atheroma progression, following the consumption of quercetin (Shen et al., 2013), anthocyanins (Mauray et al., 2012), and phenolic acids (Wang et al., 2010).

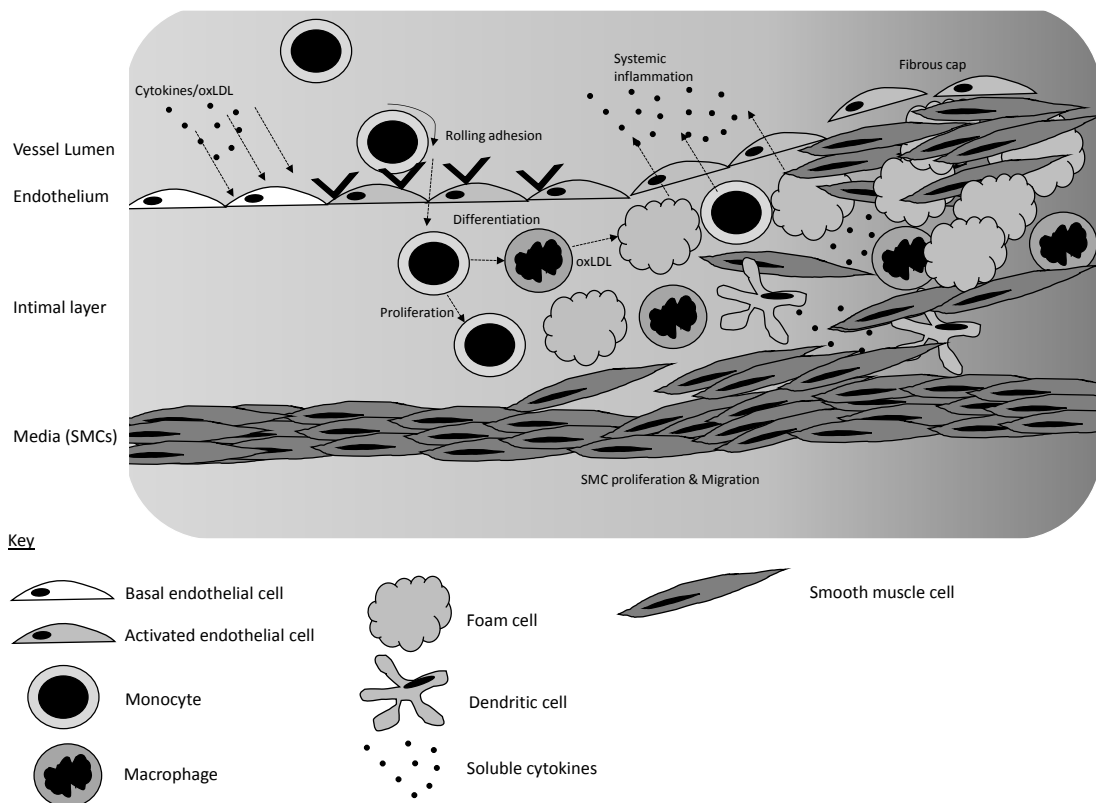


**Figure 1.3. Pathogenesis of atherosclerosis.** 1) Chronic low-level inflammation of the endothelium by any of a number of stimulants, such as cytokines (e.g.  $\text{TNF-}\alpha$ ), high ox-LDL, or shear stress, leads to expression of surface adhesion molecules (e.g. E-selectin, VCAM-1). 2) Monocytes adhere to the endothelial cell surface by rolling and tethering. 3) Cytokine secretion by endothelial and monocytic cells, leads to monocyte infiltration, proliferation, and differentiation into macrophages. 4) Macrophages absorb oxLDL to form foam cells. 5) Foam cells die to form a necrotic core. 6) Smooth muscle cells (SMCs) migrate to stabilise the core and form a fibrous cap. 6) The atheroma may eventually rupture and lead to thrombosis, which may induce myocardial infarction or stroke. Abbreviations: OxLDL, oxidised low density lipoprotein; SMCs. Smooth muscle cells. Adapted from Full et al., 2009.

### 1.3.3 Endothelial dysfunction

Endothelial dysfunction is an early-stage pathology in the development of atherosclerosis; characterised as the reduced availability of nitric oxide (NO) and consequential imbalance of endothelial homeostasis held by the 'healthy' endothelium (**Figure 1.4**; Rajendran et al., 2013). Under normal conditions, endothelial cells primarily regulate vasodilation by NO and prostacyclin ( $\text{PGI}_2$ ) levels (Deanfield et al., 2007). The presence of NO aids in the suppression of  $\text{NF}\kappa\text{B}$  activation and the consequent expression of inflammatory proteins, such as VCAM-1 and  $\text{TNF-}\alpha$ . Additionally, blood clotting is inhibited by the expression of anti-thrombotic proteins such as plasminogen activator inhibitor 1 (PAI-1) and von Willebrand factor (vWF)

(van Hinsbergh, 2012). In 'healthy' individuals, there is an absence of circulating cell stress markers, such as circulating endothelial cells (CECs) and endothelial microparticles (EMPs), and markers which mediate endothelial repair, such as endothelial progenitor cells (EPCs), are increased (Burger and Touyz, 2012). Conversely, in the presence of endothelial dysfunction, vasodilation is impaired and coagulation factors and inflammation are upregulated and there is a high level of circulating endothelial stress markers. It is postulated that flavonoids may prevent the development of atherosclerosis by restoring endothelial homeostasis and preventing endothelial dysfunction, such as by the induction of vasodilators and anticoagulants (Angelone et al., 2011, Jimenez et al., 2015) and inhibition of cytokines and adhesion molecules (Burris et al., 2014, Chen et al., 2002, Noll et al., 2012).

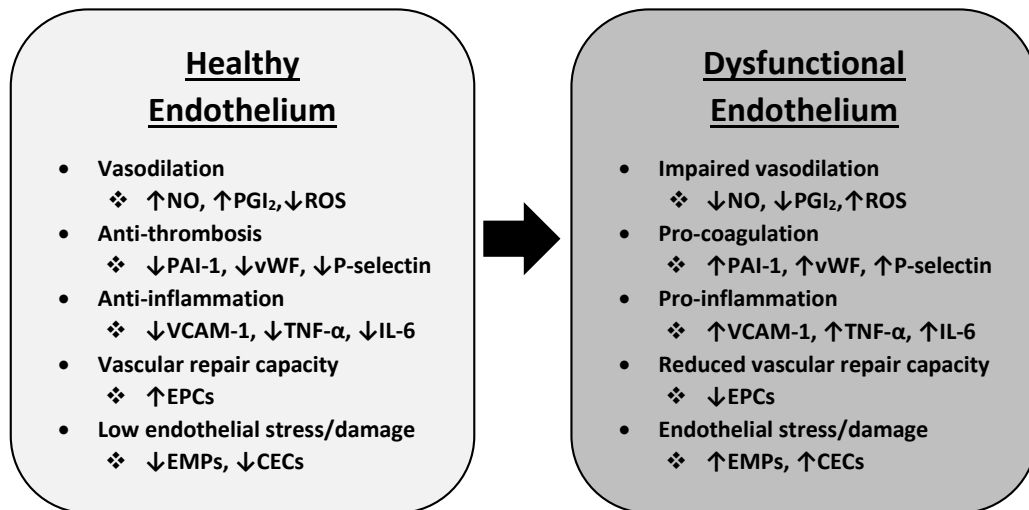


**Figure 1.4. Characteristics of the healthy and dysfunctional endothelium.** Abbreviations: CECs, circulating endothelial cells; EMPs, endothelial microparticles; EPCs, endothelial progenitor cells; IL-6, interleukin-6; NO, nitric oxide; PAI-1, plasminogen activator inhibitor-1; PGI<sub>2</sub>, prostacyclin; ROS, reactive oxygen species; TNF-α, tumour necrosis factor alpha; VCAM-1, vascular cellular adhesion molecule-1; vWF, von Willebrand factor. Adapted from Rajendran et al., 2013.

### 1.3.2. Biomarkers of endothelial dysfunction

#### 1.3.2.1. Nitric oxide homeostasis and oxidative stress

##### a) Endothelial nitric oxide synthase

A disruption of nitric oxide (NO) homeostasis is a contributing factor in the progression of endothelial dysfunction, which can lead to atherosclerosis. Endothelial nitric oxide synthase (eNOS) is considered a critical regulator of NO homeostasis and is therefore a key clinical target for the treatment or management of chronic cardiovascular disorders (Heiss et al.,

2015). Clinical measures of vascular function, such as flow-mediated vasodilation (FMD; Grassi et al., 2015), are, at least in part, regulated by endothelium-derived nitric oxide (NO) levels (Green et al., 2014). Cellular NO levels has therefore been a target of interest for previous flavonoid studies (Tribolo et al., 2013). Certain flavonoids may enhance vascular function through modulating the expression of eNOS (Woodman and Chan, 2004), which subsequently increases NO.

eNOS produces NO by the oxidation of L-arginine to L-citrulline (**Figure 1.5**), which is catalysed via a cofactor, tetrahydrobiopterin ( $BH_4$ ), by electron transfer to the amine group of L-arginine (Alp and Channon, 2004). Disruption of eNOS is referred to as eNOS uncoupling, which can promote the transition of a normal endothelium into a dysfunctional endothelium by the increase in reactive oxygen species (ROS) production. eNOS uncoupling occurs in the presence of oxidative stress, where there are reduced levels of substrates L-arginine and  $BH_4$ ; in this state the enzyme produces ROS, such as superoxide ( $O_2^-$ ), peroxynitrite ( $ONOO^-$ ) and hydrogen peroxide ( $H_2O_2$ ; Kawashima and Yokoyama, 2004). The transcriptional, post-transcriptional and post-translational regulation of eNOS expression is affected by a number of physical, chemical and hormonal factors such as bradykinin, oestradiol, intracellular calcium ( $Ca^{2+}$ ), shear stress and vascular endothelial growth factor (VEGF; Rafikov et al., 2011). *In vitro* studies have shown that eNOS expression is increased in response to multiple subclasses of flavonoids, such as anthocyanins (Lazze et al., 2006), flavan-3-ols (Martinez-Fernandez et al., 2015), and flavanones (Rizza et al., 2011), though the study of phenolic metabolites on eNOS expression is relatively contemporary (Edwards et al, 2015).

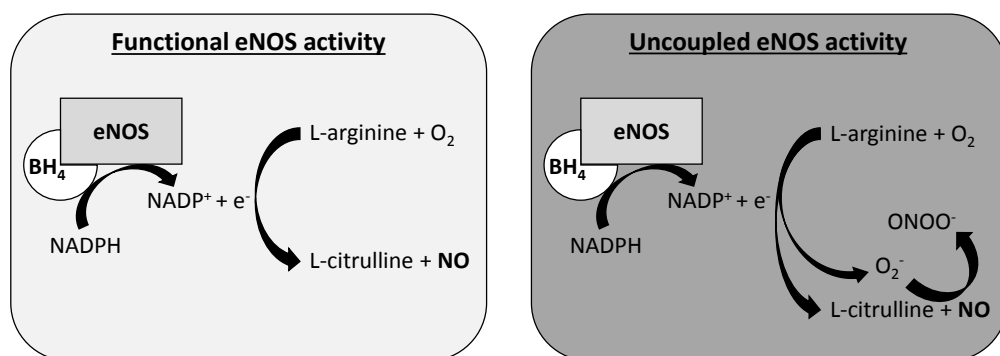


**Figure 1.5. Functional and dysfunctional eNOS activity.** A) Functional eNOS activity produces NO under normal physiological conditions. B) Dysfunctional eNOS activity produces superoxide radicals which may react with NO, reduced its bioavailability and producing  $ONOO^-$  radicals.

Interestingly, the flavonol, quercetin has been shown at supraphysiological concentrations to decrease eNOS expression, which appears to be blocked when the structure is metabolically conjugated with glucuronide, however this effect has not been demonstrated at physiologically achievable concentrations (Tribolo et al., 2013), conversely, concentrations of  $\leq 10 \mu\text{M}$  of quercetin has been seen to increase eNOS expression (Shen et al., 2012). These studies further support the requirement for *in vitro* studies to utilise concentrations which resemble physiologically achievable concentrations observed *in vivo*. A recent study into structure-activity relationships, at a physiologically achievable concentration of  $1 \mu\text{M}$ , of multiple flavonoids suggested that chemical structure significantly affects the ability to increase eNOS mRNA expression *in vitro* (Martinez-Fernandez et al., 2015). Furthermore, it has been seen that common phenolic metabolites of flavonoids, protocatechuic acid (PCA) and vanillic acid (VA) also upregulate eNOS expression (Edwards et al., 2015) in a concentration dependent manner. These studies suggest that flavonoids and/or their metabolites, may influence eNOS expression in endothelial cells, though their effects at physiologically achievable concentrations, or additive effects of multiple metabolites in combination, have yet to be explored.

#### **b) Haem oxygenase-1**

Haem oxygenase-1 (HO-1) catalyses the oxidation and degradation of intracellular haem (**Figure 1.6**). The by-products of this reaction are carbon monoxide (CO), ferrous iron ( $\text{Fe}^{2+}$ ), and biliverdin IX $\alpha$ , which is subsequently reduced in the presence of NADPH and biliverdin reductase to produce the bilirubin IX $\alpha$  (Araujo et al., 2012). Intracellular HO-1 protein expression is low in the absence of cellular stress, but can be induced in response to a number of physical and chemical stimuli, such as NO, cytokines, oxLDL, and phytochemicals. HO-1 is of interest as a therapeutic target due to the bioactivity of its by-products, particularly CO and bilirubin; CO at low levels confers vasodilatory (Leffler et al., 2011) and anti-inflammatory activity (Ryter et al., 2006), whereas bilirubin increases NO in mice (Liu et al., 2015) and is known to scavenge ROS *in vitro* (Abraham and Kappas, 2008).

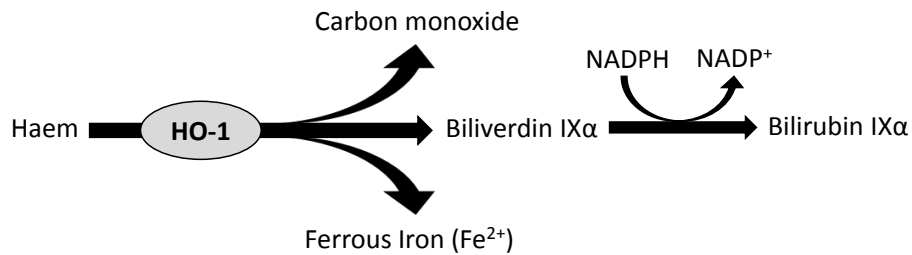


**Figure 1.6. Degradation of Haem by Haem oxygenase-1 (HO-1)**

ApoE-deficient mice fed a high fat diet with quercetin expressed raised levels of HO-1 protein in the aorta against those not fed quercetin and this appeared to be protective against the development of atherosclerosis (Shen et al., 2013). *In vitro* studies have identified links between the upregulation of HO-1 in response to quercetin and the reduction in the expression of inflammatory biomarkers (Sun et al., 2015). Likewise, the flavanone naringenin attenuates smooth muscle cell proliferation and migration by upregulation of HO-1 (Chen et al., 2012) and similar effects have been observed in endothelial cells in response to the anthocyanin cyanidin-3-glucoside (C3G; Speciale et al., 2013, Sorrenti et al., 2007). Previously, few studies reported increased HO-1 protein expression in response to physiological concentrations of these flavonoids and recently one study observed HO-1 protein expression in response to phenolic metabolites of flavonoids (protocatechuic acid and vanillic acid; Edwards et al., 2015). Given the diversity of flavonoid metabolites and the impact of flavonoids on multiple cells types, study into the effects of phenolic metabolites on HO-1 expression is warranted.

### **1.3.2.2. Low level chronic inflammation**

#### **a) Tumour necrosis factor-α**

Tumor necrosis factor-alpha (TNF-α) is a cytokine that plays a central role in the pathogenesis of a number of diseases, such as atherosclerosis, inflammatory bowel diseases (IBDs) and rheumatoid arthritis (Brenner et al., 2015). TNF-α functions as either a membrane-traversing protein or may be cleaved from the cell surface by TNF-α converting enzyme (TACE) to circulate as a soluble protein (Hehlgans and Pfeffer, 2005). The progression of atherosclerosis is strongly associated with circulating TNF-α levels in the blood (Bruunsgaard et al., 2000). In a study of 32 males aged  $58.2 \pm 12$  y with a particular variant of atherosclerosis, coronary artery ectasia, circulating TNF-α expression levels were  $15.6 \pm 11.2$  pg/mL vs.  $7.8 \pm 3.7$  pg/mL compared to an age and sex matched control group (Aydin et al.,

2009). The knockout of TNF- $\alpha$  in ApoE-deficient mice reduced atherosclerotic lesion size by 50%, again suggesting that TNF- $\alpha$  is a major contributing factor to the development of atherosclerosis (Branen et al., 2004). There have been many clinical studies investigating the effects of flavonoids on TNF- $\alpha$  expression, however, a meta-analysis of 32 RCTs found no direct effects of flavonoids on TNF- $\alpha$  expression in humans (Peluso et al., 2013). A lack of consistency and poor controls between and within the studies was noted and may be a factor in the lack of positive findings.

#### **b) Vascular cell adhesion molecule-1**

Vascular adhesion molecule-1 (VCAM-1) is primarily expressed in endothelial cells, but may also be present to a lesser extent in other inflammatory cell types (e.g. macrophages, myoblasts, dendrites). The earliest stages of atherosclerosis pathogenesis involve the systematic expression of adhesion molecules which mediate the tethering (L- and P-selectins), rolling attachment, and arrest at cell surface (VCAM-1, E-selectins, and ICAMs) and transmigration (ICAMs and PECAMs) of monocytes into the arterial intima (Galkina and Ley, 2007, Blankenberg et al., 2003; **Figure 1.7**). Of these proteins, VCAM-1 is considered critical and essential to atherosclerosis pathogenesis (Ley and Huo, 2001) and mice with defective VCAM-1 expression (VCAM-1<sup>D4D</sup>; 2-8% VCAM-1 relative to wild-type), fed a high cholesterol diet, had lesser-developed lesions after 8 weeks relative to wild-type mice (Cybulsky et al., 2001). VCAM-1 expression is upregulated following activation of the NF $\kappa$ B transcription factor pathway in response to a number of stimuli, such as TNF- $\alpha$ , oxLDL (Yurdagul et al., 2016), and cluster of differentiation 40 ligand (CD40L; expressed by CD4+ T lymphocytes; Pamukcu et al., 2011). Membrane-bound VCAM-1 may be cleaved from the endothelial cell surface forming a soluble molecule (sVCAM-1), though the exact mechanism for this is not certain. Previous studies have suggested that VCAM-1 shedding may be mediated by TNF- $\alpha$  converting enzymes (TACE; e.g. ADAM17) following stimulation with phorbol 12-myristate 13-acetate (PMA; Garton et al., 2003) and TNF- $\alpha$  (via TIMP-3; Singh et al., 2005).

Expression levels of circulating adhesion molecules have been postulated to be predictive of clinical events, despite the uncertainty of their roles in CVD pathology (Hope and Meredith, 2003). sVCAM-1 is found at considerably high levels in the plasma of patients with atherosclerosis (Miwa et al., 1997) and considered an important predictor of risk of death from coronary heart disease (Blankenberg et al., 2001). Furthermore, sVCAM-1 expression directly correlates with membrane-bound VCAM-1 levels (Kjaergaard et al., 2013) and

remains stable in plasma (Hartweg et al., 2007), which makes it an ideal experimental biomarker in models of endothelial dysfunction.

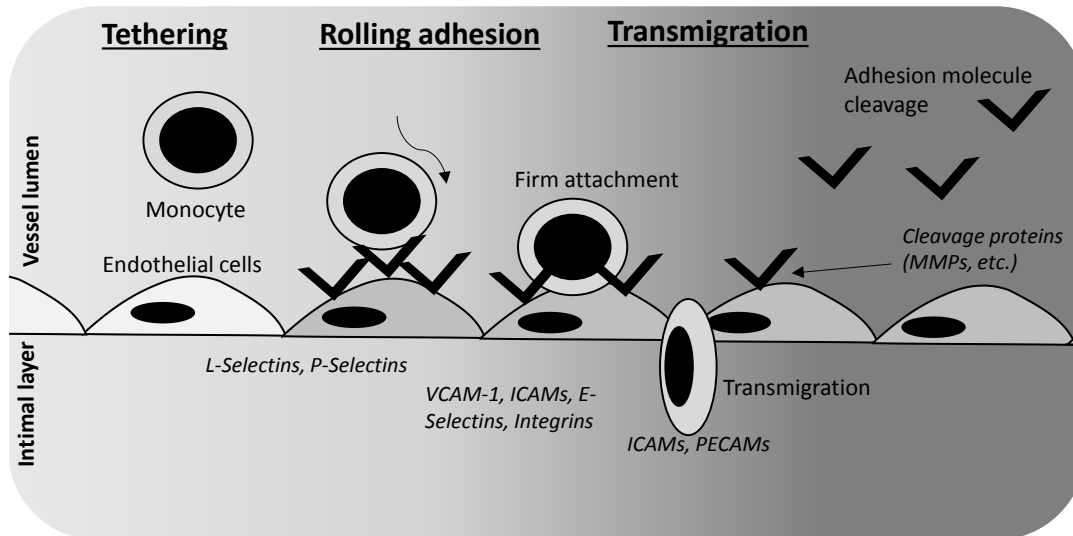


**Figure 1.7. Cell adhesion and roles of adhesion molecules during early stages of atherosclerosis.** 1) L- and P-Selectins function primarily in the process of tethering and rolling of monocytes on the endothelial membrane. 2) Vascular cell adhesion molecule-1 (VCAM-1), intercellular adhesion molecules (ICAMs), E-selectins, and integrins induce firm adhesion. 3) ICAMs and platelet endothelial cellular adhesion molecules (PECAMs) are involved in transmigration of cells from the vessel lumen into the underlying intimal layer. 4) Cellular adhesion molecules, except integrins, may be cleaved by proteolytic enzymes (e.g. metalloproteases (MMPs)) from the cell surface and circulate as soluble forms (sVCAM-1, sICAM-1, etc.). Adapted from Blankenberg et al., 2003.

*In vitro* studies using human endothelial cells have observed an inhibition of VCAM-1 in response to various subclasses of flavonoids, such as flavan-3-ols (Ludwig et al., 2004), anthocyanins (Speciale et al., 2010), flavones (Choi et al., 2004), and flavanones (Nizamutdinova et al., 2008). However, these studies observed activity at concentrations from 5 to 60  $\mu$ M, which does not reflect physiologically achievable concentrations. Therefore, future studies should investigate the activity of flavonoids at physiologically achievable concentrations and account for the extensive metabolism of flavonoids.

More recently, studies have focused on the effects of flavonoid metabolites on the inhibition of VCAM-1 and monocyte adhesion (Claude et al., 2014, Chanet et al., 2013), though these have looked primarily at the phase II conjugated parent structures, rather than the bacterial catabolites. Until recently, only a few studies from our group have focused on unconjugated

and conjugated phenolic metabolites (di Gesso et al., 2015, Amin et al., 2015), where one has reported bioactivities of mixtures of flavonoid metabolites.

### **c) Interleukin-6**

Raised serum IL-6 expression has been shown as highly predictive of CVD (Cesari et al., 2003) and of future cardiac events and is involved in the induction of endothelial dysfunction (Bhagat et al., 1997) and the activation of acute-phase proteins (Scheller et al., 2011). In a study of 718 patients, high levels of serum IL-6 was significantly associated with cardiovascular mortality (Su et al., 2013) and atherosclerotic lesion size was significantly increased in ApoE-deficient mice injected with recombinant IL-6 (Huber et al., 1999). *In vitro*, IL-6 has been shown to induce the proliferation of smooth muscle cells (Garcia-Lafuente et al., 2009). Following a 4-week anthocyanin-rich bilberry juice intervention, significantly lower plasma concentrations of IL-6 were reported in subjects who consumed the treatment relative to the placebo control (Karlsen et al., 2010). IL-1 $\beta$  stimulated IL-6 expression in Grave's orbital fibroblasts was significantly reduced by >50  $\mu$ M quercetin and by the flavanones, hesperetin and naringenin (100  $\mu$ M) in murine adipocytes (Yoshida et al., 2010). As previously mentioned, there are few studies which have looked at physiologically achievable concentrations of flavonoids and of their phenolic metabolites on IL-6 secretion. This is particularly pertinent given that conjugated phenolic metabolites of flavonoids have recently been seen by our group to significantly reduce the secretion of sIL-6 by human endothelial cells (Amin et al., 2015).

### **1.3.3. Regulatory mechanisms of endothelial dysfunction**

#### **1.3.3.1. Transcription factor regulation**

##### **a) Nuclear factor-erythroid-2-related factor 2**

The nuclear factor-erythroid-2-related factor 2 (Nrf2) transcription factor is a key sensor and master regulator of oxidative stress and is expressed ubiquitously in all tissues (Uhlen et al., 2015). Activation of Nrf2 leads to the transcription of proteins which have antioxidant and anti-inflammatory properties, which may protect against endothelial dysfunction, and is therefore a potential therapeutic target for CVD (Reuland et al., 2013). Nrf2 protein levels in the cytosol are negatively regulated by association with Kelch-like ECH associated protein 1 (Keap1). Keap1 is a scaffold protein that recruits Cul-3/Rbx1 E3 ubiquitin ligase, which leads to the ubiquitination and degradation of Nrf2 by the 26S proteasome (Niture et al., 2014). This mechanism has been demonstrated by the increase in Nrf2 expression following proteasome inhibition (Sekhar et al., 2000). Following translocation to the nucleus, activated

Nrf2 binds to an enhancer, the antioxidant response element (ARE), in the regulatory regions of over 250 cellular antioxidants, detoxification enzymes and other cytoprotective proteins, including haem oxygenase-1 (HO-1), NAD(P)H dehydrogenase quinone-1 (NQO1), and glutamate–cysteine ligase (GCL; Hybertson et al., 2011). It has been observed that certain flavonoids may have regulatory effects on the Nrf2 pathway (Moosavi et al., 2016). In aged rat hearts, Nrf2 expression was upregulated in response to hesperidin (Elavarasan et al., 2012) and Nrf2-dependent HO-1 expression in response to quercetin is thought to be dependent on ERK1/2 phosphorylation (Liu et al., 2012).

The mechanism(s) by which Nrf2-regulated transcription (**Figure 1.8**) is activated has been a topic of much debate. Initially, it was postulated that Keap1/Nrf2 binding was destabilised by modification of the cysteines of Keap1 in the presence of oxidative stress (Dinkova-Kostova et al., 2002), leading to the liberation of Nrf2 from the complex. This mechanism has not been unequivocally demonstrated *in vitro*, in fact, the presence of inducers of Nrf2 activation, such as sulforaphane, were not able to separate the proteins (Egler et al., 2005). An alternative proposal is that the ubiquitination of Nrf2, which signals degradation by the 26S proteasome is inhibited, potentially by disruption of the binding site. This then leads to the accumulation of Keap1/Nrf2 in the cytoplasm, eventually resulting in the saturation of Keap1, increase of free Nrf2 in the cytoplasm, and subsequent translocation and activation of transcription (Lee and Johnson, 2004). This stabilisation mechanism is most commonly accepted and resembles other characterised mechanisms, such as p53 in response to ionising and ultraviolet (UV) radiation, which leads to a reduction in Mdm2 E3 ubiquitin ligase binding ability (Honda and Yasuda, 2000). Additionally, Nrf2 activation has been shown to be upregulated in the presence of the phosphorylation, and targeted degradation, of negative regulators of Nrf2, such as Keap1 and Bach1, as demonstrated following 1 h treatment with tert-butylhydroquinone (t-BHQ), a potent phenolic antioxidant (Kaspar and Jaiswal, 2010, Kaspar et al., 2012).

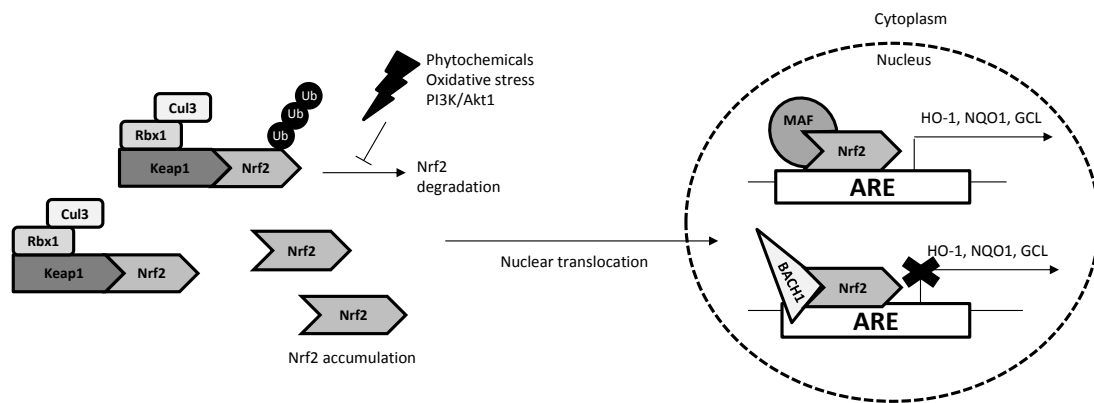


**Figure 1.8. Regulation of the Nrf2-mediated transcription pathway.** The binding of Nrf2/MAF to ARE initiates the transcription of antioxidant, stress-responsive and phase II detoxifying proteins. Abbreviations: ARE, antioxidant-response element; Bach1, BTB And CNC Homology 1; Cul3, cullin-3; GCL,  $\gamma$ -glutamate cysteine ligase; HO-1, haem oxygenase-1; Keap1, kelch-like ECH-associated protein-1; NQO1, NAD(P)H:quinone oxidoreductase; Nrf2, nuclear factor-erythroid-2-related factor 2; Rbx1, RING-box protein-1; Ub, ubiquitin. Adapted from Kim et al., 2010.

It has been postulated that Keap1 directly interacts with inhibitors of the TNF- $\alpha$  stimulated NF $\kappa$ B transcription pathway, leading to the inhibition of pro-inflammatory protein expression (Jiang et al., 2012), as was also observed in endothelial cells treated with epigallocatechin gallate (EGCG; Han et al., 2012). Additionally, Nrf2-dependant HO-1 and NQO1 induction causes a reduction in pathological biomarkers of atherosclerosis, such as MCP-1 (Kim et al., 2010) and VCAM-1 (Zakkar et al., 2009), suggesting that there is cross talk between the pathways in activated endothelial cells and that there is the potential for flavonoids to have an effect, directly or indirectly, on these interactions (Chan et al., 2011).

## b) NF $\kappa$ B

The phenotypic switch of endothelial cells to a dysfunctional state is partly as a result of low level chronic inflammation, and the expression of many pro-inflammatory biomarkers, such as adhesion molecules, cytokines, growth factors and chemokines, are under the transcriptional regulation of the nuclear factor  $\kappa$ B (NF $\kappa$ B; **Figure 1.9**; Ferre et al., 2010). NF $\kappa$ B is implicated in the initiation of atherosclerosis by the induction of inflammatory and immune responses (Ramji et al., 2015) and flavonoids have been seen to inhibit targets within this pathway (Gonzalez et al., 2011). In resting cells, the NF- $\kappa$ B family of proteins (p65, RelB, c-Rel, p50, and p52), are retained in the cytoplasm as homo- or hetero-dimers bound to inhibitors of  $\kappa$ B (I $\kappa$ B; Hayden et al., 2004).

NF $\kappa$ B-mediated transcription is activated by a number of upstream signalling cascades, in response to various stimuli, such as pro-inflammatory cytokines (e.g. TNF- $\alpha$ ), phorbol esters, lipopolysaccharide (LPS), and antigens (Sakurai et al., 2003). Following TNF- $\alpha$  binding to the TNF- $\alpha$  receptor-1 (TNFR1), a scaffold referred to as the TNFR1-associated death domain (TRADD) protein is recruited. TRADD recruits a number of adaptor proteins, such as receptor-interacting protein (RIP) kinases and TNFR-associated factors (TRAF2/5). These are responsible for the activation of downstream kinases, including several mitogen-activated protein kinase kinases (MAPKKKs), such as TGF- $\beta$ -activated kinase 1 (TAK1). TAK1 is an endogenous inhibitor of a family of proteins called inhibitors of I $\kappa$  kinases (IKKs) in resting cells and previous studies have shown that TNF- $\alpha$  stimulated NF- $\kappa$ B activation is dependent on TAK1 phosphorylation (Sakurai et al., 2003).

The IKK complex consists of two kinase subunits, IKK $\beta$  and IKK $\alpha$ , and a regulatory subunit, IKK $\gamma$  (Bremner et al., 2002). The phosphorylation of these kinase subunits leads to the phosphorylation of I $\kappa$ Bs, such as I $\kappa$ B $\alpha$  at Ser32 and Ser36, and p65 at Ser538, leading to the ubiquitination and rapid proteasome-mediated degradation of I $\kappa$ B, the translocation of NF $\kappa$ B to the nucleus, and the subsequent transcription of pro-inflammatory proteins, such as VCAM-1 and IL-6 (Kempe et al., 2005). Previous studies have shown that I $\kappa$ B $\alpha$  is significantly upregulated in rats fed soybean isoflavones (Yuan et al., 2012), which is inversely related to NF $\kappa$ B transcription levels and therefore the expression of pro-inflammatory proteins. The phenolic metabolite, protocatechuic acid (PCA), has been shown to inhibit monocyte adhesion to TNF- $\alpha$  activated mouse aortic endothelial cells (MAEC) by reducing the NF $\kappa$ B-DNA binding ability (Wang et al., 2010) and reduces the LPS stimulated production of inflammatory cytokines through inhibiting the activation of JNK, ERK and p38 in macrophages (Min *et al.*, 2010).

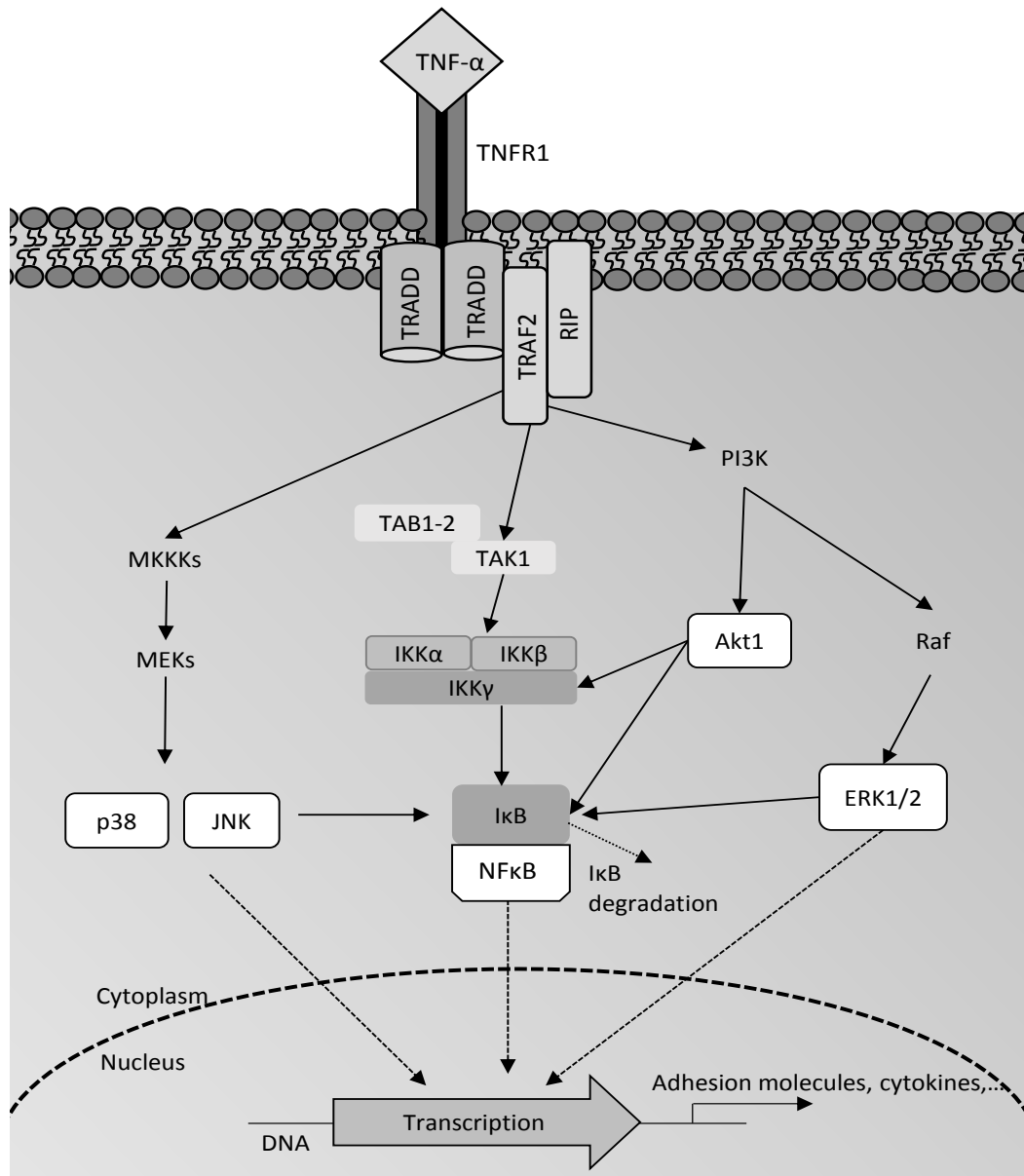


**Figure 1.9. TNF- $\alpha$  activated NF $\kappa$ B transcription factor and signalling kinase cascades.** ERK1/2, extracellular-signal-regulated kinase 1/2; I $\kappa$ B, inhibitor of  $\kappa$ B; IKK, inhibitor of  $\kappa$ B kinase; JNK, c-Jun N-terminal kinases; MAPKKKs, mitogen-activated protein kinase kinase kinases; MEKs, mitogen-activated protein kinase kinases; NF $\kappa$ B, nuclear factor  $\kappa$ B; p38, mitogen-activated protein kinase; PI3K, phosphoinositide 3-kinase; TAB1-2, TAK1 binding protein; TAK1, TGF $\beta$ -activated kinase 1; TRADD, TNFR1-associated DEATH domain; TNF- $\alpha$ , tumour necrosis factor- $\alpha$ ; TNFR1, TNF receptor-1. Adapted from Wilson et al., 2009.

As previously mentioned, other MAPKKs upstream of IKK are activated by proteins in the TRADD complex. Downstream MAPKs, such as extracellular signal-regulated kinases (ERK1/2), c-Jun N-terminal kinase (JNK), and p38 MAPK, have been shown to be rapidly phosphorylated in response to TNF- $\alpha$  in endothelial cells (Yoshizumi et al., 2004). TAK1 has been seen to phosphorylate MEKKs leading to the activations of JNK and p38 (Landstrom, 2010) as well as PI3K (Faurischou and Gniadecki, 2008), which leads to the activations of Akt1 and ERKs (Wang et al., 2012). NF $\kappa$ B activation can be partly suppressed by inhibitors of ERK1/2 (PD98059), JNK (SP600125), and p38 (SB203580; Kang et al., 2006), suggesting that the activation of these proteins may, in part, be dependent on the TNF- $\alpha$  stimulated phosphorylation of these protein kinases. TNF- $\alpha$  induced Akt1 phosphorylation has been reported to activate the NF $\kappa$ B pathway by inducing the phosphorylation of IKK $\alpha$  at Tyr32 (Ozes et al., 1999). It has been previously demonstrated that inhibitors of Akt1 phosphorylation (LY294002 and wortmannin) partially inhibit TNF- $\alpha$  induced NF $\kappa$ B-DNA binding, suggesting that Akt1 phosphorylation, at least in part, is also associated with the activation of the NF $\kappa$ B pathway (Kang et al., 2006). Rat aortic endothelial cells transfected with RNAi for ERK2 and Akt1 had increased expression of VCAM-1 following stimulation with 10 ng/mL TNF- $\alpha$ , suggesting that these kinases are negative regulators of NF $\kappa$ B-mediated VCAM-1 expression (Pott et al., 2016).

The inhibition of TNF- $\alpha$  stimulated lipolysis by flavanones hesperetin and naringenin in mouse adipocytes has been shown to be dependent on ERK1/2 phosphorylation, suggesting that flavonoids may target NF $\kappa$ B indirectly through other kinases. Flavanol metabolites have also been found to inhibit both NF $\kappa$ B and p38-MAPK regulated monocyte adhesion to endothelial cells (Claude et al., 2014), indicating also that flavonoid metabolite are active in both these pathways, as has been seen for butein, which inhibited the expression of adhesion molecules via JNK inhibition, as well as by inhibiting I $\kappa$ B degradation (Kojima et al., 2014), further suggesting that flavonoids may act on signal transduction kinases dependent and independent of NF $\kappa$ B. These studies together suggest that flavonoid metabolites may act in multiple simultaneous pathways which may ultimately reduce the expression of pro-inflammatory proteins which drive the pathogenesis of atherosclerosis. This therefore warrants the exploration of multiple mechanisms of action, rather than focusing on NF $\kappa$ B in isolation.

## 1.4. Hypotheses, Rationale, & Aims

**Rationale for study design.** The lack of dietary relevance of contemporary cell culture studies in the field of nutrition is apparent, given the use of precursor structures at supraphysiological concentrations, which may explain why the underlying mechanisms of action of many phytochemicals (such as flavonoids) are still unknown (Kay, 2010).

**Rationale for culture models.** The modulation of acute vascular responses, such as flow-mediated dilation, post-consumption of flavonoids have been shown to correlate with modulations in flavonoid metabolite profiles (Rodriguez-Mateos et al., 2014a, Schar et al., 2015), while anti-inflammatory effects are observed following more chronic intervention (Zhu et al., 2013).

**Primary Hypothesis.** It is therefore hypothesised that flavonoid metabolite profiles are associated with specific mechanisms affecting differential physiological responses as they are systematically metabolised and eliminated from the body.

### **Thesis aims.**

1. Determine whether metabolism of flavonoids affected their bioactivity on vascular (Chapters 3 & 4) and inflammatory (Chapter 5) biomarkers of endothelial dysfunction.
2. Determine potential additive or synergistic activity of flavonoids and their metabolites in combination (Chapters 3-6).
3. Determine the effects of concentration on bioactivity (Chapters 3, 5, & 6).
4. Determine potential mechanisms of action (Chapters 3, 5, & 6).
5. Determine the structure-activity relationship between metabolite treatments (Chapter 5).

### **Aim-specific rationales.**

#### **1) Flavonoids and their phenolic metabolites have differential bioactivities on vascular and inflammatory biomarkers of endothelial dysfunction.**

Flavonoids undergo extensive metabolism by the activities of colonic bacteria and phase II metabolism. The resultant structures are diverse in their structural nature and, for the purpose of this investigation, focus was given to phenolic B-ring metabolites that differ

by the 3' and 4' configuration patterns. 6 flavonoids, 14 conjugated and unconjugated phenolic metabolites, and 25 combinations thereof, were screened across 4 biomarkers, in biological triplicate, totalling 408 experiments, each in technical duplicate. Biomarkers investigated were eNOS and HO-1 (Chapters 3 & 4) in vascular cells and sVCAM-1 in TNF- $\alpha$  stimulated endothelial cells (Chapter 5). Active treatments from these screens were utilised in further experiments, which include mRNA and mechanistic studies (Chapters 3 & 5).

**2) Flavonoids and their phenolic metabolites have additive or synergistic bioactivities in combination.**

Flavonoids and their metabolites do not circulate in isolation following ingestion, but exist as complex mixtures of metabolites at various concentrations (Czank et al., 2013, Pereira-Caro et al., 2014, Serra et al., 2012), thus it is important that this is reflected in the design of cell culture experiments exploring the bioactivities of dietary components (Kerimi and Williamson, 2016). Few studies have explored the effects of flavonoids in combination, despite some indication of differential activities when in combination relative to isolation (Koga and Meydani, 2001, Harasstani et al., 2010). Mixtures of equal-molar concentrations of structurally similar compounds were screened for their effect on HO-1 (Chapter 3 & 4) and sVCAM-1 (Chapter 5). It was hypothesised that this method of screening would provide better understanding of structure-activity relationships, and which may help elucidate potential additive effects in future studies. Further investigations were then conducted in the inflammatory model utilising unique human peak plasma compositions of metabolites (Chapter 6) identified in a <sup>13</sup>C-labelled cyanidin-3-glucoside conducted by our group previously.

**3) Flavonoids and their phenolic metabolites have differential bioactivities at physiologically achievable concentrations relative to supraphysiological concentrations.**

The effects of flavonoids on biomarkers of endothelial dysfunction are not necessarily amplified by increased concentration, making it feasible that flavonoids and their metabolites may be more active at the lowest concentrations, as seen by others in our group (di Gesso et al., 2015). For this reason, active treatments from each screen (HO-1 and sVCAM-1) were further explored for their effect on increasing concentrations on HO-1 (Chapter 3) and sVCAM-1 (Chapter 5).

**4) Flavonoid phenolic metabolites are active in transcription factor and signalling kinase cascade pathways.**

Flavonoids and their metabolites regulate the activity of a number of vascular and inflammatory pathways. The present investigation focused on the effects of active treatments from each screen on basal Nrf2 transcription factor expression, Akt1, and ERK1/2 phosphorylation (Chapter 3). For active treatments from the sVCAM-1 screen (Chapter 5), their effect on TNF- $\alpha$  stimulated NF $\kappa$ B (phosphorylated p65) expression, and phosphorylation of TNF- $\alpha$  stimulated Akt1, ERK1/2, p38, and JNK was also investigated (Chapter 5 & 6).

**5) Structure-activity relationships can be determined between structurally similar flavonoids and metabolites.**

Investigations of structure-activity relationships (SAR) are important to improving our understanding of how metabolism alters phytochemical activity. As previous studies have reported the SAR of flavonoids and their metabolites (Lotito and Frei, 2006, Chen et al., 2004a, Krga et al., 2016, di Gesso et al., 2015), we aimed to draw conclusions based on relationships between conjugated and unconjugated phenolic metabolites in vascular cells (Chapter 5).

## Chapter 2. Methods & Materials

### 2.1. General Materials and Equipment

T75, 6-well, 24-well, and 96-well cell culture plates were purchased from Greiner Bio-one (Stonehouse, UK). Nalgene General Long-Term Storage Cryogenic Tubes (1.5 mL) and Nunclon 12-well plates were purchased from Fisher Scientific (Loughborough, UK). Human plasma-derived fibronectin (lyophilized powder, BioReagent) and Trypan Blue solution (0.4%, liquid, sterile-filtered) were purchased from Sigma Aldrich (Dorset, UK).

### 2.2. General Reagents and Buffers

**Water.** All water utilised was of Milli-Q grade ( $18.2 \text{ M}\Omega \text{ cm}^{-1}$ ), with the exception of that used for RNA extraction, which was diethylpyrocarbonate (DEPC) treated (RNase-free) water purchased from Fisher Scientific (Loughborough, UK). Water and buffers used for cell culture were sterilised by autoclaving in-house.

**Phosphate Buffer Solution.** For Western blotting experiments, Phosphate Buffer Solution (PBS) tablets were purchased from Thermofisher Scientific (Loughborough, UK; 1 x solution, pH 7.4 with no correction). For ELISA kits, PBS from tablets was not utilised following manufacturer recommendation that this may affect assay sensitivity (R&D Systems), instead, a solution of 137 mM NaCl, 2.7 mM KCl, 10 mM  $\text{Na}_2\text{HPO}_4 \cdot 2 \text{H}_2\text{O}$  and  $\text{KH}_2\text{PO}_4$  (pH corrected to 7.4) was prepared using in-house reagents.

**Cell lysis buffers.** For protein samples for Western blotting, NP-40 lysis buffer (containing 1 % (octylphenoxy)polyethoxyethanol, 150 mM NaCl, 20 mM Tris and 10 % glycerol (pH 8.0)) was prepared using in-house reagents and supplemented with Complete Protease Inhibitor Cocktail (Roche Applied Bioscience; Burgess Hill, UK; 1 tablet/10 mL) and phosphatase inhibitor (in 100 % DMSO solution; Sigma Aldrich; 0.1 % final concentration). For preparation of protein samples for eNOS and HO-1 ELISAs, Sample Buffer #1 (R&D Systems, Abingdon; containing 1 mM EDTA, 0.5 % Triton X-100 in PBS) was used. For preparation of protein samples for rat Hmox-1, an Extraction Reagent 2 (lysis buffer) was provided in the Hmox-1 ELISA kit purchased from Enzo LifeSciences (Exeter, UK).

## 2.3. Treatment Solutions

### a) Materials

**Flavonoids and phenolic metabolites.** Conjugated metabolites (protocatechuic acid-3-glucuronide (PCA3G), protocatechuic acid-4-glucuronide (PCA4G), protocatechuic acid-3-sulfate (PCA3S), protocatechuic acid-4-sulfate (PCA4S), vanillic acid-4-glucuronide (VA4G), vanillic acid-4-sulfate (VA4S), isovanillic acid-3-glucuronide (IVA3G), isovanillic acid-3-sulfate (IVA3S), benzoic acid-4-glucuronide (BA4G), and benzoic acid-4-sulfate (BA4S)) were synthesised at the University of St. Andrews, UK (Zhang et al., 2012). All flavonoids and unconjugated phenolic acids were obtained from Sigma Aldrich (Dorset, UK), with the exception of cyanidin-3-glucoside and peonidin-3-glucoside (Extrasynthase, France).

**Cell culture assay treatments.** Human tumour necrosis factor- $\alpha$  (TNF- $\alpha$ ; recombinant, expressed in *E.Coli*), (E)-3-(4-t-Butylphenylsulfonyl)-2-propenenitrile (BAY 11-7085; NF $\kappa$ B/I $\kappa$ B inhibitor), PD98059 (ERK1/2 inhibitor), and dimethyl sulfoxide (DMSO; Hybri max, sterile filtered, bioreagent (99.7%)) were purchased from Sigma Aldrich (Dorset, UK). InSolution™ LY294002 (Akt/PI3K inhibitor) was purchased from Millipore (Watford, UK).

### b) Preparation of treatment solutions

**Individual treatments.** Stock solutions of all compounds were prepared in 100 % DMSO at 200 mM and stored at -80 °C, with the exception of cyanidin-3-glucoside and peonidin-3-glucoside, which were stored at 40 mM, and sulfate- conjugated phenolic acids, which were stored at 25 mM in 50 % DMSO (50 % PBS) to maintain stability whilst reducing final DMSO concentrations in working solutions. Working solutions of all treatments were added to supplemented media to the appropriate concentrations (0.01  $\mu$ M, 0.1  $\mu$ M, 1  $\mu$ M, 10  $\mu$ M, 50  $\mu$ M, or 100  $\mu$ M) immediately prior to treatment.

**Combination treatments.** Treatments containing mixtures of compounds consisted of equimolar concentrations of the constituent treatment compounds to a cumulative concentration of 1  $\mu$ M or 10  $\mu$ M, for example, a combination comprising of four constituents would require 0.25  $\mu$ M of each to equate to a cumulative concentration of 1  $\mu$ M or 2.5  $\mu$ M of each to equate to 10  $\mu$ M.

## 2.4. Cell Culture Techniques

### 2.4.1. General Cell Culture Protocols

**Culture plate coating.** Cell culture plates were washed once with PBS prior to the addition of 5 µg/mL fibronectin coating solution (**Table 2.1**) and incubated at room temperature for 1 h. Fibronectin solution was then removed and plates were washed twice with sterile PBS. Remaining PBS was aspirated and plates were incubated at 37°C for >2 h, or until dry. Plates were then stored at 4°C for <1 month, if not used immediately.

**Table 2.1. Fibronectin coating solution for cell culture plates**

Culture plate	Surface Area (cm <sup>2</sup> )	Volume of solution (µL)	Fibronectin/cm <sup>2</sup>
96 well	0.3	25	0.41*
24 well	2	100	0.25
12 well	4	200	0.25
6 well	10	500	0.25
T75	75	4000	0.26

\*Higher volume of coating solution utilised due to relatively large meniscus effect

**Thawing cells.** All cells were purchased frozen in 10 % DMSO (90 % media) in cryogenic tubes in a liquid nitrogen storage container and transported on dry ice when required. Vials were thawed briefly in a water bath at 37°C and cells transferred into 20-25 mL supplemented cell culture medium in a pre-warmed (37°C), fibronectin-coated, T75 cell culture flask. Cells were examined in the first instance under an inverted phase contrast microscope for evidence of contaminants or artefacts, before being incubated at 37°C, 5 % CO<sub>2</sub>, in a humidified atmosphere. Supplemented media was replenished <24 h following thawing to remove remaining DMSO from solution.

**Cell counting.** Cells were counted using a haemocytometer. Monolayers were detached by use of either Trypsin Passage Pack (HUVEC and RASMC) or DetachKit (HCAEC). Briefly, cell culture media was removed and cells washed with Hank's Balanced Salt Solution (HBSS). Trypsin was added to the appropriate volume and plates were incubated at room temperature for <5 min. Detachment was confirmed under a light microscope. An equal volume of Trypsin Neutralising Solution (TNS; containing phosphate and HEPES-buffered saline solution and 10 % foetal bovine serum (FBS)) was then added and cell solutions transferred to a 15 mL falcon tube and mixed by inversion. 10 µL of cell solution in media was then removed and mixed with 10 µL of trypan blue and loaded onto a haemocytometer

slide. Cell viability was determined by visual inspection under an inverted phase contrast microscope at x20 magnification. The number of cells in four 1 mm x 1 mm grids were totalled and a mean was established. This value was then doubled to account for the 1:1 trypan blue dilution. The number of cells/mL was determined using the following equation:

$$\text{Cells/ml of suspension} = \text{Number of cells counted (dilution corrected)} \times 10^4$$

#### **2.4.2. Human umbilical vein endothelial cells**

##### **a) Materials**

Early passage human umbilical vein endothelial cells (HUVECs) (cryopreserved, pooled donors), large vessel endothelial growth medium (containing 2 % FBS, human epidermal growth factor, human fibroblast growth factor, 25 µg/mL gentamycin, 50 ng/mL amphotericin, hydrocortisone and heparin) and Trypsin Passage Packs (containing 0.025 % trypsin and 0.01 % EDTA, TNS, and HBSS solution) were purchased from Caltag Medsystems (Buckingham, UK).

##### **b) Methods**

Cells were routinely cultured in fibronectin-coated T75 flasks, using supplemented large vessel endothelial cell growth medium at 37°C and 5 % CO<sub>2</sub>. HUVECs were sub-cultured using a Trypsin Passage Pack according to manufacturer's instructions, as described in '2.4.1 Cell Counting' and were used at passage 3 or 4.

#### **2.4.3. Rat aortic smooth muscle cells**

##### **a) Materials**

Cryopreserved, second passage, pooled Clonetics rat aortic smooth muscle cells (RASMCs) from adult Sprague Dawley rats were purchased from Lonza Biologics (Slough, UK). Dulbecco's modified Eagle's medium: F12 (DMEM), gentamycin/amphotericin (GA-1000), FBS, Trypsin Passage Pack (containing 0.025 % trypsin and 0.01 % EDTA) were purchased from Caltag Medsystems (Buckingham, UK). Final growth media in DMEM contained 0.1 % gentamycin/amphotericin and 20 % FBS.

##### **b) Methods**

Cells were routinely cultured in fibronectin coated T75 flasks, using Dulbecco's modified Eagle's medium: F12 containing 0.1 % antibiotics (GA-1000) and 20 % FBS, at 37°C and 5 % CO<sub>2</sub>. RASMC were sub-cultured using Trypsin Passage Pack according to manufacturer's

instructions, as described in '2.4.1 Cell Counting', and were starved in serum-free DMEM for 24 h prior to experiments. Cells were starved due to a high volume of serum (20 %), which favours the growth of RASMC, but which is believed to negatively affect assay outcomes (Boulton et al., 1998, Steffen et al., 2008), thus a serum-free assay was selected, as also described by others (Kim et al., 2009). Cells were used between passages 3 and 6.

#### **2.4.4. Human coronary artery endothelial cells**

##### **a) Materials**

Cryopreserved, second passage, single donor human coronary artery endothelial cells (HCAECs), endothelial cell medium MV (containing 5 % v/v foetal calf serum, endothelial cell growth supplement, recombinant human epidermal growth factor, heparin, and hydrocortisone) and Detach Kit (containing 0.04 % trypsin and 0.03 % EDTA) were purchased from PromoCell GmbH (Heidelberg, Germany).

##### **b) Methods**

Cells were routinely cultured in fibronectin coated T75 flasks, using endothelial cell medium MV at 37°C and 5 % CO<sub>2</sub>. HCAEC were sub-cultured using a Detach Kit, according to manufacturer's instructions, as described in '2.4.1 Cell Counting'. Cells were used between passages 3 and 6.

### **2.5. Biochemical Techniques**

#### **2.5.1. WST-1 cell viability assay**

##### **a) Materials**

Cell proliferation reagent WST-1 [(4-[3-(4-Iodophenyl)-2-(4-nitrophenyl)-2H-5-tetrazolio]-1,3-benzene disulphonate)] was purchased from Roche Applied Science (Burgess Hill, UK). Absorbance values were recorded using an OMEGA Plate Reader from BMG LABTECH (Bucks, UK).

##### **b) Methods**

Cell viability was measured using the WST-1 assay according to conditions optimised previously by our lab group (M.Edwards, PhD Thesis, 2013). Specific assay conditions are given in respective chapters. Cells were seeded in triplicate into fibronectin coated 96-well plates and incubated for 24 h at 37°C, 5 % CO<sub>2</sub>, in a humidified atmosphere. Treatments were added to confluent cells at the maximum concentration utilised in subsequent experiments. Controls included a blank (media only) as a negative control (no effect on cell proliferation)

and were treated with PBS only as a positive control (inhibitor of cell proliferation). Following 24 h treatment, 10  $\mu$ L WST-1 Cell Proliferation Reagent was added to each well and incubated as before for 4 h, and absorbance was measured at 450 nm using a BMG plate reader.

### **2.5.2. Enzyme-linked immunosorbent assay**

#### **a) Materials**

DuoSet human VCAM-1 ELISA kit, DuoSet human IL-6 ELISA kit, and DuoSet human HO-1 were purchased from R&D systems (Abingdon, UK). Additional reagents: optical ELISA plates, ELISA plate sealers, Reagent Diluent 2 (blocking buffer; containing 1 % BSA, 0.05 %  $\text{NaN}_3$  in PBS), Streptavidin-horseradish peroxidase (HRP) solution (1:1), Substrate Solution kit (containing Colour Reagent A ( $\text{H}_2\text{O}_2$ ) and Colour Reagent B (Tetramethylbenzidine)) were purchased from R&D systems (Abingdon, UK). A stop solution (containing 2N  $\text{H}_2\text{SO}_4$ ) was made using in-house reagents. Rat Hmox-1 ELISA Kits (containing a microtiter plate, 5X Extraction reagent 2, Sample diluent, Wash buffer concentrate, Antibody, Conjugate, TMB Substrate, and Stop solution 2) were purchased from Enzo Lifesciences (Exeter, UK). Absorbance values for all ELISA plates were recorded using an OMEGA plate reader from BMG LABTECH (Bucks, UK).

#### **b) Methods**

**Human eNOS.** Human eNOS protein levels were determined using an eNOS Quantikine Kit (R&D Systems; Abingdon, UK) according to manufacturer's instructions. Briefly, 100  $\mu$ L Assay Diluent RDW1 was added to each well, followed by the addition of 100  $\mu$ L samples or standards in duplicate. Plates were sealed using ELISA plate sealers and incubated for 2 h with shaking. Samples were removed and plates were washed 6 times with 1x Wash Buffer (containing buffer surfactant with preservatives). 200  $\mu$ L of Enzyme Conjugate was then added to each well. Plates were sealed and incubated for 2 h with shaking. The wash step was repeated prior to the addition of 200  $\mu$ L of Substrate Solution to each strip at 10 sec intervals. After 15 min, 50  $\mu$ L Stop Solution was added to each strip at 10 sec intervals as before. Plates were placed briefly on plate shaker to ensure thorough mixing, and read immediately at 450 nm (corrected for 570 nm) using an optical BMG microplate reader.

**Human HO-1.** Human HO-1 protein levels in recovered cell culture supernatants were assayed using a Human HO-1 DuoSet ELISA kit (R&D Systems; Abingdon, UK), according to the manufacturer's instructions. Briefly, 96-well optical ELISA plates were incubated with 100  $\mu$ L Capture Antibody Solution (containing 8.0  $\mu$ g/mL rat anti-human HO-1 antibody in

PBS) overnight at room temperature. Solutions were removed and plates were washed 6 times with 0.05 % Tween 20 in PBS. Reagent Diluent 2 (1x) was added to each well and plates were incubated for 1 h at room temperature. Plates were washed prior to the addition of 100 µL samples or standards in duplicate and incubated for 1 h at room temperature with shaking. The previous wash step was repeated prior to addition of a Detection Antibody Solution (containing 0.2 µg/mL goat anti-human HO-1 antibody in Reagent Diluent 2 (1x)) for 2 h at room temperature with shaking. The wash step was repeated prior to the addition of 100 µL Streptavidin-HRP solution for 20 min. Following a final wash step, 100 µL Colour Substrate Solution was added to each strip at 10 sec intervals. After 20 min, 50 µL of Stop Solution was added to each strip at 10 sec intervals as before. Plates were placed briefly on plate shaker to ensure thorough mixing, and read immediately at 450 nm (corrected for 570 nm) using an optical BMG microplate reader.

**Rat Hmox-1.** Hmox-1 protein expression was determined by rat HO-1 ELISA according to the manufacturer's instructions. Briefly, lysates were prepared using Extraction Buffer and dilutions were made in Sample Buffer. 100 µL of prepared samples or standards were loaded to anti-rat HO-1 Immunoassay plates in duplicate. Plates were sealed using ELISA plate sealers and incubated for 1 h with shaking. Samples were removed and plates were washed 4 times with 1x Wash Buffer (containing buffer surfactant with preservatives). 100 µL of rat HO-1 antibody (containing rabbit anti-rat HO-1 antibody). 200 µL of rat HO-1 Conjugate (containing HRP conjugated rabbit IgG) was then added. Plates were sealed and incubated for 30 min with shaking as before. The wash step was repeated prior to the addition of 100 µL of TMB Substrate to each strip at 10 sec intervals. After 15 min, 100 µL Stop Solution 2 was added to each strip at 10 sec intervals as before. Plates were placed briefly on plate shaker to ensure thorough mixing, and read immediately at 450 nm using an optical BMG microplate reader

**sVCAM-1 and sIL-6.** Human sVCAM-1 and sIL-6 protein levels in recovered cell culture supernatants were assayed using a Human VCAM-1/CD106 DuoSet ELISA kit or Human IL-6 ELISA kit (R&D Systems; Abingdon, UK), according to the manufacturer's instructions. Briefly, 96-well optical ELISA plates were incubated with 100 µL Capture Antibody Solution (containing mouse anti-human VCAM-1 or mouse anti-human IL-6 antibody in PBS) overnight at room temperature. Solutions were removed and plates were washed 6 times with 0.05 % Tween 20 in PBS. Reagent Diluent 2 (1x) was added to each well and plates were incubated for 1 h at room temperature. Supernatants were centrifuged at 2000 x g for 5 minutes and diluted 1:5 in Reagent Diluent 2 (R&D Systems; Abingdon, UK), except for basal

and negative controls, which were not diluted (due to basal protein expression levels near the lower detection limit of the standard curve). The wash step was repeated prior to the addition of 100  $\mu$ L samples or standards and incubated for 1 h at room temperature with shaking. The wash step was repeated prior to the addition of a Detection Antibody Solution (containing biotinylated sheep anti-human VCAM-1 or biotinylated goat anti-IL-6 antibody in Reagent Diluent 2 (1x)) for 2 h at room temperature with shaking. Plates were washed prior to the addition of 100  $\mu$ L Streptavidin-HRP solution for 20 min. Following a final wash step, 100  $\mu$ L of Colour Substrate Solution was added at 10 sec intervals. After 20 min, 50  $\mu$ L of Stop Solution was added to each strip at 10 sec intervals as before. Plates were placed briefly on plate shaker to ensure thorough mixing, and read immediately at 450 nm (corrected for 570 nm) using an optical BMG microplate reader.

### 2.5.3. Real Time-qPCR

#### a) Materials

TRIzol reagent, SuperScript II Reverse Transcriptase (with 5x first strand buffer and 100 mM dithiothreitol (DTT)), and MicroAmp optical microplates were obtained from Life Technologies (Paisley, UK). Chloroform and propan-2-ol were purchased from Thermofisher Scientific (Loughborough, UK) and 200 proof ethanol (absolute; for molecular biology) was purchased from Sigma Aldrich (Dorset, UK). RiboLock RNase inhibitor, DNase I (with 10x reaction buffer with  $MgCl_2$ , and 50 mM EDTA), dNTP PCR mix (10 mM), and oligo (dT) primers (100  $\mu$ M) were purchased from Thermofisher Scientific (Loughborough, UK). PrecisionPLUS 2x qPCR Master Mix with SYBR Green and custom primers for all target genes (human HO-1, VCAM-1, IL-6 and rat HMOX-1) were purchased from Primer Design (Southampton, UK; **Table 2.2**), as were human and rat geNORM housekeeping gene primers (**Table 2.3**). The NanoDrop2000 spectrophotometer and ABI7500 RT-qPCR system were purchased from Thermofisher Scientific (Loughborough, UK).

**Table 2.2. Primers of target genes for RT-qPCR**

Gene	Species	Sense primer (5'-3')	Antisense primer (3'-5')
HO1	Human	ATGGCCTCCCTGTACCACATC	TGTTGCGCTCAATCTCCTCTCT
Hmox1	Rat	TTCAGAAGGGTCAGGTGTCC	GGAAGTAGAGTGGGGCATAGA
VCAM1	Human	CAGGCTAAGTTACATATTGATGACAT	GAGGAAGGGCTGACCAAGAC
IL6	Human	GCAGAAAACAACCTGAACCTT	ACCTCAAACCTCCAAAAGACCA

**Table 2.3. Reference genes from geNORM kit description**

Gene name	Host	Description
PPIA	Human	Peptidylprolyl isomerase A (cyclophilin A)
PRDM4	Human	PR domain containing 4
TYW1	Human	tRNA-yW synthesizing protein-1
UBE2D2	Human	Ubiquitin-conjugating enzyme E2D2
UBE4A	Human	Ubiquitination factor E4A
VIPAS39	Human	VPS33B interacting protein, apical-basolateral polarity regulator, spe-39
18S	Rat	18S Ribosomal RNA
Gapdh	Rat	Glyceraldehyde-3-phosphate dehydrogenase
Nupl2	Rat	Nucleoporin-like protein 2
Stau1	Rat	Staufen double-stranded RNA binding protein 1
Tomm22	Rat	Translocase of outer mitochondrial membrane 22
Zgpat	Rat	Zinc Finger, CCCH-Type With G Patch Domain

## b) Methods

**RNA extraction & quantification.** Total RNA was extracted from cells by phenol-chloroform extraction using TRIzol reagent according to the manufacturer's protocol with minor adjustments. Briefly, following media removal and cell wash steps, 1 mL of TRIzol reagent was added to each well, mixed repeatedly by pipetting to homogenise the cells, and the plate was frozen overnight at -80°C. Upon complete thawing, homogenates were transferred to 1.5 mL Eppendorf tubes and 200 µL of chloroform was added. Tubes were shaken vigorously by hand for 15 sec and vortexed for 10 sec, followed by incubation at room temperature (RT) for 10 min. Samples were centrifuged for 20 min at 12,000 x g, 4°C. 400 µL of the uppermost, clear, aqueous layer was transferred to a new tube. 500 µL of propan-2-ol was added and samples were vortexed for 10 sec. Tubes were then incubated at RT for 10 min prior to centrifugation for 15 min at 12,000 x g, 4°C. Supernatants were discarded and 1 mL 70 % ethanol (30 % RNase-free water) was added to each tube. Samples were again centrifuged for 10 min at 12,000 x g, 4°C. All ethanol was removed from the pellet via pipetting and evaporation at RT. Twenty microliters of RNase-free water was added to each sample and mixed by pipette prior to freezing overnight at -80°C. RNA was quantified by use of the NanoDrop2000 spectrophotometer and the quality of samples was determined by its purity ratio ( $A_{260/280}$ ).

**Reverse transcription PCR.** 1 µg of each RNA sample was incubated with DNase I, DNase I buffer, and RiboLock for 30 min at 37°C. Each sample was then incubated with oligo(dT) primers, dNTP PCR mix, and EDTA for 10 min at 65°C, followed by the addition of first strand

buffer, DTT, and RiboLock for 2 min at 42°C. Reverse transcription of RNA to cDNA was performed by the addition of SuperScript® II Reverse Transcriptase and incubated for 50 min at 42°C. The reaction was then stopped by incubation for 15 min at 70°C.

**Real time-qPCR.** Real-time quantitative PCR (RT-qPCR) was carried out using 25 ng of cDNA of each sample, with the addition of target gene primers (Table 2.1) added to PCR Precision master mix with SYBR Green (Primer Design) and nuclease-free water to a final reaction volume of 20 µL. RT-qPCR was carried out using the ABI7500 system, wherein the reaction was activated at 95°C for 10 min prior to 50 cycles of denaturation and data collection (15 sec at 95°C and 1 min at 60°C per cycle, respectively). Recorded  $C_t$  values for target genes were normalised to two geNORM reference/housekeeping genes, selected based on their stability, as established using qPCR data analysis software qbase<sup>PLUS2</sup> (Biogazelle; Zwinjaarde, Belgium).

**geNORM analysis.** Identification of reference genes utilised for normalisation of  $C_t$  data was conducted using a geNormPLUS kit (PrimerDesign; Southampton UK). Primer sets for six stably expressed human and rat reference genes (Table 2.2) were designed, pre-validated and supplied by PrimerDesign. These were used to select optimal reference genes for RASMC, and TNF- $\alpha$  stimulated HCAEC. Reference genes for HUVEC were pre-determined by our group following the same protocol (Amin, PhD thesis, 2014).  $C_t$  values obtained from RT-qPCR were analysed by use of qbasePLUS software (version 2.3; Biogazelle; Zwinjaarde, Belgium) which determined relative gene stability across a number of treated samples, as well as optimal number of reference genes (Hellemans et al., 2007).

**Melt-curve analysis.** All primers were purchased pre-validated for their specificity, though melt curve data ( $T_m$ ) were checked against their expected values to confirm specificity of primer annealing and monitor presence of contaminants, as recommended in the MIQE guidelines (Taylor et al., 2010). Acceptable melt curves displayed a single sharp peak at expected  $T_m$ . A no-reverse-transcription control and a no-template control (no DNA) were also included in every run for each primer set tested to confirm no DNA contamination and to assess primer-dimer formation. Example melt curves for each gene of interest are provided in the Appendix, **Chapter 9.6**).

**Determination of fold change values.** Fold change from specified control was calculated using  $2^{-\Delta\Delta C_t}$  determination, as described by others (Livak and Schmittgen, 2001), where:

$C_t$  = raw amplification data value

$\Delta C_t = C_t[\text{control}] - C_t[\text{treatment}]$

$\Delta\Delta C_t = \Delta C_t[\text{target gene}] - \Delta C_t[\text{reference gene}]$

Fold change from control =  $2^{-\Delta\Delta C_t}$

## 2.5. Western blotting

### A) Materials

Pierce BCA Protein Assay Kit was purchased from Thermofisher Scientific (Loughborough, UK). NuPAGE Tris-Glycine Sodium Dodecyl Sulfate (SDS) and LDS Sample Buffer (2X) was purchased from Life Technologies (Paisley, UK). Tween 20 and Brilliant Blue were purchased from Sigma Aldrich (Dorset, UK). PrecisionPlus Protein Dual Colour Ladder, 10 % Mini-PROTEAN TGX Precast Gels, Trans-Blot SD Semi-Dry Transfer Cell, Mini-PROTEAN Cell, BioRad Tris-SDS (20x) and TGS (20x) were purchased from Bio-Rad Laboratories (Hemel Hempstead, UK). Immobilon-FL polyvinylidene difluoride (PVDF) membrane was purchased from Millipore (Watford, UK). Protein-Free T20 (TBS) blocking buffer was purchased from Thermofisher Scientific (Loughborough, UK). Odyssey Infrared Imaging System and Odyssey Infrared Imaging System Application Software (version 3.0.21) were purchased from Li-Cor Biosciences (Cambridge, UK).

### B) Methods

**Sample preparation.** Protein concentrations of each sample were determined against a standard curve of known albumin concentrations by use of a Pierce BCA Assay Kit, according to the manufacturer's instructions. 25  $\mu\text{g}$  of total protein was used in each experiment. In preparation for gel electrophoresis, lysates were reduced using NuPAGE sample reducing agent (1 M DTT) in NuPAGE LDS sample buffer, vortexed for 5 sec and heated to 95°C for 5-10 minutes, followed by 5 sec vortex and brief centrifugation at 12000 x g prior to gel loading.

**Polyacrylamide gel electrophoresis.** PrecisionPlus Protein Dual Colour standards (containing comparative molecular weight markers 250 kDa-10 kDa) or prepared protein samples were loaded onto 10 % SDS-PAGE gels and run using a BioRad Mini-PROTEAN Cell at 25 mA (one gel) or 35 mA (two gels) until completion.

**Western transfer.** Filter papers and membranes were equilibrated for at least 15 min in 20 % methanol (80 % 1x Tris-glycine buffer). Immobilon-FL PVDF membranes were activated by

incubation with 100 % methanol for 60 sec and equilibrated in 20 % methanol (80 % 1x Tris-glycine buffer) for at least 15 min prior to transfer. Proteins were then transferred onto methanol-activated membranes at 25 V for 60 min using a BioRad Trans-Blot SD Semi-Dry Transfer Cell.

**Gel staining.** Equal protein transfers were confirmed visually using Brilliant Blue staining of the gels, as described by others (Dong et al., 2011). Briefly, following transfer, gels were placed into 0.25 % Brilliant Blue stain (10 % acetic acid, 20 % methanol, 70 % water) for 1 h at room temperature with gentle rocking. Staining solution was collected for re-use and gels were washed several times in distilled water and imaged at 700 nm using Odyssey Infrared Imaging System (Li-Cor (version 3.0.21)). Gel staining solutions were recycled <3 times.

**Western blot.** Membranes were blocked using T20 blocking buffer for 1 h at room temperature, and incubated overnight at 4°C in the appropriate concentration of primary and loading control antibodies (**Table 2.4**). Primary antibody solutions were collected and replaced with infrared (IR)-labelled secondary antibodies in PBS (0.1 % Tween; 10 % T20 blocking buffer) and incubated at room temperature for 1 h away from light. Antibody solutions were again collected and membranes were washed with 0.1 % Tween in PBS for 3 x 10 min. After the final wash step, membranes were briefly washed 2 x with PBS (no Tween) and imaged and quantified by densitometry at 700 nm and 800 nm using Odyssey Infrared Imaging System and Odyssey Infrared Imaging System Application Software, respectively (Li-Cor (version 3.0.21)).

**Table 2.4. Primary and secondary antibodies used in Western blotting assays**

Target	Host	Supplier	Product code	Dilution
p-p65(Ser536)	Rabbit	Abcam	ab28856	1:2000
pAkt1 (Ser473)	Rabbit	Abcam	ab81283	1:5000
Akt1	Rabbit	Abcam	ab32505	1:5000
pErk1/2*	Rabbit	Abcam	ab76165	1:200
ERK1/2	Rabbit	Abcam	ab17942	1:2000
p-SAPK/JNK (Thr183/Tyr185)	Mouse	CST <sup>1</sup>	CS 9255	1:2000
SAPK/JNK	Rabbit	CST <sup>1</sup>	CS 9258	1:2000
p-p38 MAPK (Thr180/Tyr182)	Mouse	CST <sup>1</sup>	CS 9216	1:2000
p38 MAPK	Rabbit	CST <sup>1</sup>	CS 9212	1:2000
Nrf2	Rabbit	Abcam	ab62352	1:1000
GAPDH	Chicken	Millipore	ab2302	1:15000
Chicken IgG (IRDye® 680LT)	Donkey	Li-Cor	926-68075	1:15000
Rabbit IgG (IRDye® 800CW)	Goat	Li-Cor	926-32211	1:15000
Mouse IgG (IRDye®800CW)	Goat	Li-Cor	926-32210	1:15000

\*pErk1(pT202/pY204)+ pErk2(pT185/pY187) <sup>1</sup>Cell Signalling Technologies (Hitchin, UK).

## 2.6. Statistical analysis

Specific data analyses are described in each respective chapter. In general, effects between treatment and control in cell viability assays, and in assays where controls were not included in multiple comparisons (such as unstimulated and negative controls in TNF- $\alpha$  stimulated VCAM-1 assays), were determined by use of Student's t-test using Microsoft Excel (version 2013). Treatment effects (and multiple comparisons) were established by one-way analysis of variance (ANOVA) followed by post-hoc test of least square difference (LSD) using SPSS for Windows (version 22.0; IBM, New York, USA). Data were considered significant where  $p \leq 0.05$  and, for the purpose of screening, statistical trends were identified where  $p \leq 0.15$ . Data are presented graphically or in tabular form as percentage or fold change of the positive control  $\pm$  SD, as specified.

## **Chapter 3. Effect of flavonoids and their metabolites on the basal expression of vascular biomarkers in endothelial cells.**

### **3.1. Introduction**

Epidemiological studies have demonstrated positive associations between diets high in flavonoid-rich foods and the reduced risk of cardiovascular disease (CVD; Wang et al., 2014, Rodriguez-Mateos et al., 2014b), though the underlying mechanisms of action of flavonoids have been elusive. Human feeding studies have observed that certain flavonoids have beneficial effects on vascular function, such as blood flow and flow-mediated vasodilation (FMD; Grassi et al., 2015), both of which are regulated by endothelium-derived nitric oxide (NO) levels (Green et al., 2014). NO homeostasis has therefore been a target of interest for previous flavonoid *in vitro* studies (Tribolo et al., 2013). The disruption of NO homeostasis is a driving factor in the progression of endothelial dysfunction, which can lead to atherosclerosis (Lusis, 2000, Chapidze et al., 2007).

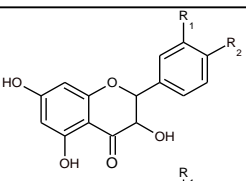
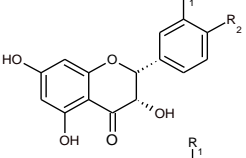
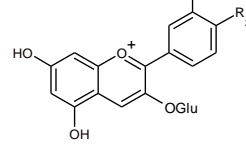
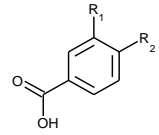
NO homeostasis in endothelial cells is disrupted in response to high levels of reactive oxygen species (ROS), such as superoxide ( $O_2^{\cdot-}$ ). The production of  $O_2^{\cdot-}$  is stimulated by NADPH oxidase (NOX) activity, and it has previously been hypothesised that flavonoids may decrease  $O_2^{\cdot-}$  production by inhibition of NOX (Schewe et al., 2008), thus subsequently increasing NO and justifying the observed improvements in FMD following consumption of flavonoids (Hooper et al., 2012). However, many previous *in vitro* studies attempting to elucidate the mechanisms underlying this activity have utilised supraphysiological concentrations of precursor flavonoids and have not determined the bioactivity of their more bioavailable phenolic degradants (Kay, 2010). Additionally these treatments have been studied in isolation, which does not take into account their potential additive, antagonistic or synergistic effects (Kerimi and Williamson, 2016).

Our group have previously demonstrated that a number of anthocyanin degradants/phenolic acids decreased  $O_2^{\cdot-}$  but did not have detectable effects on NOX activity in endothelial cells (Edwards et al., 2015). Activity was instead suggested to be due to other, indirect proteins involved in the maintenance of vascular homeostasis, such as endothelial nitric oxide synthase (eNOS) and haem oxygenase-1 (HO-1). Certain flavonoids may enhance vascular function through modulating expression levels of eNOS (Woodman and Chan, 2004), which subsequently increases NO. Furthermore, eNOS expression is stabilised in response to cellular bilirubin, derived from haem degradation by HO-1 (Kawamura et al.,

2005). HO-1 expression has been shown to be induced in response to certain polyphenols, such as curcumin and epigallocatechin-gallate (Scapagnini et al., 2011) through activation of the oxidative stress sensor, Nrf2 (Zhang et al., 2008) and associated signalling kinases, Akt1 and ERK1/2 (Niture et al., 2014, Moosavi et al., 2016). The effects of phenolic metabolites of flavonoids on these targets context have yet to be explored.

The present study aimed to establish if physiologically relevant concentrations of phenolic metabolites have differential bioactivities relative to their unmetabolised precursor structures (**Table 3.1**) in the modulation of eNOS and HO-1 protein expression in human umbilical vein endothelial cells (HUVEC). The secondary aim was to establish whether flavonoids and their metabolites act additively when in combination. Finally, we aimed to determine whether the magnitude of response of the most active treatments were in response to increased concentration and whether these affected regulatory signalling pathways, such as Nrf2, Akt1 and ERK1/2.

**Table 3.1. Structures of flavonoids and metabolites included in treatments.**

Name	General structure	Substituents <sup>1</sup>
Naringenin Hesperetin Quercetin		R <sub>1</sub> = H; R <sub>2</sub> = OH R <sub>1</sub> = H; R <sub>2</sub> = OCH <sub>3</sub> R <sub>1</sub> = OH; R <sub>2</sub> = OH
(-)-Epicatechin		R <sub>1</sub> = OH; R <sub>2</sub> = OH
Peonidin-3-glucoside Cyanidin-3-glucoside		R <sub>1</sub> = H; R <sub>2</sub> = OCH <sub>3</sub> R <sub>1</sub> = H; R <sub>2</sub> = OH
4-hydroxybenzoic acid Benzoic acid-4-glucuronide Benzoic acid-4-sulfate Protocatechuic acid Protocatechuic acid-3-glucuronide Protocatechuic acid-4-glucuronide Protocatechuic acid-3-sulfate Protocatechuic acid-4-sulfate Vanillic acid Vanillic acid-4-glucuronide Vanillic acid-4-sulfate Isovanillic acid Isovanillic acid-3-glucuronide Isovanillic acid-3-sulfate		R <sub>1</sub> = H; R <sub>2</sub> = OH R <sub>1</sub> = H; R <sub>2</sub> = Glc R <sub>1</sub> = H; R <sub>2</sub> = Sul R <sub>1</sub> = OH; R <sub>2</sub> = OH R <sub>1</sub> = Glc; R <sub>2</sub> = OH R <sub>1</sub> = OH; R <sub>2</sub> = Glc R <sub>1</sub> = Sul; R <sub>2</sub> = OH R <sub>1</sub> = OH; R <sub>2</sub> = Sul R <sub>1</sub> = OCH <sub>3</sub> ; R <sub>2</sub> = OH; R <sub>1</sub> = OCH <sub>3</sub> ; R <sub>2</sub> = Glc; R <sub>1</sub> = OCH <sub>3</sub> ; R <sub>2</sub> = Sul; R <sub>1</sub> = OH; R <sub>2</sub> = OCH <sub>3</sub> R <sub>1</sub> = Glc; R <sub>2</sub> = OCH <sub>3</sub> R <sub>1</sub> = Sul; R <sub>2</sub> = OCH <sub>3</sub>

Abbreviations: OH, hydroxyl; Glc, oxygen-linked-glucuronide; Glu, glucoside; Sul, sulfate; OCH<sub>3</sub>, oxygen-linked methyl group. Adapted from Warner et al., 2016.

## **3.2. Methods**

Experiment specific details are provided below while comprehensive methodological descriptors are provided in detail in Chapter 2.

### **3.2.1. Treatment solutions**

Stock solutions of flavonoids and metabolites (listed in Table 3.1) were prepared in DMSO and stored as described in Chapter 2. Working solutions of 1 mM of each analyte were made up in supplemented media before being diluted to a final concentration of 0.1  $\mu$ M, 1  $\mu$ M, 10  $\mu$ M, or 50  $\mu$ M, or to equimolar concentrations for combined treatments (for example, in a 10  $\mu$ M mixture consisting of 4 constituents, each would contain 2.5  $\mu$ M of each constituent). Treatment combinations were designed based on their structural similarities and based on activity when screened in isolation. Treatment solutions were prepared in supplemented media and stored at 4°C, with the exception of cyanidin-3-glucoside and peonidin-3-glucoside, which were added immediately prior to the experiments to maintain stability.

### **3.2.2. Cell culture**

Cryogenically stored, pooled donor, human umbilical vein endothelial cells (HUVECs) were cultured and maintained as described in Chapter 2. All cells were incubated for at least 24 hours at 37°C, 5 % CO<sub>2</sub>, in a humidified atmosphere, prior to experiment commencement. HUVECs were used between passages 3 and 4.

### **3.2.3. Cell viability**

HUVEC were seeded at 20,000 cells/well in fibronectin coated 96-well plates and grown to confluence in supplemented media. Cells were treated with 10  $\mu$ M of each treatment, or 0.02 % DMSO (vehicle control) in media. PBS (cells, no media) was used as a positive assay control. The WST-1 assay was carried out as described in Chapter 2.

### **3.2.4. eNOS and HO-1 protein expression**

HUVEC were seeded at 100,000 cells/well in fibronectin coated 12-well plates. Cells were treated with 0.1  $\mu$ M, 1  $\mu$ M, 10  $\mu$ M, or 50  $\mu$ M treatment solution or 0.02 % DMSO (vehicle control) and incubated for 18 h (eNOS) or 16 h (HO-1) at 37°C, 5 % CO<sub>2</sub>, in a humidified atmosphere. Cell culture supernatants were then removed and cells were washed 3 x with PBS on ice. Cell lysates were stored at -80°C until required. Samples underwent a single freeze-thaw cycle, incubated to room temperature, and vortexed for 3 x 5 sec then centrifuged at 2000 x g, 10 min, at 4°C immediately prior to use. Protein expression of eNOS and HO-1 were determined by commercially available enzyme-linked immunosorbent assays (ELISAs), as described in Chapter 2.

### **3.2.5. HO-1 mRNA expression**

HUVEC were seeded at 200,000 cells/well in fibronectin coated 6-well plates. Cells were treated with 10  $\mu$ M treatment solution or 0.02 % DMSO (vehicle control). Cell culture supernatant was removed and cells washed 3 x with PBS on ice. Total RNA was extracted, reverse transcribed, and RT-qPCR was conducted as described in Chapter 2. Reference genes, UBE2D2 and PRDM4, were used to normalise the data, as described in Chapter 2.

### **3.2.6. Total Nrf2 protein expression and signalling kinase Akt1 and ERK1/2 phosphorylation.**

HUVEC were seeded at 200,000 cells/well in fibronectin coated 6-well plates. Cells were treated with inhibitors, LY294002 (Akt1) or PD98059 (ERK1/2), for 1 h prior to treatment with 10  $\mu$ M treatment solutions or 0.02 % DMSO (vehicle control) for 6 h (Nrf2) or 15 min (Akt, pAkt, ERK1/2, pERK1/2). Cells were washed 3 x with PBS on ice and lysed with NP-40 lysis buffer and frozen at -80°C until required. Samples underwent a single freeze-thaw cycle, incubated to room temperature, vortexed for 3 x 5 sec, and centrifuged at 2000 x g, 10 min, at 4°C immediately prior to use. Protein concentrations were determined by BCA assay, and protein separated and probed by SDS-PAGE and Western blotting, as described in Chapter 2. Densitometry values were normalised to GAPDH reference gene. Normalised densitometry values for phosphorylated Akt1 and ERK1/2 were normalised to their total protein Akt1 and ERK1/2.

### **3.2.7. Data analysis**

For cytotoxicity experiments, absorbance values were reported as a mean of three independent replicates and differences from an untreated control were determined by use of Student's t-test using Microsoft Excel (version 2013). eNOS and HO-1 protein (pg/mL) and HO-1 mRNA (fold change) were recorded as the mean of two technical duplicates and reported as a mean of three independent replicates  $\pm$  SD (n=3), relative to an untreated control (no DMSO). Protein expression data determined by Western blotting were reported relative to the vehicle control (DMSO only) where data represent the mean  $\pm$  SD of three independent replicates as above. Treatment effects were determined relative to the vehicle control (DMSO) and established by one-way analysis of variance (ANOVA) with post-hoc least square difference (LSD) using SPSS for Windows (version 22.0). For screening purposes, treatments displaying non-significant values of  $p \leq 0.15$  were taken forward, for validation in subsequent concentration-response analysis.

### 3.2.8. Method optimisation

Method optimisation experiments were conducted to identify a positive control and optimal treatment time for the upregulation of HO-1 expression (Appendix; **Chapter 9.1.1; Figure 3.1**). Endogenous reference genes for normalisation of  $C_t$  data for target genes (UBE2D2 and PRDM4) were selected based on previously established method optimisation by our group (Amin PhD thesis, 2014).

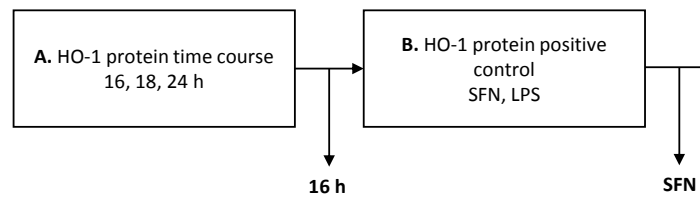


**Figure 3.1. Method optimisation experiments for Chapter 3.** See Appendix 9.1. Abbreviations: HO-1, haem oxygenase-1; LPS, lipopolysaccharide; SFN, sulforaphane. Abbreviations for mRNA reference genes can be found in Chapter 2.5.3.

### 3.3 Results

#### 3.3.1. Effect of treatments on cell viability.

6 flavonoids and 13 phenolic acid metabolites were screened in endothelial cells (HUVEC) for their effect at 10  $\mu$ M for 24 h on cell viability by use of WST-1 (**Table 3.2**). No significant effects ( $p \leq 0.05$ ) on cell viability were observed in either cell type in response to treatments used.

**Table 3.2. Effects on cell viability**

	Absorbance value (% of untreated control)	
	Average $\pm$ SD	p
Vehicle control (VC)	103.21 $\pm$ 4.47	0.67
Hesperetin (HES)	95.33 $\pm$ 5.72	0.57
Peonidin-3-Glucoside (P3G)	108.00 $\pm$ 0.86	0.29
Naringenin (NAR)	86.61 $\pm$ 1.76	0.20
(-)-Epicatechin (EPI)	101.58 $\pm$ 1.70	0.33
Quercetin (QUE)	112.70 $\pm$ 12.08	0.07
Cyanidin-3-Glucoside (C3G)	104.70 $\pm$ 1.34	0.77
4-hydroxybenzoic acid (4HBA)	96.69 $\pm$ 6.24	0.70
Benzoic acid-4- Glc (BA4G)	100.50 $\pm$ 4.47	0.74
Benzoic acid-4-Sul (BA4S)	104.68 $\pm$ 3.74	0.24
Protocatechuic acid (PCA)	93.97 $\pm$ 2.32	0.55
Protocatechuic acid -3-Glc (PCA4G)	102.77 $\pm$ 7.80	0.76
Protocatechuic acid -4- Glc (PCA4S)	101.91 $\pm$ 4.99	0.94
Protocatechuic acid -3-Sul (PCA3S)	99.15 $\pm$ 4.55	0.81
Protocatechuic acid -4-Sul (PCA4S)	103.77 $\pm$ 5.63	0.62
Vanillic acid (VA)	98.44 $\pm$ 4.06	0.85
Isovanillic acid (IVA)	102.32 $\pm$ 9.39	0.91
Vanillic acid-4-Glc (VA4G)	99.85 $\pm$ 3.08	0.80
Isovanillic acid-3-Glc (IVA3G)	102.79 $\pm$ 2.41	0.29
Vanillic acid-4-Sul (VA4S)	96.76 $\pm$ 9.67	0.45

Cell viability was assessed after 4 h incubation with WST-1 reagent and is presented as a percentage of an untreated control. Columns represent the mean of three independent replicates  $\pm$  SD. Treatment effects were determined relative to an untreated control by use of Student's t-test using Microsoft Excel (version 2013). Abbreviations: Glc, glucuronide; Sul, sulfate.

### 3.3.2. Effect of flavonoids and their metabolites on eNOS protein.

6 flavonoids and 13 phenolic metabolites were screened for their effect at 1  $\mu$ M on eNOS protein in HUVEC (**Figure 3.2**). No treatments were significantly different from the vehicle control (VC; 0.02 % DMSO), therefore no treatments were taken forward from this screen for further exploration of combined activity and dose response.

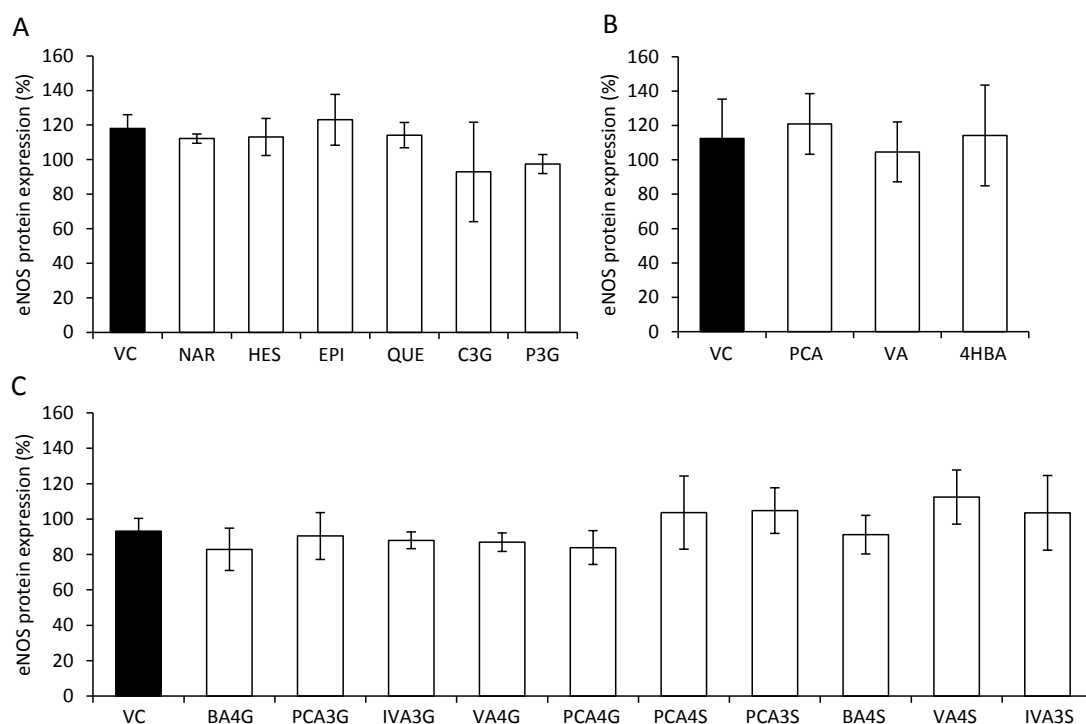


**Figure 3.2. Effect of flavonoids and metabolites on eNOS protein.** HUVEC were treated to a final concentration of 1  $\mu$ M or 0.02 % DMSO (VC) for 18 h. eNOS protein was quantified by ELISA and presented as a percentage of an untreated control. Data represents the average of 3 independent replicates  $\pm$  SD (n=3). Analysis was performed relative to vehicle control by use of one-way ANOVA with post-hoc LSD. Abbreviations: 4HBA, 4-hydroxybenzoic acid; BA4G, benzoic acid-4-glucuronide; BA4S, benzoic acid-4-sulfate; C3G, cyanidin-3-glucoside; EPI, (-)-epicatechin; HES, hesperetin; IVA3G, isovanillic acid-3-glucuronide; IVA3S, isovanillic acid-3-sulfate; NAR, naringenin; P3G, peonidin-3-glucoside; PCA, protocatechuic acid; PCA3G, protocatechuic acid-3-glucuronide; PCA4G, protocatechuic acid-4-glucuronide; PCA3S, protocatechuic acid-3-sulfate; PCA4S, protocatechuic acid-4-sulfate; QUE, quercetin; VA, vanillic acid; VA4G, vanillic acid-4-glucuronide; VA4S, vanillic acid-4-sulfate; VC, vehicle control.

### 3.3.4. Effect of flavonoids and their metabolites on HO-1 protein.

6 flavonoids and 13 phenolic metabolites were screened for their effect at 1  $\mu$ M on HUVEC HO-1 protein expression (**Figure 3.3**). HO-1 protein was significantly upregulated in response to 2 phenolic metabolites, 4HBA ( $121.63 \pm 1.31$ ,  $p \leq 0.001$ ) and PCA4S ( $122.72 \pm 8.73$ ,  $p = 0.05$ ), and there was a trend for an increase of HO-1 in response to quercetin ( $132.24 \pm 30.77$ ,  $p = 0.07$ ).

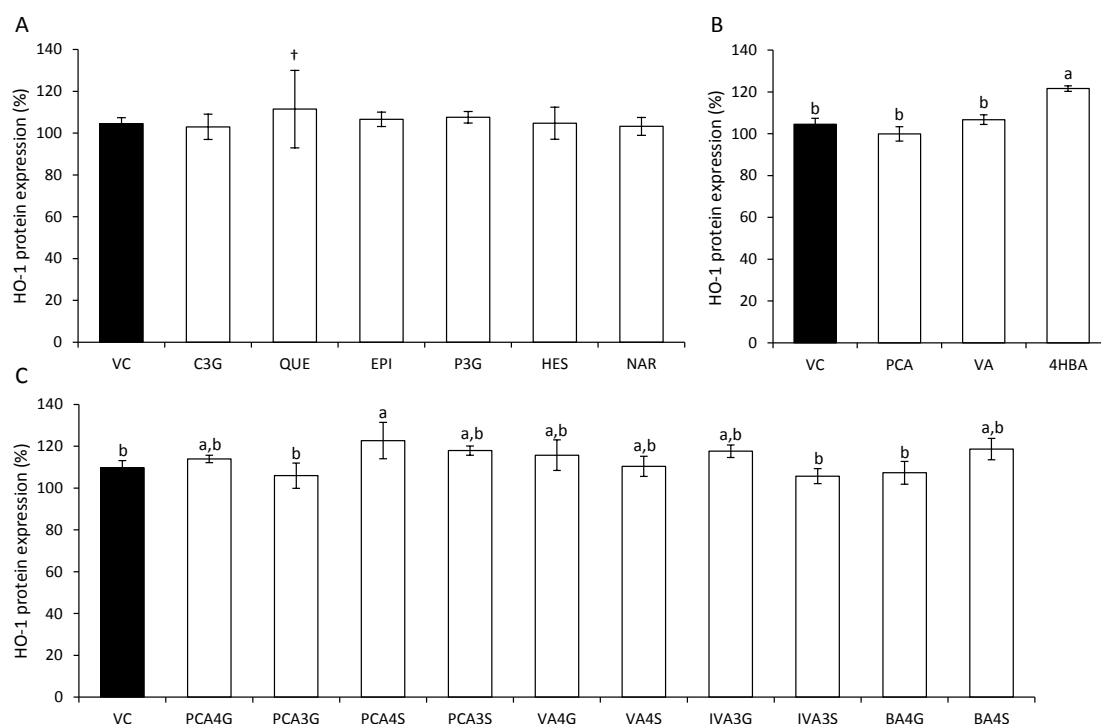


**Figure 3.3. Effect of flavonoids and metabolites on HO-1 protein.** HUVEC were treated to a final concentration of 1  $\mu$ M or 0.02 % DMSO (VC) for 16 h. HO-1 protein was quantified by ELISA and presented as a percentage of an untreated control. Data represents the average of 3 independent replicates  $\pm$  SD (n=3). Labelled means without a common letter differ (one-way ANOVA with post-hoc LSD),  $p \leq 0.05$ ; †  $p \leq 0.15$  to VC. Abbreviations: 4HBA, 4-hydroxybenzoic acid; BA4G, benzoic acid-4-glucuronide; BA4S, benzoic acid-4-sulfate; C3G, cyanidin-3-glucoside; EPI, (-)-epicatechin; HES, hesperetin; IVA3G, isovanillic acid-3-glucuronide; IVA3S, isovanillic acid-3-sulfate; NAR, naringenin; P3G, peonidin-3-glucoside; PCA, protocatechuic acid; PCA3G, protocatechuic acid-3-glucuronide; PCA4G, protocatechuic acid-4-glucuronide; PCA3S, protocatechuic acid-3-sulfate; PCA4S, protocatechuic acid-4-sulfate; QUE, quercetin; VA, vanillic acid; VA4G, vanillic acid-4-glucuronide; VA4S, vanillic acid-4-sulfate; VC, vehicle control.

Selected treatments containing one or more of the active compounds were taken forward to explore concentration responsiveness and additive effects. No combination treatments actively increased HO-1 protein (**Figure 3.4**).

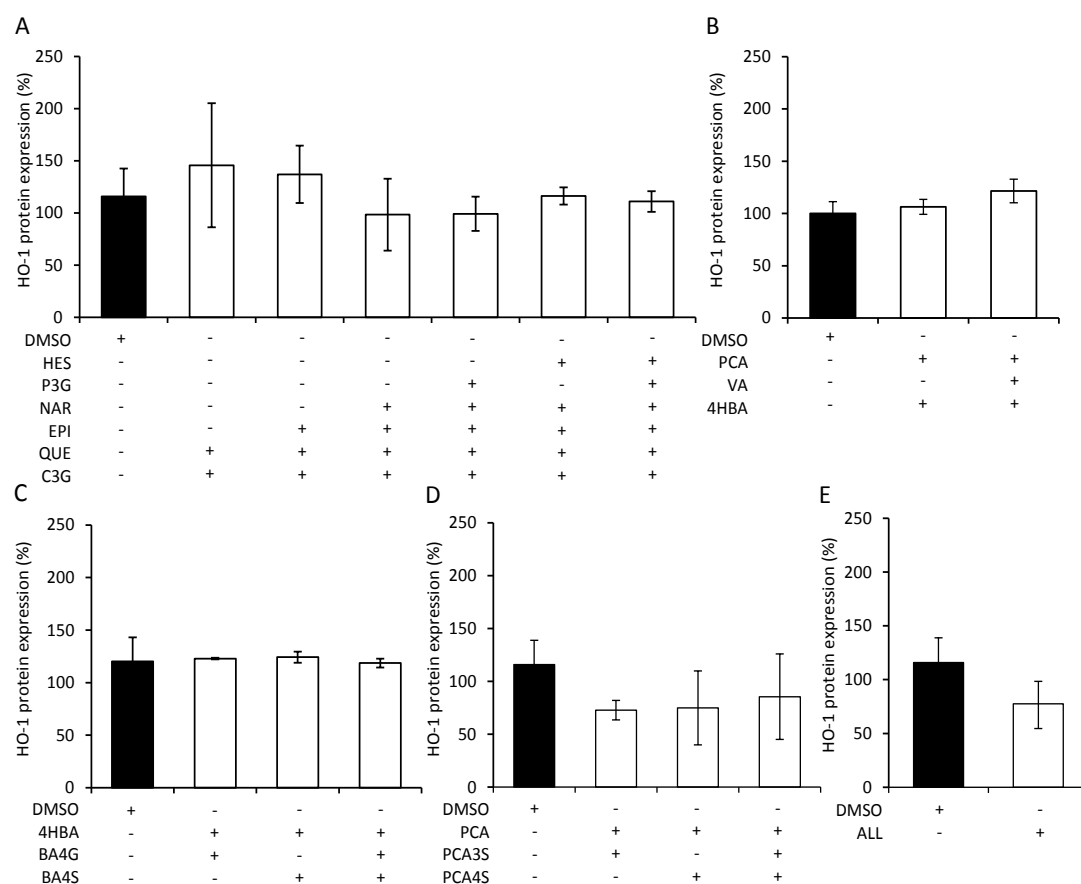


**Figure 3.4. Effect of mixtures of flavonoids and metabolites on HO-1.** HUVEC were treated to a cumulative concentration of 10  $\mu$ M or 0.02 % DMSO (VC) for 16 h. HO-1 protein was quantified by ELISA. Data represents the average of 3 independent replicates  $\pm$  SD (n=3). Treatment effects were determined by one-way ANOVA with post hoc LSD. Abbreviations: 4HBA, 4-hydroxybenzoic acid; BA4G, benzoic acid-4-glucuronide; BA4S, benzoic acid-4-sulfate; C3G, cyanidin-3-glucoside; EPI, (-)-epicatechin; HES, hesperetin; NAR, naringenin; P3G, peonidin-3-glucoside; PCA, protocatechuic acid; PCA3S, protocatechuic acid-3-sulfate; PCA4S, protocatechuic acid-4-sulfate; QUE, quercetin; VA, vanillic acid; VC, vehicle control.

Three analytes, quercetin, 4HBA, and PCA4S, were investigated for the effect of increasing concentration (0.1-50  $\mu\text{M}$ ) on HO-1 protein expression (**Figure 3.5**). HO-1 protein expression was increased by <20% in response to 1  $\mu\text{M}$  of each treatment, though this effect was not amplified by increasing the concentration above 1  $\mu\text{M}$ .

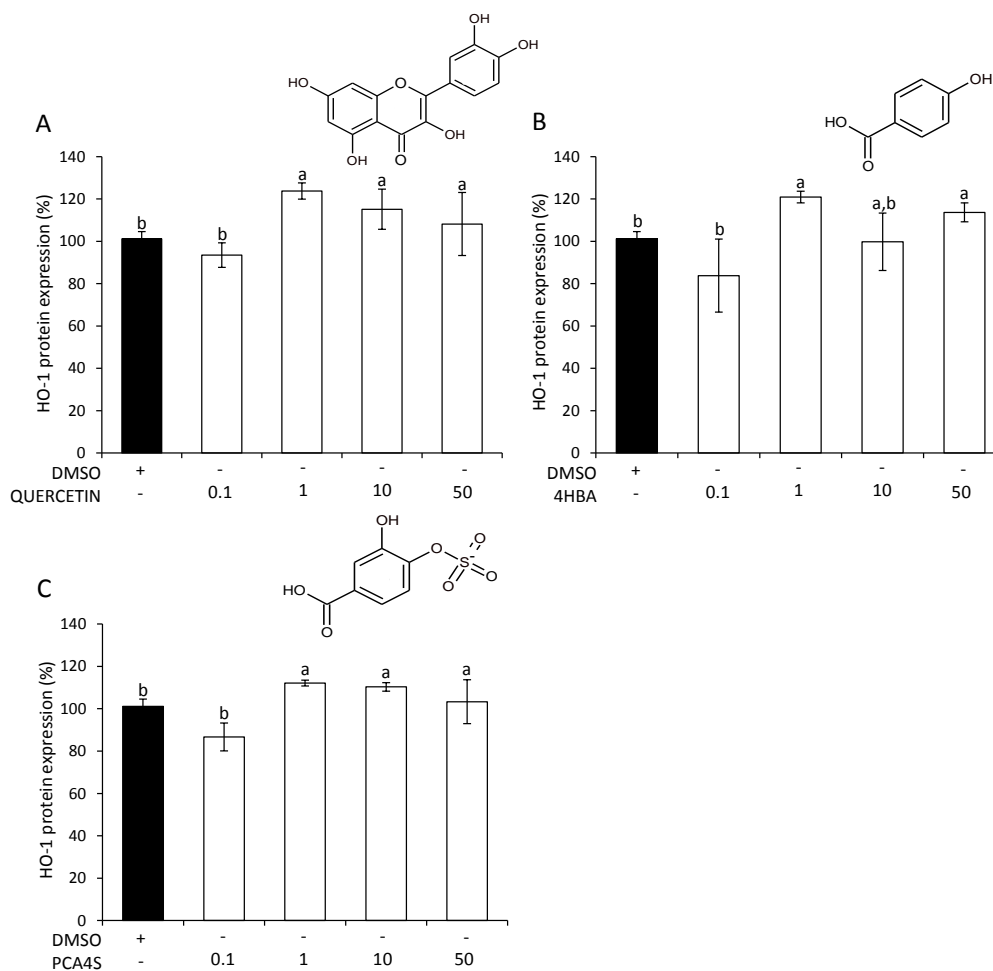


**Figure 3.5. Effect of dose of quercetin and 2 phenolic metabolites on HO-1 protein.** A) Quercetin B) 4-hydroxybenzoic acid (4HBA), C) Protocatechuic acid-4-sulfate (PCA4S). HUVEC were treated with specified concentration ( $\mu\text{M}$ ) of each treatment or 0.02 % DMSO (VC) for 16 h. HO-1 protein was quantified by ELISA. Columns represent mean of three independent replicates  $\pm$  SD (n=3). Labelled means without a common letter differ significantly,  $p \leq 0.05$  (ANOVA with post hoc LSD). Abbreviations: 4HBA, 4-hydroxybenzoic acid; PCA4S, protocatechuic acid-4-sulfate.

### 3.3.5. Effect of flavonoids and metabolites on HO-1 mRNA expression.

Quercetin, 4HBA, and PCA4S were investigated for their effect on HO-1 mRNA expression (**Figure 3.6**). HO-1 mRNA, relative to 0.02 % DMSO (vehicle control), was upregulated in response to quercetin (2.25 fold,  $p \leq 0.01$ ) and 4HBA (1.26 fold,  $p \leq 0.05$ ), but not PCA4S

( $p=0.67$ ). Quercetin and 4HBA were taken forward to explore their effect on transcription factor (Nrf2) expression.

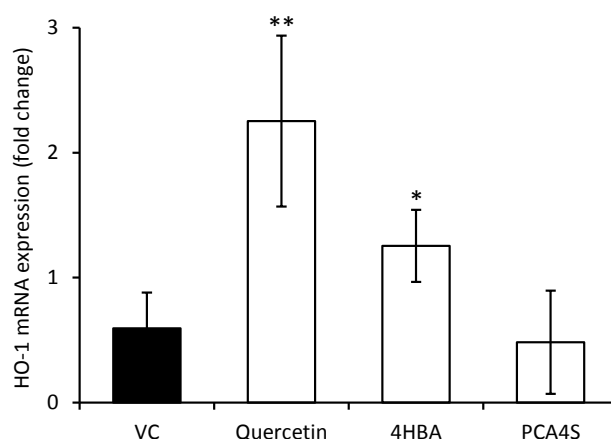


**Figure 3.6. Effect of quercetin, 4-hydroxybenzoic acid, and PCA-4-sulfate on HO-1 mRNA expression.**

Treatments were added to HUVEC at a final concentration of 10  $\mu\text{M}$  or 0.02 % DMSO for 6 h, HO-1 mRNA is presented relative to an untreated control (no DMSO) following normalisation to reference genes UBE2D2 and PRDM4. Data represents the average of 3 independent replicates  $\pm$  SD ( $n=3$ ). Analysis was performed by one-way ANOVA with post-hoc LSD,  $**p \leq 0.01$ ,  $*p \leq 0.05$ . Abbreviations: 4HBA, 4-hydroxybenzoic acid; PCA4S, protocatechuic acid-4-sulfate; VC, vehicle control.

### **3.3.6. Effect of quercetin and 4-hydroxybenzoic acid on total Nrf2 protein expression in the presence of Akt1 and ERK1/2 inhibitors.**

Quercetin and 4HBA were measured for their effect on total Nrf2 protein expression in HUVEC, and their apparent effect in the presence of inhibitors of Akt1 (LY294002) or ERK1/2 (PD98059; **Figure 3.7**). Nrf2 expression was increased in response to quercetin relative to the vehicle control (2.89 fold,  $p=0.002$ ), and there was a moderate, though not significant, reduction in this effect when cells had been pre-treated with LY294002 (Akt1 inhibitor;  $p=0.11$ ). 4HBA had no significant effect on Nrf2 protein expression ( $p=0.52$ ).

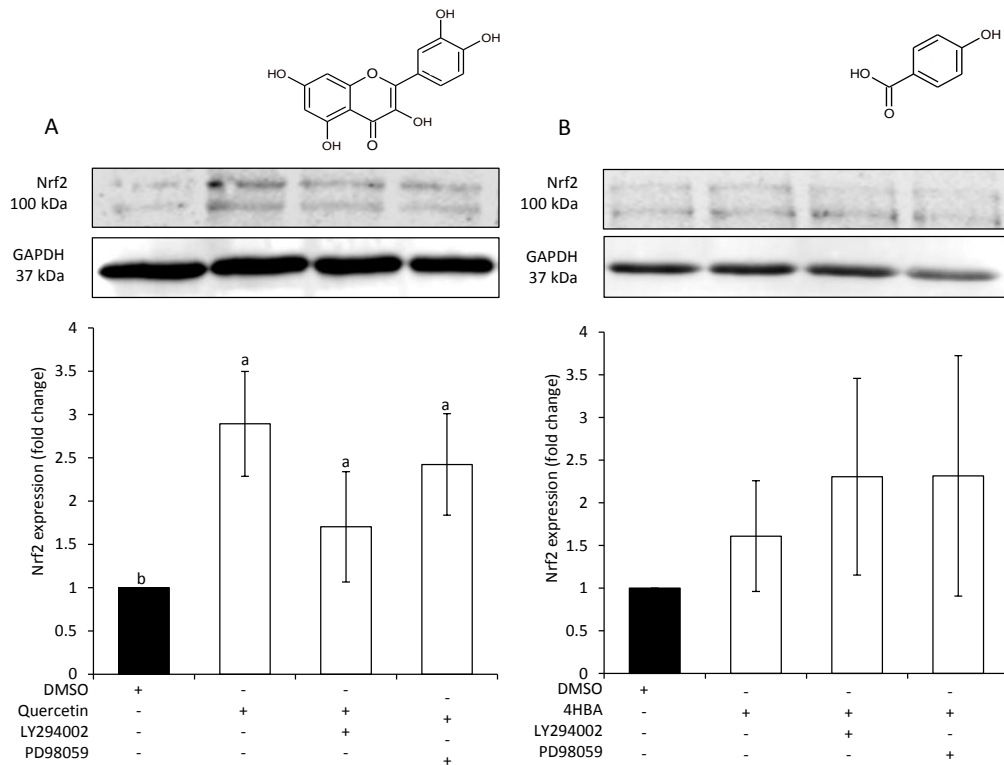


**Figure 3.7. Effect of inhibitors of Akt1 and ERK1/2 on quercetin and 4-hydroxybenzoic acid induced total Nrf2 protein expression.** A) Quercetin, B) 4-hydroxybenzoic acid. Inhibitors of Akt1 phosphorylation (LY294002) and ERK1/2 phosphorylation (PD98059) were added to HUVEC media 1 h prior to the addition of 10  $\mu$ M quercetin, 10  $\mu$ M 4HBA, or 0.02 % DMSO (vehicle control), for 6 h. Total Nrf2 protein was determined by densitometry, normalised to reference gene, GAPDH, and presented relative to vehicle control (0.02 % DMSO). Blots are representative of one of three independent replicates and columns are representative of three independent replicates  $\pm$  SD (n=3). Labelled means without a common letter differ significantly,  $p \leq 0.05$  (ANOVA with post hoc LSD). Abbreviations: 4HBA, 4-hydroxybenzoic acid.

### 3.3.7. Effect of quercetin, 4-hydroxybenzoic acid and protocatechuic acid-4-sulfate on vascular signal transduction pathways.

Quercetin, 4HBA and PCA4S (10  $\mu$ M) were measured for their effect on Akt1 and ERK1/2 phosphorylation in HUVEC (**Figure 3.8**). Quercetin induced the phosphorylation of Akt1 (1.50 fold,  $p=0.03$ ) and ERK1/2 (1.57 fold,  $p=0.04$ ) relative to the vehicle control, whereas no effects were observed in response to 4HBA or PCA4S on the phosphorylation of either protein. Inhibitors of Akt1 (LY294002) and ERK1/2 (PD98059) phosphorylation significantly inhibited the phosphorylation of their respective targets in each experiment.

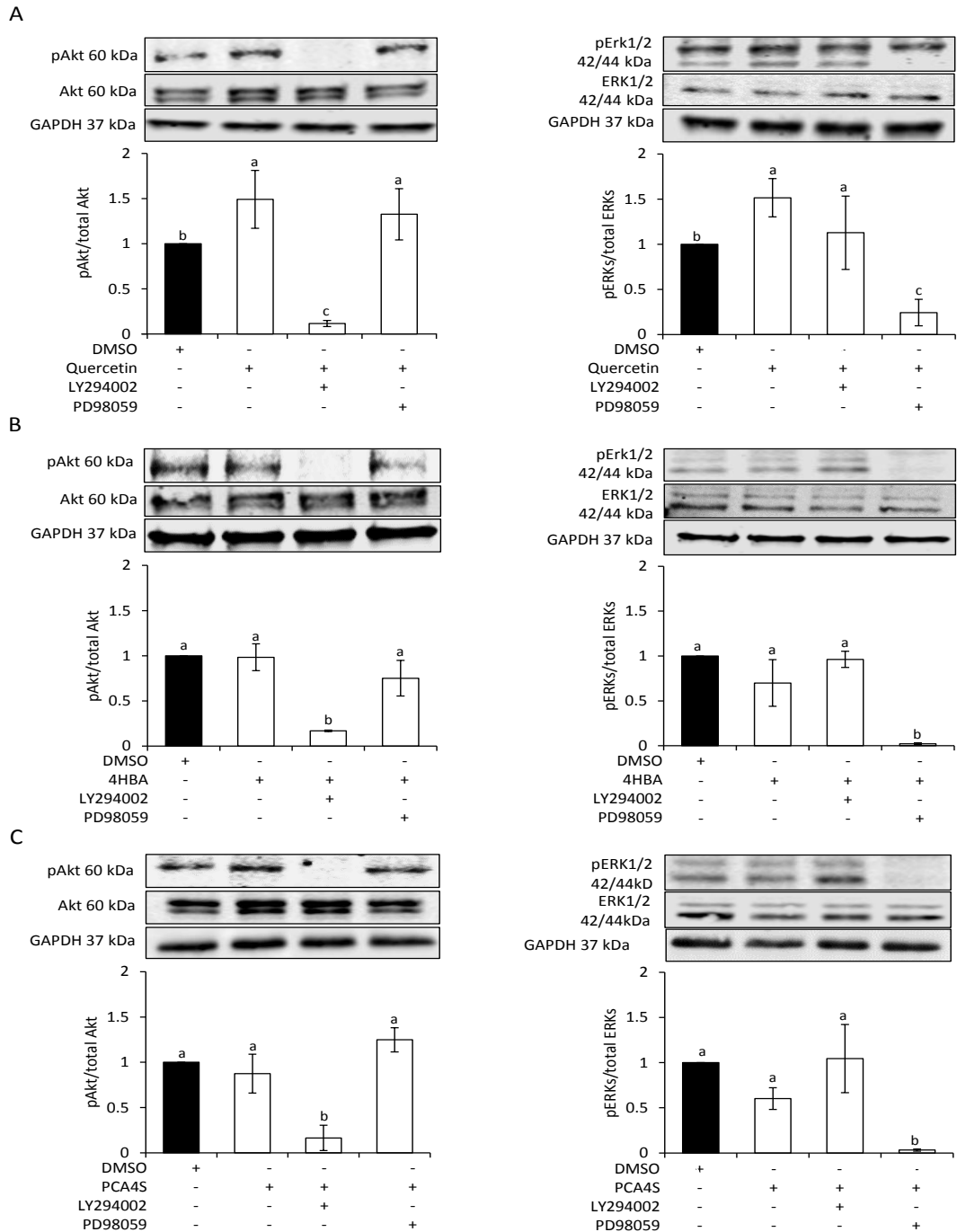


**Figure 3.8. Effect of quercetin, 4-hydroxybenzoic acid and protocatechuic acid-4-sulfate on Akt1 and ERK1/2 phosphorylation.** A) Quercetin, B) 4-hydroxybenzoic acid (4HBA), C) Protocatechuic acid-4-sulfate (PCA4S). Inhibitors of Akt1 phosphorylation (LY294002) and ERK1/2 phosphorylation (PD98059) were added to HUVEC 1 h prior to the addition of 10  $\mu$ M quercetin, 4HBA, PCA4S, or 0.02 % DMSO (vehicle control), for 15 min. Relative concentrations of phosphorylated and total protein were determined by densitometry, normalised to reference gene, GAPDH, and presented relative to the vehicle control. Blots are representative of one of three independent replicates and columns are representative of three independent replicates  $\pm$  SD (n=3). Labelled means without a common letter differ significantly,  $p \leq 0.05$  (ANOVA with post hoc LSD).

### 3.4. Discussion

Flavonoid intake has been positively associated with the reduced risk of cardiovascular diseases and defining this relationship will aid our knowledge regarding how diet may influence and optimise health (Feliciano et al., 2015). Flavonoids have been linked to improvements in vascular function and blood pressure (Grassi et al., 2015), though their mechanisms of action have yet to be elucidated. It has been suggested that flavonoids and their metabolites improve vascular function through regulation of endothelial nitric oxide synthase (eNOS; Shen et al., 2012) and the oxidant-response protein, HO-1 (Liu et al., 2012, Sorrenti et al., 2007). The expression of HO-1 is primarily mediated by the transcription factor Nrf2, which is activated in response to a number of stimuli, such as oxidative stress or through signalling kinase activation, such as Akt1 and ERK1/2 (Niture et al., 2014, Moosavi et al., 2016).

It has been postulated that phenolic metabolites of flavonoids, which are present at higher concentrations for longer periods of time than their precursors, underlie flavonoids' cardiovascular bioactivity (Kay et al., 2009, Heleno et al., 2015). Recent work from our group have studied the effects of phenolic metabolites of flavonoids (protocatechuic acid (PCA) and vanillic acid (VA)) on eNOS and HO-1 expression (Edwards et al., 2015), though the study of their phase II metabolites in this context is relatively novel, as is the study of their combined effects.

6 commonly consumed flavonoids and 13 metabolites, identified in human feeding studies (Clifford et al., 2013, de Ferrars et al., 2014b, McKay et al., 2015, Pimpão et al., 2015, Schar et al., 2015), were screened for their effects on eNOS (Figure 3.2) and HO-1 (Figure 3.3) protein expression in human endothelial cells (HUVEC). Of the treatments screened, 1 flavonoid (quercetin) and 2 phenolic acid metabolites (4-hydroxybenzoic acid (4HBA) and protocatechuic acid-4-sulfate (PCA4S)) increased HO-1 protein expression >20 %. Quercetin, 4HBA, and PCA4S were further investigated for the effect of increased concentration (Figure 3.5), where each treatment again increased HO-1 protein in response to 1  $\mu$ M, but this response was not amplified in response to increased concentration (10  $\mu$ M- 50  $\mu$ M). Subsequent experiments demonstrated that quercetin and 4HBA significantly upregulated HO-1 mRNA expression (Figure 3.6) but only quercetin increased total Nrf2 protein (Figure 3.7) and additionally induced the phosphorylation of Akt1 and ERK1/2 signalling kinases (Figure 3.8). These data suggest that quercetin, but not 4HBA and PCA4S is active in these signalling pathways and that phenolic metabolites act via alternative mechanisms. Mixtures of quercetin and structurally similar flavonoids (7 equimolar mixtures) and 11 mixtures of

4HBA and PCA4S and their structurally similar metabolites, to a cumulative concentration of 10  $\mu\text{M}$ , were screened for their effect on HO-1 protein (Figure 3.4), though no effects were observed, suggesting no additive effects.

It has been postulated that flavonoids may exert their vascular effects by the increase of eNOS expression, which leads to an increase in nitric oxide (NO) bioavailability (Rodriguez-Mateos et al., 2014). The increase in NO may, in part, contribute to improved flow-mediated dilation observed following the consumption of certain flavonoids (Hooper et al., 2008). Previous *in vitro* studies which have observed the effects of flavonoids on eNOS expression lack dietary relevance, as precursor flavonoids at supraphysiological concentrations are commonly utilised (Kay, 2010). In the present study, eNOS protein expression did not increase in response to 1  $\mu\text{M}$  of any treatment and it is possible that the concentration utilised was not high enough to elicit a response. Lazze *et al.*, who utilised the anthocyanin cyanidin (an aglycone of cyanidin-3-glucoside), demonstrated a 46 % increase in eNOS protein at 100  $\mu\text{M}$  (Lazze et al., 2006), whereas serum concentrations of a  $^{13}\text{C}$ -labelled cyanidin-3-glucoside (C3G) has been reported several magnitudes lower (0.14  $\mu\text{M}$ ; de Ferrars et al., 2014b), which suggests that these studies are not reflective of a physiologically achievable response. Increasing the screening concentration may therefore have elicited a response. That said, certain studies suggest that the concentration response of eNOS may be non-linear (such that increasing the concentration may not increase response). Most notably, eNOS expression has been shown to increase in response to <10  $\mu\text{M}$  quercetin (Shen et al., 2012), whereas it is significantly reduced following treatment with 30  $\mu\text{M}$ -100  $\mu\text{M}$  quercetin (Jackson and Venema, 2006), suggestive of a non-linear concentration response. Bovine endothelial cells (BAEC) treated with cyanidin-3-glucoside showed increased eNOS levels at 0.1  $\mu\text{M}$  (Xu et al., 2004), with more modest increases in eNOS at 1  $\mu\text{M}$  and 0.01  $\mu\text{M}$ , which is again indicative of a non-linear, 'bell-curve' response. A similar response was observed by others in our group (H.Amin PhD thesis, 2014), which does not correspond to the response in the present study, though it should be noted that these previous studies utilised a 24 h treatment time whereas the present study utilised 18 h, suggesting this response may be time-dependent. Concentrations of <1  $\mu\text{M}$  of precursor flavonoids are therefore indicated for future studies. In contrast, phenolic metabolites of flavonoids are present at much higher concentrations in the serum relative to their precursor structures (Schar et al., 2015, Pimpão et al., 2015), for example serum vanillic acid (VA) levels have been reported as high as 2.7  $\mu\text{M}$  following consumption of 500 mg C3G (de Ferrars et al., 2014b) and 4  $\mu\text{M}$  following consumption of a Montmorency tart cherry extract (Keane et

al., 2015). VA has previously been shown to increase eNOS expression between 1  $\mu$ M- 10  $\mu$ M in an apparently concentration-dependent manner, suggesting that, whereas eNOS response to precursor flavonoids is non-linear, the response to phenolic metabolites is linear, though further evidence, such as through a thorough concentration-response experiment (e.g. 0.01  $\mu$ M-100  $\mu$ M) utilising multiple phenolic metabolites, are required to verify these conclusions.

The oxidant-response protein HO-1 has been implicated in cellular defence activity of flavonoids, potentially through its enzymatic by-products, bilirubin and carbon monoxide (CO; Szabo et al., 2004). In agreement with previous studies (Lin et al., 2004, Chow et al., 2005, Sun et al., 2015), the present study demonstrated that HO-1 was upregulated in response to quercetin in human endothelial cells. A recent study from our group utilising monocytic cells (J. di Gesso PhD thesis, 2015) also demonstrated that quercetin upregulated HO-1 at 10  $\mu$ M and 50  $\mu$ M. Phenolic acid metabolites, PCA4S and 4HBA, increased endothelial HO-1 protein by >20% (Figure 3.3), suggesting that these may be involved in antioxidant defence at a physiologically achievable concentration (1  $\mu$ M; de Ferrars et al., 2014b). It is interesting that PCA4S increased HO-1 protein where its unconjugated structure, protocatechuic acid (PCA), did not. PCA has previously been shown to induce the HO-1 transcription regulator, Nrf2 in murine macrophages (Vari et al., 2011), though the concentration used in this study was 25  $\mu$ M, and so the result of the present study may again be due to the utilisation of a low, physiologically achievable concentration (de Ferrars et al., 2014b). The data from the present study does suggest that metabolic conjugation increases bioactivity, as has been suggested by others, such as by Edwards *et al.*, who demonstrated that methyl conjugation of PCA to vanillic acid (VA) increased HO-1 protein (Edwards et al., 2015) and similar conclusions have been made for phenolic acids in inflammatory models of endothelial dysfunction (Amin et al., 2015).

Few studies have explored the combined effects of flavonoids and their metabolites (di Gesso et al., 2015, Krga et al., 2016), despite some indication of differential activities relative to their constituents in isolation (Heeba et al., 2012, Khandelwal et al., 2012, Koga and Meydani, 2001, Liebgott et al., 2000), which suggest that flavonoids and their metabolites may have additive or synergistic effects. In the present study, the vast majority of treatments screened in isolation at 1  $\mu$ M did not have an effect on HO-1 expression. *In vivo*, total phenolic metabolite concentrations are >10  $\mu$ M (Pimpão et al., 2015, Schar et al., 2015), which was the rationale behind utilising a cumulative 10  $\mu$ M concentration, and equimolar concentrations of structurally similar compounds were used to potentially elucidate

structure-activity relationships. In the present study we explored 7 mixtures of flavonoids and 10 mixtures of conjugated and unconjugated phenolic metabolites, based on the active treatments in the HO-1 screen and their structurally similar treatments, as well as one treatment, which contained 13 phenolic metabolites (0.77  $\mu\text{M}$  of each constituent). None of the treatments utilised appear to affect HO-1 protein expression. Interestingly, this suggests not only that there are no apparent additive effects in combination, but that the presence of the treatments which were previously active in isolation at 1  $\mu\text{M}$  are not active in combination treatments up to 5  $\mu\text{M}$  (in the case of treatments with 2 constituents). Although direct comparison between isolated and combined treatments was not possible in this case, it does, to some extent, suggest antagonistic activity. Theoretically, structurally similar, though non-bioactive, treatments may block the target activity site, or interaction may occur between compounds in the mixture, as has been seen in acellular experiments (Hidalgo et al., 2010). It is possible that this activity is as a result of the 'artificial' equimolar construction of the mixtures, whereas the unique molar ratios of metabolites observed *in vivo* may elicit additive or synergistic activities, which are explored in future investigations (Chapter 6). Wallerath *et al.* observed the effects of red wine polyphenols relative to their constitutive anthocyanins and phenolic acids in isolation (1  $\mu\text{M}$ -33  $\mu\text{M}$ ; Wallerath et al., 2005), on eNOS expression in human EA.hy 926 endothelial cells. It was observed that the red wine polyphenol mixture greatly increased eNOS expression relative to its constituents in isolation. A key limitation of this study was that the polyphenol composition of red wine is not equivalent its composition following consumption due to extensive polyphenol metabolism (Kroon et al., 2004). Nevertheless, this work does present interesting data regarding the cumulative effects of flavonoid relative to in isolation, and it remains to be seen whether physiologically relevant metabolites of flavonoids equally possess additive or synergistic effects following consumption.

Quercetin, 4HBA and PCA4S were investigated for their effect on HO-1 mRNA expression, which was increased significantly in response to quercetin, as has been advocated by others (Zerin et al., 2013), and was also increased in response to 4HBA, which has not been previously demonstrated. No response was observed in response to PCA4S, suggesting that it may not be active in the transcriptional pathways affecting HO-1 (such as Nrf2), but may act post-translationally. Alternatively, there may be a discrepancy due to the use of a single treatment time, suggesting that the use of multiple time points may provide further insight into regulation of HO-1 protein and mRNA by flavonoid metabolites.

HO-1 expression is regulated by the transcription factor Nrf2, which is activated in response to a number of stimuli, such as phytochemicals, reactive oxygen species (ROS) and signalling kinase activation (e.g. Akt1 and ERK1/2; Niture et al., 2014). Total Nrf2 protein was significantly upregulated following treatment with 10  $\mu$ M quercetin, which is in agreement with previous studies at 5-50  $\mu$ M (Granado-Serrano et al., 2012, Zerin et al., 2013). This effect may be dependent on Akt1, which could be validated in future studies by use of a basal inhibitor control (Weng et al., 2011). Nrf2 protein was not significantly increased in response to 4HBA, which may be due to the low magnitude of response, which magnified the variation observed between replicates.

Finally, the effect of quercetin, 4HBA and PCA4S on Akt1 and ERK1/2 signalling kinase phosphorylation were determined. Akt1 and ERK1/2 were phosphorylated in response to quercetin which may be potential mechanisms of Nrf2 activation (and subsequent HO-1 protein expression). 4HBA and PCA4S did not affect Akt1 and ERK1/2 phosphorylation, though these may be active in other molecular pathways influencing HO-1 expression, such as PKC, JNK, and p38 MAPK (Tanigawa et al., 2007), or by receptor binding effects (Surh, 2003). It has also been suggested that flavonoids may act on endogenous inhibitors of signalling kinases, such as thioredoxin (inhibits ASK1, upstream of JNK and p38 MAP kinases; Lu et al., 2006). The present study highlights the requirement for future studies to explore alternative mechanisms of action which metabolites of flavonoids may be active, for example in inflammatory mechanisms such as NF $\kappa$ B (di Gesso et al., 2015, Amin et al., 2015). The present study provides unique insight into the effects of flavonoid phenolic metabolites on biomarkers of vascular homeostasis, and into their combined activity. However, there are certain limitations to this work. The use of human umbilical vein endothelial cells (HUVECs) may be seen as a limitation, as they do not originate from the arterial wall. Previous work from our group demonstrated that the expression of HO-1 protein in HUVEC in response to vanillic acid (0.1  $\mu$ M -10  $\mu$ M) were comparable to the more physiologically relevant cell type, human coronary artery endothelial cells (HCAEC; Edwards et al., 2015). This suggests that HUVEC are a suitable model to screen for the effects of flavonoids, but that data should be validated in HCAEC in future studies. The use of single treatment times for screening all treatments may have been a limitation as treatments may differ between uptake and time to act upon target site, depending on their structural characteristics. Rizza *et al.*, who utilised the flavanone, hesperidin (glycoside-conjugated hesperetin), investigated the effect of increased concentration (0.01  $\mu$ M – 10  $\mu$ M) in the first instance, followed by the concentration of the greatest effect size (10  $\mu$ M) across several time points (Rizza et al.,

2011). A similar system for each of the treatments in the present study would have optimised the current screen; this would have been extremely time and cost ineffective but may be indicated for future studies. The magnitude of effect on Nrf2 protein observed in the present study was relatively small, which may have magnified the variation between replicates. Additionally, it is possible that the vehicle (DMSO) masked the effect on Nrf2 signalling, as DMSO is known to upregulate Nrf2-regulated protein expression (Liang et al., 2011), this could be verified in future studies by use of a basal control. An alternative solution would be to dissolve treatment directly into media, thus negating the requirement of a vehicle; this would not have been possible for quercetin given its low water solubility (Ribeiro et al., 2009), though is a future consideration for the more soluble phenolic acid metabolites, such as utilised for VA (Edwards et al., 2015). Nrf2 expression in HUVECs is relatively low compared to other tissues, such as liver and brain (Vallejo et al., 2000), and thus detection via Western blotting proved difficult. Future studies should consider the use of a negative cellular control, such as RNA interference directed against Nrf2 (siNrf2), as used by others (Zhai et al., 2013). For the purpose of elucidating mechanisms, a more appropriate model of Nrf2 pathway activation could be the use of hepatocytes, such as HepG2 cells, as expression of Nrf2 expression is much higher, potentially increasing the measurable effect at lower concentrations (Krajka-Kuzniak et al., 2015). It should be noted, however, that the uptake of flavonoids and their metabolites is dependent on cell type (Spencer et al., 2004) and hepatocytes contain multiple phase II metabolites, which may therefore alter treatments differentially to endothelial cells into a more/less bioactive form. Validation in endothelial cells would still therefore be necessary in this case.

In conclusion, data collected on the vascular bioactivity and mechanisms of flavonoids and their phenolic metabolites suggest that conjugated metabolites of flavonoids do not appear to be active on the targets investigated at concentrations achievable through diet, suggesting that they have alternative mechanisms of action. It has been postulated that endothelial dysfunction, a key pathological driver of atherosclerosis (Hopkins, 2013), is influenced by low-level inflammation, which has a direct impact of NO availability in endothelial and smooth muscle cells (Chapidze et al., 2007). Therefore the present evidence suggests the phenolic metabolites of flavonoids are acting via another mechanism, possibly inflammatory (Amin et al., 2015, di Gesso et al., 2015), and these mechanisms are further explored in the chapters following.

## **Chapter 4. Effect of flavonoids and their metabolites on the basal expression of haem oxygenase-1 in vascular smooth muscle cells.**

### **4.1. Introduction**

Beneficial effects of flavonoids have been observed on vascular function, such as in blood flow and flow-mediated vasodilation (Grassi et al., 2015), which are regulated in-part by endothelium-derived nitric oxide (NO) levels (Green et al., 2014). Work presented previously (Chapter 3) suggested that certain flavonoid metabolites may indirectly affect intracellular NO by the upregulation of oxidant-response protein, haem oxygenase-1 (HO-1), which leads to the reduction in ROS, and maintenance of endothelial homeostasis. Vascular smooth muscle cells (VSMCs) contain various sources of ROS, such as NADPH oxidases (NOX; Louis and Zahradka, 2010), which under conditions of stress lead to VSMC proliferation, migration and cytokine production, which are critical to the progression of atherosclerosis (Lusis, 2000).

HO-1 and HO-2 are rate-limiting enzymes in the catabolism of haem to form biliverdin (converted to antioxidant bilirubin by biliverdin reductase), carbon monoxide (CO), and free iron. HO-1, specifically, is upregulated under conditions of oxidative-stress, which is believed to be a protective mechanism in the prevention of atherosclerosis (Araujo et al., 2012). HO-1 and CO inhibit NOX1 and prevent VSMC migration (Rodriguez et al., 2010), which makes HO-1 a key therapeutic target in the pathogenesis of atherosclerosis (Kim et al., 2011). Previous studies have shown that HO-1 expression is upregulated in VSMCs in response to various phytochemicals such as, quercetin (Lin et al., 2004), naringenin (Chen et al., 2012), and curcumin (Pae et al., 2007), though many past studies have utilised supraphysiological concentrations of flavonoids and the studies into the bioactivity of their more bioavailable phenolic metabolites is relatively novel (Edwards et al., 2015). Additionally, previous studies have suggested synergistic or additive activity of flavonoids and their metabolites in combination in VSMC (Keane et al., 2015, Pantan et al., 2016), though these studies have not explore the combined effects of conjugated phenolic metabolites of flavonoids identified in human feeding studies (Pimpão et al., 2015, de Ferrars et al., 2014a, Schar et al., 2015).

The primary aim of the present study was to determine the activity of 6 dietary flavonoids common to the Western diet and 13 phenolic metabolites identified in human feeding

studies (Chapter 3, Table 3.1) on Hmox-1 (human HO-1 orthologue in rats) expression in rat aortic smooth muscle cells (RASMCs), to assess their relative vascular bioactivity. The secondary aim was to identify whether flavonoids and their metabolites possess additive activity on Hmox-1 expression in combination. Finally, we aimed to determine whether active treatments affected Hmox-1 mRNA expression, with a view to suggesting potential mechanisms of action.

## **4.2. Methods.**

Experiment specific details are provided below while comprehensive methodological descriptors are provided in detail in Chapter 2.

### **4.2.1. Treatment solutions**

Stock solutions of flavonoids and metabolites were prepared in DMSO and stored as described in Chapter 2. Working solutions of 1 mM of each analyte were made up in supplemented media before being diluted to a final concentration of 10  $\mu$ M, or to equimolar concentrations for combined treatments (for example, in 10  $\mu$ M mixtures consisting of 4 constituents, each would contain 2.5  $\mu$ M of each constituent). Treatment combinations were designed based on their structural similarities and based on activity when screened in isolation. Treatment solutions were prepared in supplemented media and stored at 4°C, with the exception of cyanidin-3-glucoside and peonidin-3-glucoside, which were added immediately prior to the experiments to maintain stability.

### **4.2.2. Cell culture**

Cryogenically stored, rat aortic smooth muscle cells (RASMC) were cultured and maintained as described in Chapter 2. All cells were incubated for at least 24 hours at 37°C, 5 % CO<sub>2</sub>, in a humidified atmosphere, prior to experiment commencement. Cells were used between passages 3 and 6.

### **4.2.3. Cell viability**

RASMC were seeded at 10,000 cells/well in fibronectin coated 96-well plates and grown to confluence in supplemented media. Cells were treated with 10  $\mu$ M of each treatment, or 0.02 % DMSO (vehicle control) in media. PBS (cells, no media) was used as a negative control. WST-1 protocol was carried out as described in Chapter 2.

### **4.2.4. Hmox-1 protein expression**

RASMC were seeded at 300,000 cells/well in fibronectin coated 6-well plates. Supplemented media was replaced by serum free media 24 h prior to experiment commencement. Cells were treated with 10  $\mu$ M treatment or 0.02 % DMSO (vehicle control) and incubated for 24 h at 37°C, 5 % CO<sub>2</sub>, in a humidified atmosphere. Cells were washed 3 x with PBS, lysed with Extraction Reagent Buffer, and stored at -80°C until required. Protein expression of rat Hmox-1 was determined by commercially available enzyme-linked immunosorbent assay (ELISA), as described in Chapter 2.

#### **4.2.5. Hmox-1 mRNA expression.**

RASMC were seeded at 100,000 cells/well in fibronectin coated 12-well plates. Supplemented media was replaced by serum-free media 24 h prior to experiment commencement. Cells were treated with 10  $\mu$ M treatment solution or 0.02 % DMSO (vehicle control) for 6 h at 37°C, 5 % CO<sub>2</sub>, in a humidified atmosphere. Cell culture supernatant was removed and cells washed 3 x with PBS on ice. RNA was extracted, reverse transcribed and RT-qPCR was conducted as described in Chapter 2. Reference gene expression, Zgpat and Stau1, were determined by geNORM analysis as the most appropriate stable genes, the geometric mean of which were used to normalise the data in subsequent experiments, as described in Chapter 2.

#### **4.2.6. Data analysis**

For cytotoxicity experiments, absorbance values were reported as a mean of three independent replicates and differences relative to an untreated control (no DMSO) were determined by use of Student's t-test using Microsoft Excel (version 2013). Hmox-1 proteins (pg/mL) and mRNA (fold change) were recorded as the mean of two technical duplicates and reported relative to an untreated control. Treatment effects were determined relative to the vehicle control (DMSO) and established by one-way analysis of variance (ANOVA) with post-hoc least square difference (LSD). Analyses were conducted using SPSS for Windows (version 22.0; IBM, New York, USA). Data were considered significant where  $p \leq 0.05$ . For screening purposes, treatments displaying non-significant values of  $\leq 0.15$  were taken forward, for validation in subsequent combination and mRNA experiments.

#### **4.2.7. Method optimisation**

Method optimisation experiments were conducted to identify the appropriate screening concentration for the upregulation of Hmox-1 expression in RASMC (Appendix; **Chapter 9.2.1.; Figure 4.1**). Endogenous reference genes for normalisation of C<sub>t</sub> data for target genes were selected by use of rat geNORM kit and qBASE analysis software as described in Chapter 2 (Appendix; **Chapter 9.2.2**).

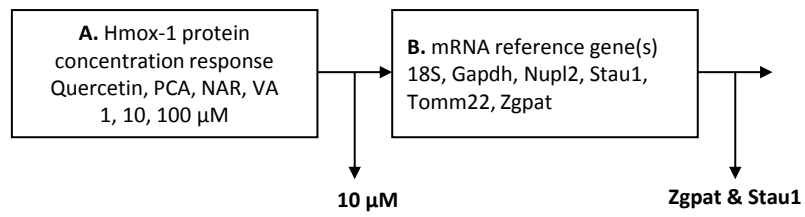


**Figure 4.1. Method optimisation experiments for Chapter 4.** See Appendix 9.2. Abbreviations: Hmox-1, haem oxygenase-1; NAR, naringenin; PCA, protocatechuic acid; VA, vanillic acid. Abbreviations for mRNA reference genes can be found in Chapter 2.5.3.

### 4.3. Results

#### 4.3.1. Effect of treatments on cell viability.

6 flavonoids and 13 phenolic acid metabolites were screened in RASMC for their effect at 10  $\mu$ M for 24 h on cell viability by use of WST-1 (**Table 4.1**). No significant effects ( $p \leq 0.05$ ) on cell viability were observed in response to treatments used.

**Table 4.1. Effects on cell viability**

	Absorbance value (% of untreated control)	
	Average $\pm$ SD	p-value
Vehicle control (VC)	85.98 $\pm$ 11.83	0.21
Hesperetin (HES)	100.15 $\pm$ 24.35	0.92
Peonidin-3-Glucoside (P3G)	94.11 $\pm$ 15.70	0.55
Naringenin (NAR)	96.55 $\pm$ 19.32	0.72
(-)-Epicatechin (EPI)	105.63 $\pm$ 11.08	0.53
Quercetin (QUE)	141.61 $\pm$ 21.49	0.06
Cyanidin-3-Glucoside (C3G)	92.90 $\pm$ 12.86	0.50
4-hydroxybenzoic acid (4HBA)	94.67 $\pm$ 13.59	0.65
Benzoic acid-4- Glc (BA4G)	115.85 $\pm$ 15.06	0.21
Benzoic acid-4-Sul (BA4S)	96.36 $\pm$ 11.83	0.74
Protocatechuic acid (PCA)	97.67 $\pm$ 9.36	0.68
Protocatechuic acid -3-Glc (PCA4G)	92.96 $\pm$ 6.95	0.20
Protocatechuic acid -4- Glc (PCA4S)	97.97 $\pm$ 17.97	0.81
Protocatechuic acid -3-Sul (PCA3S)	102.94 $\pm$ 12.08	0.67
Protocatechuic acid -4-Sul (PCA4S)	103.71 $\pm$ 19.83	0.77
Vanillic acid (VA)	91.58 $\pm$ 3.24	0.07
Isovanillic acid-3-Sul (IVA3S)	112.20 $\pm$ 7.47	0.09
Vanillic acid-4-Glc (VA4G)	109.25 $\pm$ 8.75	0.19
Isovanillic acid-3-Glc (IVA3G)	113.52 $\pm$ 15.00	0.28
Vanillic acid-4-Sul (VA4S)	117.57 $\pm$ 12.37	0.12

Cell viability following 10  $\mu$ M treatment for 24 h was assessed after 4 h incubation with WST-1 reagent and is presented as a percentage of an untreated control (no DMSO). Columns represent the mean of three biological replicates  $\pm$  SD. Effects relative to an untreated control were determined by use of Student t-test using Microsoft Excel (version 2013). Abbreviations: Glc, glucuronide; Sul, sulfate.

### 4.3.2. Effect of flavonoids and metabolites on Hmox-1

6 flavonoids and 13 phenolic metabolites were screened for their effect at 10  $\mu$ M on RASMC Hmox-1 protein expression after 24 h treatment (**Figure 4.2**). Hmox-1 expression was increased in response to 2 flavonoids, quercetin ( $189.39 \pm 29.92$  %,  $p=0.01$ ) and peonidin-3-glucoside ( $175.76 \pm 33.71$  %,  $p=0.02$ ), and there was a non-significant increase in Hmox-1 in response to protocatechuic acid (PCA;  $122.00 \pm 13.77$  %,  $p=0.09$ ). Treatment mixtures containing quercetin, peonidin-3-glucoside or PCA were taken forward to observe their effects in combinations of structurally similar compounds.

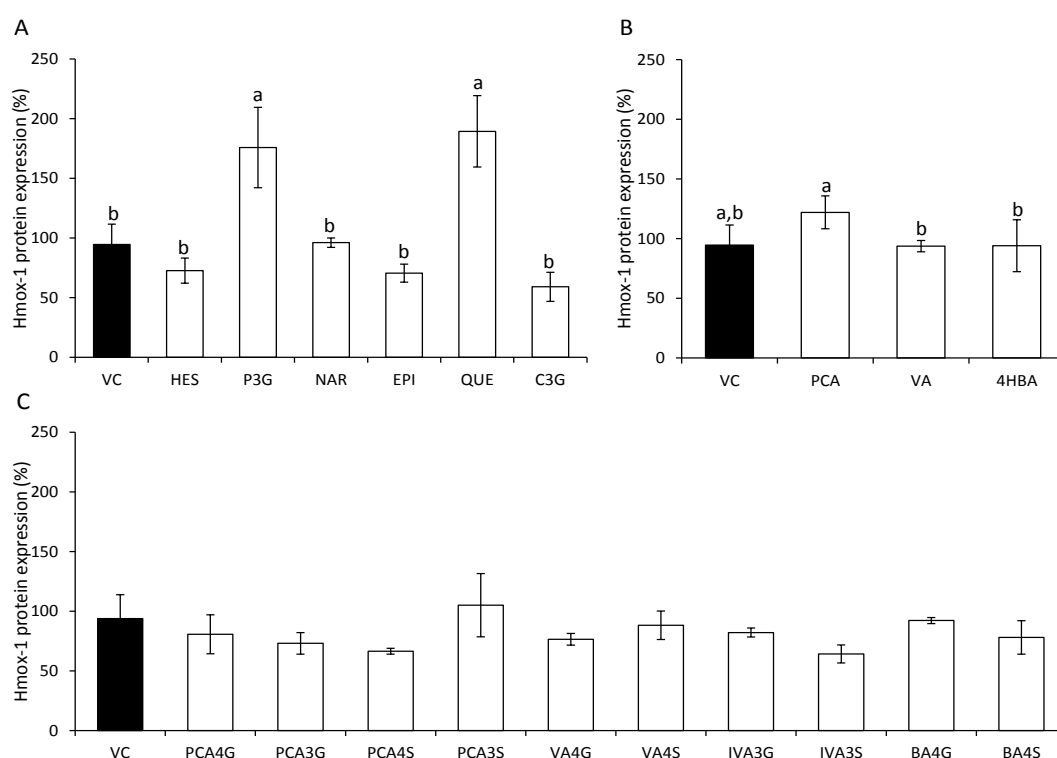


**Figure 4.2. Effect of flavonoids and their metabolites on Hmox-1 protein.** Treatments were added to RASMC to a final concentration of 10  $\mu$ M or 0.02 % DMSO (VC) for 24 h, Hmox-1 protein was quantified by ELISA and presented as a percentage of an untreated control (no DMSO). Data represents the average of 3 independent replicates  $\pm$  SD ( $n=3$ ). Labelled means without a common letter differ significantly (ANOVA with post hoc LSD,  $p \leq 0.05$ ). Abbreviations: 4HBA, 4-hydroxybenzoic acid; BA4G, benzoic acid-4-glucuronide; BA4S, benzoic acid-4-sulfate; C3G, cyanidin-3-glucoside; EPI, (-)-epicatechin; HES, hesperetin; IVA3G, isovanillic acid-3-glucuronide; IVA3S, isovanillic acid-3-sulfate; NAR, naringenin; P3G, peonidin-3-glucoside; PCA, protocatechuic acid; PCA3G, protocatechuic acid-3-glucuronide; PCA4G, protocatechuic acid-4-glucuronide; PCA3S, protocatechuic acid-3-sulfate; PCA4S, protocatechuic acid-4-sulfate; QUE, quercetin; VA, vanillic acid; VA4G, vanillic acid-4-glucuronide; VA4S, vanillic acid-4-sulfate; VC, vehicle control.

7 mixtures of flavonoids and 11 mixtures of conjugated and unconjugated phenolic metabolites were screened at 10  $\mu$ M for their effect on RASMC Hmox-1 protein expression after 24 h treatment (**Figure 4.3**). Hmox-1 expression was increased relative to vehicle control (DMSO) following treatment with the mixture consisting of equimolar concentrations of hesperetin and peonidin-3-glucoside ( $43.62 \pm 1.58$  %,  $p \leq 0.001$ ). 4 of the 11 mixtures of conjugated and unconjugated metabolites (PCA and VA; PCA and PCA3G; PCA and PCA4G; PCA and PCA3S) increased Hmox-1 expression ( $p \leq 0.05$ ) by  $\geq 8.72$  % (PCA and PCA3G).

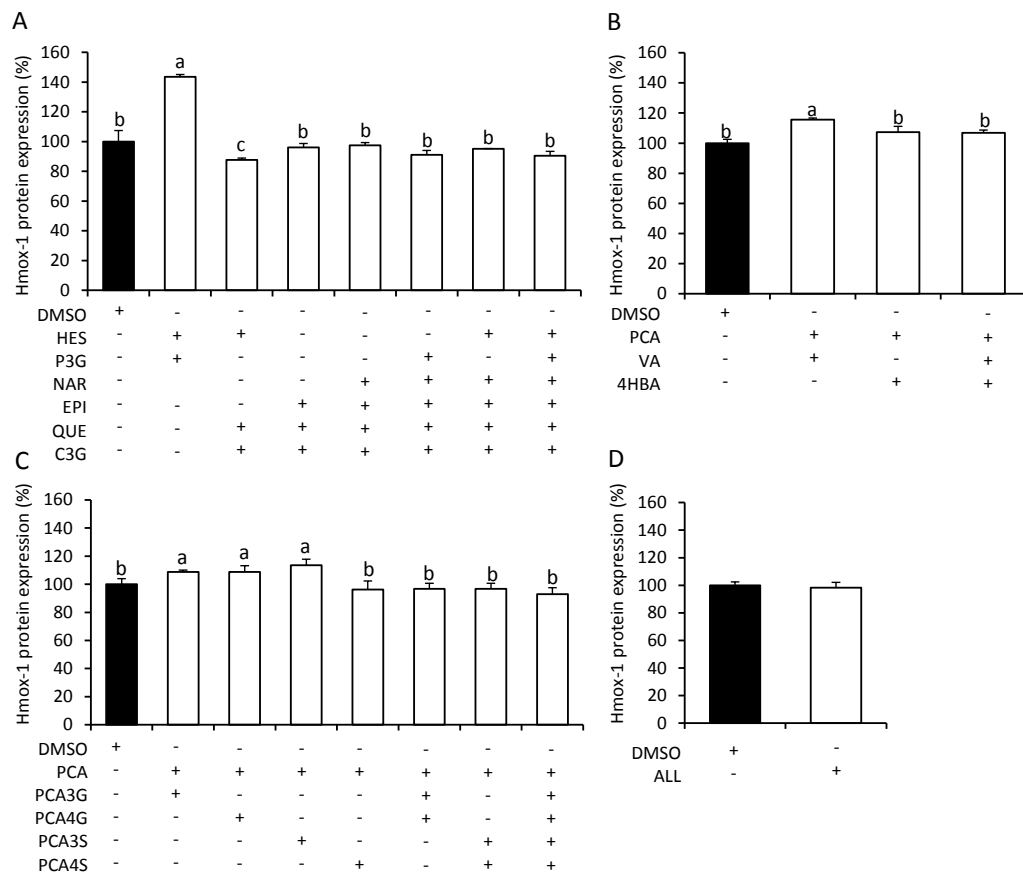


**Figure 4.3. Effect of mixtures of flavonoids and metabolites on Hmox-1 protein.** RASMC were treated to a cumulative concentration of 10  $\mu$ M for 24 h or 0.02 % DMSO (vehicle control), Hmox-1 protein was quantified by ELISA. Data represents the average of 3 independent replicates  $\pm$  SD ( $n=3$ ). Labelled means without a common letter differ significantly (ANOVA with Post Hoc LSD,  $p \leq 0.05$ ). Abbreviations: ALL, combination of 13 phenolic metabolites; C3G, cyanidin-3-glucoside; EPI, (-)-epicatechin; HES, hesperetin; naringenin; P3G, peonidin-3-glucoside; PCA, protocatechuic acid; PCA3G, protocatechuic acid-3-glucuronide; PCA4G, protocatechuic acid-4-glucuronide; PCA3S, protocatechuic acid-3-sulfate; PCA4S, protocatechuic acid-4-sulfate; QUE, quercetin; VA, vanillic acid; VC, vehicle control.

### 4.3.2. Effect of quercetin, peonidin-3-glucoside, and protocatechuic acid on Hmox-1 mRNA expression in RASMC

Quercetin, P3G, and PCA were screened for their effect on Hmox-1 mRNA expression in RASMCs after 6 h treatment (**Figure 4.4**). Hmox-1 mRNA expression appeared to increase in response to quercetin (3.09 fold, n=2). No apparent response was observed in response to P3G or PCA.

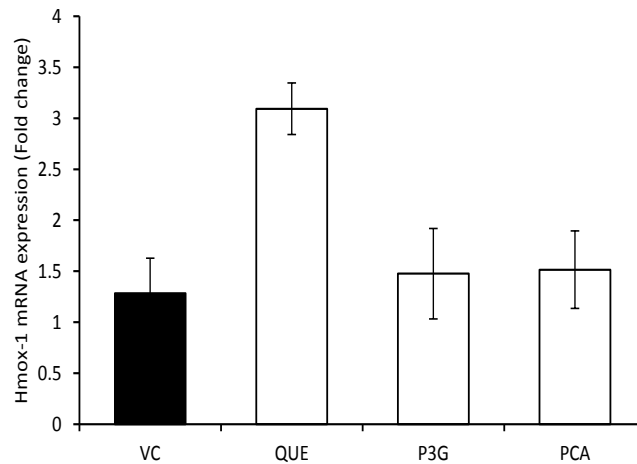


**Figure 4.4. Effect of quercetin, peonidin-3-glucoside, and PCA on Hmox-1 mRNA.** Treatments were added to RASMC at a final concentration of 10  $\mu$ M for 6 h or 0.02 % DMSO (VC), Hmox-1 protein was quantified by RT-qPCR relative to reference genes Stau1 and Zgpat and presented as fold change relative to an untreated control (no DMSO). Data represents the average of 2 independent replicates  $\pm$  SD (n=2).

#### 4.4. Discussion

Flavonoid consumption has been positively associated with the reduced risk of cardiovascular diseases (Wang et al., 2014), partially thought to be through their apparent effects on vascular function (Grassi et al., 2015), though their mechanisms of action have yet to be elucidated. It is now well understood that bacterial catabolism of flavonoids reduces the bioavailability of the parent flavonoids and produces a number of phenolic metabolites (Keppler and Humpf, 2005, Feliciano et al., 2015), though the study of their bioactivity is relatively contemporary (Heleno et al., 2015), as is the study of their additive or synergistic effects in combination (Krga et al., 2016, di Gesso et al., 2015, Keane et al., 2015). The present study aimed to investigate the effects of 6 flavonoids and 13 phenolic metabolites on haem oxygenase-1 (Hmox-1) protein expression in rat aortic smooth muscle cells (RASMC) and to observe their potential additive or synergistic effects in equimolar combinations. Hmox-1 prevents VSMC migration by the inhibition of superoxide producing NAPDH oxidases (Rodriguez et al., 2010), which makes Hmox-1 a key therapeutic target in the prevention of atherosclerosis (Kim et al., 2011) and an appropriate target for the present investigation.

2 flavonoids (quercetin and peonidin-3-glucoside (P3G)) and one metabolite (protocatechuic acid (PCA)) upregulated Hmox-1 protein in RASMCs (Figure 4.2), as did 1 mixture, consisting of hesperetin and peonidin-3-glucoside, 1 mixture consisting of PCA and VA and 3 mixtures containing PCA and its sulfate (PCA3S) or glucuronide (PCA3G and PCA4G) conjugates (Figure 4.3). These data suggest that conjugated metabolites of flavonoids do not actively increase Hmox-1 protein in isolation, but may act additively or synergistically.

Quercetin significantly induced Hmox-1 protein in the present study which is in accordance with previous studies, where it has previously been shown to upregulate Hmox-1 and other oxidant response genes through activity on transcription factor, Nrf2 (Chow et al., 2005a, Shih et al., 2004, Lin et al., 2004, Tanigawa et al., 2007, Granado-Serrano et al., 2012, Liang et al., 2013, Sun et al., 2015). It has been observed that 10 – 30  $\mu\text{M}$  quercetin significantly induced HO-1 protein in murine macrophages (Cho and Kim, 2013) and 50  $\mu\text{M}$  quercetin induced HO-1 protein levels between 4 - 12 h in rat hepatocytes (Liu et al., 2012). It should be noted that quercetin circulates as its aglycone structure at very low concentrations. In a feeding study of fried onions (equivalent of 64 mg of quercetin aglycone), a peak mean plasma concentration of 0.65  $\mu\text{M}$  was detected at 3 h (Hollman et al., 1996). Certain studies have been unable to detect the quercetin aglycone post-consumption (Heeba et al., 2012). Given that phenolic metabolites exist at higher concentrations for longer periods of time in

the circulation, greater focus should be given to their bioactivity is indicated in future studies.

Quercetin largely circulates as glucuronide/sulfate metabolites, which are considered to be significantly less bioactive relative to the aglycone structure (Lodi et al., 2008, Tribolo et al., 2008, Tribolo et al., 2013). Quercetin-glucuronides may anionically bind to the cell surface of circulating macrophages leading to the cleavage of glucuronic acid and release of the quercetin aglycone (Ishisaka et al., 2013). However, a recent *in vitro* study on the effect of quercetin-3-glucuronide on NOX1 inhibition (Jimenez et al., 2015), suggested that a high concentration (100  $\mu$ M) of the conjugated metabolite was required to de-conjugate enough glucuronic acid to exert a significant effect on NOX inhibition. Quercetin-3-glucuronide is thought to act by different mechanisms to its aglycone, as it has been shown to inhibit JNK phosphorylation and subsequent transcription of inflammatory genes in vascular smooth muscle cells (VSMCs; Yoshizumi et al., 2002). These studies suggest that flavonoid aglycones may be active on vascular mechanisms of action (such as NOX inhibition or Hmox-1 expression), but that metabolic conjugation may alter activity the target toward inflammatory mechanisms of action, such as the expression of adhesion molecules (Amin et al., 2015).

The anthocyanin, P3G, also upregulated Hmox-1 protein to an equivalent extent as quercetin (Figure 4.2). The effect of P3G in this pathway is lesser studied relative to quercetin and so it is difficult to compare these data directly to previous studies, and, to our knowledge, this is the first time that this effect has been reported on Hmox-1 expression, although retinal epithelial (ARPE-19) cells preincubated with bilberry extract (containing P3G) demonstrated increased HO-1 expression by 5.5 fold (Milbury et al., 2007). It should be noted that P3G is unstable and rapidly degrades to phenolic acid derivatives at physiological pH and therefore has low plasma bioavailability, which has also been shown *in vivo* for the structurally similar anthocyanin, cyanidin-3-glucoside (de Ferrars et al., 2014b). The relevance of these data to physiologically achievable effects in a nutritional context therefore remains to be established. Of greater interest is the apparent reduction of activity between P3G and its B-ring derivative, vanillic acid (VA), suggesting that the activity of anthocyanins on Hmox-1 expression observed *in vitro* may in fact be lost *in vivo* due to chemical degradation or bacterial catabolism. This is contrary to findings of others in our group, who have concluded that conjugation increases bioactivity in inflammatory mechanisms in endothelial and monocytic cell types (Amin et al., 2015, di Gesso et al., 2015), which further suggests that

conjugation may reduce efficacy of phenolic metabolites on oxidant-response mechanisms but may increase efficacy in inflammatory mechanisms.

It was surprising that no effect on Hmox-1 was observed in the present study in response to VA, given that a significant increase in HO-1 protein in human endothelial cells has previously been observed at this concentration (Edwards et al., 2015), which suggests cell type- and/or species-specific effects. A recent study of P3G on TNF- $\alpha$  stimulated adhesion molecules by endothelial cells (Krga et al., 2016) demonstrated that it was only bioactive at the physiologically achievable concentration of 0.1  $\mu$ M, but not at concentrations  $\geq$ 0.2  $\mu$ M. These data suggest that whereas effect on vascular biomarkers may be apparent *in vitro* at supraphysiological concentrations (as in the present study), this anthocyanin may act in inflammatory pathways at low, physiologically relevant concentrations (Kuntz et al. 2015).

PCA, a prominent metabolite common to multiple flavonoids subclasses (Schar et al., 2015, de Ferrars et al., 2014b), modestly (though not significantly,  $p=0.09$ ), increased Hmox-1 protein. It may be predicted that with increased concentration, this result may have reached significance, given that plasma concentrations may reach 16  $\mu$ M (Keane et al., 2015) and this could be validated in future studies. It should be noted that PCA does not circulate for extended periods of time, but is more likely to be methylated by catechol-O-methyl transferase (COMT) enzymes (Zhu, 2002) and circulate at higher levels as vanillic acid (de Ferrars et al., 2014b). Past studies have suggested that the catechol moiety was likely responsible for the activity of PCA (Kakkar and Bais, 2014). As such, further work is required on the effect of conjugation of the catechol group to establish its effects on mechanisms and magnitudes of effect.

7 mixtures of flavonoids and 11 mixtures of phenolic metabolites were designed based on their structural similarities and where activity was observed in our original screen (Figure 4.2; quercetin, P3G and PCA), and studied for their effect on Hmox-1 protein expression (Figure 4.3). Here, equimolar mixtures of substituents were utilised (to a cumulative concentration of 10  $\mu$ M, such that a mixture of 2 constituents would have equivalent concentrations of 5  $\mu$ M). Hmox-1 protein was increased in response to a mixture containing equimolar concentrations of hesperetin and P3G, though this was to the same relative magnitude as P3G in isolation at 10  $\mu$ M. These data either suggest additive activity or that this bioactivity is sustained by P3G at 5  $\mu$ M, which future studies could confirm by use of a concentration-response experiment. 4 mixtures of phenolic metabolites containing PCA actively increased Hmox-1 protein, which is of particular interest as the concentration used is achievable following flavonoid consumption (Schar et al., 2015) and therefore is a

potentially physiologically achievable effect. In a study by Keane *et al.*, following the feeding of 30 mL or 60 mL Montmorency tart cherry extract (equivalent to 90 or 180 cherries) to 12 healthy males (Keane *et al.*, 2015), mean peak concentrations of PCA and VA in plasma were 16  $\mu\text{M}$  and 2  $\mu\text{M}$ , respectively. These concentrations were doubled to 32  $\mu\text{M}$  and 4  $\mu\text{M}$  *in vitro* to include maximum achievable concentrations *in vivo* and utilised to determine their effect on VSMC proliferation and migration. No effect was observed in response to either metabolite in isolation, but a mixture of PCA+VA increased VSMC migration, suggestive of a beneficial, additive effect. Interestingly, the present study observed that PCA and VA, in isolation, also did not significantly increase Hmox-1 expression, but a combination consisting of 5  $\mu\text{M}$  of each metabolite (to a cumulative concentration of 10  $\mu\text{M}$ ) significantly upregulated Hmox-1 protein. This firstly may support the hypothesis that these abundant metabolites act additively on Hmox-1 expression and, secondly, may present a potential mechanism of action for the aforementioned *in vivo* experiment (Keane *et al.*, 2015), as Hmox-1 protein upregulation is positively associated with VSMC migration *in vitro*, which may prevent lesion rupture (Araujo *et al.*, 2012). Additionally, it has recently been demonstrated that angiotensin II-induced inflammation is inhibited by the synergistic activity of atorvastatin and cyanidin-3-glucoside in vascular smooth muscle cells (Pantan *et al.*, 2016), though an unmetabolised flavonoid, these data do support the evidence of additive or synergistic effects in VSMC and merit further exploration in future studies.

Effects of active treatments on Hmox-1 mRNA were investigated to infer potential mechanisms of action. Hmox-1 mRNA was only apparently increased in response to quercetin, but not to P3G or PCA. These data may suggest, as previously demonstrated in Chapter 3, that only quercetin is active on Hmox-1 transcription, which indicates activation of upstream transcription factor, Nrf2, which may be confirmed in future studies. The present investigation focused on the putative mechanisms of action of the phenolic metabolites, the vast majority of which were not active on downstream protein, Hmox-1. In addition, the effects observed for quercetin are already established in the literature (Liang *et al.*, 2013, Cho and Kim, 2013, Granado-Serrano *et al.*, 2012, Tanigawa *et al.*, 2007, Lin *et al.*, 2004) and therefore no mechanistic studies were carried forward.

The present study has provided novel insight into the effects of flavonoids and their metabolites on oxidant response protein, Hmox-1, in VSMCs, however, there were certain limitations to this work. The use of a rat-derived cell type, as opposed to human cells, may be seen as a limitation as the phenotypes and expression levels of cellular proteins may not be conserved between species (Kotokorpi *et al.*, 2007). An advantage to the use of RASMC

is that there is direct relevance of such bioactivity studies to animal studies which have observed the effects of quercetin-glucuronides/sulfate metabolites (Lodi et al., 2009) and anthocyanins (Ziberna et al., 2013). Effect size of vascular biomarkers in response to flavonoids may differ in rat relative to human cell types, and therefore, although cost prohibitive, future work should validate key findings in a human cell type, such as human coronary artery smooth muscle cells (HCASMCs), to confirm their relevance.

The treatment concentration (10  $\mu$ M) utilised in the present study may be seen as a limitation, certainly for the precursor flavonoids, and conjugated and unconjugated metabolites circulate at a vast range of concentrations (de Ferrars et al., 2014b). A more appropriate screening model would have been to screen the precursor flavonoids at 0.1  $\mu$ M and phenolic metabolites at 10  $\mu$ M, this would allow comparison at physiologically relevant concentrations but would not have allowed direct comparisons for structure-activity relationship investigations. Furthermore, 10  $\mu$ M may not be a concentration to which VSMC are exposed to, as these cells are not directly exposed to circulating factors in the blood, unlike endothelial cells. Future studies could improve the physiological relevance of this study by the development of an endothelial/VSMC co-culture model (Truskey, 2010).

In conclusion, the present study has demonstrated that 2 precursor flavonoids relevant to the UK diet and 1 associated metabolite induced Hmox-1 total protein in VSMCs, and that bioactivity is apparently increased in combination by additive or synergistic activity. To further these conclusions, future work is required to elucidate the individual bioactivities of the treatment constituents of these combinations and bioactivity within cellular signalling experiments should be explored to identify which mechanism(s) of action these treatments may act upon. The primary outcome of the present investigation was that only one of the investigated metabolites was (moderately) active on the biomarker investigated, whereas recent studies suggest that flavonoid metabolites may be more active in inflammatory mechanisms of action, such as inflammation-driven adhesion molecule expression (Krga et al., 2016, Amin et al., 2015), which will be the focus of the succeeding work (Chapters 5 & 6).

### **Acknowledgements**

Dr Ildefonso Rodriguez-Ramiro, a Research Assistant at Norwich Medical School, collected the raw data utilised for Figures 4.2-4.4 and Dr. Jason Kerr, previously a Research Associate at Norwich Medical School and UEA School of Pharmacy, collected the raw WST-1 data for Table 4.1.

## Chapter 5. Effect of flavonoids and their metabolites on inflammatory mechanisms in human endothelial cells.

### 5.1. Introduction

Positive associations have been made between diets high in flavonoid-rich foods and the reduced risk of cardiovascular disease (CVD; Wang et al., 2014), leading to studies focusing on biomarkers relating to direct vascular reactivity, affecting blood pressure, heart rate variability and flow mediated vasodilation (Kay et al., 2012, Ried et al., 2012). However, low level chronic inflammation, attributed to the expression of vascular adhesion molecules on the surface of the endothelium, has long been implicated as a driving factor in the early stages of atherosclerosis (Ley and Huo, 2001, Lusis, 2000). Tumour necrosis factor-alpha (TNF- $\alpha$ ) is a cytokine that serves as a mediator in a number of diseases, such as atherosclerosis, and stimulates the production of a number of pro-inflammatory biomarkers (Nakao et al., 2003), such as circulating levels of soluble vascular adhesion molecule-1 (sVCAM-1), an important predictor of risk of death from coronary heart disease (Blankenberg et al., 2001). TNF- $\alpha$  stimulated sVCAM-1 expression therefore provided a logical target for exploring the potential mechanisms of action of flavonoid metabolites in the present investigation.

Previous studies have demonstrated potentially beneficial effects of flavonoids on some inflammatory mechanisms *in vitro*, including inhibition of the adhesion of leukocytes to endothelial cells (Chanet et al., 2013, Chen et al., 2004, Claude et al., 2014). The mechanisms underlining these effects are unknown, potentially as previous *in vitro* investigations have focused on the activity of unmetabolised flavonoids, which are found in relatively low abundance in the circulation compared to their metabolites, and have considerably shorter half-lives (de Ferrars et al., 2014b, Pereira-Caro et al., 2014, Rodriguez-Mateos et al., 2014a, McKay et al., 2015). It has therefore been suggested that the biological activity observed in human studies results from the activity of products of flavonoid metabolism (i.e., products of bacterial catabolism, absorption and further phase II metabolism; Kay et al., 2009). Additionally, many past *in vitro* studies have utilised supraphysiological concentrations of precursor/unmetabolised flavonoids, while only a limited few have reported the activity of free phenolic acids (Edwards et al., 2015). Until recently (Amin et al., 2015, di Gesso et al., 2015) few have explored the activity of phase II conjugates of phenolic acid derivatives (Kling et al., 2014, Olejarz et al., 2014, Sevgi et al.,

2014, Juurlink et al., 2014), primarily as a result of the lack of availability of synthetic standards (Rodriguez-Mateos et al., 2014d).

The present study explored the hypothesis that phenolic metabolites of flavonoids have differential biological activities to their precursor structures, and that metabolites in combination may have additive or synergistic effects on inflammation. We therefore screened 6 flavonoids found commonly in the Western diet, 14 human metabolites, as previously reported (Czank et al., 2013, de Ferrars et al., 2014b, Rodriguez-Mateos et al., 2014a, Pereira-Caro et al., 2014), and 25 combinations of the flavonoids and their metabolites (at equimolar concentrations), for their ability to reduce sVCAM-1 protein secretion by TNF- $\alpha$  stimulated human umbilical vein endothelial cells (HUVECs). Concentration response relationships of the active treatments were also explored for their effect on protein and mRNA, including four physiological (between 0.01  $\mu$ M and 10  $\mu$ M) and one supraphysiological (100  $\mu$ M) concentration. The most active treatment was further assessed for activity on the transcription factor NF $\kappa$ B and on key kinases reported to regulate TNF- $\alpha$  –induced adhesion molecule expression (p38, JNK, ERK1/2, and Akt1).

## **5.2. Methods**

Experiment specific details are provided below while comprehensive methodological descriptors are provided in detail in Chapter 2.

### **5.2.1. Treatment solutions**

Stock solutions of flavonoids and metabolites were prepared in DMSO and stored as described in Chapter 2. Working solutions of 1 mM of each analyte were made up in supplemented media before being diluted to a final concentration of 0.01  $\mu\text{M}$ , 0.1  $\mu\text{M}$ , 1  $\mu\text{M}$ , 10  $\mu\text{M}$ , or 100  $\mu\text{M}$ , or to equimolar concentrations for treatments (for example, each in a mixture consisting of 4 constituents, each would be 0.25  $\mu\text{M}$ , to a cumulative concentration of 1  $\mu\text{M}$ ).

### **5.2.2. Cell culture**

Cryogenically stored, pooled donor, human umbilical vein endothelial cells (HUVECs) were cultured and maintained as described in Chapter 2. All cells were incubated for at least 24 hours at 37°C, 5 % CO<sub>2</sub>, in a humidified atmosphere, prior to experiment commencement. All cells were used between passages 3 and 4.

### **5.2.3. sVCAM-1 and sIL-6 protein expression**

HUVEC were seeded at 80,000 cells/well in fibronectin coated 24-well plates. For treatment effect experiments, cells were pre-treated for 30 min with 0.01  $\mu\text{M}$ , 0.1  $\mu\text{M}$ , 1  $\mu\text{M}$ , 10  $\mu\text{M}$ , or 100  $\mu\text{M}$  treatment solution, or 0.02 % DMSO (vehicle control) prior to the addition 10 ng/mL TNF- $\alpha$ , followed by 18 h incubation at 37°C, 5 % CO<sub>2</sub>, in a humidified atmosphere. Supernatants were collected on ice, centrifuged at 2000 x g for 10 min at 4°C, and stored at -80°C until required. Samples underwent a single freeze-thaw cycle, incubated to room temperature, and vortexed for 3 x 5 sec immediately prior to use. Supernatants were diluted 1:5 in Reagent Diluent #2 (R&D Systems) prior to commencing the assay, with the exception of the unstimulated control, which was not diluted. Protein expression of sVCAM-1 and sIL-6 were determined by commercially available enzyme-linked immunosorbent assay (ELISA), as described in Chapter 2.

### **5.2.4. VCAM-1 mRNA expression**

HUVEC were seeded at 200,000 cells/well in fibronectin coated 6-well plates. For treatment effect experiments, cells were pre-treated for 30 min with 0.01  $\mu\text{M}$ , 0.1  $\mu\text{M}$ , 1  $\mu\text{M}$ , 10  $\mu\text{M}$ , or 100  $\mu\text{M}$  treatment solution, 0.02 % DMSO (vehicle control) or 10  $\mu\text{M}$  BAY-11 7085 (NF $\kappa$ B inhibitor), prior to 4 h stimulation with 10 ng/mL TNF- $\alpha$ . Cell culture supernatants were removed and cells washed 3 x with PBS. Total RNA was extracted, reverse transcribed and

RT-qPCR carried out as described in Chapter 2. Reference genes, UBE2D2 and PRDM4, were used to normalise the data in subsequent experiments.

#### **5.2.5. NF $\kappa$ B p65, p38 MAPK, JNK, Akt, and ERK1/2 protein expression**

HUVEC were seeded at 200,000 cells/well in fibronectin coated 6-well plates. Cells were treated with 0.1  $\mu$ M, 1  $\mu$ M, 10  $\mu$ M, or 100  $\mu$ M protocatechuic acid (PCA) or 0.02 % DMSO (vehicle control) for 30 min followed by addition of TNF- $\alpha$  (10 ng/mL) for 15 min. Cells were washed 3x with PBS and cells lysed with NP-40 lysis buffer. Total protein concentrations were determined by BCA assay and proteins were separated and probed by SDS-PAGE and Western blotting, respectively, as described in Chapter 2. Densitometry values were normalised to GAPDH reference protein.

#### **5.2.6. Data analysis**

Protein (pg/mL) or mRNA (fold change) were recorded as the mean of two technical duplicates, and reported relative to the TNF- $\alpha$  positive control (containing TNF- $\alpha$  without DMSO) as a mean of three independent replicates  $\pm$  SD (n=3). Protein from Western blotting (infrared density) were reported as singular measures relative to TNF- $\alpha$  positive control (containing TNF- $\alpha$  without DMSO). Treatment effects for ELISAs, PCRs, and Western blots were established by one-way analysis of variance (ANOVA) with post-hoc least square difference (LSD) conducted using SPSS for Windows (version 22.0; IBM, New York, USA). Untreated and negative controls were not included in the ANOVA for treatment effect but presented graphically, where a student t-test established difference relative to vehicle control (DMSO) using Microsoft Excel (version 2013). Data were considered significant where  $p \leq 0.05$ . For screening purposes, treatments displaying nonsignificant values ( $p \leq 0.15$ ) were taken forward for validation in subsequent concentration analysis.

#### **5.2.7. Method optimisations**

Method optimisation experiments were conducted to identify the TNF- $\alpha$  concentration (10 ng/mL), stimulation time (18 h), for the upregulation of sVCAM-1 expression (**Figure 5.1**; Appendix, **Chapter 9.3**). The effect of concentration of PCA across each time point was determined when cells were either pre-treated or co-incubated with TNF- $\alpha$  (pre-treatment). The effect of PCA was in TNF- $\alpha$  stimulated HUVEC was also validated in HCAEC. Endogenous reference genes for normalisation of  $C_t$  data for target genes were selected based on previous optimisation experiments conducted by our group (Amin PhD thesis, 2014). TNF- $\alpha$  stimulated expression time of NF $\kappa$ B p65 and the phosphorylation of signalling kinases, Akt1, ERK1/2, p38 and JNK were determined (15 min).

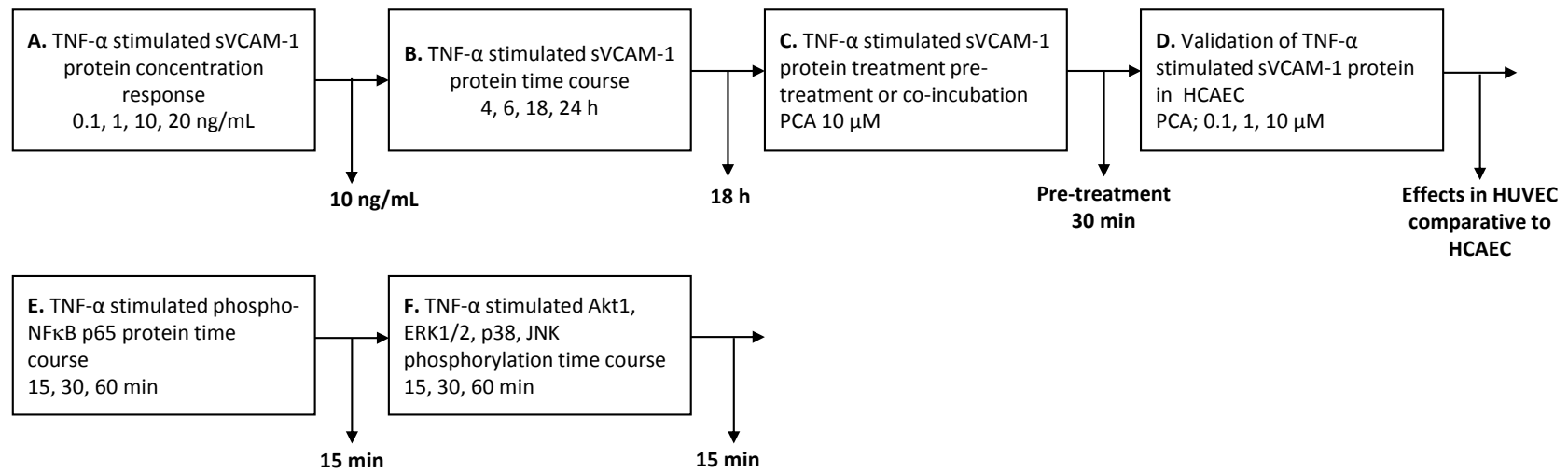


**Figure 5.1. Method optimisation experiments for Chapter 5- A-D) sVCAM-1 protein, E-F) NFκB p65 expression and signalling kinase expression.** See Appendix 9.3. Abbreviations: HCAEC, human coronary artery endothelial cells; HUVEC, human umbilical vein endothelial cells; PCA, protocatechuic acid; TNF-α, tumour necrosis factor α.

### **5.3. Results**

#### **5.3.1. Effect of flavonoids and their metabolites on TNF- $\alpha$ stimulated sVCAM-1 secretion**

6 flavonoids and 14 phenolic metabolites were screened at a concentration of 1  $\mu$ M for their ability to reduce TNF- $\alpha$  stimulated sVCAM-1 secretion by HUVECs (**Figure 5.2**). Precursor flavonoids had no effect on sVCAM-1 secretion, although there was a moderate, but non-significant ( $p=0.14$ ) increase in the secretion of sVCAM-1 following treatment with (-)-epicatechin. The metabolite PCA significantly decreased sVCAM-1 secretion ( $p=0.05$ ) and moderate but non-significant effects were observed for treatment with sulfate (PCA4S,  $p=0.07$ ; PCA3S  $p=0.14$ ) and glucuronide (IVA3G,  $p=0.15$ ) conjugates of PCA. Active treatments were taken forward to explore concentration response.

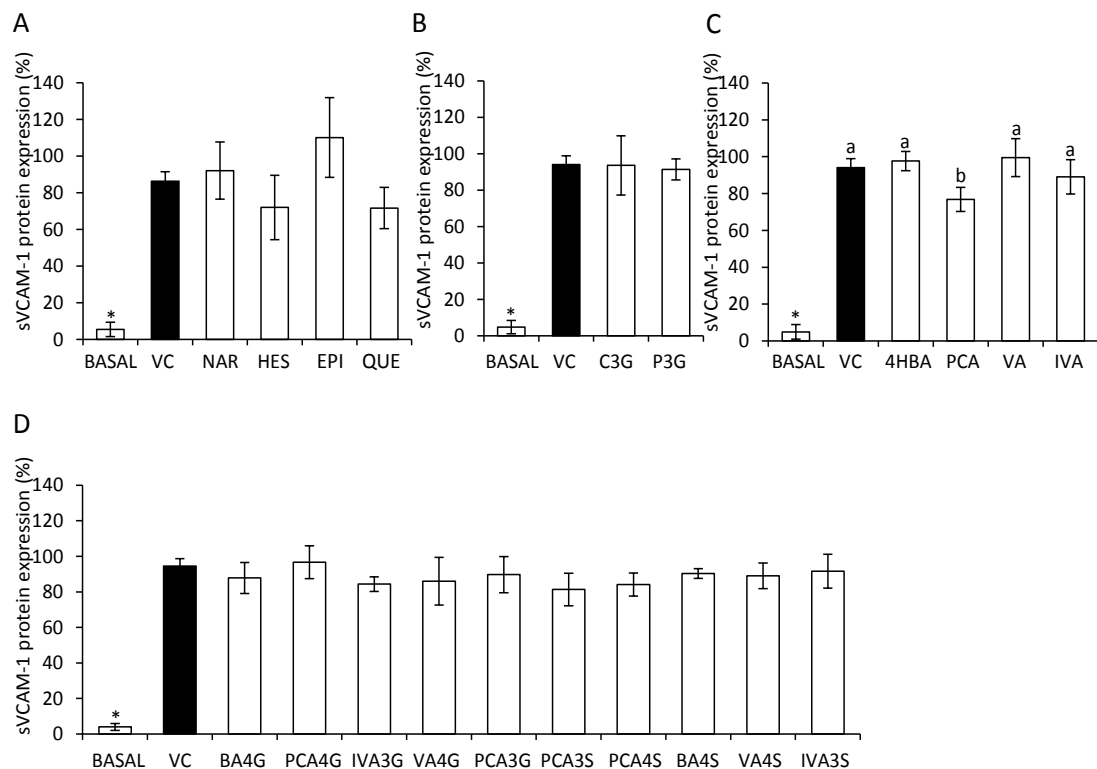


**Figure 5.2. Effect of flavonoids and phenolic acid metabolites on TNF- $\alpha$  stimulated sVCAM-1 protein secretion.** A) Flavonoids, B) Anthocyanin glucosides, C) Unconjugated phenolic acids, D) Conjugated phenolic acids. Data were normalized to a TNF- $\alpha$  control and columns represent the mean  $\pm$  SD of three independent experiments, n=3. Different letters indicate significant difference following post hoc LSD ( $p \leq 0.05$ ). Comparisons of untreated control relative to vehicle control (DMSO) were established via student t-test, \* $p \leq 0.05$ . Abbreviations: 4HBA, 4-hydroxybenzoic acid; BA4G, benzoic acid-4-glucuronide; BA4S, benzoic acid-4-sulfate; C3G, cyanidin-3-glucoside; EPI, (-) epicatechin; HES, hesperetin; IVA, isovanillic acid; IVA3G, isovanillic acid-3-glucuronide; IVA3S, isovanillic acid-3-sulfate; NAR, naringenin; P3G, peonidin-3-glucoside; PCA, protocatechuic acid; PCA3G, protocatechuic acid-3-glucuronide; PCA4G, protocatechuic acid-4-glucuronide; PCA3S, protocatechuic acid-3-sulfate; PCA4S, protocatechuic acid-4-sulfate; QUE, quercetin; VA, vanillic acid; VA4G, vanillic acid-4-glucuronide; VA4S, vanillic acid-4-sulfate.

Seven treatments containing mixtures of flavonoids and 18 treatments containing combinations of phenolic metabolites were also investigated for their effect on sVCAM-1 secretion (**Figure 5.3**), however, no activity was observed at a cumulative concentration of 1  $\mu$ M of the compounds.

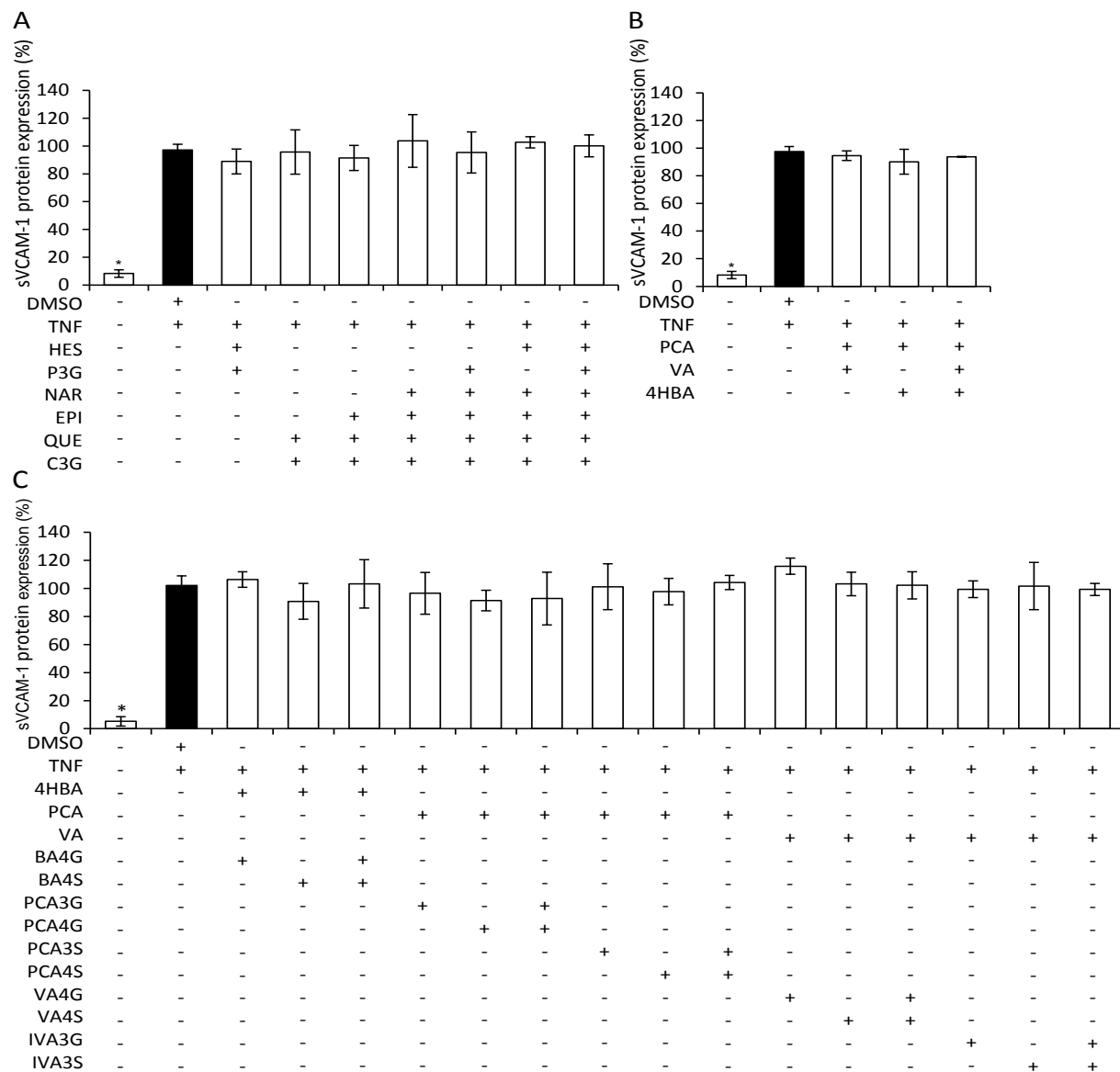


**Figure 5.3. Effect of mixtures of flavonoids and phenolic acid metabolites on TNF- $\alpha$  stimulated sVCAM-1 protein secretion.** A) Flavonoid mixtures, B) Phenolic acid mixtures, C) Conjugated and unconjugated phenolic metabolite mixtures. Data were normalized to a TNF- $\alpha$  control and columns represent the mean  $\pm$  SD of three independent experiments, n=3. Different letters infer significant difference following post hoc LSD ( $p \leq 0.05$ ). Comparisons of untreated control relative to vehicle control (DMSO) were established via student t-test. \* $p \leq 0.05$ . Abbreviations: 4HBA, 4-hydroxybenzoic acid; BA4G, benzoic acid-4-glucuronide; BA4S, benzoic acid-4-sulfate; C3G, cyanidin-3-glucoside; EPI, (-) epicatechin; HES, hesperetin; IVA, isovanillic acid; IVA3G, isovanillic acid-3-glucuronide; IVA3S, isovanillic acid-3-sulfate; NAR, naringenin; P3G, peonidin-3-glucoside; PCA, protocatechuic acid; PCA3G, protocatechuic acid-3-glucuronide; PCA4G, protocatechuic acid-4-glucuronide; PCA3S, protocatechuic acid-3-sulfate; PCA4S, protocatechuic acid-4-sulfate; QUE, quercetin; VA, vanillic acid; VA4G, vanillic acid-4-glucuronide; VA4S, vanillic acid-4-sulfate.

### **5.3.2. Effect of concentration of PCA and IVA metabolites on sVCAM-1 secretion.**

sVCAM-1 secretion was investigated following treatment with 0.01  $\mu\text{M}$  -100  $\mu\text{M}$  of the active treatments PCA, PCA3S, PCA4S, and IVA3G (**Figure 5.4**). IVA, although not active in the sVCAM-1 protein screen, was also included in order to establish structure-activity relationships with PCA and IVA conjugates. Here, PCA significantly reduced sVCAM-1 levels in a concentration dependent manner between 1  $\mu\text{M}$  and 100  $\mu\text{M}$ , while PCA3S and IVA were only active at levels between 10  $\mu\text{M}$  and 100  $\mu\text{M}$ , and PCA4S and IVA3G were only active at 100  $\mu\text{M}$

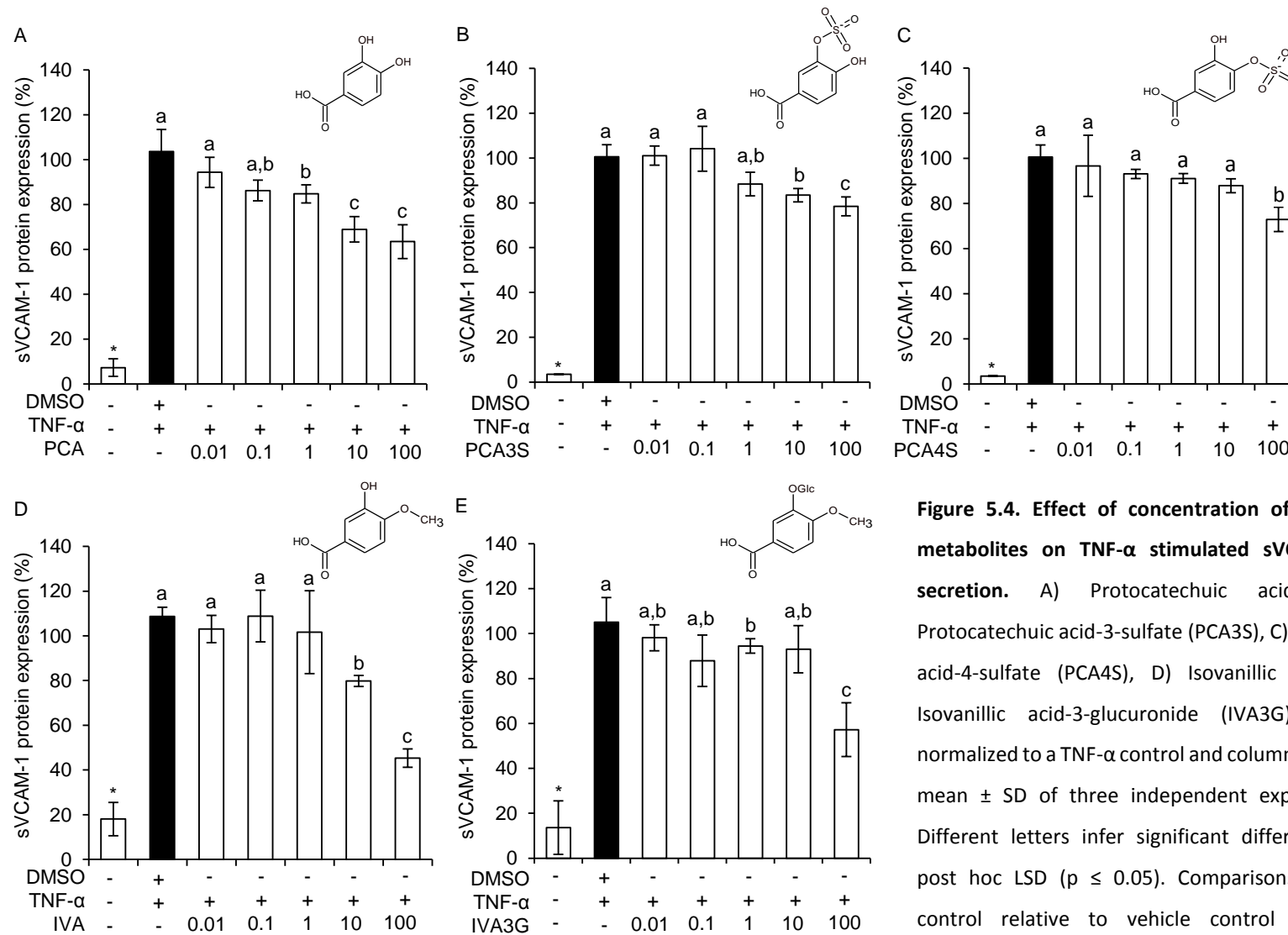


**Figure 5.4. Effect of concentration of phenolic acid metabolites on TNF-α stimulated sVCAM-1 protein secretion.** A) Protocatechuic acid (PCA), B) Protocatechuic acid-3-sulfate (PCA3S), C) Protocatechuic acid-4-sulfate (PCA4S), D) Isovanillic acid (IVA), E) Isovanillic acid-3-glucuronide (IVA3G). Data were normalized to a TNF-α control and columns represent the mean ± SD of three independent experiments, n=3. Different letters infer significant difference following post hoc LSD ( $p \leq 0.05$ ). Comparisons of untreated control relative to vehicle control (DMSO) were established via Student's t-test, \* $p \leq 0.05$

### 5.3.3. Effect of PCA metabolites on sIL-6 protein expression.

To determine whether the apparent concentration responsive effects of PCA, PCA3S, and PCA4S on sVCAM-1 were pathway specific, the effects of these metabolites were investigated for a differentially regulated, secreted inflammatory biomarker, soluble interleukin-6 (sIL-6), in response to TNF- $\alpha$  stimulation (**Figure 5.5**). sIL-6 protein expression was significantly increased up to 14 fold ( $p \leq 0.001$ ) following 18 h stimulation with TNF- $\alpha$ . Pre-incubation with PCA, PCA3S or PCA4S did not have any significant effects on sIL-6 secretion.

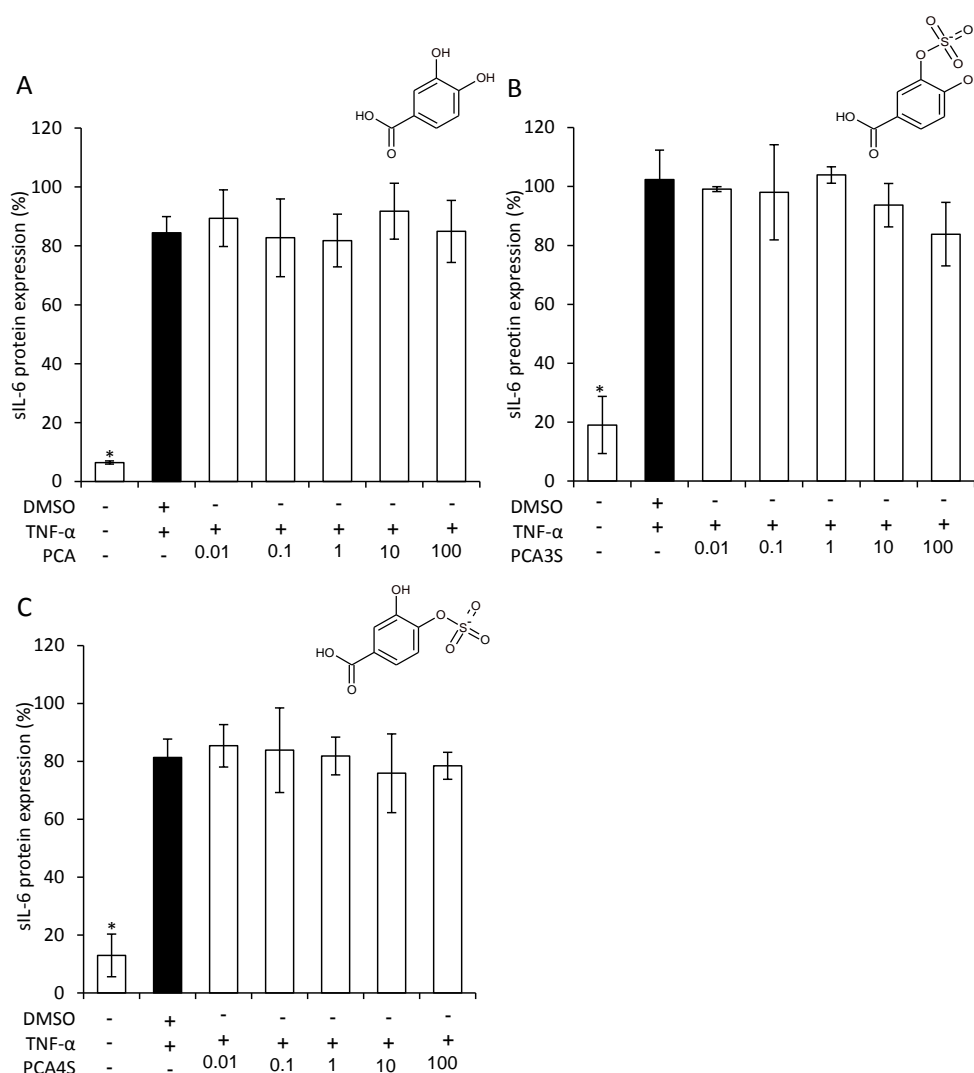


**Figure 5.5. Effect of concentration of phenolic acid metabolites on TNF- $\alpha$  stimulated sIL-6 protein secretion.** A) Protocatechuic acid (PCA), B) Protocatechuic acid-3-sulfate (PCA3S), C) Protocatechuic acid-4-sulfate (PCA4S). Data were normalized to a TNF- $\alpha$  control and columns represent the mean  $\pm$  SD of three independent replicates ( $n=3$ ). Comparisons between treatments were determined using one-way ANOVA with post hoc LSD. The comparisons between an untreated control relative to vehicle control (DMSO) were established via Student's t-test,  $*p \leq 0.001$ .

#### **5.3.4. Effect of PCA and IVA metabolites on VCAM1 mRNA expression**

To identify whether the effects on sVCAM-1 protein were mirrored in VCAM1 mRNA expression, HUVECs were treated with PCA, PCA3S, PCA4S, IVA or IVA3G at concentrations between 0.01  $\mu$ M and 100  $\mu$ M (**Figure 5.6**). TNF- $\alpha$  significantly induced VCAM-1 mRNA expression after 4 h ( $p \leq 0.01$ ), and this effect was fully inhibited by treatment with the negative control ( $\text{I}\kappa\text{B}\alpha$ -inhibitor, BAY 11-7085). Treatment with 100  $\mu$ M PCA was the only treatment to significantly inhibit VCAM-1 mRNA expression (78 % inhibition).

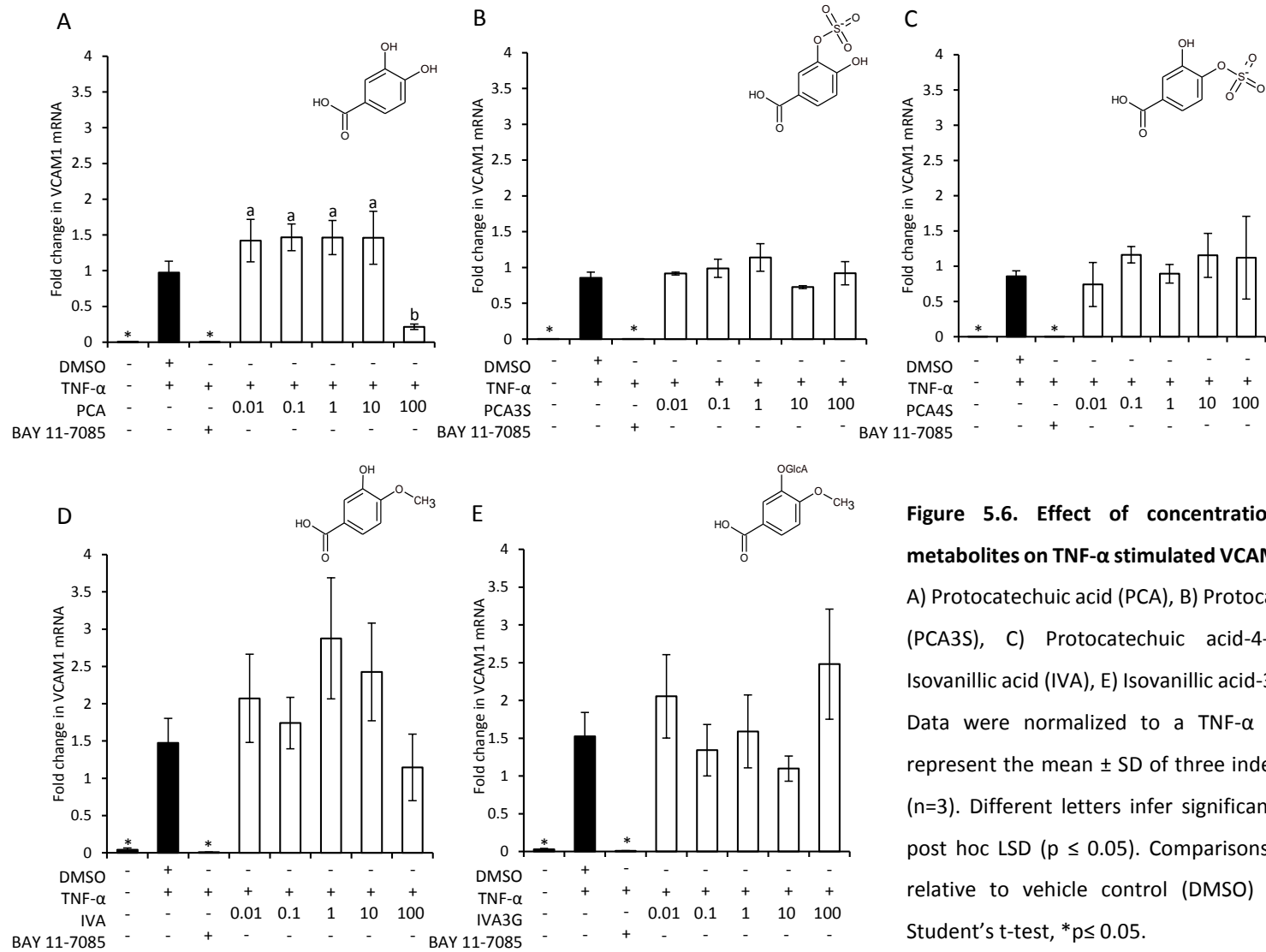


**Figure 5.6. Effect of concentration of phenolic acid metabolites on TNF- $\alpha$  stimulated VCAM-1 mRNA expression.** A) Protocatechuic acid (PCA), B) Protocatechuic acid-3-sulfate (PCA3S), C) Protocatechuic acid-4-sulfate (PCA4S), D) Isovanillic acid (IVA), E) Isovanillic acid-3-glucuronide (IVA3G). Data were normalized to a TNF- $\alpha$  control and columns represent the mean  $\pm$  SD of three independent experiments (n=3). Different letters infer significant difference following post hoc LSD ( $p \leq 0.05$ ). Comparisons of untreated control relative to vehicle control (DMSO) were established via Student's t-test, \* $p \leq 0.05$ .

### 5.3.5. Effect of TNF- $\alpha$ stimulation on NF $\kappa$ B pathway activation

The effects of PCA (0.1  $\mu$ M - 100  $\mu$ M) were tested for their effect on NF $\kappa$ B pathway activation. Expression of phosphorylated p65 (Figure 5.7) was significantly increased relative to the vehicle control, whereas the I $\kappa$ B $\alpha$  inhibitor, Bay 11-7085, significantly inhibited this expression ( $p \leq 0.001$ ). No differential effects were observed on either biomarker in response to PCA. Other TNF- $\alpha$  activated signalling kinases were therefore further investigated to elucidate PCA mechanism of action.

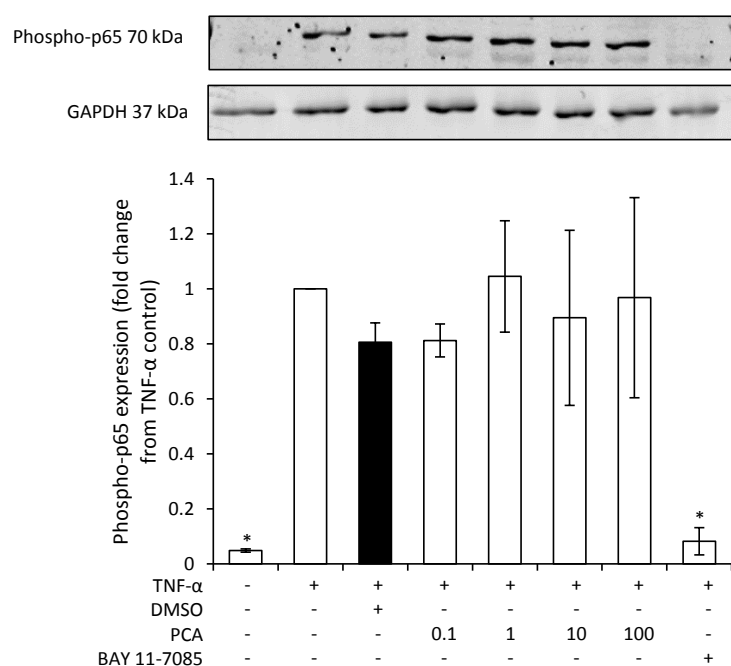


**Figure 5.7. Concentration response of PCA on NF $\kappa$ B p65 phosphorylation.** Data were normalized to an unstimulated control and columns represent the mean  $\pm$  SD of three independent replicates ( $n=3$ ). Treatment effects were compared by use of a one-way ANOVA with post hoc LSD ( $p \leq 0.05$ ). Comparisons of untreated or negative control relative to vehicle control (DMSO) were established via Student's t-test,  $*p \leq 0.05$ .

### 5.3.6. Effect of PCA on TNF- $\alpha$ stimulated signalling kinase phosphorylation

The effects of PCA (0.1  $\mu$ M - 100  $\mu$ M) were tested for their effect on TNF- $\alpha$  stimulated Akt1, ERK, p38, and JNK phosphorylation (Figure 5.8). No differential effects were observed on kinase phosphorylation following treatment with PCA.

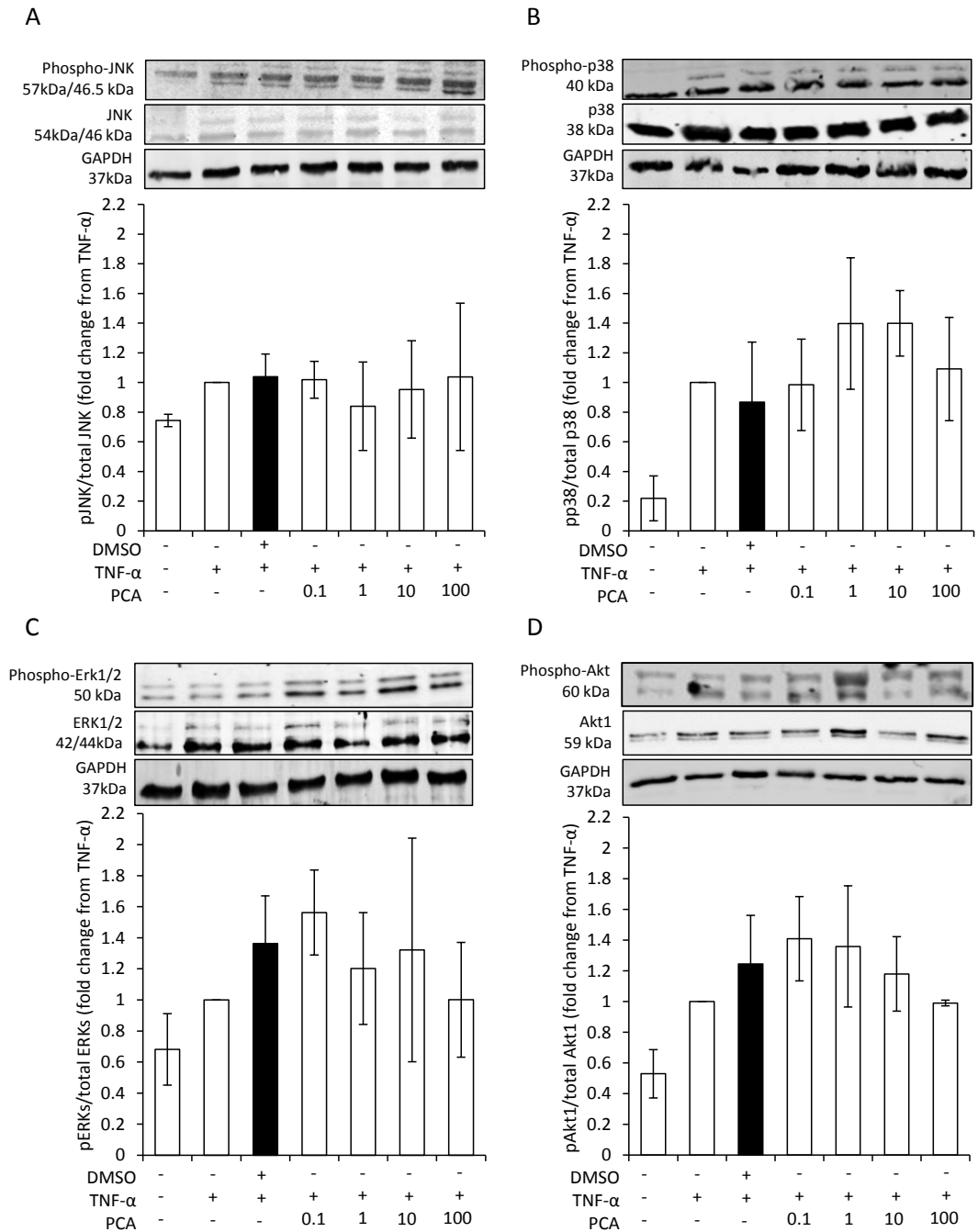


**Figure 5.8. Concentration response of PCA on signalling kinase phosphorylation.** Data were normalized to a TNF- $\alpha$  control and columns represent the mean of three independent replicates  $\pm$  SD (n=3). Blots are representative of one of three independent replicates. Treatment effects were compared by use of a one-way ANOVA with post hoc LSD ( $p \leq 0.05$ ). Comparisons of untreated or negative control relative to vehicle control (DMSO) were established via Student's t-test, \* $p \leq 0.05$ .

## 5.4. Discussion

Previous studies have demonstrated potentially beneficial effects of flavonoids on inflammation *in vivo*, including inhibition of the adhesion of leukocytes to endothelial cells (Chen et al., 2002, Wang et al., 2010). However, the mechanisms underlining these effects are unknown, potentially as previous *in vitro* investigations have focused on the activity of unmetabolised flavonoids, which are found in low abundance in the circulation compared to their chemical degradants, bacterial catabolites, and phase II metabolites (Kay, 2010, Murota and Terao, 2003).

sVCAM-1 was a logical target to investigate the vasoprotective activity of flavonoids as it is a clinical predictor of risk of death from cardiovascular disease (Blankenberg et al., 2001) and previous studies have demonstrated beneficial effects of flavonoids on adhesion of leukocytes to endothelial cells (Chanet et al., 2013, Chen et al., 2004b, Claude et al., 2014). Only the phenolic metabolites of flavonoids inhibited sVCAM-1 protein secretion in a model of pro-inflammatory stress (i.e. TNF- $\alpha$  stimulation), which supports the hypothesis that common phenolic metabolites have differential activities to their precursor structures. These findings are supported by additional recent studies demonstrating that metabolites were active on sIL-6 and sVCAM-1 production following stimulation with CD40 and oxidised-LDL (oxLDL) in vascular endothelial cells and TNF- $\alpha$  following LPS stimulation in human monocytes (Amin et al., 2015, di Gesso et al., 2015).

In the present study, 20 flavonoids and their metabolites and 25 combinations of structurally similar compounds were explored for their effects in TNF- $\alpha$  stimulated HUVECs. Four phenolic metabolites demonstrated inhibitory activity on sVCAM-1 secretion. PCA demonstrated the greatest activity, displaying a strong inhibitory effect on sVCAM-1, which appeared to be amplified with increased concentration. Inhibition of VCAM-1 mRNA was observed in response to PCA, however, this was only apparent at a supraphysiological concentration of 100  $\mu$ M and did not appear to affect NF $\kappa$ B pathway activation or other signalling kinase activations at any of the concentrations used (0.1  $\mu$ M- 100  $\mu$ M). Furthermore, mixtures of metabolites and flavonoids showed no activity toward sVCAM-1, suggesting no additive activity at sub-micromolar concentrations (cumulative concentrations adding up to 1  $\mu$ M).

Five treatments were further explored for their concentration-responsive effects on sVCAM-1 protein (Figure 5.4), four of these (PCA, PCA3S, PCA4S, and IVA3G) demonstrated inhibition of sVCAM-1, and one (IVA) was selected to draw conclusions regarding structure-activity relationships between the PCA and IVA conjugates. Of the compounds screened,

PCA was the most active across the concentration range tested, and this activity is in line with previous studies, where it has been shown to inhibit the expression of inflammatory mediators, including adhesion molecules (Kakkar and Bais, 2014, Min et al., 2010). The activity of PCA is comparable to its aldehyde equivalent (protocatechuic aldehyde), in a recent report identifying a dose-dependent reduction in the TNF- $\alpha$  stimulated sVCAM-1 (Zhou et al., 2005); this supports the premise that the catechol moiety of flavonoid metabolites holds significant anti-inflammatory activity (Rimbach et al., 2004). As discussed in Chapter 4, it should be noted that PCA, given its reactive catechol moiety, is rapidly methylated by catechol-O-methyltransferase (COMT; Zhu, 2002) and does not persist in the systemic circulation at any appreciable concentration for significant periods of time (de Ferrars et al., 2014a, Czank et al., 2013, de Ferrars et al., 2014b), whereas its metabolite, vanillic acid (VA), for example, is reported to exist at much higher concentrations and have a considerably longer half-life (de Ferrars et al., 2014a, Czank et al., 2013, de Ferrars et al., 2014b, Schar et al., 2015).

The lack of dietary relevance of contemporary cell culture studies in the field of nutrition is apparent, given the use of precursor structures at supraphysiological concentrations, which may explain why the underlying mechanisms of action of many phytochemicals (such as flavonoids) are still unknown (Kay, 2010). It is therefore interesting that we observed a trend in the inhibition of sVCAM-1 in response to PCA at concentrations as low as 0.1  $\mu$ M, as previous studies have identified serum concentrations of PCA ranging between 0.15  $\mu$ M (de Ferrars et al., 2014b) and 1.5  $\mu$ M (Vitaglione et al., 2007, de Ferrars et al., 2014a) after consumption of a pure cyanidin-3-glucoside, fruit juice, or elderberry extract, suggesting that this concentration and effect is achievable through diet.

We sought to explore if the observed effect on sVCAM-1 protein was reflected in the expression of VCAM-1 mRNA, as advocated by others (Wang et al., 2010, Amin et al., 2015). PCA was only active here at 100  $\mu$ M, suggesting PCA is not directly active on mRNA transcription or in other relevant signalling pathways investigated (NF $\kappa$ B, JNK, p38, Akt1, ERK1/2), at physiologically achievable concentrations, but it is therefore likely acting post-translationally, such as through other cellular enzymes, e.g. glutathione peroxidase (GPx; d'Alessio et al., 1998), this would be an interesting line of enquiry, as other studies have shown upregulation of GPx following treatment with quercetin (Granado-Serrano et al., 2012) and catechin (Simos et al., 2012). Additionally, it is conceivable that flavonoids or their metabolites could interact with the cleavage of the protein from the surface of endothelial cells (Videm and Albrigtsen, 2008), such as by interaction with TNF- $\alpha$  converting

enzyme, ADAM17 (Garton et al., 2003), a suggested mediator of VCAM-1 shedding from the surface of endothelial cells. Future cell culture studies exploring the mechanisms of action of PCA at physiological concentrations may elucidate alternative post-translational or receptor-binding activities.

Investigations of structure-activity relationships (SAR) are important to improving our understanding of how metabolism alters phytochemical activity. As previous studies have reported the SAR of flavonoids (Martinez-Fernandez et al., 2015, Lotito and Frei, 2006), we aimed to draw conclusions based on relationships between conjugated and unconjugated phenolic metabolites. Of the 5 metabolites studied in detail, PCA had the greatest inhibitory effect on sVCAM-1 secretion, with PCA3S, PCA4S and IVA having equally lesser activity, and IVA3G having little or no effect (**Figure 5.9**), suggesting that sequential conjugation the hydroxyl and carboxyl moieties systematically reduces potency on sVCAM-1 secretion.

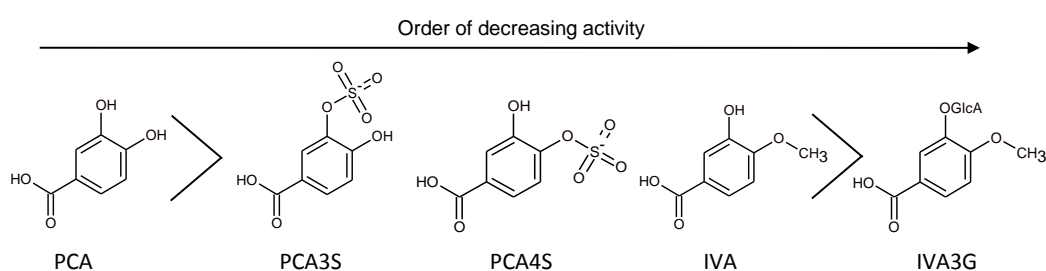


**Figure 5.9. Relative inhibition of sVCAM-1 in response to PCA, PCA3S, PCA4S, IVA, and IVA3G, at 10  $\mu$ M.** Structures are presented in the order of decreasing activity. Statistical comparisons were established using one-way ANOVA with post hoc LSD, where > sign represents a significant difference in effect between compounds ( $p \leq 0.05$ ). Abbreviations: PCA, protocatechuic acid; PCA3S, protocatechuic acid-3-sulfate; PCA4S, protocatechuic acid-4-sulfate; IVA, isovanillic acid; IVA3G, isovanillic acid-3-glucuronide.

Conjugation of certain flavonoids has been shown to reduce their inhibitory activity on monocyte adhesion, and this has been attributed to the loss of a hydroxyl group (Rimbach et al., 2004, Winterbone et al., 2009), however, the opposite has recently been reported in oxLDL stimulated HUVECs, where conjugation of PCA increased the activity on sVCAM-1 (Amin et al., 2015), suggesting that the effects of conjugation is dependent on the inflammatory stimulus, and thus the upstream signal transduction pathway involved, which has also been suggested for other precursor flavonoids (Xu et al., 2007). This again may support the hypothesis that mechanisms of action lie upstream of key signal transduction pathways. Overall, this SAR analysis supports the theory that PCA bioactivity is related to

its catechol moiety and substitution of these systematically reduces activity. Therefore, it is possible that there are differential bioactivities of flavonoid metabolites post-consumption, as they are systematically metabolised and eliminated from the circulation.

Flavonoids and their metabolites do not circulate in isolation following ingestion, but exist as complex mixtures of metabolites at various concentrations (Czank et al., 2013, Pereira-Caro et al., 2014, Serra et al., 2012), thus it is important that this is reflected in the design of cell culture experiments exploring the bioactivities of dietary components. Few studies have explored the effects of flavonoids in combination, despite some indication of differential activities when in combination relative to isolation (Koga and Meydani, 2001, Harasstani et al., 2010). In the present study we explored an extensive array of mixtures of flavonoids and flavonoid metabolites (25 mixtures in total). Inhibitory effects on sVCAM-1 secretion from mixtures totalling 1  $\mu\text{M}$  in concentration (cumulative concentration of analytes present in an equimolar ratio) were not observed in the present study. Here, treatments represented concentrations of each analyte between 0.5  $\mu\text{M}$  and 0.17  $\mu\text{M}$  and it is possible that these concentrations were too low to elicit a quantifiable response, whereas a recent human study identified total phenolic metabolites to reach 13.3  $\mu\text{M}$  following consumption of orange juice (Schar et al., 2015), thus greater cumulative concentrations are indicated in future cell culture studies. Given that mixtures of phenolic metabolites have shown differential effects to their constituents in isolation in LPS stimulated THP-1 cells (di Gesso et al., 2015), cumulative effects of these metabolites may be cell-type or stimulus specific. It is possible that the non-natural construction of equimolar concentrations of analytes does not render activity, and that a more appropriate method to investigate additive or synergistic effects would be to mimic mixtures/profiles of serum metabolites reported following human consumption studies; this was the focus of a future investigation (Chapter 6).

This study has provided novel insight into the differential activity of flavonoid metabolites compared to their precursor structures, and explored their potential for additive effects, though there are certain limitations of this work. Firstly, the measurement of soluble VCAM-1 over membrane-bound VCAM-1 could be seen as a limitation as it is the membrane-bound VCAM-1 that binds directly to leukocytes in the progression of atherosclerosis (Lusis, 2000). However, it has been reported that sVCAM-1 protein levels directly correlate with levels of surface-bound VCAM-1 (Kjaergaard et al., 2013) and sVCAM-1 has been suggested as a more appropriate biomarker of endothelial cell activation (Videm and Albrigtsen, 2008); that said, further investigation of the relative activity of these

metabolites on surface-bound VCAM-1 would verify such correlations (Kjaergaard et al., 2013). The cell culture model utilised could be considered a limitation, as HUVECs do not originate from the arterial walls, however, HUVECs are a well characterised cell type used extensively to study endothelial dysfunction and a validation study (Appendix; Chapter 9.3.4) regarding the effect of PCA on human coronary artery endothelial cells (HCAECs) appears to suggest that the two cell types have similar responses to both TNF- $\alpha$  and PCA. These data are in support of previous studies demonstrating that both cell types provide similar protein and mRNA response (Luu et al., 2010). The concentration of TNF- $\alpha$  (10 ng/mL) used to stimulate sVCAM-1 in the present study could also be viewed as a limitation. 10 ng/mL was selected as it is a commonly reported concentration utilised in the literature (Catalan et al., 2012, Chen et al., 2002, Kwon et al., 2005, Zhou et al., 2005), however, physiologically, plasma concentrations are reported as low as 0.001-0.04 ng/mL in patients with coronary artery disease (Aydin et al., 2009) but may reach 2 ng/mL in patients who have suffered myocardial infarction (Skoog et al., 2002). The secretion of sVCAM-1 in response to TNF- $\alpha$  stimulated HUVEC was ten-fold less than HCAEC, so the use of physiological concentrations of TNF- $\alpha$  may have made detection of effects difficult, as such the study presented in Chapter 6 explored the most appropriate concentration of TNF- $\alpha$  by use of a concentration-response experiment. The stimulation time of 18 h was chosen as this was consistently reported in the literature (Chen et al., 2001, Zhou et al., 2005) and validated in preliminary experiments (Appendix; Chapter 9.3), however, theoretically, each metabolite could have different time points of maximal activity, which could also be explored in future time-course experiments. Furthermore, the design of the treatment mixtures used in this investigation was quite artificial, as equimolar ratios would do not reflect serum concentrations observed in human studies, however, given the large variation in plasma metabolites observed between subjects in these studies, this was a practical way to elucidate additive effects. As discussed above, future studies could utilise metabolites at range of concentrations based on levels reported in human feeding studies (de Ferrars et al., 2014b, Pereira-Caro et al., 2014, Rodriguez-Mateos et al., 2014a), as will be the focus of Chapter 6.

It is known that flavonoids rarely survive the process of first pass metabolism in their native state (Kay et al., 2005), as evident from the low bioavailability reported for precursor flavonoids (Pimpão et al., 2014, Pimpão et al., 2015, Schar et al., 2015). Instead, flavonoids persist in the systemic circulation as methylated, glucuronidated, and sulfated forms of flavonoid and phenolic derivatives (Day et al., 2001, Mullen et al., 2006, Czank et al., 2013,

de Ferrars et al., 2014b). The present study supports previous reports that metabolism of flavonoids to phenolic acids alters their anti-inflammatory effects (Lotito et al., 2011, Al-Shalmani et al., 2011, Lodi et al., 2012, Lotito and Frei, 2006). These data indicate that the degradation of flavonoids to phenolic acids, which is believed to be largely facilitated by microbiota in the colon (de Ferrars et al., 2014b, Serra et al., 2012), increases their overall bioactivity, whereas further conjugation by phase II enzymes may have differential effects on activity (Amin et al., 2015, di Gesso et al., 2015). Therefore, certain flavonoids consumed in our habitual diet may require prior metabolism before they can exert their maximal effects and metabolites may possess differential bioactivities as they are systematically metabolised and eliminated from the circulation.

In conclusion, the present study provides novel insight into the anti-inflammatory activity of conjugated and unconjugated phenolic metabolites of flavonoids contributing to our understanding of how these dietary phytochemicals contribute to cardiovascular health.

#### **Acknowledgements**

James Catton, a Molecular Medicine MSc. Student at the University of East Anglia, collected the raw data used for Figure 5.8.

## **Chapter 6. Effect of peak serum anthocyanin metabolite profiles on inflammatory mechanisms in human coronary artery endothelial cells.**

### **6.1. Introduction**

The understanding of anthocyanin metabolism is relatively contemporary, though it is commonly accepted that their degradation is a result of their chemical instability and the impact of bacterial catabolism, resulting in a number of circulating phenolic acid metabolites (Keppler and Humpf, 2005, Kay et al., 2005). The phenolic metabolites also undergo extensive phase II metabolism (Stalmach et al., 2013), resulting in a diversity of conjugated structures (Pimpão et al., 2015). As anthocyanin metabolites do not circulate in isolation following ingestion, but exist as complex mixtures of metabolites at various concentrations (Czank et al., 2013, Pereira-Caro et al., 2014, Serra et al., 2012), it is important that this is also reflected in the design of experiments exploring the bioactivities of anthocyanins.

As anthocyanin metabolites are now known to be the primary circulating structures post consumption, the study of their activity has become the primary focus of recent works. Anthocyanin metabolites have been shown to inhibit the expression of a number of inflammatory biomarkers, such as those involved in vascular adhesion and chemotaxis (Mauray et al., 2012), which are important in the pathogenesis of chronic inflammatory diseases (Gimbrone and Garcia-Cardena, 2016). Soluble vascular cellular adhesion molecule-1 (sVCAM-1) is an important predictor of death from coronary artery disease (Blankenberg et al., 2001) and a common biomarker of endothelial activation (Videm and Albrigtsen, 2008). Equally, high levels of soluble interleukin-6 (sIL-6) is significantly associated with cardiovascular mortality (Su et al., 2013). We have recently shown that certain phenolic metabolites of flavonoids (e.g. protocatechuic acid (PCA)) inhibit TNF- $\alpha$  stimulated secretion of sVCAM-1 by human umbilical vein endothelial cells (HUVEC; Warner et al., 2016), and our group have also demonstrated this effect on sIL-6 (Amin et al., 2015). sVCAM-1 and sIL-6 therefore provided logical targets for exploring the potential mechanisms of action of anthocyanin metabolites in the present investigation.

In our recent study (Chapter 5; Warner et al., 2016), equimolar mixtures of phenolic metabolites totaling 1  $\mu$ M did not affect secretion of sVCAM-1 by HUVEC. It was suggested that these concentrations were too low to elicit a quantifiable response, whereas recent

human studies have identified total phenolic metabolites at concentrations magnitudes higher (Schar et al., 2015) and, as such, exploring greater cumulative concentrations (> 10  $\mu\text{M}$ ) are indicated. The present study therefore explored the activity of mixtures of metabolites between 0.19  $\mu\text{M}$  and 43  $\mu\text{M}$ .

The metabolism of a common dietary anthocyanin, cyanidin-3-glucoside (C3G), was recently investigated and 29 metabolites were identified following the consumption of 500 mg  $^{13}\text{C}$ -labelled cyanidin-3-glucoside (C3G; Czank et al., 2013, de Ferrars et al., 2014b; **Figure 6.1**). 3 distinct peaks in C3G metabolites were observed postprandially; one at 0.5 h -1 h, one at 6 h and one at 24 h; each spike/peak in blood levels represented distinct metabolite profiles. These peaks in blood metabolites have also been observed following consumption of cocoa flavan-3-ols (Vitaglione et al., 2013) and citrus flavanones (Pereira-Caro et al., 2015), suggesting this is a common modal response for the kinetics of flavonoids metabolites. Given that these phenolics circulate at higher concentrations for longer periods of time relative to their precursors, there is scope to investigate the collective activity of unique profiles of phenolic metabolites on inflammatory mechanisms in the present investigation.

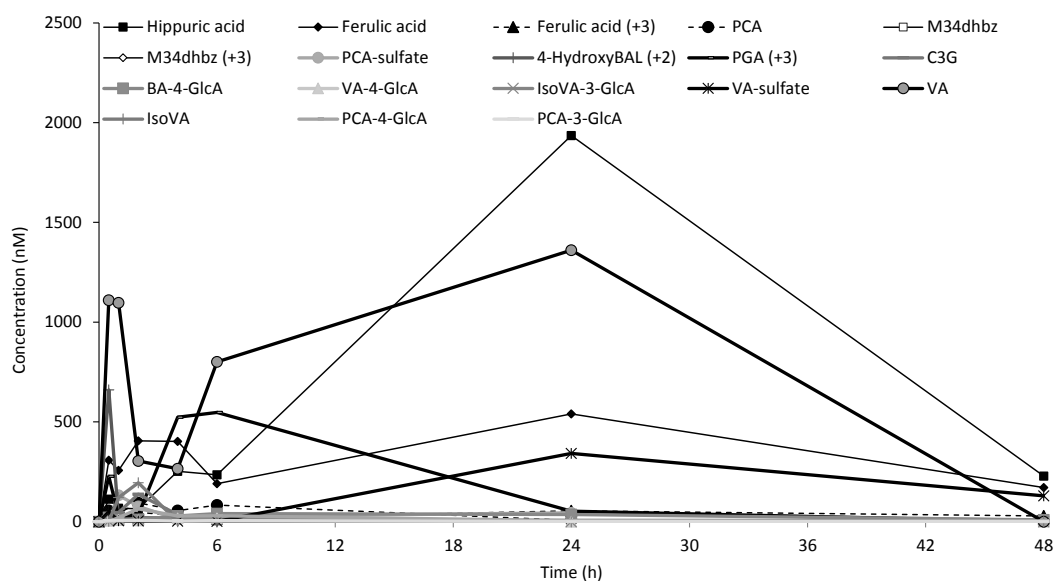


**Figure 6.1. Serum pharmacokinetic profiles of C3G and its metabolites in humans after the consumption of 500 mg  $^{13}\text{C}_5$ -C3G in eight healthy male participants.** Data represent mean concentration of specified metabolites from 8 participants. Abbreviations: BA, benzoic acid; BAL, benzaldehyde; C3G, cyanidin-3-glucoside; GlcA, glucuronide; M34dhbz, methyl-3, 4-dihydroxybenzoate; PCA, protocatechuic acid; PGA, phloroglucinaldehyde; VA, vanillic acid. Adapted from (de Ferrars et al., 2014b).

The primary aim of the present study was to investigate the effects of unique serum profiles of C3G metabolites observed to peak *in vivo* at 1 h, 6 h, and 24 h post consumption on sVCAM-1 and sIL-6 protein secretion by human coronary artery endothelial cells (HCAECs). The secondary aim was to investigate the effects of metabolite profiles across a range of concentrations, reflecting levels ten-fold lower (<0.5  $\mu\text{M}$ ) and ten-fold higher (<50  $\mu\text{M}$ ) than mean concentrations (<5  $\mu\text{M}$ ) observed by Czank *et al.* (Czank *et al.*, 2013). Finally, the effects of the highest concentrations (<50  $\mu\text{M}$ ) were studied to establish their mechanistic effects on VCAM-1 and IL-6 mRNA and by targeting key inflammatory targets (NF $\kappa$ B p65, p38 MAPK, and JNK).

## 6.2. Methods

Experiment specific details are provided below while comprehensive methodological descriptors are provided in detail in Chapter 2.

### 6.2.1. Treatment solutions

Stock solutions were prepared and stored as described in Chapter 2. Working solutions of 1 mM of each required treatment constituent were prepared in supplemented media before being diluted to their highest working concentration (1.9  $\mu$ M, 2.0  $\mu$ M, 4.4  $\mu$ M as observed at 1 h, 6 h, 24 h respectively; Czank et al., 2013; **Table 6.1**) and stored at 4°C, with the exception of cyanidin-3-glucoside, which was added immediately prior to the final dilutions in order to maintain stability. Solutions were subsequently diluted in supplemented media as required (Table 6.1) immediately prior to experiment commencement.

**Table 6.1: Serum profile mixture constituents and concentrations**

Analyte	Final profile concentration (nM)								
	1 h profile			6 h profile			24 h profile		
C3G	5	50	500	0	0	0	0	0	0
PCA	4	40	400	8	80	800	1	10	100
PGA	3	30	300	55	550	5500	5	50	500
BA -4-Glc	1	10	100	4	40	400	4	40	400
PCA-4-Glc	2	20	200	3	30	300	0	0	0
PCA-3-Sul	7	70	700	2	20	200	2	20	200
PCA-4-Sul	7	70	700	2	20	200	2	20	200
VA	110	1100	11000	80	800	8000	136	1360	13600
IVA	12	120	1200	0	0	0	0	0	0
VA-4-Glc	1	10	100	2	20	200	0	0	0
IVA-3-Glc	1	10	100	2	20	200	0	0	0
VA-4-Sul	0	0	0	0	0	0	17	170	1700
IVA-3-Sul	0	0	0	0	0	0	17	170	1700
4-HBA	1	10	100	1	10	100	1	10	100
Ferulic acid	29	290	2900	21	210	2100	59	590	5900
Hippuric acid	7	70	700	23	230	2300	194	1940	19400
	190	1900	19000	203	2030	20300	438	4380	43800

Abbreviations: 4-HBA, 4-hydroxybenzaldehyde; BA, benzoic acid; C3G, cyanidin-3-glucoside; Glc, glucuronide; IVA, isovanillic acid; PCA, protocatechuic acid; PGA, phloroglucinaldehyde; Sul, sulfate; VA, vanillic acid.

### 6.2.2. Cell culture

Three vials of human coronary artery endothelial cells (HCAEC; from different, single donors) were cultured and maintained as described in Chapter 2. All cells were incubated for at least

24 hours at 37°C, 5 % CO<sub>2</sub>, in a humidified atmosphere, prior to experiment commencement. All cells were used between passages 3 and 6.

### **6.2.3. Cell viability**

HCAEC were seeded at 20,000 cells/well in fibronectin coated 96-well plates and grown to confluence in supplemented media. Cells were treated with highest working concentrations, or 0.01% DMSO (vehicle control), with or without TNF- $\alpha$  (10 ng/mL), and PBS (cells, no media) was used as a negative assay control. WST-1 was carried out as described in Chapter 2.

### **6.2.4. sVCAM-1 and sIL-6 protein expression**

HCAEC were seeded at 60,000 cells/well in fibronectin coated 24-well plates. Cells were treated for 30 min with peak metabolites profiles identified previously at 1 h, 6 h, 24 h post consumption (Table 6.1) or 0.01 % DMSO (vehicle control) prior to the addition of 0.1 ng/mL TNF- $\alpha$ , and incubated for 18 h at 37°C, 5 % CO<sub>2</sub>, in a humidified atmosphere. Supernatants were collected on ice, centrifuged at 2000 x g for 10 min at 4°C, and stored at -80°C until required. Samples underwent a single freeze-thaw cycle, were incubated to room temperature, and vortexed for 3 x 5 sec immediately prior to use. Supernatants were diluted 1:1 in Reagent Diluent (R&D Systems) prior to commencing the assay. Protein expression of sVCAM-1 and sIL-6 were determined by commercially available enzyme-linked immunosorbent assay (ELISA), as described in Chapter 2.

### **6.2.5. VCAM-1 and IL-6 mRNA expression**

HCAEC were seeded at 200,000 cells/well in fibronectin coated 6-well plates. Cells were pre-treated for 30 min with the highest working concentrations of each serum profile or 0.01 % DMSO (vehicle control) prior to the addition of 0.1 ng/mL TNF- $\alpha$ , and incubated for 4 h at 37°C, 5 % CO<sub>2</sub>, in a humidified atmosphere. Cell culture supernatants were removed and cells washed 3 x with PBS. Total RNA was extracted, reverse transcribed, and RT-qPCR were conducted as described in Chapter 2. Aliquots were taken prior to freezing and geNORM analysis was carried out to determine stable reference genes (VIPAS39 and PRDM4), the geometric mean of which were used to normalise the data in subsequent experiments.

### **6.2.6. Phospho-NF $\kappa$ B p65, p38 MAPK and JNK expression**

HCAEC were seeded at 200,000 cells/well in fibronectin coated 6-well plates. Cells were pre-treated for 30 min with the highest working concentrations of each serum profile or 0.01 % DMSO (vehicle control) prior to the addition of 10 ng/mL TNF- $\alpha$ , and incubated for 15 min at 37°C, 5 % CO<sub>2</sub>, in a humidified atmosphere. Cells were washed 3 x with PBS and cells were

lysed with NP-40 lysis buffer; total protein concentrations were determined by BCA assay, and proteins were separated and probed by SDS-PAGE and Western blotting, respectively, as described in Chapter 2.

### 6.2.7. Data analysis

Cell viability data (optical density) were recorded as a mean of 2 technical replicates and effects were determined relative to an untreated control (media only) by Student's t-test using Microsoft Excel (version 2013). sVCAM-1 and sIL-6 protein (pg/mL) or mRNA (fold change) were recorded as the mean of two technical duplicates, and reported relative to the TNF- $\alpha$  positive control (containing TNF- $\alpha$  without DMSO). Treatment effects were established by one-way analysis of variance (ANOVA) with post-hoc least square difference (LSD) conducted using SPSS for Windows (version 22.0; IBM, New York, USA). Untreated controls were not included in the ANOVA for treatment effect but presented graphically, where Student's t-test established difference relative to vehicle control (DMSO). Phospho-NF $\kappa$ B p65 expression (infrared density) data were normalised to GAPDH reference gene and phospho-p38 MAPK and phospho-JNK data were normalized to total p38s and total JNKs, respectively, and treatment effects were established relative to the vehicle control (DMSO) by one-way analysis of variance (ANOVA) with post-hoc least square difference (LSD) conducted using SPSS. Data were presented graphically as a fold change of vehicle control (DMSO). All data represents the mean  $\pm$  SD of three biological replicates (n=3).

### 6.2.8. Method optimisations

sVCAM-1 and sIL-6 stimulation time and concentration (0.1 ng/mL TNF- $\alpha$ ; 24 h) and VCAM-1 and IL-6 mRNA stimulation time (4 h) were determined in method optimisation experiments (**Figure 6.2**; Appendix; **Chapter 9.4**). Endogenous reference genes for normalisation of C<sub>t</sub> data for target genes were selected by use of human geNORM kit and qBASE analysis software as described in Chapter 2. Stimulation time for phospho-protein expressions (15 min) were as optimised for Chapter 5.

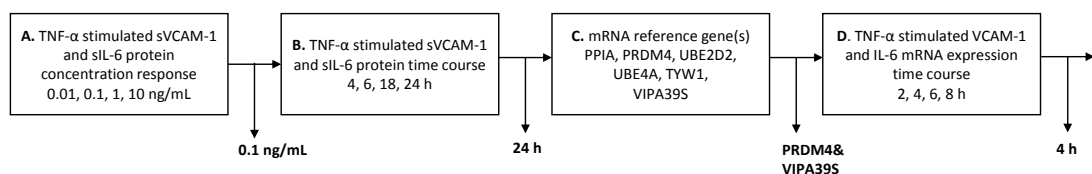


**Figure 6.2. Method optimisation experiments for Chapter 6.** See Appendix 9.4. Abbreviations: sIL-6, soluble interleukin-6; sVCAM-1, soluble vascular cell adhesion molecule-1; TNF- $\alpha$ , tumour necrosis factor-alpha. Abbreviations for mRNA reference genes are listed in Chapter 2.5.3.

## 6.3. Results

### 6.3.1. Effect of peak cyanidin-3-glucoside metabolite profiles on endothelial cell viability

Three unique profiles of cyanidin-3-glucoside metabolites (Table 6.1) were produced to reflect peak concentrations observed in a previous feeding intervention (Czank et al., 2013). Metabolites were prepared in media and used to treat human coronary artery endothelial cells, in the presence or absence of 10 ng/mL TNF- $\alpha$ , for 24 h (Table 6.2). Cell viability was assessed by the addition of WST-1 reagent. No cytotoxicity was observed in response to any treatment.

**Table 6.2: Effect of peak metabolite profiles on endothelial cell viability**

Treatment	Absorbance (% of untreated control)			
	Unstimulated		TNF- $\alpha$ 10 ng/mL	
	Mean $\pm$ SD	p	Mean $\pm$ SD	p
DMSO 0.01%	112.77 $\pm$ 9.42	0.17	102.90 $\pm$ 5.20	0.52
1 h profile	98.68 $\pm$ 7.57	0.77	96.37 $\pm$ 7.50	0.53
6 h profile	96.84 $\pm$ 6.67	0.53	94.21 $\pm$ 4.00	0.18
24 h profile	93.84 $\pm$ 5.19	0.23	89.10 $\pm$ 5.58	0.12

Cell viability (absorbance as percentage of untreated control absorbance), vehicle control (medium with 0.01 % DMSO) and highest working concentrations of treatment compounds (19  $\mu$ M, 20  $\mu$ M, 44  $\mu$ M at 1 h, 6 h, 24 h respectively; Czank et al., 2013), with and without 10 ng/mL TNF- $\alpha$ . Data shown as mean of three independent replicates  $\pm$  SD (n=3). Difference from untreated control (media only) were determined by Student's t-test using Microsoft Excel (version 2013).

### 6.3.2. Effect of peak cyanidin-3-glucoside metabolite profiles on sVCAM-1 protein expression

Cyanidin-3-glucoside metabolite treatments (Table 6.1) were used to determine their effect on TNF- $\alpha$  stimulated sVCAM-1 secretion by HCAEC (Figure 6.3). Effects were explored across a range of concentrations (ten-fold lower and ten-fold higher than the mean concentrations observed by Czank *et al.*; Table 6.1). sVCAM-1 expression was significantly reduced relative to the vehicle control by metabolite profiles at 6 h (-30.07  $\pm$  11.41 %,  $p \leq 0.001$ ) and 24 h (-27.84  $\pm$  3.09 %,  $p \leq 0.001$ ) at the mean (1.9  $\mu$ M, 2.0  $\mu$ M, 4.4  $\mu$ M at 1 h, 6 h, 24 h respectively) and ten-fold (19  $\mu$ M, 20  $\mu$ M, 44  $\mu$ M at 1 h, 6 h, 24 h respectively) concentrations. The lowest concentrations of each profile (0.19  $\mu$ M, 0.20  $\mu$ M, 0.44  $\mu$ M at 1 h, 6 h, 24 h respectively) significantly reduced sVCAM-1 secretion ( $p \leq 0.05$ ).

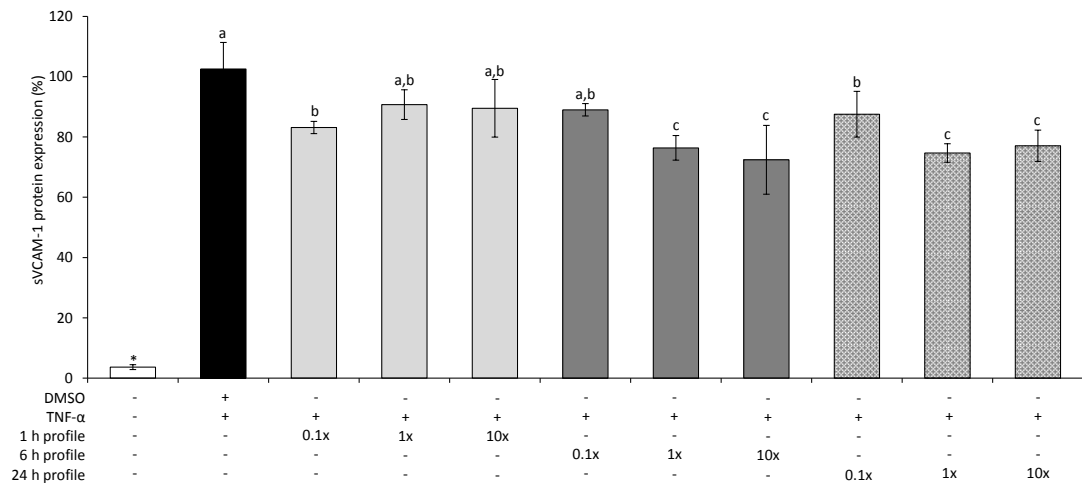


**Figure 6.3. Effect of peak metabolite profiles on sVCAM-1 protein expression.** HCAEC were treated with 3 concentrations of 3 serum metabolites profiles (ten-fold lower and ten-fold higher than the mean concentrations observed by Czank et al.; Table 6.1) prior to the addition of 0.1 ng/mL TNF- $\alpha$  for 24 h. Data were normalised to a TNF- $\alpha$  control (no DMSO) and columns represent the mean  $\pm$  SD, n = 3 biological replicates. Labelled means without a common letter differ,  $p \leq 0.05$  (ANOVA with post hoc LSD). \*Different from DMSO,  $p \leq 0.05$  (t-test).

### 6.3.3. Effect of peak cyanidin-3-glucoside metabolite profiles on VCAM-1 mRNA expression

Peak metabolite profiles were used to determine their effect on TNF- $\alpha$  stimulated VCAM-1 mRNA expression in HCAEC (**Figure 6.4**). TNF- $\alpha$  stimulated VCAM-1 mRNA was significantly reduced relative to the vehicle control, in response to metabolite profiles at 1 h ( $p=0.02$ ) and 6 h ( $p= 0.03$ ).

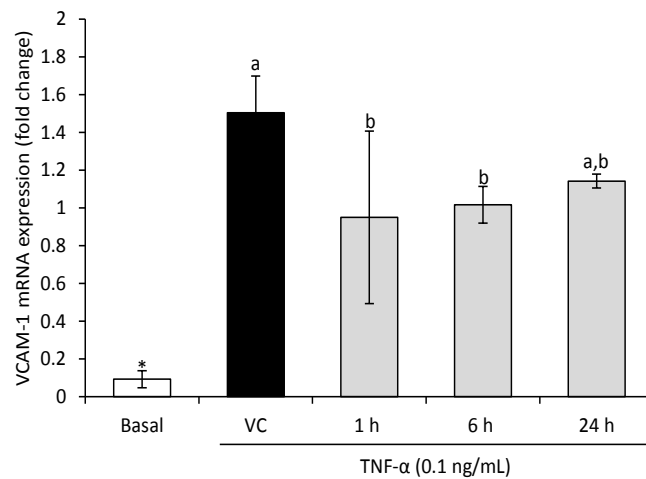


**Figure 6.4. Effect of peak metabolite profiles on VCAM-1 mRNA expression.** HCAEC were treated with the highest concentration of peak metabolite mixtures (19  $\mu$ M, 20  $\mu$ M, 44  $\mu$ M at 1 h, 6 h, 24 h respectively; Czank et al., 2013) and stimulated with 0.1 ng/mL TNF- $\alpha$  for 4 h. Data were normalised to a TNF- $\alpha$  control (no DMSO) and columns represent the mean  $\pm$  SD, n = 3 biological replicates. Labelled means without a common letter differ significantly,  $p \leq 0.05$  (ANOVA with post hoc LSD). \*Different from DMSO,  $p \leq 0.05$  (t-test).

#### 6.3.4. Effect of peak cyanidin-3-glucoside metabolite profiles on sIL-6 protein expression

Cyanidin-3-glucoside metabolite treatments (Table 6.1) were used to determine their effect on TNF- $\alpha$  stimulated sIL-6 secretion by HCAEC (**Figure 6.5**). Effects were explored across a range of concentrations (ten-fold lower and ten-fold higher than the mean concentrations observed by Czank *et al.*; Table 1). No profile reduced sIL-6 secretion relative to the vehicle control.

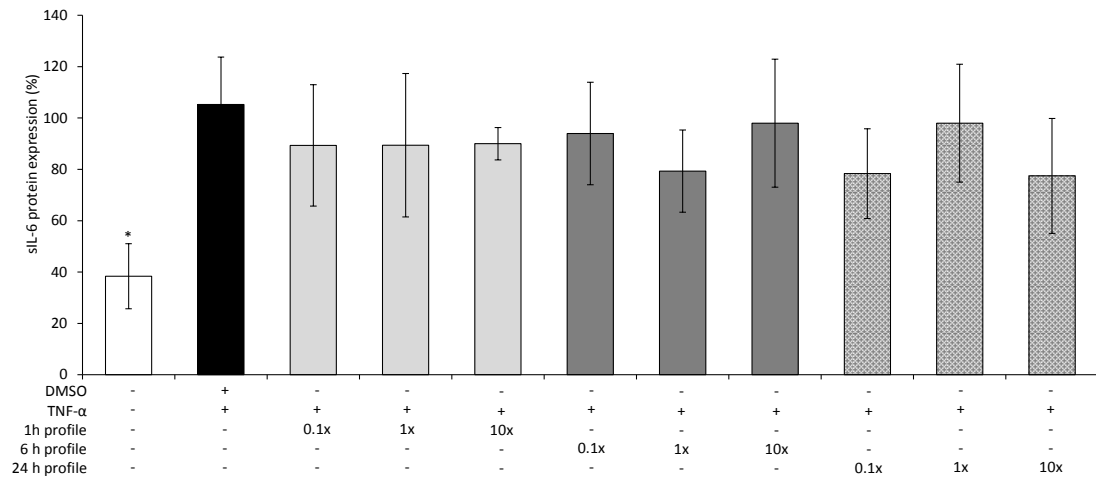


**Figure 6.5. Effect of peak metabolite profiles on sIL-6 protein expression.** HCAEC were treated with three concentrations of three serum metabolites profiles (ten-fold lower and ten-fold higher than the mean concentrations observed by Czank et al.; Table 6.1) in media prior to the addition of 0.1 ng/mL TNF- $\alpha$  for 24 h. Data were normalised to a TNF- $\alpha$  control and columns represent the mean  $\pm$  SD, n = 3 biological replicates. Labelled means without a common letter differ significantly,  $p \leq 0.05$  (ANOVA with post hoc LSD). \*Different from DMSO,  $p \leq 0.05$  (t-test).

### 6.3.6. Effect of peak cyanidin-3-glucoside metabolite profiles on IL-6 mRNA expression

Cyanidin-3-glucoside metabolite treatments (Table 6.1) were used to determine their effect on TNF- $\alpha$  stimulated IL-6 mRNA expression in HCAEC (**Figure 6.6**). TNF- $\alpha$  stimulated IL-6 mRNA expression was reduced by half in response to all treatments ( $p \leq 0.05$ ).

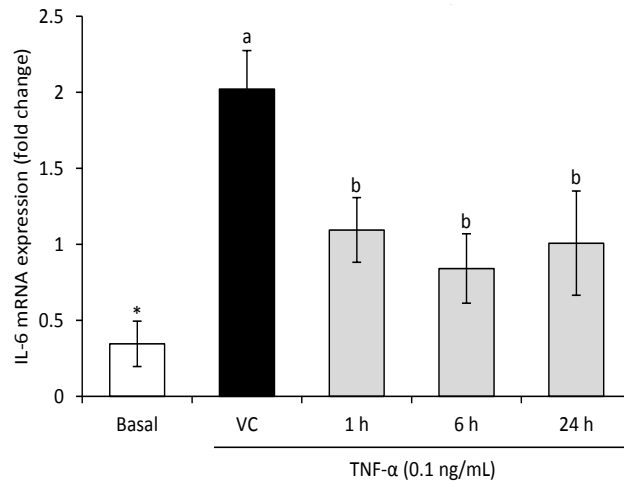


**Figure 6.6. Effect of peak metabolite profiles on IL-6 mRNA expression.**

HCAECs were treated with the highest concentration of peak metabolite mixtures (19  $\mu$ M, 20  $\mu$ M, 44  $\mu$ M at 1 h, 6 h, 24 h respectively; Czank et al., 2013) and stimulated with 0.1 ng/mL TNF- $\alpha$  for 4 h and mRNA expression was determined by RT-qPCR. Data were normalized to a TNF- $\alpha$  control and columns represent the mean  $\pm$  SD, n=3 biological replicates. Labelled means without a common letter differ significantly,  $p \leq 0.05$  (ANOVA with post hoc LSD). \*Different from DMSO,  $p \leq 0.05$  (t-test).

### 6.3.7. Effect of peak cyanidin-3-glucoside metabolite profiles on NF $\kappa$ B p65, p38 MAPK, and JNK phosphorylation.

Metabolite profiles were explored for their effect on TNF- $\alpha$  stimulated NF $\kappa$ B transcription factor p65 (**Figure 6.7**) and p38 and JNK MAP kinase phosphorylation (**Figure 6.8**). No effect was observed on TNF- $\alpha$  stimulated phospho-p65 expression, whereas p38 expression increased by approximately 1.2 fold ( $p \leq 0.05$ ) in response to all treatments, and JNK phosphorylation decreased relative to the vehicle control following treatment with the metabolite profile at 24 h (0.6-fold,  $p \leq 0.05$ ).

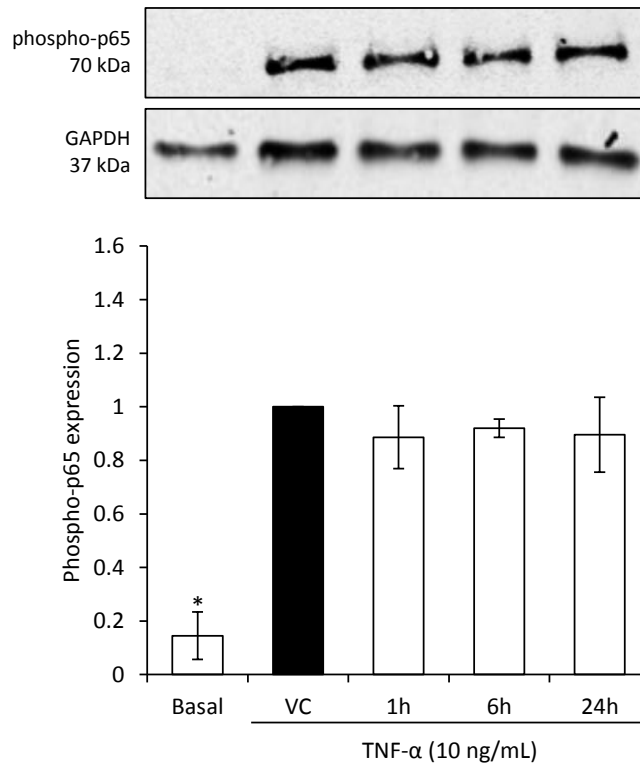


**Figure 6.7. Effect of peak metabolite profiles on phosphorylated NFκB p65 expression.** HCAEC were treated with the highest concentration of peak metabolite mixtures (19 μM, 20 μM, 44 μM at 1 h, 6 h, 24 h respectively; Czank et al., 2013), and stimulated with 10 ng/mL TNF-α for 15 min. Data were normalized to the vehicle control (DMSO) and columns represent the mean ± SD, n = 3 biological replicates. Blots are representative of one of three replicates. Labelled means without a common letter differ significantly,  $p \leq 0.05$  (ANOVA with post hoc LSD). Comparisons of untreated cells to vehicle control (DMSO) were established via Student's t-test,  $*p \leq 0.05$ .

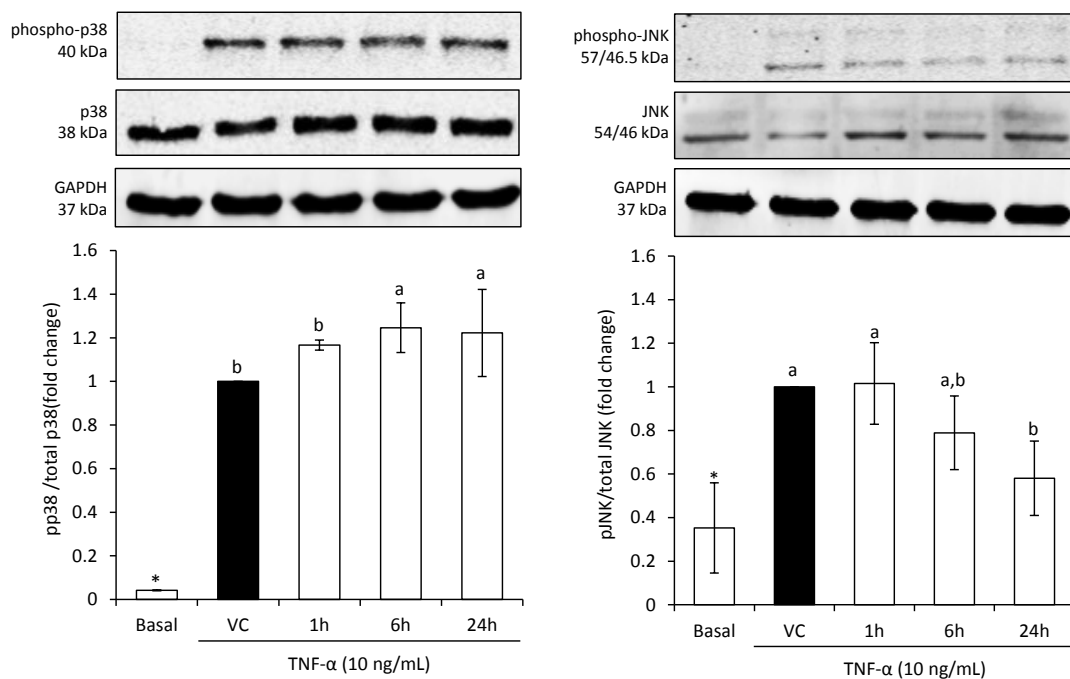


**Figure 6.8. Effect of peak metabolite profiles on phosphorylation of p38 and JNK MAP kinases.** HCAEC were treated with the highest concentration of peak metabolite mixtures (19  $\mu$ M, 20  $\mu$ M, 44  $\mu$ M at 1 h, 6 h, 24 h respectively; Czank et al., 2013), were stimulated with 10 ng/mL TNF- $\alpha$  for 15 min. Data were normalized to the vehicle control (DMSO) and columns represent the mean  $\pm$  SD, n=3 biological replicates. Blot are representative of one of three replicates. Comparisons of untreated cells to vehicle control (DMSO) were established via Student's t-test, \*p $\leq$ 0.05.

## 6.4. Discussion

Flavonoids may exert their cardiovascular benefits through the modulation of inflammatory biomarkers which drive the progression of atherosclerosis (Wallace, 2011). The vast majority of previous studies have investigated the mechanisms of action of flavonoid glycosides and aglycones using *ex vivo* and *in vitro* systems, but few have explored the effects of their more physiologically relevant metabolites, which are produced after extensive chemical and microbial degradation and metabolic conjugation (i.e. glucuronide, methyl and sulfate derivatives; de Ferrars et al., 2014a, Stalmach et al., 2013). Many past studies have also utilised foods or plant extracts containing a number of compounds (Davis et al., 2006, Kuntz et al., 2015, Taverniti et al., 2014), without knowledge of the exact composition or concentrations of individual constituents, making it difficult to determine the active components. Alternatively, the design of *in vitro* studies utilising bioactive compounds in isolation do not take into account the additive, antagonistic or synergetic activities these may have in combination. The study of the cumulative activity of phenolic metabolites is relatively novel (Warner et al., 2016, di Gesso et al., 2015, Krga et al., 2016) and its exploration may help elucidate the beneficial effects of flavonoids observed *in vivo*.

Previous investigations have noted that metabolic conversion of anthocyanins alter their biological activity (Amin et al., 2015, Edwards et al., 2015, Warner et al., 2016, Krga et al., 2016). The present study is the first to explore the activity of physiologically relevant profiles of metabolite identified following the consumption of the common dietary class of flavonoid, anthocyanins. Herein, we have utilised profiles of cyanidin-3-glucoside (C3G) metabolites identified by Czank *et al.* (Czank et al., 2013), with the aim of elucidating the potential mechanisms of action of anthocyanins. Three unique treatments were explored based on the mean concentrations of metabolites peaked in serum, representing 1 h, 6 h, and 24 h postprandial blood samples (Figure 6.1). It was hypothesised that the beneficial effects of anthocyanins may occur as a result of varying compositions and concentrations of metabolites, which could have differential biological activities, as they are systematically metabolised and eliminated from the body.

The key findings from the present study were that the mixtures of metabolites used have significant inhibitory effects on sVCAM-1 protein secretion (Figure 6.2) and this was achieved at concentrations reflective of those identified *in vivo* (de Ferrars et al., 2014b), suggesting this activity is physiologically achievable. The inhibition of sVCAM-1 in response to the mixtures of metabolites representing peak kinetic profiles at 24 h was greater than metabolite profiles identified at 6 h post-consumption. The anti-inflammatory activity of

flavonoid metabolites may therefore be modulated to a greater extent by profiles of metabolites which appear many hours post consumption (6 h -24 h), suggesting metabolites of microbial origin are responsible for the chronic anti-inflammatory activity of anthocyanins (Kay et al., 2009).

Few studies have explored the effects of flavonoids in combination (di Gesso et al., 2015), despite some indication of differential activities when in combination relative to isolation (Heeba et al., 2012, Khandelwal et al., 2012, Koga and Meydani, 2001, Liebgott et al., 2000). The present study demonstrated that the effect of mixtures mimicking blood profiles of metabolites of cyanidin-3-glucoside appear to have effect greater than the 'artificial' equal molar concentrations of mixed metabolites explored previously (Chapter 5). Previous studies have utilised rat serum post consumption of flavonoids (Koga and Meydani, 2001). Here, serum containing metabolites of (+)-catechin were shown to significantly reduce U937 adhesion to human aortic endothelial cells (HAEC) relative to the pure metabolite in isolation. Conversely, quercetin metabolism appeared to neutralise the anti-inflammatory activity of the pure compound, as has been demonstrated in other models of cellular adhesion (Winterbone et al., 2009). The limitations of this study design are that plasma contains many bioactive components other than flavonoid metabolites, making it difficult to compare treatments relative to pure compounds; in addition, rat metabolism differs from human metabolism, making it difficult to directly apply rodent findings to humans. There is scope to carry out similar experiments using human serum in future work, though limitations still exist regarding the use of appropriate controls, as described above.

The highest mean serum concentration of metabolites detected in our recent tracer study feeding 500 mg of <sup>13</sup>C-labelled anthocyanins (equivalent to the consumption of approximately 100g of blackberries; Manach et al., 2004) was observed at 24 h post consumption and totalled 4.38 µM (de Ferrars et al., 2014b). In this study the inter-individual variation was high (for example, serum C<sub>max</sub> for hippuric acid was 1962 ± 1389 nM), indicating the mean concentration could vary greatly. The present study sought to address the issue of variation in blood profiles by utilising concentrations across the lowest and highest concentrations reported between individuals (0.80 µM – 13.18 µM; Czank et al., 2013). As such, we used two serial ten-fold dilutions of the maximal concentrations observed at each time point where metabolites peaked in the serum (1 h, 6 h, 24 h) to explore effect size across a range of physiologically relevant concentrations. Surprisingly, no statistical differences in the inhibition of sVCAM-1 protein expression were observed between the observed mean (Czank et al., 2013) and ten-fold concentrations of the metabolite profiles. We initially

hypothesised that lower concentrations of metabolites would have a lesser effects size than the highest concentration, which would have supported the conclusion that the concentrations of the metabolites used in our previous experiments (Warner et al., 2016, di Gesso et al., 2015) were too low to elicit a significant response. This suggests that there is something unique about these profiles/mixtures of metabolites. This outcome is an important finding as the concentrations reflect those which could be reached following consumption of 500 mg (or less) of anthocyanins, which reflects achievable levels following dietary consumption of anthocyanin-rich foods (Rodriguez-Mateos et al., 2014a). As phenolic metabolites are common to a number of dietary flavonoids and food sources (Heleno et al., 2015), it is possible that serum profiles utilised in the present study could be exceeded following a habitual polyphenol-rich diet, given that consumption in Europe has been estimated between 744 mg/day - 1786 mg/day (Zamora-Ros et al., 2015). As effects were observed at the lowest concentrations in the present study (between 0.19  $\mu$ M and 0.44  $\mu$ M), the evidence suggests that even low levels of dietary consumption would have beneficial effects on inflammatory status.

The effects of the treatments on VCAM-1 and IL-6 mRNA expression were investigated to determine whether these would reflect the protein expression profiles and to suggest potential mechanisms of action. In our previous experiments (Chapter 5), it was observed that only PCA inhibited VCAM-1 mRNA expression at 100  $\mu$ M, which provided the rationale behind our concentration-response hypothesis. It is interesting that VCAM-1 and IL-6 mRNAs were reduced by half in response to the 3 peak serum mixtures, the total metabolite concentrations of which were 19  $\mu$ M, 23  $\mu$ M, and 44  $\mu$ M, respectively. In the case of IL-6 activity, the relative increase in total concentration of each respective treatment did not appear to alter the magnitude of response, whereas the lower concentrations (peak metabolite compositions at 1 h (19  $\mu$ M) and 6 h (22  $\mu$ M) post-consumption) appeared to reduce VCAM-1 mRNA to the greatest extent relative to the vehicle control. Given differential complexity of the metabolite structures and concentrations in the present treatment mixtures, and given that few showed activity when studied in isolation in the present thesis, it appears that certain metabolites utilised in the present study act additively or synergistically, potentially through effecting multiple pathways simultaneously. Multiple pathways are indeed thought to be affected following anthocyanin metabolite treatment, for example, aortas of ApoE-deficient mice fed an anthocyanin-rich bilberry extract, analysed by Pathway Miner (DNA microarray), demonstrated the modulation 1261 genes which code for proteins involved in the regulation of cellular processes, including adhesion and

inflammatory biomarker expression (Mauray et al., 2012). There is therefore scope for future studies to more broadly explore the activities of these serum metabolites *in vitro*.

Pharmacological methods currently exist to statistically assess the synergistic activity of particular drugs and chemicals, however these methodologies are rarely applied to mixtures as complex as those utilised herein. Harasstani *et al.* utilised a method referred to as isobolographic analysis to evaluate the inhibition of inflammatory biomarker secretion in a RAW 264.7 cell model (Harasstani et al., 2010), which identified that flavonoids chrysin, kaempferol, morin and silibinin had highly effective synergistic activity in combination compared to in isolation. The flavonoids in combination significantly lowered the overall IC<sub>50</sub> value for the three biomarkers tested, which is an interesting finding for combination treatment strategies, though it still holds limited relevance to nutrition as the IC<sub>50</sub> concentrations ranged from 2.28 µM (kaempferol + chrysin) to 14.19 µM (morin + silibinin). Even at the lowest observed concentration where effects were seen, it is clear this study holds lesser relevance to nutritional studies as feeding studies have reported maximal plasma concentrations of kaempferol and chrysin as 0.10 µM (DuPont et al., 2004) and 0.02 µM (Walle et al., 2001a), respectively. Given that flavonoid phenolic metabolite concentrations can achieve maximal plasma concentrations of 13.3 µM (Schar et al., 2015), isobolographic analysis may be utilised in future studies to assess synergistic activities of complex mixtures of physiologically relevant metabolites, as used herein.

NFκB is a key transcription factor pathway in the TNF-α stimulated expression of adhesion molecules in endothelial cells (Hopkins, 2013). In the present study, no effect was observed on the expression of phosphorylated p65 in response to any of the treatments used, suggesting that the mixtures used may not be active in the NFκB pathway, as was suggested previously in our recent work (Warner et al., 2016) and corroborated by others (Krga et al., 2016). In both these studies, it was shown that gut metabolites of flavonoids reduced TNF-α stimulated expression of adhesion molecule proteins, but showed no activity on mRNA expression, suggesting these may be active in alternative mechanisms which influence adhesion molecule expression, such as AP-1 via p38 and JNK MAP kinases.

As observed for sVCAM-1 protein, the metabolite profile at 24 h post consumption inhibited JNK activation to the greatest extent, suggesting that this profile of most likely large intestine-derived metabolites, is active in this pathway. However, the same profiles also increased p38 phosphorylation, which was an unexpected outcome as this would imply a pro-inflammatory effect (Zarubin and Han, 2005). Nevertheless, it is apparent that the effects observed on the molecular targets investigated do not fully reflect changes to protein or

mRNA expression, suggesting that other unexplored mechanisms of action, both pre- and post-transcriptional, may be affected by the treatment mixtures. Future studies should explore activity on TNF- $\alpha$  receptor 1 (TNFR1), which is a key modulator of NF $\kappa$ B induced expression of adhesion molecule expression, irrespective of p38 MAPK or JNK (Zhou et al., 2007).

The present study addressed several limitations of previous works which have applied plasma or serum post-consumption of flavonoids *in vitro*, presenting difficulties in untangling effects of metabolites relative to other serum or plasma components (i.e., proteins, electrolytes, hormones, antigens, etc.). Non-phenolic components of serum/plasma, which are often present in much greater concentrations than phenolic constituents, make it difficult to elucidate the origin of any activity observed and few studies have studied their mechanisms of action (Harasstani et al., 2010, Koga and Meydani, 2001). The novelty of the present study is that the experiments can be appropriately controlled for vehicle, which allows a more direct exploration of mechanism of action. This in itself has the limitation that the metabolites themselves may act differentially in serum relative in cell culture media, and certain flavonoids have been shown to interact with serum albumin in acellular conditions (Bi et al., 2004). Furthermore, it is feasible that not all phenolic metabolites in the serum for this study were detected in the first instance (de Ferrars et al., 2014a) due to absence of appropriate standards (Kay, 2010), likewise the sensitivity of the detection methods are a determinant, leading to variation between clinical sample concentrations and which were modelled in the present study. Concentrations of total metabolites may therefore be higher than those described. Future studies could address these limitations in a single study by comparing serum treatments from a human clinical study, to those extracted, to mixtures of pure analytes mimicking blood composition, as used herein. In such a case, appropriate controls could be utilised to establish the effects of the various treatment matrices relative to the metabolites in question.

No effects were observed on sIL-6 protein expression in the present study, though it is possible that effects were masked by large variation between replicates. A parallel study from our group conducted in TNF- $\alpha$  (10 ng/mL)-stimulated human umbilical vein endothelial cells (HUVEC) demonstrated inhibitory effects of the same profiles on sVCAM-1 and sIL-6 in response to all treatments (M.Smith PhD Thesis, 2016). It is possible that the reduced stimulus (TNF- $\alpha$ ) concentration (0.1 ng/mL in the present study relative to 10ng/mL) increased variation as a result of low sIL-6 induction, making it difficult to quantify significant activity. Therefore, the obtained results are likely associated with the use of a more

physiological relevant level of stimulus, whereas a more pharmacological dose of TNF- $\alpha$  may have allowed a greater magnitude of effect to be observed. A recent study by Kuntz *et al.* utilised two concentrations of TNF- $\alpha$ ; 1 ng/mL TNF- $\alpha$  to mimic a low-grade inflammatory state and 10 ng/mL to mimic high-grade inflammation. Replicating this model of low- vs. high- grade inflammation, future studies could explore activity across a range of stimulus concentrations from 0.1-10 ng/mL (Kuntz *et al.*, 2015a).

Limited data is available correlating acute anthocyanin metabolite profiles in human studies with inflammatory biomarkers, potentially as immediate/acute effects (aside from vascular reactivity) are rarely observed in healthy volunteers (Schar *et al.*, 2015) and only a few studies have been conducted in subjects with inflammatory conditions, such as hypercholesterolemia (Zhu *et al.*, 2013), where anti-inflammatory effects are observed over prolonged periods of time (e.g. 12-24 weeks; Zhu *et al.*, 2013). Data from the present study suggest that the metabolite profile with the maximum inflammatory effect was observed at 24 h post-consumption. Conversely, improvements in flow-mediated dilation (FMD) and blood pressure in response to the feeding to anthocyanins are observed between 1 h and 6 h post-consumption (maximum response at 2 h; Rodriguez-Mateos *et al.*, 2014a). In this study, following the consumption of a drink containing blueberry anthocyanins, benzoic and vanillic acids positively correlated with FMD at 1–2 h, whereas hippuric, hydroxyhippuric, and homovanillic acids correlated with the FMD at 6 h. These data suggests an acute-phase modulatory vascular response of phenol metabolites. Based on these findings and those of the present study it may be possible that an immediate vascular response, mediated by very low levels of parent flavonoids and their immediate degradation products, is succeeded by a delayed anti-inflammatory response, mediated by products of colonic bacterial catabolism and hepatic phase II conjugation. Future studies should establish if these peak metabolite profiles similarly affect expression levels of biomarkers of nitric oxide homeostasis (e.g. endothelial NO synthase (eNOS)) and acute antioxidant enzymes (e.g. haem oxygenase-1 (HO-1), and glutathione peroxidase (GPx)) at the same time points. As FMD is, at least in part, moderated by NO (Green *et al.*, 2014), it may be postulated that levels of these proteins, would increase as a result of profiles of flavonoids and metabolites observed at 1 h and 6 h. This would ultimately suggest a dual mechanistic activity of metabolites, which may shed light on how flavonoids act chronically to modulate a number of physiological responses.

In conclusion, the present study identified that mixtures of anthocyanin metabolites identified post consumption of dietary achievable levels of anthocyanins have significant inhibitory effects on sVCAM-1 protein secretion, suggesting this is a physiologically

achievable effect. Further work is required to elucidate the multiple mechanisms at play and their cumulative or synergistic activity at the tissue level, ultimately informing our understanding of how anthocyanins and other flavonoids impact cardiovascular health.

## Chapter 7. General Discussion & Future Perspectives

### 7.1. General Discussion

Protective effects of dietary flavonoids against cardiovascular-related disorders have been observed in numerous randomised-control trials (Barona et al., 2012, Weseler et al., 2011, Bondonno et al., 2012, Curtis et al., 2009, Faridi et al., 2008), animal feeding (Bornhoeft et al., 2012, Gandhi et al., 2009, Heeba et al., 2012, Loke et al., 2010, Nabavi et al., 2012, Sheng et al., 2009) and *in vitro* studies (Kawai et al., 2008, Tu et al., 2007, Yamagata et al., 2010). Many studies have been conducted using supraphysiological doses of single flavonoids, overlooking the potential bioactivity of flavonoid metabolites and the additive effects flavonoid metabolites may have in combination (Keane et al., 2015, Harasstani et al., 2010, Krga et al., 2016, di Gesso et al., 2015). Elucidating the cellular effects of flavonoid metabolites at concentrations obtainable through diet, will enhance our understanding of flavonoid cardiovascular bioactivity.

Flavonoids undergo extensive metabolism by the activities of colonic bacteria. The resultant structures are diverse in their structural nature and, for the purpose of this investigation, focus was given to phenolic B-ring derived metabolites, as activity has been suggested previously by our group in vascular (Edwards et al., 2015, Amin et al., 2015) and inflammatory (di Gesso et al., 2015) cells types. The selected treatments for the present investigations differ primarily by the moieties present at the 3' and 4' positions, which allow elucidation of potential structure-activity relationships. This thesis screened the effects of flavonoids common to the UK diet, and associated conjugated and unconjugated phenolic metabolites, for their effect of eNOS and HO-1 proteins in basal endothelial and vascular smooth muscle cells (VSMCs; Chapters 3 & 4) and sVCAM-1 and sIL-6 (Chapters 5 & 6) in TNF- $\alpha$  stimulated endothelial cells (**Figure 7.1**). Additionally, multiple combination treatments were designed based on their structural similarities, as would be present in the systemic circulation post-consumption of a meal rich in a particular flavonoid. Treatments were screened from 'protein-to-pathway', and were selected for further study based on their relative bioactivities, in order to elucidate potential mechanisms of action responsible for the effects on the biomarkers observed.

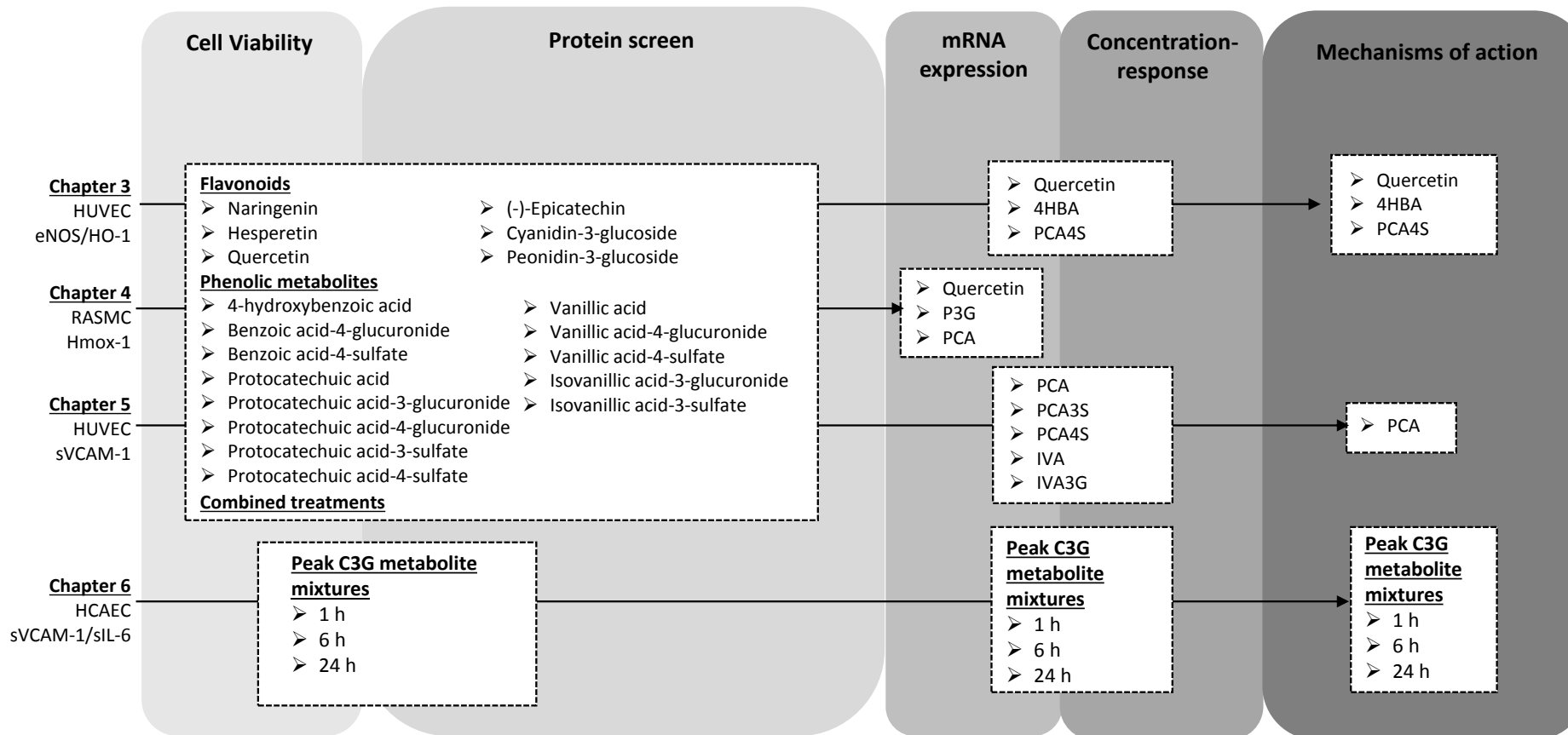


**Figure 7.1. Experiment and treatment schematic.** Abbreviations: 4-HBA, 4-hydroxybenzoic acid; C3G, cyanidin-3-glucoside; eNOS, endothelial nitric oxide synthase; HCAEC, human coronary artery endothelial cells; HO-1/Hmox-1, haem oxygenase-1; HUVEC, human umbilical vein endothelial cells; IVA, isovanillic acid; IVA3G, isovanillic acid-3-glucuronide; P3G, peonidin-3-glucoside; PCA, protocatechuic acid; PCA3S, protocatechuic acid-3-sulfate; PCA4S, protocatechuic acid-3-sulfate; RASMC, rat aortic smooth muscle cells; sIL-6, soluble interleukin-6; sVCAM-1, soluble vascular cellular adhesion molecule-1.

In order to determine the potential bioactivities of flavonoids and metabolites on vascular function, all treatments were screened in isolation (at a physiologically achievable concentration of 1  $\mu$ M) for their effects on endothelial nitric oxide synthase (eNOS) and haem oxygenase-1 (HO-1) protein in human umbilical vein endothelial cells (HUVEC; Chapter 3). One flavonoid (quercetin) and 2 phenolic acid metabolites (4-hydroxybenzoic acid (4HBA) and protocatechuic acid-4-sulfate (PCA4S)) increased HO-1 protein expression. The vast majority of phenolic metabolites had no effect on either protein, suggesting they are relatively inactive within these mechanisms. Subsequently, 7 equimolar mixtures of flavonoids containing quercetin and 11 mixtures containing 4HBA and/or PCA4S, to a cumulative concentration of 10  $\mu$ M, were screened for their effect on HO-1 protein, though no significant effects were observed, which suggests that combining these treatments does not increase their efficacy and therefore does not indicate additive or synergistic activity. Quercetin, 4HBA, and PCA4S were further investigated for the effect of increased concentration, where each treatment again resulted in increased HO-1 protein in response to 1  $\mu$ M, but this response was not amplified in response to greater concentrations (10  $\mu$ M-50  $\mu$ M), which may indicate negative feedback regulation of this protein with increased concentration of metabolites. Subsequent experiments demonstrated that quercetin and 4HBA significantly upregulated HO-1 mRNA expression but only quercetin increased total Nrf2 protein and induced the phosphorylation of Akt1 and ERK1/2 signalling kinases. These data support previous literature which cites quercetin as active in the activation of oxidant-response pathways, but also suggests that flavonoid metabolites, such as 4HBA and PCA4S upregulate HO-1 protein by alternative mechanisms.

Treatment effects were further investigated on Hmox-1 protein expression in rat aortic smooth muscle cells (RASMC; Chapter 4). Two flavonoids (quercetin and peonidin-3-glucoside) and one metabolite (protocatechuic acid (PCA)) actively upregulated Hmox-1, though, again, only quercetin significantly increased Hmox-1 mRNA expression. Quercetin has previously been shown to upregulate Nrf2-related genes (Liu et al., 2012, Chow et al., 2005, Lin et al., 2004, Tanigawa et al., 2007), though it has limited activity reported at concentrations below 1  $\mu$ M. Conjugation of quercetin has been seen to reduce the activity of quercetin in vascular pathways, whereas quercetin-3-glucuronide has been seen to inhibit inflammation, such as JNK phosphorylation (Yoshizumi et al., 2002), suggesting that conjugation of flavonoids and their metabolites may alter their target to inflammatory mechanisms of action. Likewise, P3G significantly upregulated Hmox-1 protein, but at 0.1  $\mu$ M has been shown to inhibit inflammation-driven vascular adhesion, which was not

observed at concentrations greater than 0.2  $\mu\text{M}$  (Krga et al., 2016). These data suggest that, whereas vascular pathways are activated in response to P3G at supraphysiological concentrations (as in the present study), P3G may act in inflammatory pathways at physiological concentrations (Kuntz et al., 2015). PCA, a prominent metabolite common to multiple flavonoids subclasses (Schar et al., 2015, de Ferrars et al., 2014b), modestly, though not significantly ( $p=0.09$ ), increased Hmox-1 protein. Past studies have identified the catechol hydroxyls of PCA as responsible for its bioactivity (Kakkar and Bais, 2014) and previous studies from our group have identified PCA as active within inflammatory mechanism of action, where activity was lessened upon conjugation of catechol hydroxyls to sulfate, glucuronide and methyl moieties (Warner et al., 2016). Overall, these data suggest that conjugation of metabolites may reduce their efficacy on Hmox-1 protein expression, although other sources have suggested that conjugation of metabolites may increase their efficacy in inflammatory mechanisms of action (di Gesso et al., 2015, Amin et al., 2015).

Flavonoids and their metabolites do not circulate in isolation following ingestion, but exist as complex mixtures of metabolites at various concentrations (Czank et al., 2013, Pereira-Caro et al., 2014, Serra et al., 2012), thus it is important that this is reflected in the design of cell culture experiments exploring the bioactivities of dietary components. Few studies have explored the effects of flavonoids in combination, despite some indication of differential activities when in combination relative to isolation (Koga and Meydani, 2001, Harasstani et al., 2010). Hmox-1 protein was increased in response to 4 mixtures of phenolic metabolites containing PCA, which is of particular interest as the concentrations used are achievable following flavonoid consumption (Schar et al., 2015) and therefore it is a potentially physiologically achievable effect. Interestingly, the present study observed that PCA and VA, in isolation, also did not significantly increase Hmox-1 expression, but a combination consisting of 5  $\mu\text{M}$  of each metabolite (to a cumulative concentration of 10  $\mu\text{M}$ ) significantly upregulated Hmox-1 protein; a similar effect was identified by Keane *et al.* on VSMC migration (Keane et al., 2015). These data further support the growing evidence of additive or synergistic effects between flavonoids and metabolites (Krga et al., 2016, di Gesso et al., 2015) and merits further exploration in future studies.

Given that the metabolites under investigation did not appear to actively increase basal expression of eNOS and HO-1 proteins, and that previous studies have suggested that metabolites of flavonoids may be active in inflammatory mechanisms of action (Krga et al., 2016, di Gesso et al., 2015, Amin et al., 2015), 20 flavonoids and their metabolites and 25 combinations of structurally similar compounds were explored for their effects in TNF- $\alpha$

stimulated HUVECs (Chapter 5). Four phenolic metabolites demonstrated inhibitory activity on sVCAM-1 secretion. PCA demonstrated the greatest activity, displaying a strong inhibitory effect on sVCAM-1, which appeared to be amplified with increased concentration. Inhibition of VCAM-1 mRNA was also observed in response to PCA, however, this was only apparent at a supraphysiological concentration of 100  $\mu\text{M}$  and did not appear to affect NF $\kappa$ B pathway activation or other signalling kinase activations (JNK, p38, Akt1, ERK1/2). This has been shown previously for other metabolites of anthocyanins (Krga et al., 2016), suggesting that PCA likely acts upon post-translational pathway targets, such as glutathione peroxidase (GPx; d'Alessio, Moutet et al. 1998), as studies have shown upregulation of GPx following treatment with quercetin (Granado-Serrano, Martin et al. 2012) and catechin (Simos, Verginadis et al. 2012). Additionally, it is conceivable that flavonoids and/or their metabolites could interact with the cleavage of the protein from the surface of endothelial cells (Videm and Albrigtsen 2008), such as by interaction with TNF- $\alpha$  converting enzyme, ADAM17 (Garton, Gough et al. 2003). Mixtures of metabolites and flavonoids showed no activity toward sVCAM-1, suggesting no additive activity at sub-micromolar concentrations (cumulative concentrations adding up to 1  $\mu\text{M}$ ), though the exploration of these combinations at greater concentrations requires investigation; as was the focus of the subsequent study (Chapter 6).

Three unique treatments were explored for their activity on sVCAM-1 and sIL-6 secretion by human coronary artery endothelial cells (HCAECs); where treatments were designed based on the time points of metabolites peaked in serum, representing 1 h, 6 h, and 24 h postprandial blood samples (Chapter 6). It was hypothesised that the beneficial effects of anthocyanins may occur as a result of varying profiles/compositions and concentrations of metabolites, which could have differential biological activities as anthocyanins are systematically metabolised along the gastrointestinal tract and eliminated from the body. Here, mixtures of metabolites had significant inhibitory effects on sVCAM-1 protein secretion, which was achieved at concentrations (2.0  $\mu\text{M}$ -4.4  $\mu\text{M}$ ) reflective of those identified *in vivo* (de Ferrars et al., 2014b), suggesting this activity is physiologically achievable. The inhibition of sVCAM-1 in response to the mixtures of metabolites representing peak kinetic profiles at 24 h was greater than metabolite profiles identified at 6 h post consumption, suggesting that the anti-inflammatory activity of flavonoid metabolites may be modulated to a greater extent by profiles of metabolites which appear many hours post-consumption (6 h -24 h), further supporting the hypothesis that metabolites of microbial origin are responsible for the anti-inflammatory activity of

anthocyanins (Kay et al., 2009). Although none of the constructed 'artificial' treatments (representing cumulative concentration of 1  $\mu\text{M}$ ) were active at this concentration on sVCAM-1 (Chapter 5), the serum mixtures reflecting profiles of C3G metabolites (Chapter 6) inhibited the molecule at the lowest concentrations reported (to a cumulative concentration of 0.19  $\mu\text{M}$ -0.44  $\mu\text{M}$ ), suggesting that specific combinations of metabolites increase their efficacy. These conclusions appear to support findings from a recent clinical study, which demonstrated that metabolites profiles are associated with specific physiological responses (such as seen for flow mediated dilation, which correlated with specific metabolite profiles 1 h- 6 h (Rodriguez-Mateos et al., 2014a) as they are systematically metabolised and eliminated from the body. Future studies should therefore consider multiple mechanistic activities of metabolite profiles observed *in vivo*, i.e. initial (<6 h) metabolite profiles may affect vascular responsiveness followed by a delayed (>6 h) anti-inflammatory response mediated by products of bacterial catabolism, absorption, and phase II conjugation.

## **7.2. Future perspectives**

Elucidating the mechanisms by which flavonoids and their metabolites *in vitro* may improve vascular function and inhibit inflammation *in vivo* is essential to understanding how flavonoids impact cardiovascular health. This may in turn provide insight into how flavonoids and other food bioactives influence health and therefore which specific types and quantities of certain foods are most protective against inflammation and vascular disease. In order to elucidate these mechanisms, it is important that future *in vitro* investigations optimise for physiological relevance.

The specific biomarkers investigated are a potential limitation to the present investigation, given that an anthocyanin-rich bilberry extract was reported to modulate at least 1261 genes, which may contribute to the progression or regression of atherosclerosis (Mauray et al., 2012). The use of DNA and protein microarrays may therefore be a consideration to highlight novel mechanisms of action on which flavonoid metabolites may act.

The use of human umbilical vein endothelial cells (HUVECs) may have been a limitation on the present investigations, as HUVEC do not originate from the arterial wall. Previous investigations from our group of the vascular effects of polyphenols have demonstrated that the expression of HO-1 in HUVEC and human coronary artery endothelial cells (HCAECs) in response to cyanidin-3-glucoside, PCA, and VA, are similar in both cell types (Edwards et al., 2015), thus HUVECs were a logical and financially viable model to use to screen a large number of treatments, though key results from such screens should be validated in HCAECs.

HCAEC utilised in Chapter 6 addresses this limitation and improves the physiological relevance of the study, though aortic endothelial cells could also have been used. Arterial rather than aortic cells were utilised as atherosclerosis is likely to develop in arteries where there is slow, or 'disturbed', flow (Hopkins, 2013). Endothelial cells grown on cell culture dishes are only exposed to reactants on the exposed surface of the cell, which is not reflective of their *in vivo* state. 3D-models, in which cells are grown within extracellular matrix (ECM) gels, are considered a more appropriate model as this allows cells to grow and interact with their medium at multiple surfaces, as would be situated *in vivo* (Pampaloni et al., 2007). 3D- cultures also have greater stability and longer lifespans compared to traditional 2D cultures, which may enable the chronic effects of flavonoids and their metabolites to be studied more effectively. Even more pioneering is the microfabrication of 'organs on a chip', as utilised more commonly in the fields of drug-delivery and toxicity (Huh et al., 2013). An example of such a model is the AngioChip (Zhang et al., 2016), which consists of layers resembling microchips stacked into a 3D blood vessel. Within this is a matrix of parenchymal cells surrounding a perfused, microchannel network coated with endothelial cells modelling a functional vessel lumen. The use of such models could be used in parallel to flavonoid feeding studies to more effectively study the 'real-time' effects of flavonoids and their metabolites, on processes such as monocyte adhesion in endothelial dysfunction. The use of rat smooth muscle cells (SMCs), as opposed to human, may be a limitation as the phenotypes and expression levels of cellular proteins may not be conserved between species (Kotokorpi et al., 2007). That said, the data from the present study could more easily be translated into animal models, such as in models mimicking *in vivo* anatomical structures, e.g. excised arterial rings and organ baths (Bell and Gochenaur, 2006, Sanchez et al., 2006, Ko et al., 2010). The effect size of vascular biomarkers in response to flavonoids may differ in rat relative to human cell types, and therefore, although cost prohibitive, future work should validate key findings in a human cell type, such as human coronary artery smooth muscle cells (HCASMCs), to confirm their relevance.

The use of endothelial cells or smooth muscle cell cultures in isolation may be seen as a limitation in the context of physiological relevance as, *in vivo*, the two cell types exist in close contact and cross-talk across an elastic intimal layer (Lodi et al., 2012). For example, eNOS is an endothelium derived enzyme, but ultimately its key bioactive endpoint (nitric oxide) targets the smooth muscle of the arterial vessel (Lusis, 2000). It may be interesting therefore to utilise a co-culture system, such as developed by others (Lodi et al., 2012), whereby the combined effects of these metabolites could be investigated. Ideally, these effects could be

mapped against an *ex vivo* model of rat aorta to elucidate target mechanisms. Arterial cells in particular are not static cells, but constantly cross talk with surrounding smooth muscle cells to expand and contract to facilitate blood flow, this in itself presents additional stresses and activates certain pathways in cells. Smooth muscle cells are not directly exposed to the circulation (and therefore circulating flavonoid metabolites) and so their intercellular concentrations of flavonoids would presumably be lower relative to endothelial cells. To address this, future studies could conduct an animal feeding study, followed by tissue extraction and high-resolution mass spectrometry (MS), which would elucidate the relative concentrations of flavonoid metabolites in SMCs. The metabolite profiles detected could then be mimicked *in vitro* to elucidate potential mechanisms. Alternatively, this issue may also be addressed by the use of an endothelial/SMC co-culture model (Truskey, 2010); enabling the endothelial cells to be exposed to the treatments in the first instance, where some intracellular endothelial metabolism of certain flavonoids is thought to occur (Toro-Funes et al., 2014, Rodriguez-Mateos et al., 2014c), followed by exposure to the smooth muscle cells to metabolites which diffuse or are transported from the endothelial cells.

In Chapter 6, the metabolite profiles with the maximum anti-inflammatory effect were observed at 6 h and 24 h post-consumption. Conversely, maximum effects on flow-mediated dilation (FMD) in response to the anthocyanin feeding have been observed at 2 h (Rodriguez-Mateos et al., 2014a). Overall, these data suggests an acute-phase modulatory vascular response of phenol metabolites followed by a delayed anti-inflammatory response many hours post-consumption. Based on these findings and those of the present study it may be possible that an immediate vascular response, mediated by very low levels of parent flavonoids and their immediate degradation products, is succeeded by a delayed anti-inflammatory response, mediated by products of colonic bacterial catabolism and hepatic phase II conjugation. Future studies may observe whether these peak metabolite profiles similarly affect expression levels of biomarkers of nitric oxide homeostasis at the same time points. These effects could be confirmed most effectively by the use of a randomised-control trial (RCT) which would target the effects of specific metabolite composition of labelled flavonoids across multiple time points, and their effects on vascular function, such as by FMD, and inflammatory biomarkers, such as sVCAM-1. Given that metabolites have been shown to be present in the circulation at 48 h (Czank et al., 2013), such studies should be extended to beyond this time point. Ideally, such a study would recruit a population who have relatively healthy vascular systems but elevated inflammatory biomarkers, such as those with metabolic syndrome (Scarpellini et al., 2012), especially given recent evidence

suggesting that flavonoids may be protective against this condition (Bhaswant et al., 2015). Data from such a study would better address the hypothesis of multiple mechanisms of metabolite activity, which may shed light on how flavonoids and their metabolites act chronically to modulate a number of physiological responses.

In summary, the present thesis provides novel insights into the bioactivity of flavonoids and their phenolic metabolites, their combined activities, and the potential mechanisms by which they may exert protective effects. The present investigation is, to the best of the author's knowledge, the first work to demonstrate the effects of conjugated phenolic metabolites on vascular and inflammatory biomarkers in endothelial and smooth muscle cells and the first study to observe that treatments which mimic plasma profiles following consumption of C3G appear to have greater anti-inflammatory activity relative to systematically constructed equimolar combinations of flavonoids. This thesis therefore provides evidence that may contribute to our understanding of the bioactivity of flavonoids in humans and therefore our understanding of the associations between diet and health.

## Chapter 8. References

- ABRAHAM, N. G. & KAPPAS, A. 2008. Pharmacological and clinical aspects of heme oxygenase. *Pharmacological Reviews*, 60, 79-127.
- ADEBAMOWO, C. A., CHO, E., SAMPSON, L., KATAN, M. B., SPIEGELMAN, D., WILLETT, W. C. & HOLMES, M. D. 2005. Dietary flavonols and flavonol-rich foods intake and the risk of breast cancer. *International Journal of Cancer*, 114, 628-633.
- AGATI, G., BRUNETTI, C., DI FERDINANDO, M., FERRINI, F., POLLASTRI, S. & TATTINI, M. 2013. Functional roles of flavonoids in photoprotection: new evidence, lessons from the past. *Plant Physiology & Biochemistry*, 72, 35-45.
- AL-SHALMANI, S., SURI, S., HUGHES, D. A., KROON, P. A., NEEDS, P. W., TAYLOR, M. A., TRIBOLO, S. & WILSON, V. G. 2011. Quercetin and its principal metabolites, but not myricetin, oppose lipopolysaccharide-induced hyporesponsiveness of the porcine isolated coronary artery. *British Journal of Pharmacology*, 162, 1485-97.
- ALP, N. J. & CHANNON, K. M. 2004. Regulation of endothelial nitric oxide synthase by tetrahydrobiopterin in vascular disease. *Arteriosclerosis, Thrombosis, and Vascular Biology*, 24, 413-20.
- AMIN, H. P., CZANK, C., RAHEEM, K. S., ZHANG, Q., BOTTING, N. P., CASSIDY, A. & KAY, C. D. 2015. Anthocyanin and its physiologically relevant metabolites alter the expression of IL-6 and VCAM-1 in CD40L and oxidized LDL challenged vascular endothelial cells. *Molecular Nutrition & Food Research*, 59, 1095-106.
- ANDUJAR, I., RECIO, M. C., GINER, R. M. & RIOS, J. L. 2012. Cocoa Polyphenols and Their Potential Benefits for Human Health. *Oxidative Medicine and Cellular Longevity*, 2012:906252
- ANGELONE, T., PASQUA, T., DI MAJO, D., QUINTIERI, A. M., FILICE, E., AMODIO, N., TOTA, B., GIAMMANCO, M. & CERRA, M. C. 2011. Distinct signalling mechanisms are involved in the dissimilar myocardial and coronary effects elicited by quercetin and myricetin, two red wine flavonols. *Nutrition, Metabolism, and Cardiovascular Diseases*, 21, 362-71.
- ARAÚJO, J. A., ZHANG, M. & YIN, F. 2012. Heme oxygenase-1, oxidation, inflammation, and atherosclerosis. *Frontiers in Pharmacology*, 3, 119.
- ARTS, I. C., HOLLMAN, P. C., FESKENS, E. J., BUENO DE MESQUITA, H. B. & KROMHOUT, D. 2001. Catechin intake might explain the inverse relation between tea consumption and ischemic heart disease: the Zutphen Elderly Study. *American Journal of Clinical Nutrition*, 74, 227-32.
- AYDIN, M., TEKIN, I. O., DOGAN, S. M., YILDIRIM, N., ARASLI, M., SAYIN, M. R. & AKTOP, Z. 2009. The levels of tumor necrosis factor-alpha and interleukin-6 in patients with isolated coronary artery ectasia. *Mediators of Inflammation*, 2009, 106145.
- BARONA, J., ARISTIZABAL, J. C., BLESSO, C. N., VOLEK, J. S. & FERNANDEZ, M. L. 2012. Grape polyphenols reduce blood pressure and increase flow-mediated vasodilation in men with metabolic syndrome. *Journal of Nutrition*, 142, 1626-32.
- BEECHER, G. R. 2003. Overview of dietary flavonoids: nomenclature, occurrence and intake. *Journal of Nutrition*, 133, 3248S-3254S.
- BELL, D. R. & GOCHENAUR, K. 2006. Direct vasoactive and vasoprotective properties of anthocyanin-rich extracts. *Journal of Applied Physiology* (1985), 100, 1164-70.

- BERK, B. C., ABE, J. I., MIN, W., SURAPISITCHAT, J. & YAN, C. 2001. Endothelial atheroprotective and anti-inflammatory mechanisms. *Annals of the New York Academy of Sciences*, 947, 93-109; discussion 109-11.
- BHAGAT, K. & VALLANCE, P. 1997. Inflammatory cytokines impair endothelium-dependent dilatation in human veins in vivo. *Circulation*, 96, 3042-7.
- BHASWANT, M., FANNING, K., NETZEL, M., MATHAI, M. L., PANCHAL, S. K. & BROWN, L. 2015. Cyanidin 3-glucoside improves diet-induced metabolic syndrome in rats. *Pharmacological Research*, 102, 208-17.
- BI, S. Y., DING, L., TIAN, Y., SONG, D. Q., ZHOU, X., LIU, X. & ZHANG, H. Q. 2004. Investigation of the interaction between flavonoids and human serum albumin. *Journal of Molecular Structure*, 703, 37-45.
- BIRT, D. F. & JEFFERY, E. 2013. Flavonoids. *Advances in Nutrition*, 4, 576-7.
- BLANKENBERG, S., BARBAUX, S. & TIRET, L. 2003. Adhesion molecules and atherosclerosis. *Atherosclerosis*, 170, 191-203.
- BLANKENBERG, S., RUPPRECHT, H. J., BICKEL, C., PEETZ, D., HAFNER, G., TIRET, L. & MEYER, J. 2001. Circulating cell adhesion molecules and death in patients with coronary artery disease. *Circulation*, 104, 1336-42.
- BOHN, T. 2014. Dietary factors affecting polyphenol bioavailability. *Nutrition Reviews*, 72, 429-52.
- BOKKENHEUSER, V. D., SHACKLETON, C. H. & WINTER, J. 1987. Hydrolysis of dietary flavonoid glycosides by strains of intestinal Bacteroides from humans. *The Biochemical Journal*, 248, 953-6.
- BONDONNO, C. P., YANG, X., CROFT, K. D., CONSIDINE, M. J., WARD, N. C., RICH, L., PUDDEY, I. B., SWINNY, E., MUBARAK, A. & HODGSON, J. M. 2012. Flavonoid-rich apples and nitrate-rich spinach augment nitric oxide status and improve endothelial function in healthy men and women: a randomized controlled trial. *Free Radical Biology & Medicine*, 52, 95-102.
- BORNHOEFT, J., CASTANEDA, D., NEMOSECK, T., WANG, P. W., HENNING, S. M. & HONG, M. Y. 2012. The Protective Effects of Green Tea Polyphenols: Lipid Profile, Inflammation, and Antioxidant Capacity in Rats Fed an Atherogenic Diet and Dextran Sodium Sulfate. *Journal of Medicinal Food*, 15, 726-732.
- BOULTON, D. W., WALLE, U. K. & WALLE, T. 1998. Extensive binding of the bioflavonoid quercetin to human plasma proteins. *Journal of Pharmacy and Pharmacology*, 50, 243-9.
- BRANEN, L., HOVGAARD, L., NITULESCU, M., BENGTSSON, E., NILSSON, J. & JOVINGE, S. 2004. Inhibition of tumor necrosis factor-alpha reduces atherosclerosis in apolipoprotein E knockout mice. *Arteriosclerosis, Thrombosis, and Vascular Biology*, 24, 2137-42.
- BRAVO, L. 1998. Polyphenols: Chemistry, dietary sources, metabolism, and nutritional significance. *Nutrition Reviews*, 56, 317-333.
- BRENMER, P., HEINRICH, M. (2002). Natural products as targeted modulators of the nuclear factor-KB pathway. *Journal of Pharmacy and Pharmacology* 54(4): 453-472.
- BRENNER, D., BLASER, H. & MAK, T. W. 2015. Regulation of tumour necrosis factor signalling: live or let die. *Nature Reviews Immunology*, 15, 362-74.
- BRUNETTI, C., DI FERDINANDO, M., FINI, A., POLLASTRI, S. & TATTINI, M. 2013. Flavonoids as antioxidants and developmental regulators: relative significance in plants and humans. *International Journal of Molecular Sciences*, 14, 3540-55.
- BRUUNSGAARD, H., ANDERSEN-RANBERG, K., JEUNE, B., PEDERSEN, A. N., SKINHOJ, P. & PEDERSEN, B. K. 1999. A high plasma concentration of TNF-alpha is associated with dementia in centenarians. *The Journals of Gerontology. Series A, Biological Sciences and Medical Sciences*, 54, M357-64.

- BRUUNSGAARD, H., SKINHOJ, P., PEDERSEN, A. N., SCHROLL, M. & PEDERSEN, B. K. 2000. Ageing, tumour necrosis factor-alpha (TNF-alpha) and atherosclerosis. *Clinical and Experimental Immunology*, 121, 255-60.
- BURGER, D. & TOUYZ, R. M. 2012. Cellular biomarkers of endothelial health: microparticles, endothelial progenitor cells, and circulating endothelial cells. *Journal of the American Society of Hypertension*, 6, 85-99.
- BURRIS, R. L., NG, H. P. & NAGARAJAN, S. 2014. Soy protein inhibits inflammation-induced VCAM-1 and inflammatory cytokine induction by inhibiting the NF-kappaB and AKT signaling pathway in apolipoprotein E-deficient mice. *European Journal of Nutrition*, 53, 135-48.
- CASSIDY, A., MUKAMAL, K. J., LIU, L., FRANZ, M., ELIASSEN, A. H. & RIMM, E. B. 2013. High anthocyanin intake is associated with a reduced risk of myocardial infarction in young and middle-aged women. *Circulation*, 127, 188-96.
- CASSIDY, A., O'REILLY, E. J., KAY, C., SAMPSON, L., FRANZ, M., FORMAN, J. P., CURHAN, G. & RIMM, E. B. 2011. Habitual intake of flavonoid subclasses and incident hypertension in adults. *American Journal of Clinical Nutrition*, 93, 338-47.
- CATALAN, U., FERNANDEZ-CASTILLEJO, S., PONS, L., HERAS, M., ARAGONES, G., ANGLAS, N., MORELLO, J. R. & SOLA, R. 2012. Alpha-tocopherol and BAY 11-7082 reduce vascular cell adhesion molecule in human aortic endothelial cells. *Journal of Vascular Research*, 49, 319-28.
- CAYATTE, A. J., PALACINO, J. J., HORTEN, K. & COHEN, R. A. 1994. Chronic inhibition of nitric oxide production accelerates neointima formation and impairs endothelial function in hypercholesterolemic rabbits. *Arteriosclerosis and Thrombosis*, 14, 753-9.
- CEBR 2014. The economic cost of cardiovascular disease from 2014-2020 in six European economies. August 2014 edition.
- CESARI, M., PENNINX, B. W., NEWMAN, A. B., KRITCHEVSKY, S. B., NICKLAS, B. J., SUTTON-TYRRELL, K., TRACY, R. P., RUBIN, S. M., HARRIS, T. B. & PAHOR, M. 2003. Inflammatory markers and cardiovascular disease (The Health, Aging and Body Composition [Health ABC] Study). *American Journal of Cardiology*, 92, 522-8.
- CHAN, K. H., NG, M. K. & STOCKER, R. 2011. Haem oxygenase-1 and cardiovascular disease: mechanisms and therapeutic potential. *Clinical Science*, 120, 493-504.
- CHANET, A., MILENKOVIC, D., CLAUDE, S., MAIER, J. A., KHAN, M. K., RAKOTOMANOMANA, N., SHINKARUK, S., BERARD, A. M., BENNETAU-PELISSERO, C., MAZUR, A. & MORAND, C. 2013. Flavanone metabolites decrease monocyte adhesion to TNF-alpha-activated endothelial cells by modulating expression of atherosclerosis-related genes. *British Journal of Nutrition*, 100 (4), 587-98.
- CHAPIDZE, L., KAPANADZE, S., DOLIDZE, N., BAKHUTASHVILI, Z. & LATSABIDZE, N. 2007. Endothelial dysfunction in patients with coronary atherosclerosis. *Georgian Medical News*, 142, 20-2.
- CHEN, C. C., CHOW, M. P., HUANG, W. C., LIN, Y. C. & CHANG, Y. J. 2004a. Flavonoids inhibit tumor necrosis factor-alpha-induced up-regulation of intercellular adhesion molecule-1 (ICAM-1) in respiratory epithelial cells through activator protein-1 and nuclear factor-kappaB: structure-activity relationships. *Molecular Pharmacology*, 66, 683-93.
- CHEN, J. W., LIN, F. Y., CHEN, Y. H., WU, T. C., CHEN, Y. L. & LIN, S. J. 2004b. Carvedilol inhibits tumor necrosis factor-alpha-induced endothelial transcription factor activation, adhesion molecule expression, and adhesiveness to human mononuclear cells. *Arteriosclerosis, Thrombosis, and Vascular Biology*, 24, 2075-81.

- CHEN, S., DING, Y., TAO, W., ZHANG, W., LIANG, T. & LIU, C. 2012. Naringenin inhibits TNF-alpha induced VSMC proliferation and migration via induction of HO-1. *Food and Chemical Toxicology*, 50, 3025-31.
- CHEN, Y. H., LIN, S. J., CHEN, J. W., KU, H. H. & CHEN, Y. L. 2002. Magnolol attenuates VCAM-1 expression in vitro in TNF-alpha-treated human aortic endothelial cells and in vivo in the aorta of cholesterol-fed rabbits. *British Journal of Pharmacology*, 135, 37-47.
- CHEN, Y. H., LIN, S. J., KU, H. H., SHIAO, M. S., LIN, F. Y., CHEN, J. W. & CHEN, Y. L. 2001. Salvianolic acid B attenuates VCAM-1 and ICAM-1 expression in TNF-alpha-treated human aortic endothelial cells. *Journal of Cellular Biochemistry*, 82, 512-21.
- CHO, Y. J. & KIM, S. J. 2013. Effect of quercetin on the production of nitric oxide in murine macrophages stimulated with lipopolysaccharide from *Prevotella intermedia*. *Journal of Periodontal & Implant Science*, 43, 191-7.
- CHOI, J. S., CHOI, Y. J., PARK, S. H., KANG, J. S. & KANG, Y. H. 2004. Flavones mitigate tumor necrosis factor-alpha-induced adhesion molecule - Upregulation in cultured human endothelial cells: Role of nuclear factor-kappa B. *Journal of Nutrition*, 134, 1013-1019.
- CHOW, J. M., SHEN, S. C., HUAN, S. K., LIN, H. Y. & CHEN, Y. C. 2005. Quercetin, but not rutin and quercitrin, prevention of H<sub>2</sub>O<sub>2</sub>-induced apoptosis via anti-oxidant activity and heme oxygenase 1 gene expression in macrophages. *Biochemical Pharmacology*, 69, 1839-51.
- CLAUDE, S., BOBY, C., RODRIGUEZ-MATEOS, A., SPENCER, J. P., GERARD, N., MORAND, C. & MILENKOVIC, D. 2014. Flavanol metabolites reduce monocyte adhesion to endothelial cells through modulation of expression of genes via p38-MAPK and p65-Nf-kB pathways. *Molecular Nutrition & Food Research*, 58, 1016-27.
- CLIFFORD, M. N., VAN DER HOOFT, J. J. & CROZIER, A. 2013. Human studies on the absorption, distribution, metabolism, and excretion of tea polyphenols. *American Journal of Clinical Nutrition*, 98, 1619S-1630S.
- CORCORAN, M. P., MCKAY, D. L. & BLUMBERG, J. B. 2012. Flavonoid basics: chemistry, sources, mechanisms of action, and safety. *Journal of Nutrition in Gerontology and Geriatrics*, 31, 176-89.
- CROZIER, A., JAGANATH, I. B. & CLIFFORD, M. N. 2009. Dietary phenolics: chemistry, bioavailability and effects on health. *Natural Product Reports*, 26, 1001-43.
- CURTIS, P. J., KROON, P. A., HOLLANDS, W. J., WALLS, R., JENKINS, G., KAY, C. D. & CASSIDY, A. 2009. Cardiovascular disease risk biomarkers and liver and kidney function are not altered in postmenopausal women after ingesting an elderberry extract rich in anthocyanins for 12 weeks. *Journal of Nutrition*, 139, 2266-71.
- CUTLER, G. J., NETTLETON, J. A., ROSS, J. A., HARNACK, L. J., JACOBS, D. R., SCRAFFORD, C. G., BARRAJ, L. M., MINK, P. J. & ROBIEN, K. 2008. Dietary flavonoid intake and risk of cancer in postmenopausal women: The Iowa Women's Health Study. *International Journal of Cancer*, 123, 664-671.
- CYBULSKY, M. I., IIYAMA, K., LI, H., ZHU, S., CHEN, M., IIYAMA, M., DAVIS, V., GUTIERREZ-RAMOS, J. C., CONNELLY, P. W. & MILSTONE, D. S. 2001. A major role for VCAM-1, but not ICAM-1, in early atherosclerosis. *Journal of Clinical Investigation*, 107, 1255-62.
- CZANK, C., CASSIDY, A., ZHANG, Q., MORRISON, D. J., PRESTON, T., KROON, P. A., BOTTING, N. P. & KAY, C. D. 2013. Human metabolism and elimination of the anthocyanin, cyanidin-3-glucoside: a (13)C-tracer study. *American Journal of Clinical Nutrition*, 97, 995-1003.

- D'ALESSIO, P., MOUTET, M., COUDRIER, E., DARQUENNE, S. & CHAUDIERE, J. 1998. ICAM-1 and VCAM-1 expression induced by TNF-alpha are inhibited by a glutathione peroxidase mimic. *Free Radical Biology & Medicine*, 24, 979-87.
- DAVIS, P. A., POLAGRUTO, J. A., VALACCHI, G., PHUNG, A., SOUCEK, K., KEEN, C. L. & GERSHWIN, M. E. 2006. Effect of apple extracts on NF-kappaB activation in human umbilical vein endothelial cells. *Experimental Biology and Medicine*, 231, 594-8.
- DAY, A. J., GEE, J. M., DUPONT, M. S., JOHNSON, I. T. & WILLIAMSON, G. 2003. Absorption of quercetin-3-glucoside and quercetin-4'-glucoside in the rat small intestine: the role of lactase phlorizin hydrolase and the sodium-dependent glucose transporter. *Biochemical Pharmacology*, 65, 1199-206.
- DAY, A. J., MELLON, F., BARRON, D., SARRAZIN, G., MORGAN, M. R. & WILLIAMSON, G. 2001. Human metabolism of dietary flavonoids: identification of plasma metabolites of quercetin. *Free Radical Research*, 35, 941-52.
- DE FERRARS, R. M., CASSIDY, A., CURTIS, P. & KAY, C. D. 2014a. Phenolic metabolites of anthocyanins following a dietary intervention study in post-menopausal women. *Molecular Nutrition & Food Research*, 58, 490-502.
- DE FERRARS, R. M., CZANK, C., ZHANG, Q., BOTTING, N. P., KROON, P. A., CASSIDY, A. & KAY, C. D. 2014b. The pharmacokinetics of anthocyanins and their metabolites in humans. *British Journal of Pharmacology*, 171, 3268-82.
- DEANFIELD, J. E., HALCOX, J. P. & RABELINK, T. J. 2007. Endothelial function and dysfunction: testing and clinical relevance. *Circulation*, 115, 1285-95.
- DELL'AGLI, M., BUSCIALA, A. & BOSISIO, E. 2004. Vascular effects of wine polyphenols. *Cardiovascular Research*, 63, 593-602.
- DESCH, S., SCHMIDT, J., KOBLER, D., SONNABEND, M., EITEL, I., SAREBAN, M., RAHIMI, K., SCHULER, G. & THIELE, H. 2010. Effect of Cocoa Products on Blood Pressure: Systematic Review and Meta-Analysis. *American Journal of Hypertension*, 23, 97-103.
- DI GESSO, J. L., KERR, J. S., ZHANG, Q., RAHEEM, K. S., YALAMANCHILI, S. K., O'HAGAN, D., KAY, C. D. & O'CONNELL, M. A. 2015. Flavonoid metabolites reduce tumor necrosis factor-alpha secretion to a greater extent than their precursor compounds in human THP-1 monocytes. *Molecular Nutrition & Food Research*, 59 (6), 1143-54
- DINKOVA-KOSTOVA, A. T., HOLTZCLAW, W. D., COLE, R. N., ITOH, K., WAKABAYASHI, N., KATOH, Y., YAMAMOTO, M. & TALALAY, P. 2002. Direct evidence that sulfhydryl groups of Keap1 are the sensors regulating induction of phase 2 enzymes that protect against carcinogens and oxidants. *Proceedings of the National Academy of Sciences of the United States of America*, 99, 11908-13.
- DONG, W. H., WANG, T. Y., WANG, F. & ZHANG, J. H. 2011. Simple, time-saving dye staining of proteins for sodium dodecyl sulfate-polyacrylamide gel electrophoresis using Coomassie blue. *PLoS One*, 6, e22394.
- DUPONT, M. S., DAY, A. J., BENNETT, R. N., MELLON, F. A. & KROON, P. A. 2004. Absorption of kaempferol from endive, a source of kaempferol-3-glucuronide, in humans. *European Journal of Clinical Nutrition*, 58, 947-54.
- EDWARDS, M., CZANK, C., WOODWARD, G. M., CASSIDY, A. & KAY, C. D. 2015. Phenolic metabolites of anthocyanins modulate mechanisms of endothelial function. *Journal of Agricultural and Food Chemistry*, 63, 2423-31.
- EGGLER, A. L., LIU, G., PEZZUTO, J. M., VAN BREEMEN, R. B. & MESECAR, A. D. 2005. Modifying specific cysteines of the electrophile-sensing human Keap1 protein is insufficient to disrupt binding to the Nrf2 domain Neh2. *Proceedings of the National Academy of Sciences of the United States of America*, 102, 10070-5.

- ELAVARASAN, J., VELUSAMY, P., GANESAN, T., RAMAKRISHNAN, S. K., RAJASEKARAN, D. & PERIANDAVAN, K. 2012. Hesperidin-mediated expression of Nrf2 and upregulation of antioxidant status in senescent rat heart. *Journal of Pharmacy and Pharmacology*, 64, 1472-82.
- FARIDI, Z., NJIKE, V. Y., DUTTA, S., ALI, A. & KATZ, D. L. 2008. Acute dark chocolate and cocoa ingestion and endothelial function: a randomized controlled crossover trial. *American Journal of Clinical Nutrition*, 88, 58-63.
- FAURSCHOU, A. & GNIADDECKI, R. 2008. TNF-alpha stimulates Akt by a distinct aPKC-dependent pathway in premalignant keratinocytes. *Experimental Dermatology*, 17, 992-7.
- FELGINES, C., TALAVERA, S., TEXIER, O., GIL-IZQUIERDO, A., LAMAISON, J. L. & REMESY, C. 2005. Blackberry anthocyanins are mainly recovered from urine as methylated and glucuronidated conjugates in humans. *Journal of Agricultural and Food Chemistry*, 53, 7721-7727.
- FELICIANO, R. P., PRITZEL, S., HEISS, C. & RODRIGUEZ-MATEOS, A. 2015. Flavonoid intake and cardiovascular disease risk. *Current Opinion in Food Science*, 2, 92-99.
- FERRE, S., BALDOLI, E., LEIDI, M. & MAIER, J. A. 2010. Magnesium deficiency promotes a pro-atherogenic phenotype in cultured human endothelial cells via activation of NFkB. *Biochimica et Biophysica Acta*, 1802, 952-8.
- FROSTEGARD, J. 2013. Immunity, atherosclerosis and cardiovascular disease. *BMC Medicine*, 11, 117.
- FULL, L. E., RUISANCHEZ, C. & MONACO, C. 2009. The inextricable link between atherosclerosis and prototypical inflammatory diseases rheumatoid arthritis and systemic lupus erythematosus. *Arthritis Research & Therapy*, 11, 217.
- GALKINA, E. & LEY, K. 2007. Vascular adhesion molecules in atherosclerosis. *Arteriosclerosis, Thrombosis and Vascular Biology*, 27, 2292-301.
- GANDHI, C., UPAGANALAWAR, A. & BALARAMAN, R. 2009. Protection against in vivo focal myocardial ischemia/reperfusion injury-induced arrhythmias and apoptosis by Hesperidin. *Free Radical Research*, 43, 817-827.
- GARCIA-LAFUENTE, A., GUILLAMON, E., VILLARES, A., ROSTAGNO, M. A. & MARTINEZ, J. A. 2009. Flavonoids as anti-inflammatory agents: implications in cancer and cardiovascular disease. *Inflammation Research*, 58, 537-52.
- GARTON, K. J., GOUGH, P. J., PHILALAY, J., WILLE, P. T., BLOBEL, C. P., WHITEHEAD, R. H., DEMPSEY, P. J. & RAINES, E. W. 2003. Stimulated shedding of vascular cell adhesion molecule 1 (VCAM-1) is mediated by tumor necrosis factor-alpha-converting enzyme (ADAM 17). *Journal of Biological Chemistry*, 278, 37459-64.
- GELEIJNSE, J. M., LAUNER, L. J., VAN DER KUIP, D. A., HOFMAN, A. & WITTEMAN, J. C. 2002. Inverse association of tea and flavonoid intakes with incident myocardial infarction: the Rotterdam Study. *American Journal of Clinical Nutrition*, 75, 880-6.
- GIMBRONE, M. A., JR. & GARCIA-CARDENA, G. 2016. Endothelial Cell Dysfunction and the Pathobiology of Atherosclerosis. *Circulation Research*, 118, 620-36.
- GONZALEZ, R., BALLESTER, I., LOPEZ-POSADAS, R., SUAREZ, M. D., ZARZUELO, A., MARTINEZ-AUGUSTIN, O. & SANCHEZ DE MEDINA, F. 2011. Effects of flavonoids and other polyphenols on inflammation. *Critical Reviews in Food Science and Nutrition*, 51, 331-62.

- GRANADO-SERRANO, A. B., MARTIN, M. A., BRAVO, L., GOYA, L. & RAMOS, S. 2012. Quercetin modulates Nrf2 and glutathione-related defenses in HepG2 cells: Involvement of p38. *Chemico-Biological Interactions*, 195, 154-64.
- GRASSI, D., DESIDERI, G., NECOZIONE, S., DI GIOSIA, P., BARNABEI, R., ALLEGAERT, L., BERNAERT, H. & FERRI, C. 2015. Cocoa consumption dose-dependently improves flow-mediated dilation and arterial stiffness decreasing blood pressure in healthy individuals. *Journal of Hypertension*, 33, 294-303.
- GREEN, D. J., DAWSON, E. A., GROENEWOUD, H. M., JONES, H. & THIJSSSEN, D. H. 2014. Is flow-mediated dilation nitric oxide mediated?: A meta-analysis. *Hypertension*, 63, 376-82.
- GUSTIN, J. A., OZES, O. N., AKCA, H., PINCHEIRA, R., MAYO, L. D., LI, Q., GUZMAN, J. R., KORGAONKAR, C. K. & DONNER, D. B. 2004. Cell type-specific expression of the I $\kappa$ B kinases determines the significance of phosphatidylinositol 3-kinase/Akt signaling to NF- $\kappa$ B activation. *Journal of Biological Chemistry*, 279, 1615-20.
- HAN, S. G., HAN, S. S., TOBOREK, M. & HENNIG, B. 2012. EGCG protects endothelial cells against PCB 126-induced inflammation through inhibition of AhR and induction of Nrf2-regulated genes. *Toxicology and Applied Pharmacology*, 261, 181-8.
- HARASSTANI, O. A., MOIN, S., THAM, C. L., LIEW, C. Y., ISMAIL, N., RAJAJENDRAM, R., HARITH, H. H., ZAKARIA, Z. A., MOHAMAD, A. S., SULAIMAN, M. R. & ISRAF, D. A. 2010. Flavonoid combinations cause synergistic inhibition of proinflammatory mediator secretion from lipopolysaccharide-induced RAW 264.7 cells. *Inflammation research: official journal of the European Histamine Research Society*, 59, 711-21.
- HARTWEG, J., GUNTER, M., PERERA, R., FARMER, A., CULL, C., SCHALKWIJK, C., KOK, A., TWAALFHOVEN, H., HOLMAN, R. & NEIL, A. 2007. Stability of soluble adhesion molecules, selectins, and C-reactive protein at various temperatures: implications for epidemiological and large-scale clinical studies. *Clinical Chemistry*, 53, 1858-60.
- HEEBA, G. H., MAHMOUD, M. E. & EL HANAFY, A. A. 2012. Anti-inflammatory potential of curcumin and quercetin in rats: Role of oxidative stress, heme oxygenase-1 and TNF- $\alpha$ . *Toxicology and Industrial Health*, 30, 551-560.
- HEHLGANS, T. & PFEFFER, K. 2005. The intriguing biology of the tumour necrosis factor/tumour necrosis factor receptor superfamily: players, rules and the games. *Immunology*, 115, 1-20.
- HEISS, C., RODRIGUEZ-MATEOS, A. & KELM, M. 2015. Central role of eNOS in the maintenance of endothelial homeostasis. *Antioxidant and Redox Signalling*, 22, 1230-42.
- HELENO, S. A., MARTINS, A., QUEIROZ, M. J. & FERREIRA, I. C. 2015. Bioactivity of phenolic acids: metabolites versus parent compounds: a review. *Food Chemistry*, 173, 501-13.
- HELLEMANS, J., MORTIER, G., DE PAEPE, A., SPELEMAN, F. & VANDESOMPELE, J. 2007. qBase relative quantification framework and software for management and automated analysis of real-time quantitative PCR data. *Genome Biology*, 8, R19.
- HIDALGO, M., SANCHEZ-MORENO, C. & DE PASCUAL-TERESA, S. 2010. Flavonoid-flavonoid interaction and its effect on their antioxidant activity. *Food Chemistry*, 121, 691-696.
- HOLLMAN, P. C., VD GAAG, M., MENGELERS, M. J., VAN TRIJP, J. M., DE VRIES, J. H. & KATAN, M. B. 1996. Absorption and disposition kinetics of the dietary antioxidant quercetin in man. *Free Radical Biology & Medicine*, 21, 703-7.

- HONDA, R. & YASUDA, H. 2000. Activity of MDM2, a ubiquitin ligase, toward p53 or itself is dependent on the RING finger domain of the ligase. *Oncogene*, 19, 1473-6.
- HOOPER, L., KAY, C., ABDELHAMID, A., KROON, P. A., COHN, J. S., RIMM, E. B. & CASSIDY, A. 2012. Effects of chocolate, cocoa, and flavan-3-ols on cardiovascular health: a systematic review and meta-analysis of randomized trials. *American Journal of Clinical Nutrition*, 95, 740-51.
- HOOPER, L., KROON, P. A., RIMM, E. B., COHN, J. S., HARVEY, I., LE CORNU, K. A., RYDER, J. J., HALL, W. L. & CASSIDY, A. 2008. Flavonoids, flavonoid-rich foods, and cardiovascular risk: a meta-analysis of randomized controlled trials. *American Journal of Clinical Nutrition*, 88, 38-50.
- HOPE, S. A. & MEREDITH, I. T. 2003. Cellular adhesion molecules and cardiovascular disease. Part II. Their association with conventional and emerging risk factors, acute coronary events and cardiovascular risk prediction. *Internal Medicine Journal*, 33, 450-62.
- HOPKINS, P. N. 2013. Molecular biology of atherosclerosis. *Physiological Reviews*, 93, 1317-542.
- HUBER, S. A., SAKKINEN, P., CONZE, D., HARDIN, N. & TRACY, R. 1999. Interleukin-6 exacerbates early atherosclerosis in mice. *Arteriosclerosis, Thrombosis and Vascular Biology*, 19, 2364-7.
- HUH, D., KIM, H. J., FRASER, J. P., SHEA, D. E., KHAN, M., BAHINSKI, A., HAMILTON, G. A. & INGBER, D. E. 2013. Microfabrication of human organs-on-chips. *Nature Protocols*, 8, 2135-57.
- HYBERTSON, B. M., GAO, B., BOSE, S. K. & MCCORD, J. M. 2011. Oxidative stress in health and disease: the therapeutic potential of Nrf2 activation. *Molecular Aspects of Medicine*, 32, 234-46.
- ISHISAKA, A., KAWABATA, K., MIKI, S., SHIBA, Y., MINEKAWA, S., NISHIKAWA, T., MUKAI, R., TERAOKA, J. & KAWAI, Y. 2013. Mitochondrial dysfunction leads to deconjugation of quercetin glucuronides in inflammatory macrophages. *PLoS One*, 8, e80843.
- JACKSON, S. J. & VENEMA, R. C. 2006. Quercetin inhibits eNOS, microtubule polymerization, and mitotic progression in bovine aortic endothelial cells. *Journal of Nutrition*, 136, 1178-84.
- JIANG, J., MO, Z. C., YIN, K., ZHAO, G. J., LV, Y. C., OUYANG, X. P., JIANG, Z. S., FU, Y. & TANG, C. K. 2012. Epigallocatechin-3-gallate prevents TNF- $\alpha$ -induced NF- $\kappa$ B activation thereby upregulating ABCA1 via the Nrf2/Keap1 pathway in macrophage foam cells. *International Journal of Molecular Medicine*, 29, 946-56.
- JIMENEZ, R., LOPEZ-SEPULVEDA, R., ROMERO, M., TORAL, M., COGOLLUDO, A., PEREZ-VIZCAINO, F. & DUARTE, J. 2015. Quercetin and its metabolites inhibit the membrane NADPH oxidase activity in vascular smooth muscle cells from normotensive and spontaneously hypertensive rats. *Food & Function*, 6, 409-14.
- JUURLINK, B. H., AZOUZ, H. J., ALDALATI, A. M., ALTINAWI, B. M. & GANGULY, P. 2014. Hydroxybenzoic acid isomers and the cardiovascular system. *Nutrition Journal*, 13, 63.
- KAKKAR, S. & BAIS, S. 2014. A review on protocatechuic Acid and its pharmacological potential. *ISRN Pharmacology*, 2014, 952943.
- KALTSCHMIDT, B., KALTSCHMIDT, C., HOFMANN, T. G., HEHNER, S. P., DROGE, W. & SCHMITZ, M. L. 2000. The pro- or anti-apoptotic function of NF- $\kappa$ B is determined by the nature of the apoptotic stimulus. *European Journal of Biochemistry*, 267, 3828-35.
- KANG, J. S., YOON, Y. D., HAN, M. H., HAN, S. B., LEE, K., LEE, K. H., PARK, S. K. & KIM, H. M. 2006. Glabridin suppresses intercellular adhesion molecule-1 expression in tumor necrosis factor- $\alpha$ -stimulated human umbilical vein endothelial cells by blocking sphingosine kinase pathway: implications of Akt, extracellular signal-regulated kinase, and nuclear factor- $\kappa$ B/Rel signaling pathways. *Molecular Pharmacology*, 69, 941-9.

- KARLSEN, A., PAUR, I., BOHN, S. K., SAKHI, A. K., BORGE, G. I., SERAFINI, M., ERLUND, I., LAAKE, P., TONSTAD, S. & BLOMHOFF, R. 2010. Bilberry juice modulates plasma concentration of NF-kappaB related inflammatory markers in subjects at increased risk of CVD. *European Journal of Nutrition*, 49, 345-55.
- KASPAR, J. W. & JAISWAL, A. K. 2010. Antioxidant-induced phosphorylation of tyrosine 486 leads to rapid nuclear export of Bach1 that allows Nrf2 to bind to the antioxidant response element and activate defensive gene expression. *Journal of Biological Chemistry*, 285, 153-62.
- KASPAR, J. W., NITURE, S. K. & JAISWAL, A. K. 2012. Antioxidant-induced INrf2 (Keap1) tyrosine 85 phosphorylation controls the nuclear export and degradation of the INrf2-Cul3-Rbx1 complex to allow normal Nrf2 activation and repression. *Journal of Cell Science*, 125, 1027-38.
- KAUSER, K., DA CUNHA, V., FITCH, R., MALLARI, C. & RUBANYI, G. M. 2000. Role of endogenous nitric oxide in progression of atherosclerosis in apolipoprotein E-deficient mice. *American Journal of Physiology, Heart and Circulatory Physiology*, 278, H1679-85.
- KAWAI, Y., NISHIKAWA, T., SHIBA, Y., SAITO, S., MUROTA, K., SHIBATA, N., KOBAYASHI, M., KANAYAMA, M., UCHIDA, K. & TERAOKA, J. 2008. Macrophage as a target of quercetin glucuronides in human atherosclerotic arteries - Implication in the anti-atherosclerotic mechanism of dietary flavonoids. *Journal of Biological Chemistry*, 283, 9424-9434.
- KAWAMURA, K., ISHIKAWA, K., WADA, Y., KIMURA, S., MATSUMOTO, H., KOHRO, T., ITABE, H., KODAMA, T. & MARUYAMA, Y. 2005. Bilirubin from heme oxygenase-1 attenuates vascular endothelial activation and dysfunction. *Arteriosclerosis, Thrombosis and Vascular Biology*, 25, 155-60.
- KAWASHIMA, S. & YOKOYAMA, M. 2004. Dysfunction of endothelial nitric oxide synthase and atherosclerosis. *Arteriosclerosis, Thrombosis and Vascular Biology*, 24, 998-1005.
- KAY, C. D. 2006. Aspects of anthocyanin absorption, metabolism and pharmacokinetics in humans. *Nutrition Research Reviews*, 19, 137-46.
- KAY, C. D. 2010. The future of flavonoid research. *British Journal of Nutrition*, 104 Suppl 3, S91-5.
- KAY, C. D. 2015. Rethinking paradigms for studying mechanisms of action of plant bioactives. *Nutrition Bulletins*, 40, 335-339.
- KAY, C. D., HOOPER, L., KROON, P. A., RIMM, E. B. & CASSIDY, A. 2012. Relative impact of flavonoid composition, dose and structure on vascular function: a systematic review of randomised controlled trials of flavonoid-rich food products. *Molecular Nutrition & Food Research*, 56, 1605-16.
- KAY, C. D., KROON, P. A. & CASSIDY, A. 2009. The bioactivity of dietary anthocyanins is likely to be mediated by their degradation products. *Molecular Nutrition & Food Research*, 53 Suppl 1, S92-101.
- KAY, C. D., MAZZA, G. J. & HOLUB, B. J. 2005. Anthocyanins exist in the circulation primarily as metabolites in adult men. *Journal of Nutrition*, 135, 2582-8.
- KEANE, K. M., BELL, P. G., LODGE, J. K., CONSTANTINO, C. L., JENKINSON, S. E., BASS, R. & HOWATSON, G. 2015. Phytochemical uptake following human consumption of Montmorency tart cherry (*L. Prunus cerasus*) and influence of phenolic acids on vascular smooth muscle cells in vitro. *European Journal of Nutrition*, 1-11.
- KEMPE, S., KESTLER, H., LASAR, A. & WIRTH, T. 2005. NF-kappaB controls the global pro-inflammatory response in endothelial cells: evidence for the regulation of a pro-atherogenic program. *Nucleic Acids Research*, 33, 5308-19.

- KEPPLER, K. & HUMPF, H. U. 2005. Metabolism of anthocyanins and their phenolic degradation products by the intestinal microflora. *Bioorganic & Medicinal Chemistry*, 13, 5195-205.
- KERIMI, A. & WILLIAMSON, G. 2016. At the interface of antioxidant signalling and cellular function: key polyphenol effects. *Molecular Nutrition & Food Research*, 00, 1-19.
- KHANDELWAL, A. R., HEBERT, V. Y., KLEINEDLER, J. J., ROGERS, L. K., ULLEVIG, S. L., ASMIS, R., SHI, R. & DUGAS, T. R. 2012. Resveratrol and quercetin interact to inhibit neointimal hyperplasia in mice with a carotid injury. *Journal of Nutrition*, 142, 1487-94.
- KIM, J., CHA, Y. N. & SURH, Y. J. 2010. A protective role of nuclear factor-erythroid 2-related factor-2 (Nrf2) in inflammatory disorders. *Mutation Research*, 690, 12-23.
- KIM, J. E., KANG, Y. J., LEE, K. Y. & CHOI, H. C. 2009. Isoproterenol inhibits angiotensin II-stimulated proliferation and reactive oxygen species production in vascular smooth muscle cells through heme oxygenase-1. *Biological & Pharmaceutical Bulletin*, 32, 1047-52.
- KIM, Y. M., PAE, H. O., PARK, J. E., LEE, Y. C., WOO, J. M., KIM, N. H., CHOI, Y. K., LEE, B. S., KIM, S. R. & CHUNG, H. T. 2011. Heme oxygenase in the regulation of vascular biology: from molecular mechanisms to therapeutic opportunities. *Antioxidants & Redox Signalling*, 14, 137-67.
- KJAERGAARD, A. G., DIGE, A., KROG, J., TONNESEN, E. & WOGENSEN, L. 2013. Soluble adhesion molecules correlate with surface expression in an in vitro model of endothelial activation. *Basic & Clinical Pharmacology & Toxicology*, 113, 273-9.
- KLING, B., BUCHERL, D., PALATZKY, P., MATYSIK, F. M., DECKER, M., WEGENER, J. & HEILMANN, J. 2014. Flavonoids, flavonoid metabolites, and phenolic acids inhibit oxidative stress in the neuronal cell line HT-22 monitored by ECIS and MTT assay: a comparative study. *Journal of Natural Products*, 77, 446-54.
- KNEKT, P., KUMPULAINEN, J., JARVINEN, R., RISSANEN, H., HELIOVAARA, M., REUNANEN, A., HAKULINEN, T. & AROMAA, A. 2002. Flavonoid intake and risk of chronic diseases. *American Journal of Clinical Nutrition*, 76, 560-8.
- KO, E. A., SONG, M. Y., DONTAMSETTY, R., MAKINO, A. & YUAN, J. X. 2010. Tension Measurement in Isolated Rat and Mouse Pulmonary Artery. *Drug Discovery Today: Disease Models*, 7, 123-130.
- KOGA, T. & MEYDANI, M. 2001. Effect of plasma metabolites of (+)-catechin and quercetin on monocyte adhesion to human aortic endothelial cells. *American Journal of Clinical Nutrition*, 73, 941-8.
- KOJIMA, R., KAWACHI, M. & ITO, M. 2014. Butein suppresses ICAM-1 expression through the inhibition of I $\kappa$ B $\alpha$  and c-Jun phosphorylation in TNF- $\alpha$ - and PMA-treated HUVECs. *International Immunopharmacology*, 24, 267-275.
- KOTOKORPI, P., ELLIS, E., PARINI, P., NILSSON, L. M., STROM, S., STEFFENSEN, K. R., GUSTAFSSON, J. A. & MODE, A. 2007. Physiological differences between human and rat primary hepatocytes in response to liver X receptor activation by 3-[3-[N-(2-chloro-3-trifluoromethylbenzyl)-(2,2-diphenylethyl)amino]propyloxy]phenylacetic acid hydrochloride (GW3965). *Molecular Pharmacology*, 72, 947-55.
- KRAJKA-KUZNIAK, V., PALUSZCZAK, J., SZAEFER, H. & BAER-DUBOWSKA, W. 2015. The activation of the Nrf2/ARE pathway in HepG2 hepatoma cells by phytochemicals and subsequent modulation of phase II and antioxidant enzyme expression. *Journal of Physiology and Biochemistry*, 71, 227-38.

- KRGA, I., MONFOULET, L. E., KONIC-RISTIC, A., MERCIER, S., GLIBETIC, M., MORAND, C. & MILENKOVIC, D. 2016. Anthocyanins and their gut metabolites reduce the adhesion of monocyte to TNF $\alpha$ -activated endothelial cells at physiologically relevant concentrations. *Archives of Biochemistry and Biophysics*, in press.
- KROON, P. A., CLIFFORD, M. N., CROZIER, A., DAY, A. J., DONOVAN, J. L., MANACH, C. & WILLIAMSON, G. 2004. How should we assess the effects of exposure to dietary polyphenols in vitro? *American Journal of Clinical Nutrition*, 80, 15-21.
- KUMAR, S. & PANDEY, A. K. 2013. Chemistry and biological activities of flavonoids: an overview. *Scientific World Journal*, 2013, 162750.
- KUNTZ, S., ASSEBURG, H., DOLD, S., ROMPP, A., FROHLING, B., KUNZ, C. & RUDLOFF, S. 2015a. Inhibition of low-grade inflammation by anthocyanins from grape extract in an in vitro epithelial-endothelial co-culture model. *Food & Function*, 6, 1136-49.
- KUNTZ, S., RUDLOFF, S., ASSEBURG, H., BORSCH, C., FROHLING, B., UNGER, F., DOLD, S., SPENGLER, B., ROMPP, A. & KUNZ, C. 2015b. Uptake and bioavailability of anthocyanins and phenolic acids from grape/blueberry juice and smoothie in vitro and in vivo. *British Journal of Nutrition*, 113, 1044-55.
- KWON, H. M., CHOI, Y. J., JEONG, Y. J., KANG, S. W., KANG, I. J., LIM, S. S. & KANG, Y. H. 2005. Anti-inflammatory inhibition of endothelial cell adhesion molecule expression by flavone derivatives. *Journal of Agricultural and Food Chemistry*, 53, 5150-7.
- LANDSTROM, M. 2010. The TAK1-TRAF6 signalling pathway. *International Journal of Biochemistry and Cell Biology*, 42, 585-9.
- LAZZE, M. C., PIZZALA, R., PERUCCA, P., CAZZALINI, O., SAVIO, M., FORTI, L., VANNINI, V. & BIANCHI, L. 2006. Anthocyanidins decrease endothelin-1 production and increase endothelial nitric oxide synthase in human endothelial cells. *Molecular Nutrition & Food Research*, 50, 44-51.
- LE GOUILL, E., JIMENEZ, M., BINNERT, C., JAYET, P. Y., THALMANN, S., NICOD, P., SCHERRER, U. & VOLLENWEIDER, P. 2007. Endothelial nitric oxide synthase (eNOS) knockout mice have defective mitochondrial beta-oxidation. *Diabetes*, 56, 2690-6.
- LEE, J. M. & JOHNSON, J. A. 2004. An important role of Nrf2-ARE pathway in the cellular defense mechanism. *Journal of Biochemistry and Molecular Biology*, 37, 139-43.
- LEFFLER, C. W., PARFENOVA, H. & JAGGAR, J. H. 2011. Carbon monoxide as an endogenous vascular modulator. *American Journal of Physiology, Heart and Circulatory Physiology*, 301, H1-H11.
- LEKAKIS, J., RALLIDIS, L. S., ANDREADOU, I., VAMVAKOU, G., KAZANTZOGLOU, G., MAGIATIS, P., SKALTSOUNIS, A. L. & KREMASTINOS, D. T. 2005. Polyphenolic compounds from red grapes acutely improve endothelial function in patients with coronary heart disease. *European journal of cardiovascular prevention and rehabilitation : official journal of the European Society of Cardiology, Working Groups on Epidemiology & Prevention and Cardiac Rehabilitation and Exercise Physiology*, 12, 596-600.
- LEY, K. & HUO, Y. 2001. VCAM-1 is critical in atherosclerosis. *Journal of Clinical Investigation*, 107, 1209-10.
- LIANG, C., XUE, Z., CANG, J., WANG, H. & LI, P. 2011. Dimethyl sulfoxide induces heme oxygenase-1 expression via JNKs and Nrf2 pathways in human umbilical vein endothelial cells. *Molecular Cell Biochemistry*, 355, 109-15.

- LIANG, L., GAO, C., LUO, M., WANG, W., ZHAO, C., ZU, Y., EFFERTH, T. & FU, Y. 2013. Dihydroquercetin (DHQ) induced HO-1 and NQO1 expression against oxidative stress through the Nrf2-dependent antioxidant pathway. *Journal of Agricultural and Food Chemistry*, 61, 2755-61.
- LIEBGOTT, T., MIOLLAN, M., BERCHADSKY, Y., DRIEU, K., CULCASI, M. & PIETRI, S. 2000. Complementary cardioprotective effects of flavonoid metabolites and terpenoid constituents of Ginkgo biloba extract (EGb 761) during ischemia and reperfusion. *Basic Research in Cardiology*, 95, 368-77.
- LIN, H. C., CHENG, T. H., CHEN, Y. C. & JUAN, S. H. 2004. Mechanism of heme oxygenase-1 gene induction by quercetin in rat aortic smooth muscle cells. *Pharmacology*, 71, 107-12.
- LIU, J., WANG, L., TIAN, X. Y., LIU, L., WONG, W. T., ZHANG, Y., HAN, Q. B., HO, H. M., WANG, N., WONG, S. L., CHEN, Z. Y., YU, J., NG, C. F., YAO, X. & HUANG, Y. 2015. Unconjugated bilirubin mediates heme oxygenase-1-induced vascular benefits in diabetic mice. *Diabetes*, 64, 1564-75.
- LIU, S., HOU, W., YAO, P., LI, N., ZHANG, B., HAO, L., NUSSLER, A. K. & LIU, L. 2012. Heme oxygenase-1 mediates the protective role of quercetin against ethanol-induced rat hepatocytes oxidative damage. *Toxicology In Vitro*, 26, 74-80.
- LIVAK, K. J. & SCHMITTGEN, T. D. 2001. Analysis of relative gene expression data using real-time quantitative PCR and the 2<sup>(-Delta Delta C)</sup> method. *Methods*, 25, 402-408.
- LODI, F., JIMENEZ, R., MENENDEZ, C., NEEDS, P. W., DUARTE, J. & PEREZ-VIZCAINO, F. 2008. Glucuronidated metabolites of the flavonoid quercetin do not auto-oxidise, do not generate free radicals and do not decrease nitric oxide bioavailability. *Planta Medica*, 74, 741-6.
- LODI, F., JIMENEZ, R., MORENO, L., KROON, P. A., NEEDS, P. W., HUGHES, D. A., SANTOS-BUELGA, C., GONZALEZ-PARAMAS, A., COGOLLUDO, A., LOPEZ-SEPULVEDA, R., DUARTE, J. & PEREZ-VIZCAINO, F. 2009. Glucuronidated and sulfated metabolites of the flavonoid quercetin prevent endothelial dysfunction but lack direct vasorelaxant effects in rat aorta. *Atherosclerosis*, 204, 34-9.
- LODI, F., WINTERBONE, M. S., TRIBOLO, S., NEEDS, P. W., HUGHES, D. A. & KROON, P. A. 2012. Human quercetin conjugated metabolites attenuate TNF-alpha-induced changes in vasomodulatory molecules in an HUASMCs/HUVECs co-culture model. *Planta Medica*, 78, 1571-3.
- LOKE, W. M., PROUDFOOT, J. M., HODGSON, J. M., MCKINLEY, A. J., HIME, N., MAGAT, M., STOCKER, R. & CROFT, K. D. 2010. Specific dietary polyphenols attenuate atherosclerosis in apolipoprotein E-knockout mice by alleviating inflammation and endothelial dysfunction. *Arteriosclerosis, Thrombosis, and Vascular Biology*, 30, 749-57.
- LOTITO, S. B. & FREI, B. 2006. Dietary flavonoids attenuate tumor necrosis factor alpha-induced adhesion molecule expression in human aortic endothelial cells. Structure-function relationships and activity after first pass metabolism. *Journal of Biological Chemistry*, 281, 37102-10.
- LOTITO, S. B., ZHANG, W. J., YANG, C. S., CROZIER, A. & FREI, B. 2011. Metabolic conversion of dietary flavonoids alters their anti-inflammatory and antioxidant properties. *Free Radical Biology & Medicine*, 51, 454-63.
- LOUIS, S. F. & ZAHRADKA, P. 2010. Vascular smooth muscle cell motility: From migration to invasion. *Experimental & Clinical Cardiology*, 15, e75-85.
- LU, J., PAPP, L. V., FANG, J., RODRIGUEZ-NIETO, S., ZHIVOTOVSKY, B. & HOLMGREN, A. 2006. Inhibition of Mammalian thioredoxin reductase by some flavonoids: implications for myricetin and quercetin anticancer activity. *Cancer Research*, 66, 4410-8.

- LUDWIG, A., LORENZ, M., GRIMBO, N., STEINLE, F., MEINERS, S., BARTSCH, C., STANGL, K., BAUMANN, G. & STANGL, V. 2004. The tea flavonoid epigallocatechin-3-gallate reduces cytokine-induced VCAM-1 expression and monocyte adhesion to endothelial cells. *Biochemical & Biophysical Research Communications*, 316, 659-665.
- LUSIS, A. J. 2000. Atherosclerosis. *Nature*, 407, 233-41.
- LUU, N. T., RAHMAN, M., STONE, P. C., RAINGER, G. E. & NASH, G. B. 2010. Responses of endothelial cells from different vessels to inflammatory cytokines and shear stress: evidence for the pliability of endothelial phenotype. *Journal of Vascular Research*, 47, 451-61.
- MACREADY, A. L., GEORGE, T. W., CHONG, M. F., ALIMBETOV, D. S., JIN, Y., VIDAL, A., SPENCER, J. P., KENNEDY, O. B., TUOHY, K. M., MINIHANE, A. M., GORDON, M. H., LOVEGROVE, J. A. & GROUP, F. S. 2014. Flavonoid-rich fruit and vegetables improve microvascular reactivity and inflammatory status in men at risk of cardiovascular disease--FLAVURS: a randomized controlled trial. *American Journal of Clinical Nutrition*, 99, 479-89.
- MANACH, C., SCALBERT, A., MORAND, C., REMESY, C. & JIMENEZ, L. 2004. Polyphenols: food sources and bioavailability. *American Journal of Clinical Nutrition*, 79, 727-747.
- MANACH, C., WILLIAMSON, G., MORAND, C., SCALBERT, A. & REMESY, C. 2005. Bioavailability and bioefficacy of polyphenols in humans. I. Review of 97 bioavailability studies. *American Journal of Clinical Nutrition*, 81, 230s-242s.
- MANN, G. E., ROWLANDS, D. J., LI, F. Y., DE WINTER, P. & SIOW, R. C. 2007. Activation of endothelial nitric oxide synthase by dietary isoflavones: role of NO in Nrf2-mediated antioxidant gene expression. *Cardiovascular Research*, 75, 261-74.
- MARTIN, M. A., SERRANO, A. B., RAMOS, S., PULIDO, M. I., BRAVO, L. & GOYA, L. 2010. Cocoa flavonoids up-regulate antioxidant enzyme activity via the ERK1/2 pathway to protect against oxidative stress-induced apoptosis in HepG2 cells. *Journal of Nutritional Biochemistry*, 21, 196-205.
- MARTINEZ-FERNANDEZ, L., PONS, Z., MARGALEF, M., AROLA-ARNAL, A. & MUGUERZA, B. 2015. Regulation of vascular endothelial genes by dietary flavonoids: structure-expression relationship studies and the role of the transcription factor KLF-2. *Journal of Nutritional Biochemistry*, 26, 277-84.
- MAURAY, A., FELGINES, C., MORAND, C., MAZUR, A., SCALBERT, A. & MILENKOVIC, D. 2012. Bilberry anthocyanin-rich extract alters expression of genes related to atherosclerosis development in aorta of apo E-deficient mice. *Nutrition, Metabolism and Cardiovascular Diseases*, 22, 72-80.
- MCGILL, H. C., JR., MCMAHAN, C. A. & GIDDING, S. S. 2008. Preventing heart disease in the 21st century: implications of the Pathobiological Determinants of Atherosclerosis in Youth (PDAY) study. *Circulation*, 117, 1216-27.
- MCKAY, D. L., CHEN, C. Y., ZAMPARIELLO, C. A. & BLUMBERG, J. B. 2015. Flavonoids and phenolic acids from cranberry juice are bioavailable and bioactive in healthy older adults. *Food Chemistry*, 168, 233-40.
- MENDIS, S., DAVIS, S. & NORRIVING, B. 2015. Organizational update: the world health organization global status report on noncommunicable diseases 2014; one more landmark step in the combat against stroke and vascular disease. *Stroke*, 46, e121-2.
- MILBURY, P. E., GRAF, B., CURRAN-CELENTANO, J. M. & BLUMBERG, J. B. 2007. Bilberry (*Vaccinium myrtillus*) anthocyanins modulate heme oxygenase-1 and glutathione S-transferase-pi expression in ARPE-19 cells. *Investigative Ophthalmology & Visual Science*, 48, 2343-9.

- MIN, S. W., RYU, S. N. & KIM, D. H. 2010. Anti-inflammatory effects of black rice, cyanidin-3-O-beta-D-glycoside, and its metabolites, cyanidin and protocatechuic acid. *International Immunopharmacology*, 10, 959-66.
- MINK, P. J., SCRAFFORD, C. G., BARRAJ, L. M., HARNACK, L., HONG, C. P., NETTLETON, J. A. & JACOBS, D. R., JR. 2007. Flavonoid intake and cardiovascular disease mortality: a prospective study in postmenopausal women. *American Journal of Clinical Nutrition*, 85, 895-909.
- MIWA, K., IGAWA, A. & INOUE, H. 1997. Soluble E-selectin, ICAM-1 and VCAM-1 levels in systemic and coronary circulation in patients with variant angina. *Cardiovascular Research*, 36, 37-44.
- MONAGAS, M., URPI-SARDA, M., SANCHEZ-PATAN, F., LLORACH, R., GARRIDO, I., GOMEZ-CORDOVES, C., ANDRES-LACUEVA, C. & BARTOLOME, B. 2010. Insights into the metabolism and microbial biotransformation of dietary flavan-3-ols and the bioactivity of their metabolites. *Food & Function*, 1, 233-53.
- MOOSAVI, F., HOSSEINI, R., SASO, L. & FIRUZI, O. 2016. Modulation of neurotrophic signaling pathways by polyphenols. *Drug Design, Development and Therapy*, 10, 23-42.
- MUDAU, M., GENIS, A., LOCHNER, A. & STRIJDOM, H. 2012. Endothelial dysfunction: the early predictor of atherosclerosis. *Cardiovascular Journal of Africa*, 23, 222-31.
- MULLEN, W., EDWARDS, C. A. & CROZIER, A. 2006. Absorption, excretion and metabolite profiling of methyl-, glucuronyl-, glucosyl- and sulpho-conjugates of quercetin in human plasma and urine after ingestion of onions. *British Journal of Nutrition*, 96, 107-16.
- MUROTA, K. & TERAOKA, J. 2003. Antioxidative flavonoid quercetin: implication of its intestinal absorption and metabolism. *Archives of Biochemistry and Biophysics*, 417, 12-7.
- NABAVI, S. F., NABAVI, S. M., MIRZAEI, M. & MOGHADDAM, A. H. 2012. Protective effect of quercetin against sodium fluoride induced oxidative stress in rat's heart. *Food & Function*, 3, 437-441.
- NAKAO, S., KUWANO, T., ISHIBASHI, T., KUWANO, M. & ONO, M. 2003. Synergistic effect of TNF-alpha in soluble VCAM-1-induced angiogenesis through alpha 4 integrins. *Journal of Immunology*, 170, 5704-11.
- NICE 2014. Prevention of cardiovascular disease: Evidence Update January 2014.
- NITURE, S. K., KHATRI, R. & JAISWAL, A. K. 2014. Regulation of Nrf2-an update. *Free Radical Biology & Medicine*, 66, 36-44.
- NIZAMUTDINOVA, I. T., JEONG, J. J., XU, G. H., LEE, S. H., KANG, S. S., KIM, Y. S., CHANG, K. C. & KIM, H. J. 2008. Hesperidin, hesperidin methyl chalone and phellopterin from *Poncirus trifoliata* (Rutaceae) differentially regulate the expression of adhesion molecules in tumor necrosis factor-alpha-stimulated human umbilical vein endothelial cells. *International Immunopharmacology*, 8, 670-8.
- NOLL, C., LAMETH, J., PAUL, J. L. & JANEL, N. 2012. Effect of catechin/epicatechin dietary intake on endothelial dysfunction biomarkers and proinflammatory cytokines in aorta of hyperhomocysteinemic mice. *European Journal of Nutrition*, 52, 1243-50.
- OLEJARZ, W., BRYK, D., ZAPOLSKA-DOWNAR, D., MALECKI, M., STACHURSKA, A. & SITKIEWICZ, D. 2014. Mycophenolic acid attenuates the tumour necrosis factor-alpha-mediated proinflammatory response in endothelial cells by blocking the MAPK/NF-kappaB and ROS pathways. *European Journal of Clinical Investigation*, 44, 54-64.
- OYAMA, J., MAEDA, T., SASAKI, M., KOZUMA, K., OCHIAI, R., TOKIMITSU, I., TAGUCHI, S., HIGUCHI, Y. & MAKINO, N. 2010. Green tea catechins improve human forearm vascular function and have potent anti-inflammatory and anti-apoptotic effects in smokers. *Internal Medicine*, 49, 2553-9.

- OZES, O. N., MAYO, L. D., GUSTIN, J. A., PFEFFER, S. R., PFEFFER, L. M. & DONNER, D. B. 1999. NF-kappaB activation by tumour necrosis factor requires the Akt serine-threonine kinase. *Nature*, 401, 82-5.
- PAE, H. O., JEONG, G. S., JEONG, S. O., KIM, H. S., KIM, S. A., KIM, Y. C., YOO, S. J., KIM, H. D. & CHUNG, H. T. 2007. Roles of heme oxygenase-1 in curcumin-induced growth inhibition in rat smooth muscle cells. *Experimental & Molecular Medicine*, 39, 267-77.
- PAMPALONI, F., REYNAUD, E. G. & STELZER, E. H. 2007. The third dimension bridges the gap between cell culture and live tissue. *Nature Reviews Molecular Cell Biology*, 8, 839-45.
- PAMUKCU, B., LIP, G. Y., SNEZHITSKIY, V. & SHANTSILA, E. 2011. The CD40-CD40L system in cardiovascular disease. *Annals of Internal Medicine*, 43, 331-40.
- PANTAN, R., TOCHARUS, J., SUKSAMRARN, A. & TOCHARUS, C. 2016. Synergistic effect of atorvastatin and Cyanidin-3-glucoside on angiotensin II-induced inflammation in vascular smooth muscle cells. *Experimental Cell Research*, 342, 104-12.
- PELUSO, I., RAGUZZINI, A. & SERAFINI, M. 2013. Effect of flavonoids on circulating levels of TNF-alpha and IL-6 in humans: a systematic review and meta-analysis. *Molecular Nutrition & Food Research*, 57, 784-801.
- PEREIRA-CARO, G., BORGES, G., VAN DER HOOFT, J., CLIFFORD, M. N., DEL RIO, D., LEAN, M. E., ROBERTS, S. A., KELLERHALS, M. B. & CROZIER, A. 2014. Orange juice (poly)phenols are highly bioavailable in humans. *American Journal of Clinical Nutrition*, 100, 1378-84.
- PEREIRA-CARO, G., OLIVER, C. M., WEERAKODY, R., SINGH, T., CONLON, M., BORGES, G., SANGUANSRI, L., LOCKETT, T., ROBERTS, S. A., CROZIER, A. & AUGUSTIN, M. A. 2015. Chronic administration of a microencapsulated probiotic enhances the bioavailability of orange juice flavanones in humans. *Free Radical Biology & Medicine*, 84, 206-14.
- PEREZ-VIZCAINO, F., DUARTE, J. & SANTOS-BUELGA, C. 2012. The flavonoid paradox: conjugation and deconjugation as key steps for the biological activity of flavonoids. *Journal of the Science of Food and Agriculture*, 92, 1822-1825.
- PIMPÃO, R. C., DEW, T., FIGUEIRA, M. E., MCDUGALL, G. J., STEWART, D., FERREIRA, R. B., SANTOS, C. N. & WILLIAMSON, G. 2014. Urinary metabolite profiling identifies novel colonic metabolites and conjugates of phenolics in healthy volunteers. *Molecular Nutrition & Food Research*, 58, 1414-25.
- PIMPÃO, R. C., VENTURA, M. R., FERREIRA, R. B., WILLIAMSON, G. & SANTOS, C. N. 2015. Phenolic sulfates as new and highly abundant metabolites in human plasma after ingestion of a mixed berry fruit puree. *British Journal of Nutrition*, 113, 454-63.
- POTT, G. B., TSURUDOME, M., BAMFO, N. & GOALSTONE, M. L. 2016. ERK2 and Akt are negative regulators of insulin and Tumor Necrosis Factor-alpha stimulated VCAM-1 expression in rat aorta endothelial cells. *Journal of Inflammation*, 13, 6.
- RAFIKOV, R., FONSECA, F. V., KUMAR, S., PARDO, D., DARRAGH, C., ELMS, S., FULTON, D. & BLACK, S. M. 2011. eNOS activation and NO function: structural motifs responsible for the posttranslational control of endothelial nitric oxide synthase activity. *Journal of Endocrinology*, 210, 271-84.
- RAJENDRAN, P., RENGARAJAN, T., THANGAVEL, J., NISHIGAKI, Y., SAKTHISEKARAN, D., SETHI, G. & NISHIGAKI, I. 2013. The vascular endothelium and human diseases. *International Journal of Biological Sciences*, 9, 1057-69.
- RAMJI, D. P. & DAVIES, T. S. 2015. Cytokines in atherosclerosis: Key players in all stages of disease and promising therapeutic targets. *Cytokine & Growth Factor Reviews*, 26, 673-685.

- RANGEL-HUERTA, O. D., PASTOR-VILLAESCUSA, B., AGUILERA, C. M. & GIL, A. 2015. A Systematic Review of the Efficacy of Bioactive Compounds in Cardiovascular Disease: Phenolic Compounds. *Nutrients*, 7, 5177-216.
- REULAND, D. J., MCCORD, J. M. & HAMILTON, K. L. 2013. The role of Nrf2 in the attenuation of cardiovascular disease. *Exercise Sport Science Reviews*, 41, 162-8.
- RIBEIRO, M. E., VIEIRA, I. G., CAVALCANTE, I. M., RICARDO, N. M., ATTWOOD, D., YEATES, S. G. & BOOTH, C. 2009. Solubilisation of griseofulvin, quercetin and rutin in micellar formulations of triblock copolymers E62P39E62 and E137S18E137. *International Journal of Pharmacology*, 378, 211-4.
- RIED, K., SULLIVAN, T. R., FAKLER, P., FRANK, O. R. & STOCKS, N. P. 2012. Effect of cocoa on blood pressure. *Cochrane Database of Systematic Reviews*, 8, CD008893.
- RIMBACH, G., WEINBERG, P. D., DE PASCUAL-TERESA, S., ALONSO, M. G., EWINS, B. A., TURNER, R., MINIHANE, A. M., BOTTING, N., FAIRLEY, B., MATSUGO, S., UCHIDA, Y. & CASSIDY, A. 2004. Sulfation of genistein alters its antioxidant properties and its effect on platelet aggregation and monocyte and endothelial function. *Biochimica et Biophysica Acta*, 1670, 229-37.
- RIZZA, S., MUNIYAPPA, R., IANTORNO, M., KIM, J. A., CHEN, H., PULLIKOTIL, P., SENESE, N., TESAURO, M., LAURO, D., CARDILLO, C. & QUON, M. J. 2011. Citrus polyphenol hesperidin stimulates production of nitric oxide in endothelial cells while improving endothelial function and reducing inflammatory markers in patients with metabolic syndrome. *Journal of Clinical Endocrinology and Metabolism*, 96, E782-92.
- ROBAK, J. & GRYGLEWSKI, R. J. 1988. Flavonoids are scavengers of superoxide anions. *Biochemical Pharmacology*, 37, 837-41.
- RODRIGUEZ-MATEOS, A., DEL PINO-GARCIA, R., GEORGE, T. W., VIDAL-DIEZ, A., HEISS, C. & SPENCER, J. P. 2014a. Impact of processing on the bioavailability and vascular effects of blueberry (poly)phenols. *Molecular Nutrition & Food Research*, 58, 1952-61.
- RODRIGUEZ-MATEOS, A., HEISS, C., BORGES, G. & CROZIER, A. 2014b. Berry (poly)phenols and cardiovascular health. *Journal of Agricultural and Food Chemistry*, 62, 3842-51.
- RODRIGUEZ-MATEOS, A., TORO-FUNES, N., CIFUENTES-GOMEZ, T., CORTESE-KROTT, M., HEISS, C. & SPENCER, J. P. 2014c. Uptake and metabolism of (-)-epicatechin in endothelial cells. *Archives of Biochemistry & Biophysics*, 559, 17-23.
- RODRIGUEZ-MATEOS, A., VAUZOUR, D., KRUEGER, C. G., SHANMUGANAYAGAM, D., REED, J., CALANI, L., MENA, P., DEL RIO, D. & CROZIER, A. 2014d. Bioavailability, bioactivity and impact on health of dietary flavonoids and related compounds: an update. *Archives of Toxicology*, 88, 1803-53.
- RODRIGUEZ, A. I., GANGOPADHYAY, A., KELLEY, E. E., PAGANO, P. J., ZUCKERBRAUN, B. S. & BAUER, P. M. 2010. HO-1 and CO decrease platelet-derived growth factor-induced vascular smooth muscle cell migration via inhibition of Nox1. *Arteriosclerosis, Thrombosis and Vascular Biology*, 30, 98-104.
- ROTHWELL, J. A., PEREZ-JIMENEZ, J., NEVEU, V., MEDINA-REMON, A., M'HIRI, N., GARCIA-LOBATO, P., MANACH, C., KNOX, C., EISNER, R., WISHART, D. S. & SCALBERT, A. 2013. Phenol-Explorer 3.0: a major update of the Phenol-Explorer database to incorporate data on the effects of food processing on polyphenol content. Database (Oxford), 2013, bat070.
- RYTER, S. W., ALAM, J. & CHOI, A. M. 2006. Heme oxygenase-1/carbon monoxide: from basic science to therapeutic applications. *Physiological Reviews*, 86, 583-650.

- SAKURAI, H., SUZUKI, S., KAWASAKI, N., NAKANO, H., OKAZAKI, T., CHINO, A., DOI, T. & SAIKI, I. 2003. Tumor necrosis factor-alpha-induced IKK phosphorylation of NF-kappaB p65 on serine 536 is mediated through the TRAF2, TRAF5, and TAK1 signaling pathway. *Journal of Biological Chemistry*, 278, 36916-23.
- SANCHEZ, M., GALISTEO, M., VERA, R., VILLAR, I. C., ZARZUELO, A., TAMARGO, J., PEREZ-VIZCAINO, F. & DUARTE, J. 2006. Quercetin downregulates NADPH oxidase, increases eNOS activity and prevents endothelial dysfunction in spontaneously hypertensive rats. *Journal of Hypertension*, 24, 75-84.
- SCAPAGNINI, G., VASTO, S., ABRAHAM, N. G., CARUSO, C., ZELLA, D. & FABIO, G. 2011. Modulation of Nrf2/ARE pathway by food polyphenols: a nutritional neuroprotective strategy for cognitive and neurodegenerative disorders. *Molecular Neurobiology*, 44, 192-201.
- SCARPELLINI, E. & TACK, J. 2012. Obesity and metabolic syndrome: an inflammatory condition. *Digestive Diseases and Sciences*, 30, 148-53.
- SCHAR, M. Y., CURTIS, P. J., HAZIM, S., OSTERTAG, L. M., KAY, C. D., POTTER, J. F. & CASSIDY, A. 2015. Orange juice-derived flavanone and phenolic metabolites do not acutely affect cardiovascular risk biomarkers: a randomized, placebo-controlled, crossover trial in men at moderate risk of cardiovascular disease. *American Journal of Clinical Nutrition*, 101, 931-8.
- SHELLER, J., CHALARIS, A., SCHMIDT-ARRAS, D. & ROSE-JOHN, S. 2011. The pro- and anti-inflammatory properties of the cytokine interleukin-6. *Biochimica et Biophysica Acta*, 1813, 878-88.
- SCHEWE, T., STEFFEN, Y. & SIES, H. 2008. How do dietary flavanols improve vascular function? A position paper. *Archives of Biochemistry & Biophysics*, 476, 102-6.
- SEKHAR, K. R., SOLTANINASSAB, S. R., BORRELLI, M. J., XU, Z. Q., MEREDITH, M. J., DOMANN, F. E. & FREEMAN, M. L. 2000. Inhibition of the 26S proteasome induces expression of GLCLC, the catalytic subunit for gamma-glutamylcysteine synthetase. *Biochemical & Biophysical Research Communications*, 270, 311-7.
- SERRA, A., MACIA, A., ROMERO, M. P., REGUANT, J., ORTEGA, N. & MOTILVA, M. J. 2012. Metabolic pathways of the colonic metabolism of flavonoids (flavonols, flavones and flavanones) and phenolic acids. *Food Chemistry*, 130, 383-393.
- SERRAINO, I., DUGO, L., DUGO, P., MONDELLO, L., MAZZON, E., DUGO, G., CAPUTI, A. P. & CUZZOCREA, S. 2003. Protective effects of cyanidin-3-O-glucoside from blackberry extract against peroxynitrite-induced endothelial dysfunction and vascular failure. *Life Sciences*, 73, 1097-1114.
- SEVGI, K., TEPE, B. & SARIKURKCU, C. 2014. Antioxidant and DNA damage protection potentials of selected phenolic acids. *Food Chemistry & Toxicology*, 77, 12-21.
- SHEN, Y., CROFT, K. D., HODGSON, J. M., KYLE, R., LEE, I. L., WANG, Y., STOCKER, R. & WARD, N. C. 2012. Quercetin and its metabolites improve vessel function by inducing eNOS activity via phosphorylation of AMPK. *Biochemical Pharmacology*, 84, 1036-44.
- SHEN, Y., WARD, N. C., HODGSON, J. M., PUDDEY, I. B., WANG, Y., ZHANG, D., MAGHZAL, G. J., STOCKER, R. & CROFT, K. D. 2013. Dietary quercetin attenuates oxidant-induced endothelial dysfunction and atherosclerosis in apolipoprotein E knockout mice fed a high-fat diet: a critical role for heme oxygenase-1. *Free Radical Biology & Medicine*, 65, 908-15.
- SHENG, R., GU, Z. L., XIE, M. L., ZHOU, W. X. & GUO, C. Y. 2009. EGCG inhibits proliferation of cardiac fibroblasts in rats with cardiac hypertrophy. *Planta Medica*, 75, 113-20.

- SHIH, C. M., LIN, H., LIANG, Y. C., LEE, W. S., BI, W. F. & JUAN, S. H. 2004. Concentration-dependent differential effects of quercetin on rat aortic smooth muscle cells. *European Journal of Pharmacology*, 496, 41-8.
- SIMOS, Y. V., VERGINADIS, II, TOLIOPOULOS, I. K., VELALOPOULOU, A. P., KARAGOUNIS, I. V., KARKABOUNAS, S. C. & EVANGELOU, A. M. 2012. Effects of catechin and epicatechin on superoxide dismutase and glutathione peroxidase activity, in vivo. *Redox Report*, 17, 181-6.
- SINGH, M., ARSENEAULT, M., SANDERSON, T., MURTHY, V. & RAMASSAMY, C. 2008. Challenges for research on polyphenols from foods in Alzheimer's disease: bioavailability, metabolism, and cellular and molecular mechanisms. *Journal of Agricultural and Food Chemistry*, 56, 4855-73.
- SINGH, R. J., MASON, J. C., LIDINGTON, E. A., EDWARDS, D. R., NUTTALL, R. K., KHOKHA, R., KNAUPER, V., MURPHY, G. & GAVRILOVIC, J. 2005. Cytokine stimulated vascular cell adhesion molecule-1 (VCAM-1) ectodomain release is regulated by TIMP-3. *Cardiovascular Research*, 67, 39-49.
- SITIA, S., TOMASONI, L., ATZENI, F., AMBROSIO, G., CORDIANO, C., CATAPANO, A., TRAMONTANA, S., PERTICONE, F., NACCARATO, P., CAMICI, P., PICANO, E., CORTIGIANI, L., BEVILACQUA, M., MILAZZO, L., CUSI, D., BARLASSINA, C., SARZI-PUTTINI, P. & TURIEL, M. 2010. From endothelial dysfunction to atherosclerosis. *Autoimmunity Reviews*, 9, 830-4.
- SKOOG, T., DICHTL, W., BOQUIST, S., SKOGLUND-ANDERSSON, C., KARPE, F., TANG, R., BOND, M. G., DE FAIRE, U., NILSSON, J., ERIKSSON, P. & HAMSTEN, A. 2002. Plasma tumour necrosis factor-alpha and early carotid atherosclerosis in healthy middle-aged men. *European Heart Journal*, 23, 376-83.
- SORRENTI, V., MAZZA, F., CAMPISI, A., DI GIACOMO, C., ACQUAVIVA, R., VANELLA, L. & GALVANO, F. 2007. Heme oxygenase induction by cyanidin-3-O-beta-glucoside in cultured human endothelial cells. *Molecular Nutrition & Food Research*, 51, 580-6.
- SPECIALE, A., ANWAR, S., CANALI, R., CHIRAFISI, J., SAIJA, A., VIRGILI, F. & CIMINO, F. 2013. Cyanidin-3-O-glucoside counters the response to TNF-alpha of endothelial cells by activating Nrf2 pathway. *Molecular Nutrition & Food Research*, 57, 1979-87.
- SPECIALE, A., CANALI, R., CHIRAFISI, J., SAIJA, A., VIRGILI, F. & CIMINO, F. 2010. Cyanidin-3-O-glucoside protection against TNF-alpha-induced endothelial dysfunction: involvement of nuclear factor-kappaB signaling. *Journal of Agricultural and Food Chemistry*, 58, 12048-54.
- SPENCER, J. P. 2009. Flavonoids and brain health: multiple effects underpinned by common mechanisms. *Genes & Nutrition*, 4, 243-50.
- SPENCER, J. P., ABD-EL-MOHSEN, M. M. & RICE-EVANS, C. 2004. Cellular uptake and metabolism of flavonoids and their metabolites: implications for their bioactivity. *Archives of Biochemistry & Biophysics*, 423, 148-61.
- SPENCER, J. P. E. A. C., A. 2012. *Flavonoids and Related Compounds- Bioavailability and Function*, Boca Raton, CRC Press.
- STALMACH, A., EDWARDS, C. A., WIGHTMAN, J. D. & CROZIER, A. 2013. Colonic catabolism of dietary phenolic and polyphenolic compounds from Concord grape juice. *Food & Function*, 4, 52-62.
- STEFFEN, Y., GRUBER, C., SCHEWE, T. & SIES, H. 2008. Mono-O-methylated flavanols and other flavonoids as inhibitors of endothelial NADPH oxidase. *Archives of Biochemistry and Biophysics*, 469, 209-19.
- STROUD, J. C., OLTMAN, A., HAN, A., BATES, D. L. & CHEN, L. 2009. Structural basis of HIV-1 activation by NF-kappaB--a higher-order complex of p50:RelA bound to the HIV-1 LTR. *Journal of Molecular Biology*, 393, 98-11

- SU, D., LI, Z., LI, X., CHEN, Y., ZHANG, Y., DING, D., DENG, X., XIA, M., QIU, J. & LING, W. 2013. Association between serum interleukin-6 concentration and mortality in patients with coronary artery disease. *Mediators of Inflammation*, 2013, 726178.
- SU, Z. Y., SHU, L., KHOR, T. O., LEE, J. H., FUENTES, F. & KONG, A. N. 2012. A Perspective on Dietary Phytochemicals and Cancer Chemoprevention: Oxidative Stress, Nrf2, and Epigenomics. *Topics in Current Chemistry*, 329, 133-62.
- SUN, G. Y., CHEN, Z., JASMER, K. J., CHUANG, D. Y., GU, Z., HANNINK, M. & SIMONYI, A. 2015. Quercetin Attenuates Inflammatory Responses in BV-2 Microglial Cells: Role of MAPKs on the Nrf2 Pathway and Induction of Heme Oxygenase-1. *PLoS One*, 10, e0141509.
- SURH, Y. J. 2003. Cancer chemoprevention with dietary phytochemicals. *Nature Reviews Cancer*, 3, 768-80.
- SZABO, M. E., GALLYAS, E., BAK, I., RAKOTOVAO, A., BOUCHER, F., DE LEIRIS, J., NAGY, N., VARGA, E. & TOSAKI, A. 2004. Heme oxygenase-1-related carbon monoxide and flavonoids in ischemic/reperfused rat retina. *Investigative Ophthalmology & Vision Science*, 45, 3727-32.
- TANIGAWA, S., FUJII, M. & HOU, D. X. 2007. Action of Nrf2 and Keap1 in ARE-mediated NQO1 expression by quercetin. *Free Radical Biology & Medicine*, 42, 1690-703.
- TAVERNITI, V., FRACASSETTI, D., DEL BO, C., LANTI, C., MINUZZO, M., KLIMIS-ZACAS, D., RISO, P. & GUGLIEMETTI, S. 2014. Immunomodulatory effect of a wild blueberry anthocyanin-rich extract in human Caco-2 intestinal cells. *Journal of Agricultural and Food Chemistry*, 62, 8346-51.
- TAYLOR, S., WAKEM, M., DIJKMAN, G., ALSARRAJ, M. & NGUYEN, M. 2010. A practical approach to RT-qPCR—Publishing data that conform to the MIQE guidelines. *Methods*, 50, S1-5.
- THEODORATOU, E., KYLE, J., CETNARSKYJ, R., FARRINGTON, S. M., TENESA, A., BARNETSON, R., PORTEOUS, M., DUNLOP, M. & CAMPBELL, H. 2007. Dietary flavonoids and the risk of colorectal cancer. *Cancer Epidemiology Biomarkers & Prevention*, 16, 684-693.
- TOFIELD, A. 2013. European Cardiovascular Disease Statistics 2012 Summary. *European Heart Journal*, 34, 1086-1086.
- TORO-FUNES, N., MORALES-GUTIERREZ, F. J., VECIANA-NOGUES, M. T., VIDAL-CAROU, M. C., SPENCER, J. P. & RODRIGUEZ-MATEOS, A. 2014. The intracellular metabolism of isoflavones in endothelial cells. *Food & Function*, 6, 98-108.
- TRESSERRA-RIMBAU, A., RIMM, E. B., MEDINA-REMON, A., MARTINEZ-GONZALEZ, M. A., DE LA TORRE, R., CORELLA, D., SALAS-SALVADO, J., GOMEZ-GRACIA, E., LAPETRA, J., AROS, F., FIOL, M., ROS, E., SERRA-MAJEM, L., PINTO, X., SAEZ, G. T., BASORA, J., SORLI, J. V., MARTINEZ, J. A., VINYOLES, E., RUIZ-GUTIERREZ, V., ESTRUCH, R., LAMUELA-RAVENTOS, R. M. & INVESTIGATORS, P. S. 2014. Inverse association between habitual polyphenol intake and incidence of cardiovascular events in the PREDIMED study. *Nutrition, Metabolism and Cardiovascular Diseases*, 24, 639-47.
- TRIBOLO, S., LODI, F., CONNOR, C., SURI, S., WILSON, V. G., TAYLOR, M. A., NEEDS, P. W., KROON, P. A. & HUGHES, D. A. 2008. Comparative effects of quercetin and its predominant human metabolites on adhesion molecule expression in activated human vascular endothelial cells. *Atherosclerosis*, 197, 50-6.
- TRIBOLO, S., LODI, F., WINTERBONE, M. S., SAHA, S., NEEDS, P. W., HUGHES, D. A. & KROON, P. A. 2013. Human metabolic transformation of quercetin blocks its capacity to decrease endothelial nitric oxide synthase (eNOS)

- expression and endothelin-1 secretion by human endothelial cells. *Journal of Agricultural and Food Chemistry*, 61, 8589-96.
- TRUSKEY, G. A. 2010. Endothelial Cell Vascular Smooth Muscle Cell Co-Culture Assay For High Throughput Screening Assays For Discovery of Anti-Angiogenesis Agents and Other Therapeutic Molecules. *International Journal of High Throughput Screening*, 2010, 171-181.
- TU, Y. C., LIAN, T. W., YEN, J. H., CHEN, Z. T. & WU, M. J. 2007. Antiatherogenic effects of kaempferol and rhamnocitrin. *Journal of Agricultural and Food Chemistry*, 55, 9969-9976.
- UHLEN, M., FAGERBERG, L., HALLSTROM, B. M., LINDSKOG, C., OKSVOLD, P., MARDINOGLU, A., SIVERTSSON, A., KAMPF, C., SJOSTEDT, E., ASPLUND, A., OLSSON, I., EDLUND, K., LUNDBERG, E., NAVANI, S., SZIGYARTO, C. A., ODEBERG, J., DJUREINOVIC, D., TAKANEN, J. O., HOBER, S., ALM, T., EDQVIST, P. H., BERLING, H., TEGEL, H., MULDER, J., ROCKBERG, J., NILSSON, P., SCHWENK, J. M., HAMSTEN, M., VON FEILITZEN, K., FORSBERG, M., PERSSON, L., JOHANSSON, F., ZWAHLEN, M., VON HEIJNE, G., NIELSEN, J. & PONTEN, F. 2015. Proteomics. Tissue-based map of the human proteome. *Science*, 347, 1260419.
- VALLEJO, C. G., ESCRIVA, H. & RODRIGUEZ-PENA, A. 2000. Evidence of tissue-specific, post-transcriptional regulation of NRF-2 expression. *Biochimie*, 82, 1129-33.
- VAN HINSBERGH, V. W. 2012. Endothelium--role in regulation of coagulation and inflammation. *Seminars in Immunopathology*, 34, 93-106.
- VARI, R., D'ARCHIVIO, M., FILESI, C., CAROTENUTO, S., SCAZZOCCHIO, B., SANTANGELO, C., GIOVANNINI, C. & MASELLA, R. 2011. Protocatechuic acid induces antioxidant/detoxifying enzyme expression through JNK-mediated Nrf2 activation in murine macrophages. *Journal of Nutritional Biochemistry*, 22, 409-17.
- VIDEM, V. & ALBRIGTSEN, M. 2008. Soluble ICAM-1 and VCAM-1 as markers of endothelial activation. *Scandinavian Journal of Immunology*, 67, 523-31.
- VITAGLIONE, P., BARONE LUMAGA, R., FERRACANE, R., SELLITTO, S., MORELLO, J. R., REGUANT MIRANDA, J., SHIMONI, E. & FOGLIANO, V. 2013. Human bioavailability of flavanols and phenolic acids from cocoa-nut creams enriched with free or microencapsulated cocoa polyphenols. *British Journal of Nutrition*, 109, 1832-43.
- VITAGLIONE, P., DONNARUMMA, G., NAPOLITANO, A., GALVANO, F., GALLO, A., SCALFI, L. & FOGLIANO, V. 2007. Protocatechuic acid is the major human metabolite of cyanidin-glucosides. *Journal of Nutrition*, 137, 2043-8.
- VOGIATZOGLOU, A., MULLIGAN, A. A., BHANIANI, A., LENTJES, M. A., MCTAGGART, A., LUBEN, R. N., HEISS, C., KELM, M., MERX, M. W., SPENCER, J. P., SCHROETER, H., KHAW, K. T. & KUHNLE, G. G. 2015. Associations between flavan-3-ol intake and CVD risk in the Norfolk cohort of the European Prospective Investigation into Cancer (EPIC-Norfolk). *Free Radical Biology & Medicine*, 84, 1-10.
- WALLACE, T. C. 2011. Anthocyanins in cardiovascular disease. *Advances in Nutrition*, 2, 1-7.
- WALLACE, T. C., SLAVIN, M. & FRANKENFELD, C. L. 2016. Systematic Review of Anthocyanins and Markers of Cardiovascular Disease. *Nutrients*, 8, 1.
- WALLE, T. 2004. Absorption and metabolism of flavonoids. *Free Radical Biology & Medicine*, 36, 829-37.
- WALLE, T., OTAKE, Y., BRUBAKER, J. A., WALLE, U. K. & HALUSHKA, P. V. 2001a. Disposition and metabolism of the flavonoid chrysin in normal volunteers. *British Journal of Clinical Pharmacology*, 51, 143-6.
- WALLE, T., WALLE, U. K. & HALUSHKA, P. V. 2001b. Carbon dioxide is the major metabolite of quercetin in humans. *Journal of Nutrition*, 131, 2648-2652.

- WALLERATH, T., LI, H., GODTEL-AMBRUST, U., SCHWARZ, P. M. & FORSTERMANN, U. 2005. A blend of polyphenolic compounds explains the stimulatory effect of red wine on human endothelial NO synthase. *Nitric Oxide*, 12, 97-104.
- WANG, D., WEI, X., YAN, X., JIN, T. & LING, W. 2010. Protocatechuic acid, a metabolite of anthocyanins, inhibits monocyte adhesion and reduces atherosclerosis in apolipoprotein E-deficient mice. *Journal of Agricultural and Food Chemistry*, 58, 12722-8.
- WANG, X., OUYANG, Y. Y., LIU, J. & ZHAO, G. 2014. Flavonoid intake and risk of CVD: a systematic review and meta-analysis of prospective cohort studies. *British Journal of Nutrition*, 111, 1-11.
- WANG, Y., WANG, W., WANG, L., WANG, X. & XIA, J. 2012. Regulatory mechanisms of interleukin-8 production induced by tumour necrosis factor-alpha in human hepatocellular carcinoma cells. *Journal of Cellular & Molecular Medicine*, 16, 496-506.
- WANG, Z. M., NIE, Z. L., ZHOU, B., LIAN, X. Q., ZHAO, H., GAO, W., WANG, Y. S., JIA, E. Z., WANG, L. S. & YANG, Z. J. 2012. Flavonols intake and the risk of coronary heart disease: a meta-analysis of cohort studies. *Atherosclerosis*, 222, 270-3.
- WARNER, E. F., ZHANG, Q., RAHEEM, K. S., O'HAGAN, D., O'CONNELL, M. A. & KAY, C. D. 2016. Common Phenolic Metabolites of Flavonoids, but Not Their Unmetabolized Precursors, Reduce the Secretion of Vascular Cellular Adhesion Molecules by Human Endothelial Cells. *Journal of Nutrition*, 146, 465-73.
- WENG, C. J., CHEN, M. J., YEH, C. T. & YEN, G. C. 2011. Hepatoprotection of quercetin against oxidative stress by induction of metallothionein expression through activating MAPK and PI3K pathways and enhancing Nrf2 DNA-binding activity. *Nature Biotechnology*, 28, 767-77.
- WESELER, A. R., RUIJTERS, E. J., DRITTIJ-REIJNDERS, M. J., REESINK, K. D., HAENEN, G. R. & BAST, A. 2011. Pleiotropic benefit of monomeric and oligomeric flavanols on vascular health--a randomized controlled clinical pilot study. *PLoS one*, 6, e28460.
- WHO 2014. GLOBAL STATUS REPORT on noncommunicable diseases.
- WILSON, N. S., DIXIT, V. & ASHKENAZI, A. 2009. Death receptor signal transducers: nodes of coordination in immune signaling networks. *Nature Immunology*, 10, 348-55.
- WINTERBONE, M. S., TRIBOLO, S., NEEDS, P. W., KROON, P. A. & HUGHES, D. A. 2009. Physiologically relevant metabolites of quercetin have no effect on adhesion molecule or chemokine expression in human vascular smooth muscle cells. *Atherosclerosis*, 202, 431-438.
- WOHLFART, P., XU, H., ENDLICH, A., HABERMEIER, A., CLOSS, E. I., HUBSCHLE, T., MANG, C., STROBEL, H., SUZUKI, T., KLEINERT, H., FORSTERMANN, U., RUETTEN, H. & LI, H. 2008. Antiatherosclerotic effects of small-molecular-weight compounds enhancing endothelial nitric-oxide synthase (eNOS) expression and preventing eNOS uncoupling. *Journal of Pharmacology and Experimental Therapeutics*, 325, 370-9.
- WOODMAN, O. L. & CHAN, E. 2004. Vascular and anti-oxidant actions of flavonols and flavones. *Clinical and Experimental Pharmacology and Physiology*, 31, 786-90.
- XU, J. W., IKEDA, K. & YAMORI, Y. 2004. Upregulation of endothelial nitric oxide synthase by cyanidin-3-glucoside, a typical anthocyanin pigment. *Hypertension*, 44, 217-22.
- XU, J. W., IKEDA, K. & YAMORI, Y. 2007. Inhibitory effect of polyphenol cyanidin on TNF-alpha-induced apoptosis through multiple signaling pathways in endothelial cells. *Atherosclerosis*, 193, 299-308.

- YAMAGATA, K., MIYASHITA, A., MATSUFUJI, H. & CHINO, M. 2010. Dietary flavonoid apigenin inhibits high glucose and tumor necrosis factor alpha-Induced adhesion molecule expression in human endothelial cells. *Journal of Nutritional Biochemistry*, 21, 116-124.
- YANG, X. B. & ZHAO, Y. 2012. Absorption and metabolism of red wine polyphenols and their potential health benefits in cardiovascular function. *American Journal of Clinical Nutrition*, 95, 1496-1497.
- YOSHIDA, H., TAKAMURA, N., SHUTO, T., OGATA, K., TOKUNAGA, J., KAWAI, K. & KAI, H. 2010. The citrus flavonoids hesperetin and naringenin block the lipolytic actions of TNF-alpha in mouse adipocytes. *Biochemical & Biophysical Research Communications*, 394, 728-32.
- YOSHIZUMI, M., FUJITA, Y., IZAWA, Y., SUZAKI, Y., KYAW, M., ALI, N., TSUCHIYA, K., KAGAMI, S., YANO, S., SONE, S. & TAMAKI, T. 2004. Ebselen inhibits tumor necrosis factor-alpha-induced c-Jun N-terminal kinase activation and adhesion molecule expression in endothelial cells. *Experimental Cell Research*, 292, 1-10.
- YOSHIZUMI, M., TSUCHIYA, K., SUZAKI, Y., KIRIMA, K., KYAW, M., MOON, J. H., TERAOKA, J. & TAMAKI, T. 2002. Quercetin glucuronide prevents VSMC hypertrophy by angiotensin II via the inhibition of JNK and AP-1 signaling pathway. *Biochemical & Biophysical Research Communications*, 293, 1458-65.
- YUAN, L., ZHOU, X., LI, D., MA, W., YU, H., XI, Y. & XIAO, R. 2012. Pattern recognition receptors involved in the inflammatory attenuating effects of soybean isoflavone in beta-amyloid peptides 1-42 treated rats. *Neuroscience Letters*, 506, 266-70.
- YURDAGUL, A., JR., SULZMAIER, F. J., CHEN, X. L., PATTILLO, C. B., SCHLAEPFER, D. D. & ORR, A. W. 2016. Oxidized LDL induces FAK-dependent RSK signaling to drive NF-kappaB activation and VCAM-1 expression. *Journal of Cell Science*, 129, 1580-1591.
- ZAKKAR, M., VAN DER HEIDEN, K., LUONG LE, A., CHAUDHURY, H., CUHLMANN, S., HAMDULAY, S. S., KRAMS, R., EDIRISINGHE, I., RAHMAN, I., CARLSEN, H., HASKARD, D. O., MASON, J. C. & EVANS, P. C. 2009. Activation of Nrf2 in endothelial cells protects arteries from exhibiting a proinflammatory state. *Arteriosclerosis, Thrombosis, and Vascular Biology*, 29, 1851-7.
- ZAMORA-ROS, R., KNAZE, V., ROTHWELL, J. A., HEMON, B., MOSKAL, A., OVERVAD, K., TJONNELAND, A., KYRO, C., FAGHERAZZI, G., BOUTRON-ROUAULT, M. C., TOUILLAUD, M., KATZKE, V., KUHN, T., BOEING, H., FORSTER, J., TRICHOPOULOU, A., VALANOU, E., PEPPA, E., PALLI, D., AGNOLI, C., RICCERI, F., TUMINO, R., DE MAGISTRIS, M. S., PEETERS, P. H., BUENO-DE-MESQUITA, H. B., ENGESET, D., SKEIE, G., HJARTAKER, A., MENENDEZ, V., AGUDO, A., MOLINA-MONTES, E., HUERTA, J. M., BARRICARTE, A., AMIANO, P., SONESTEDT, E., NILSSON, L. M., LANDBERG, R., KEY, T. J., KHAW, K. T., WAREHAM, N. J., LU, Y., SLIMANI, N., ROMIEU, I., RIBOLI, E. & SCALBERT, A. 2015. Dietary polyphenol intake in Europe: the European Prospective Investigation into Cancer and Nutrition (EPIC) study. *European Journal of Nutrition*, Jun 17, in press.
- ZARUBIN, T. & HAN, J. 2005. Activation and signaling of the p38 MAP kinase pathway. *Cell Research*, 15, 11-8.
- ZERIN, T., KIM, Y. S., HONG, S. Y. & SONG, H. Y. 2013. Quercetin reduces oxidative damage induced by paraquat via modulating expression of antioxidant genes in A549 cells. *Journal of Applied Toxicology*, 33, 1460-7.
- ZHAI, X., LIN, M., ZHANG, F., HU, Y., XU, X., LI, Y., LIU, K., MA, X., TIAN, X. & YAO, J. 2013. Dietary flavonoid genistein induces Nrf2 and phase II detoxification gene expression via ERKs and PKC pathways and protects against oxidative stress in Caco-2 cells. *Molecular Nutrition & Food Research*, 57, 249-59.
- ZHANG, B., MONTGOMERY, M., CHAMBERLAIN, M. D., OGAWA, S., KOROLJ, A., PAHNKE, A., WELLS, L. A., MASSE, S., KIM, J., REIS, L., MOMEN, A., NUNES, S. S., WHEELER, A. R., NANTHAKUMAR, K., KELLER, G., SEFTON, M. V.

- & RADISIC, M. 2016. Biodegradable scaffold with built-in vasculature for organ-on-a-chip engineering and direct surgical anastomosis. *Nature Materials*, Mar 7, in press.
- ZHANG, Q. Z., RAHEEM, K. S., BOTTING, N. P., SLAWIN, A. M. Z., KAY, C. D. & O'HAGAN, D. 2012. Flavonoid metabolism: the synthesis of phenolic glucuronides and sulfates as candidate metabolites for bioactivity studies of dietary flavonoids. *Tetrahedron*, 68, 4194-4201.
- ZHANG, Y., GUAN, L., WANG, X., WEN, T., XING, J. & ZHAO, J. 2008. Protection of chlorophyllin against oxidative damage by inducing HO-1 and NQO1 expression mediated by PI3K/Akt and Nrf2. *Free Radical Research*, 42, 362-71.
- ZHOU, Z., CONNELL, M. C. & MACEWAN, D. J. 2007. TNFR1-induced NF-kappaB, but not ERK, p38MAPK or JNK activation, mediates TNF-induced ICAM-1 and VCAM-1 expression on endothelial cells. *Cell Signalling*, 19, 1238-48.
- ZHOU, Z., LIU, Y., MIAO, A. D. & WANG, S. Q. 2005. Protocatechuic aldehyde suppresses TNF-alpha-induced ICAM-1 and VCAM-1 expression in human umbilical vein endothelial cells. *European Journal of Pharmacology*, 513, 1-8.
- ZHU, B. T. 2002. Catechol-O-Methyltransferase (COMT)-mediated methylation metabolism of endogenous bioactive catechols and modulation by endobiotics and xenobiotics: importance in pathophysiology and pathogenesis. *Current Drug Metabolism*, 3, 321-49.
- ZHU, Y., LING, W., GUO, H., SONG, F., YE, Q., ZOU, T., LI, D., ZHANG, Y., LI, G., XIAO, Y., LIU, F., LI, Z., SHI, Z. & YANG, Y. 2013. Anti-inflammatory effect of purified dietary anthocyanin in adults with hypercholesterolemia: a randomized controlled trial. *Nutrition, Metabolism and Cardiovascular Diseases*, 23, 843-9.
- ZIBERNA, L., LUNDER, M., TRAMER, F., DREVENSEK, G. & PASSAMONTI, S. 2013. The endothelial plasma membrane transporter bilitranslocase mediates rat aortic vasodilation induced by anthocyanins. *Nutrition, Metabolism and Cardiovascular Diseases*, 23, 68-74.

## Chapter 9. Appendices & Method Optimisation

### 9.1. Appendices for Chapter 3

#### 9.1.1. Effect of time on naringenin, sulforaphane, and lipopolysaccharide on HO-1

Sulforaphane (SFN), lipopolysaccharide (LPS) and naringenin were screened for their effect on HUVEC haem oxygenase-1 (HO-1) protein at 16 h, 18 h, and 24 h, in order to identify a time point and suitable positive control (**Figure 9.1**). HO-1 was significantly upregulated in response to SFN at all time-points tested, and there was an apparent, but non-significant increase in HO-1 in response to naringenin relative to basal at 16 h ( $2908.85 \pm 453.86$  pg/mL,  $p=0.10$ ), therefore 16 h was used in subsequent HO-1 assays.

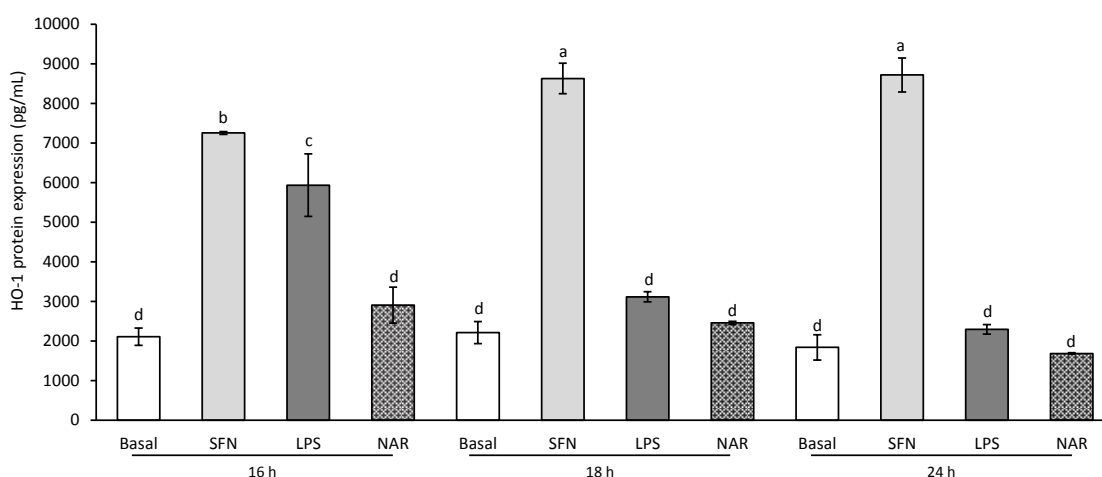


**Figure 9.1. Effect of positive controls on expression of HO-1 protein.** Treatments were added to HUVEC to a final concentration of 10  $\mu$ M (SFN and NAR) or 10 ng/mL (LPS) for 16 h, 18 h and 24 h, HO-1 protein was quantified by ELISA. Data represents the average of 3 independent replicates. Labelled means without a common letter differ significantly,  $p \leq 0.05$  (ANOVA with post hoc LSD). Abbreviations: LPS, lipopolysaccharide; NAR, naringenin; SFN, sulforaphane.

### 9.2. Appendices for Chapter 4

#### 9.2.1. Determination of screening concentration for phenolics on Hmox-1

In order to select an optimal screening concentration as an appropriate positive control for the induction of Hmox-1 in rat aortic smooth muscle cells (RASMCs), the effect 10  $\mu$ M sulforaphane (SFN), 1  $\mu$ M- 100  $\mu$ M of quercetin, naringenin, protocatechuic acid (PCA) and vanillic acid (VA) on Hmox-1 protein expression was determined by ELISA following 16 h, 18 h, and 24 h treatment (**Figure 9.2**). Hmox-1 protein expression was increased by the greatest

magnitude in response to 100  $\mu\text{M}$  quercetin, SFN and 100  $\mu\text{M}$  naringenin. Effects on Hmox-1 protein appeared to increase with concentration, thus the maximum physiological concentration of 10  $\mu\text{M}$  was selected to screen the effects of chosen treatments in subsequent experiments.

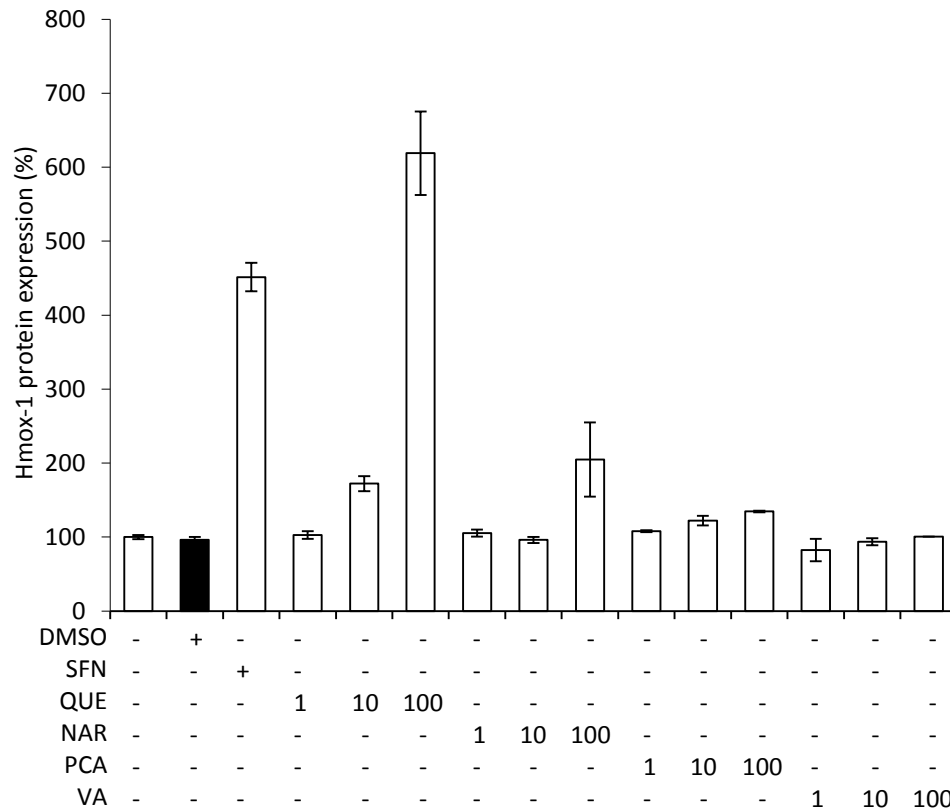


**Figure 9.2. Effect of sulforaphane (SFN) and flavonoids on the on Hmox-1 protein expression in RASMC.** Concentrations are in  $\mu\text{M}$  or 0.1 % DMSO. 10  $\mu\text{M}$  SFN was utilised as a positive control. Columns represent percentage values of Hmox-1 relative to an untreated control (no DMSO), of two independent replicates  $\pm$  SD ( $n=2$ ). Abbreviations: NAR, naringenin; QUE, quercetin; PCA, protocatechuic acid; VA, vanillic acid.

### 9.2.2. Determination of suitable reference genes for RT-qPCR

Optimal reference genes were selected using geNormPLUS kit (PrimerDesign Ltd). Six pre-validated, stably expressed, rat reference genes were run in parallel to Hmox-1 mRNA experiments (**Figure 9.3**). Resultant  $C_t$  values were analysed using the geNorm function in qbasePLUS software (version 2.3, Biogazelle NV, Zwijnaarde, Belgium) to assess gene stability across all samples, and the optimal number of genes was also determined as described by others (Hellemans et al., 2007).

It was determined that 2 reference genes were required for normalisation and Zgpat and Stau1 were identified to be the most stable reference genes. The geometric mean of the  $C_t$  values obtained for Zgpat and Stau1 were therefore used as a normalisation factor in the determination of Hmox-1 mRNA expression in response to selected treatments.

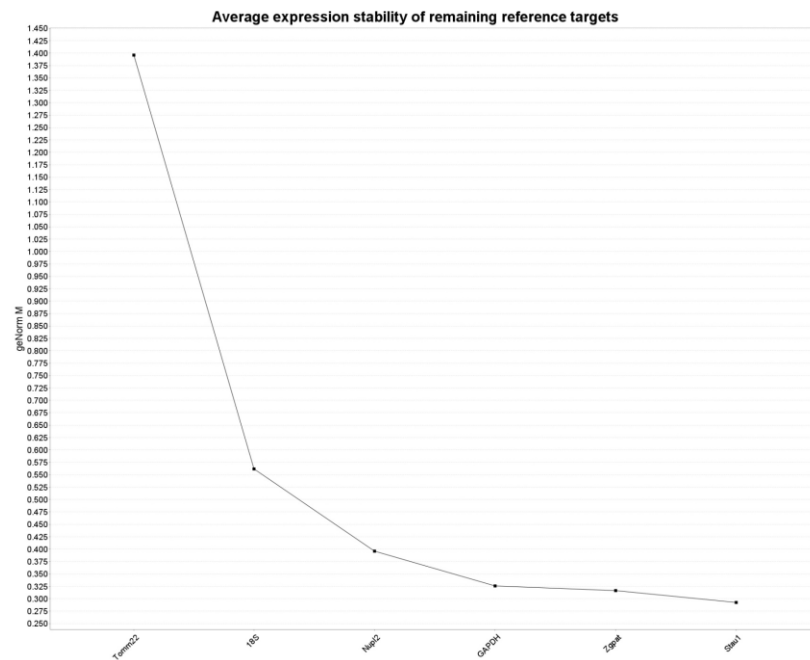


**Figure 9.3. Reference gene stability (geNorm M) for RASMC.** Cells were treated with 10  $\mu$ M quercetin, protocatechuic acid, peonidin-3-glucoside or 0.02 % DMSO for 6 h and RT-qPCR was used to determine relative amplification. Genes are arranged in order of increasing stability from left to right.

### 9.3. Appendices for Chapter 5

#### 9.3.1. Determination of TNF- $\alpha$ stimulation concentration on sVCAM-1 secretion

A concentration-dependent increase in sVCAM-1 expression was observed between 0.1 ng/mL - 20 ng/mL TNF- $\alpha$  after 24 h (**Figure 9.4**). The apparent effect size appears to stabilise between 10 ng/mL and 20 ng/mL, which may limit the observed effect size in response to select treatments, therefore a stimulation concentration of 10 ng/mL was utilised in subsequent experiments.

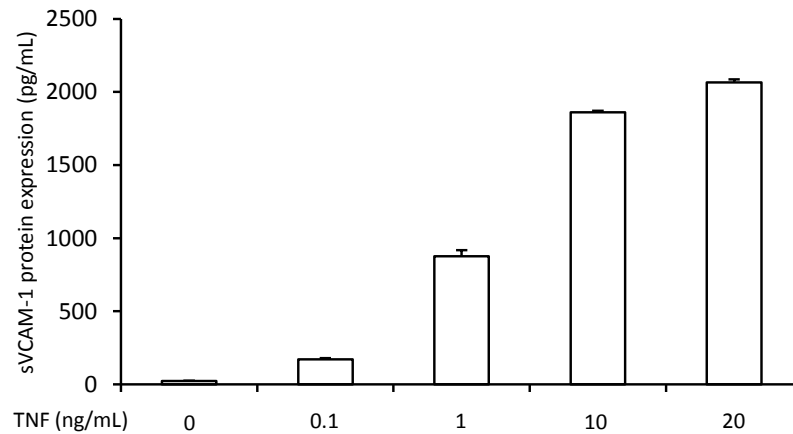


**Figure 9.4. Effect of TNF- $\alpha$  concentration on sVCAM-1 production.**

HUVEC were stimulated with TNF- $\alpha$  at concentrations between 0 and 20 ng/mL for 24 h. sVCAM-1 in cell culture supernatants was measured in duplicate by ELISA. The experiment was carried out using a single cell population, where error bars represent the standard deviation between two technical measurements.

### 9.3.2. Effect of TNF- $\alpha$ stimulation time on sVCAM-1 secretion by HUVEC.

A time-dependent increase in sVCAM-1 expression was observed between 4 h and 18 h TNF- $\alpha$  (10 ng/mL) stimulation (**Figure 9.5**). A stimulation time of 18 h was therefore utilised in subsequent experiments.

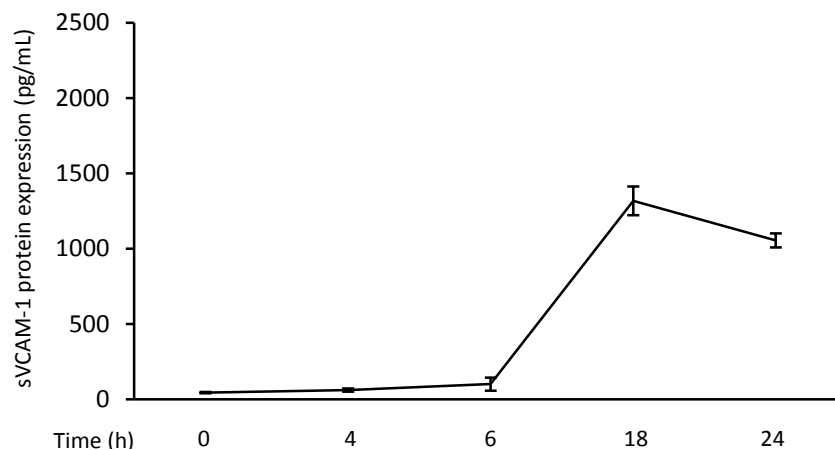


**Figure 9.5. Effect of TNF- $\alpha$  incubation time on sVCAM-1 expression in HUVEC.**

Cells were then stimulated with 10 ng/mL TNF- $\alpha$  for 4 h, 6 h, 18 h or 24 h. sVCAM-1 protein levels were determined by ELISA. The experiment was carried out using a single cell population; error bars represent the SD between technical replicates.

### 9.3.3. Effect of pre- or co-incubation of PCA with TNF- $\alpha$ .

To determine whether a pre-treatment or co-incubation of select treatments and TNF- $\alpha$  stimulants was the most appropriate assay for subsequent screening experiments, two experiments were conducted (**Figure 9.6**). Firstly, HUVEC were treated for 30 min with (10  $\mu$ M PCA) followed by 4-24 h stimulation with TNF- $\alpha$  (10 ng/mL; pre-treatment). Secondly, 10  $\mu$ M PCA and TNF- $\alpha$  (10 ng/mL) were co-incubated for 4-24 h with no pre-treatment (co-incubation). Following 30 min pre-treatment with PCA, there was a significant difference in sVCAM-1 protein relative to the vehicle control (DMSO) after 18 h ( $p \leq 0.01$ ) and 24 h ( $p \leq 0.05$ ) stimulation. A pre-treatment assay was therefore selected for subsequent experiments.

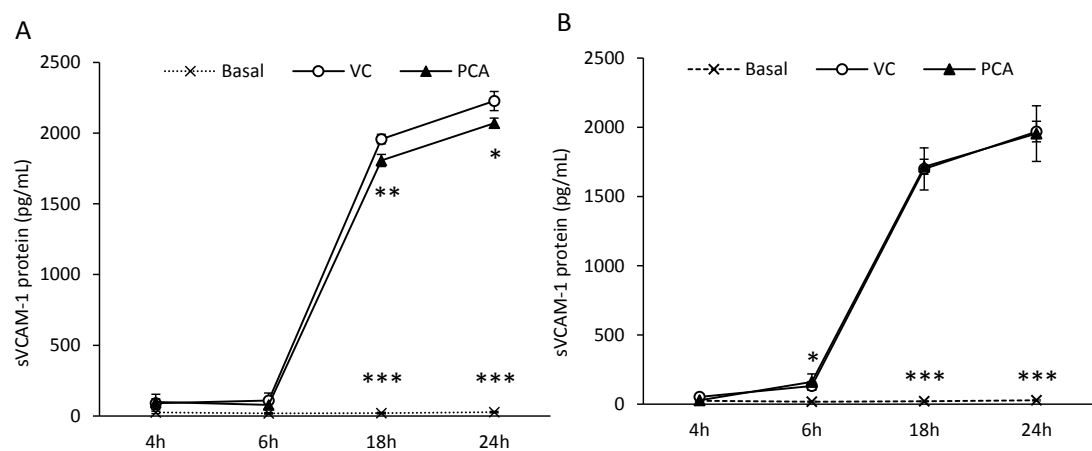


**Figure 9.6. Effect of treatment assay on inhibition of TNF- $\alpha$  stimulated sVCAM-1 by PCA with A) Pre-treatment or B) Co-incubation.** A) HUVEC were pre-treated for 30 min with 10  $\mu$ M PCA followed by 4-24 h stimulation with 10 ng/mL TNF- $\alpha$ . B) HUVEC were treated with 10  $\mu$ M PCA and 10 ng/mL TNF- $\alpha$  (co-incubation) for 4-24 h. Effects relative to vehicle control (0.02 % DMSO) at each time point were determined at each time point by one-way ANOVA (post hoc LSD), \* $p < 0.05$ , \*\* $p < 0.01$ , \*\*\* $p < 0.001$ . Abbreviations: PCA, protocatechuic acid; VC, vehicle control.

### 9.3.4. Determination of HUVEC as suitable cell type relative to HCAEC

To confirm that the response of TNF- $\alpha$  stimulated sVCAM-1 protein expression in human umbilical vein endothelial cells (HUVECs) were comparable to their more physiological cell type, human coronary artery endothelial cells (HCAECs), a concentration-response experiment utilising 0.1  $\mu$ M- 10  $\mu$ M PCA, 0.02 % DMSO (vehicle control), or 10  $\mu$ M BAY 11-7085 (NF $\kappa$ B inhibitor) was conducted on HUVEC and HCAEC in parallel (**Figure 9.7**). sVCAM-1 protein secreted by HCAEC appeared to be 10x greater than HUVEC, and the effect at 10  $\mu$ M was greater, suggesting some concentration response activity between 1  $\mu$ M-10  $\mu$ M. HUVEC were therefore confirmed as an appropriate cell model for subsequent experiments.

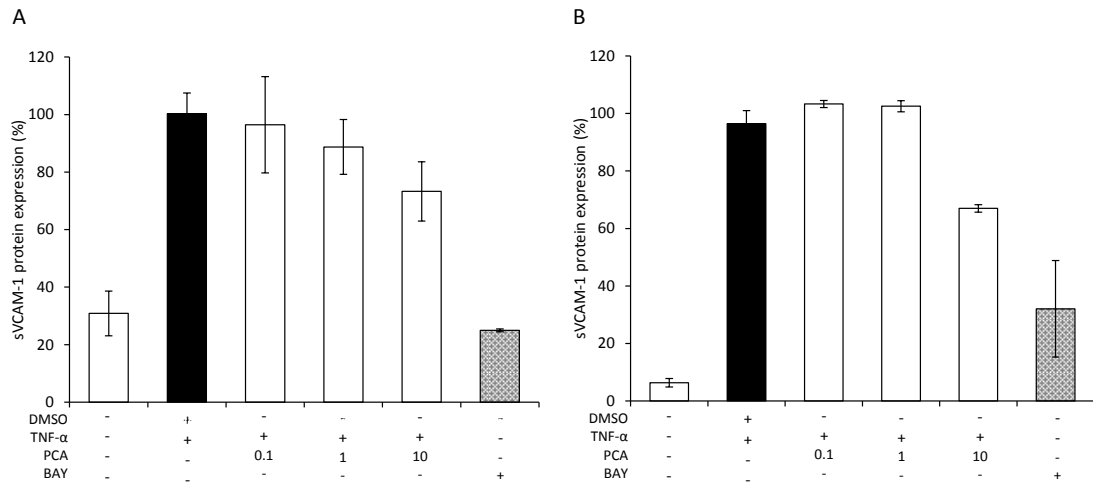


**Figure 9.7. Effect of PCA concentration of TNF- $\alpha$  stimulated sVCAM-1 protein in A) HUVEC and B) HCAEC.** Cells were treated for 30 min with 0.1  $\mu$ M-10  $\mu$ M PCA, 0.02 % DMSO, or 10  $\mu$ M BAY 11-7085, followed by addition of TNF- $\alpha$  (10 ng/mL), for 18 h. Columns represent the mean of two independent replicate  $\pm$  SD (n=2). Abbreviations: BAY, BAY 11-7085; HCAEC, human coronary artery endothelial cell; HUVEC, human umbilical vein endothelial cell; PCA, protocatechuic acid.

### 9.3.5. Determination of TNF- $\alpha$ stimulation time on phospho-NF $\kappa$ B p65 expression

NF $\kappa$ B pathway activation was determined by p65 phosphorylation in response to TNF- $\alpha$  (10 ng/mL) stimulation for 15-60 min (**Figure 9.8**). Phosphorylated p65 expression was increased 17.7 fold in response to 10 ng/mL TNF- $\alpha$  after 15 min ( $p \leq 0.001$ ), followed by an apparent time-dependent decrease with increased incubation time. 15 min was therefore used to screen for the effects of PCA on NF $\kappa$ B activation.

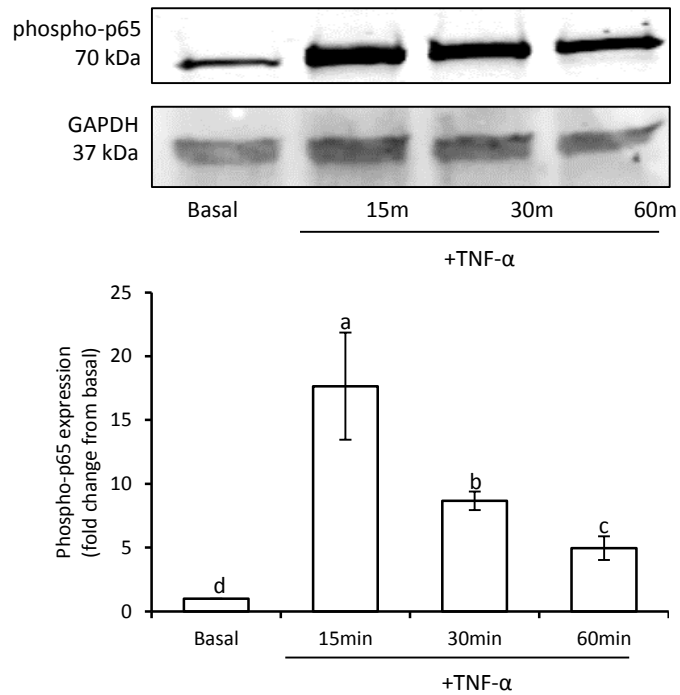


**Figure 9.8. Stimulation time response of TNF- $\alpha$  on NF $\kappa$ B p65 phosphorylation.** Data were normalized to a TNF- $\alpha$  control and columns represent the mean  $\pm$  SD of three independent replicates, n=3. Blots represent one of three independent replicates. Different letters infer significant difference following post hoc LSD ( $p \leq 0.05$ ).

### 9.3.6. Effect of TNF- $\alpha$ stimulated signalling kinase phosphorylation

Phosphorylation of multiple signalling kinases was determined following TNF- $\alpha$  stimulation following incubation for 15 min, 30 min, and 60 min (**Figure 9.9**). Akt1 phosphorylation was increased  $>2$  fold and p38 and JNK phosphorylation was increased by 15 and 4 fold, respectively, in response to TNF- $\alpha$  after 15 min, followed by an apparent time-dependent decrease with increased incubation time. 15 min was used to screen for the effects of PCA on TNF- $\alpha$  stimulated signalling kinase activation.

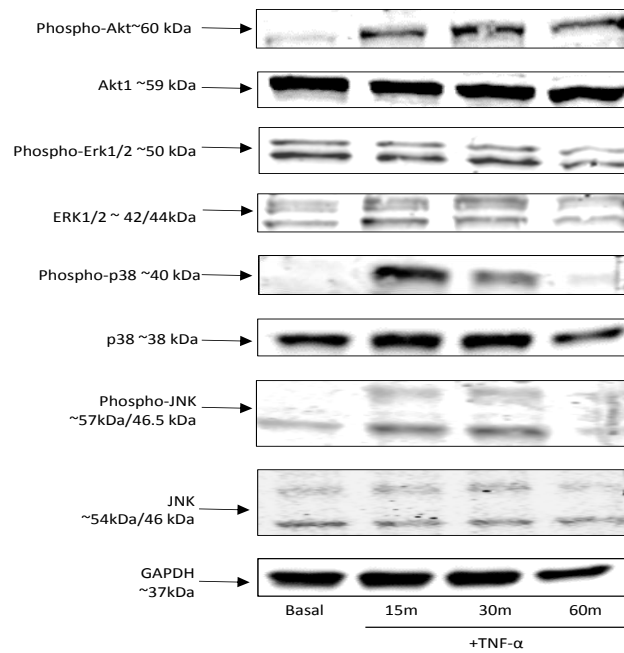


**Figure 9.9. Stimulation time response of TNF- $\alpha$  on signalling kinase phosphorylation.** Blots are representative of a single cell population (n=1).

## 9.4. Appendices for Chapter 6

### 9.4.1. Determination of TNF- $\alpha$ stimulus on sVCAM-1

In order to identify an optimal time point at which to study the effects of the serum mimic mixtures on the induction of sVCAM-1, a time course study was conducted (**Figure 9.10A**). TNF- $\alpha$  (10 ng/mL) significantly upregulated sVCAM-1 secretion by HCAEC after 6 h, 18 h, and 24 h incubation, with the largest induction relative to basal observed at 24 h ( $1570.48 \pm 29.37$  %,  $p \leq 0.001$ ). This time point (24 h) was taken forward to test for the effect of concentration response to TNF- $\alpha$  (**Figure 9.10B**). sVCAM-1 secretion was amplified with increasing concentration and an initial aim of the study was to reduce TNF- $\alpha$  concentration close to physiological concentrations, whilst enabling detectable levels of sVCAM-1 protein. As 0.1 ng/mL TNF- $\alpha$  significantly increased sVCAM-1 relative to basal ( $1056.59 \pm 60.26$  %,  $p \leq 0.001$ ), this concentration was taken forward for subsequent experiments.

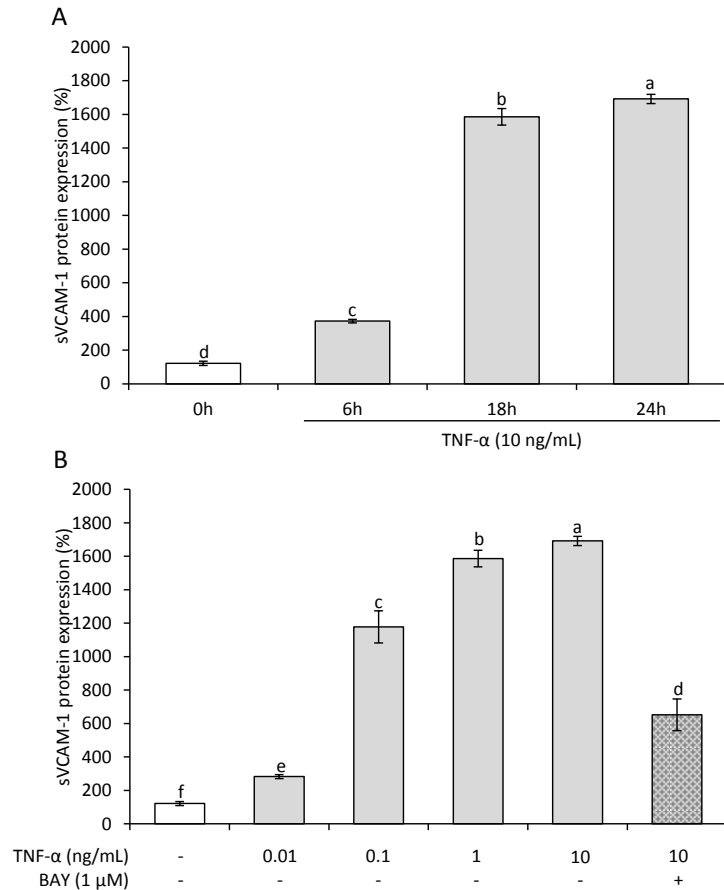


**Figure 9.10. Determination of time and concentration of TNF- $\alpha$  stimulus on sVCAM-1.** Data were recorded for each replicate as the mean of two technical replicates. Columns represent mean sVCAM-1 protein expression of three independent replicates  $\pm$  SD (n=3). Labelled means without a common letter differ significantly,  $p \leq 0.05$  (ANOVA with post hoc LSD). Abbreviation: BAY, BAY 11-7085.

#### 9.4.2. Determination of TNF- $\alpha$ stimulus on sIL-6

TNF- $\alpha$  (10 ng/mL) significantly upregulated sIL-6 secretion by HCAEC after 6 h, 18 h, and 24 h incubation, with the largest induction relative to basal observed at 24 h ( $566.81 \pm 39.87\%$ ,  $p \leq 0.001$ ) (**Figure 9.11**). sIL-6 secretion was amplified with increasing concentration, 0.1 ng/mL TNF- $\alpha$  significantly increased sVCAM-1 relative to basal ( $106.78 \pm 31.72\%$ ,  $p \leq 0.01$ ).

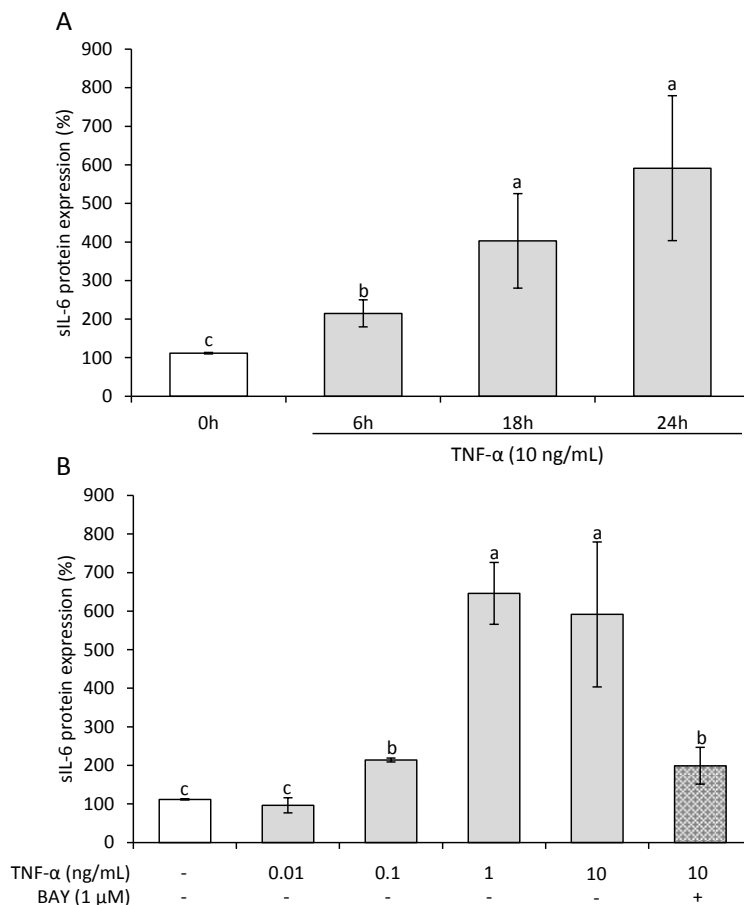


**Figure 9.11. Determination of time and concentration of TNF- $\alpha$  stimulus on sIL-6.** Data were recorded for each replicate as the mean of two technical replicates. Columns represent mean sVCAM-1 protein expression of three independent replicates  $\pm$  SD (n=3). Labelled means without a common letter differ significantly,  $p \leq 0.05$  (ANOVA with post hoc LSD). Abbreviation: BAY, BAY 11-7085.

#### 9.4.3. Validation of TNF- $\alpha$ stimulation time on VCAM-1 and IL-6 mRNA

In order to identify an optimal time point at which to study the treatment effects on TNF- $\alpha$  stimulated VCAM-1 and IL-6 mRNAs, a time course was carried out (**Figure 9.12**). The maximal response was observed at 4h where there was a fourteen fold increase VCAM-1 mRNA, and a 3 fold increase in IL-6, thus 4 h was selected as the optimal time point to take forward.

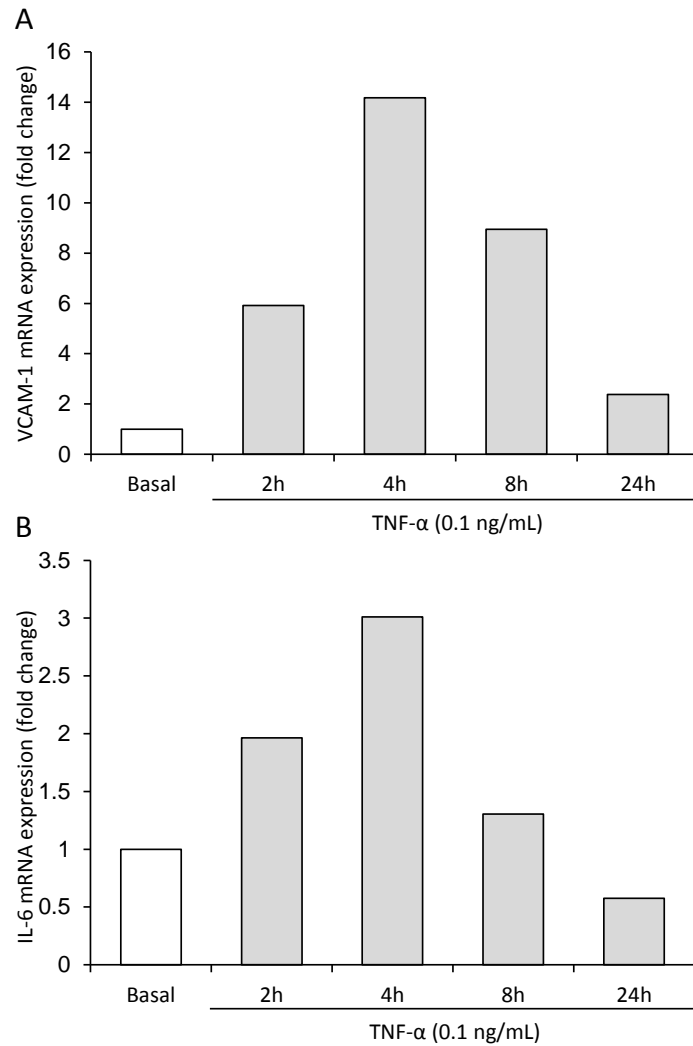


**Figure 9.12. Effect of TNF- $\alpha$  stimulation time on VCAM-1 and IL-6 mRNA expression. A) VCAM-1 B) IL-6.** Columns represent mRNA expression, normalised to reference genes VIPA39 and PRDM4, relative to an untreated control of a single cell population (n=1).

#### 9.4.4. Determination of suitable reference genes for RT-qPCR

Optimal reference genes were selected using geNorm<sup>PLUS</sup> kit (PrimerDesign Ltd). Six pre-validated stably expressed human reference genes were run in parallel to stimulated and unstimulated HCAEC (**Figure 9.13**). Resultant Ct values were analysed using the geNorm function in qbase<sup>PLUS</sup> software (version 2.3, Biogazelle NV, Zwijnaarde, Belgium) to assess gene stability across all samples, and the optimal number of genes was also determined as described by others (Hellemans et al., 2007).

It was determined that 2 reference genes were required for normalisation and VIPA39 and PRDM4 were identified to be the most stable reference genes. The geometric mean of the Ct values obtained for VIPA39 and PRDM4 were therefore used as a normalisation factor in the determination of VCAM-1 and IL-6 mRNA expression in response to selected treatments.

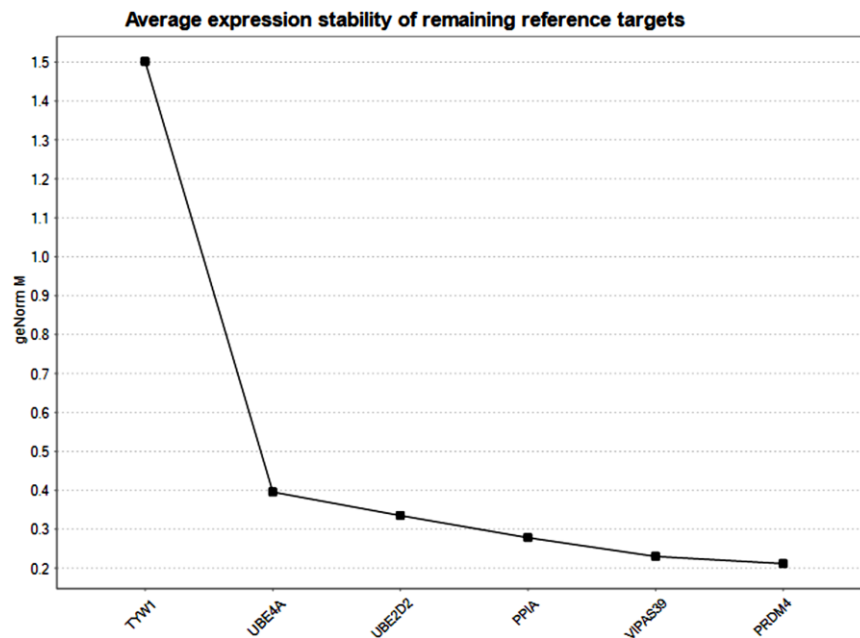


**Figure 9.13. Reference gene stability (geNorm M) for stimulated and unstimulated HCAEC.** Genes are arranged in order of increasing stability from left to right.

### 9.5. Melt curve analysis for target genes

Specific target gene primers were purchased pre-validated from Primer Design (Southampton, UK), though specificities were additionally confirmed by melt-curve analysis following data collections. Samples with a melting temperature ( $T_m$ ) not within the expected value range provided on the batch specific data sheet, or that had multiple  $T_m$ , were disregarded.

### 9.5.1. Example melt curves for Chapter 3

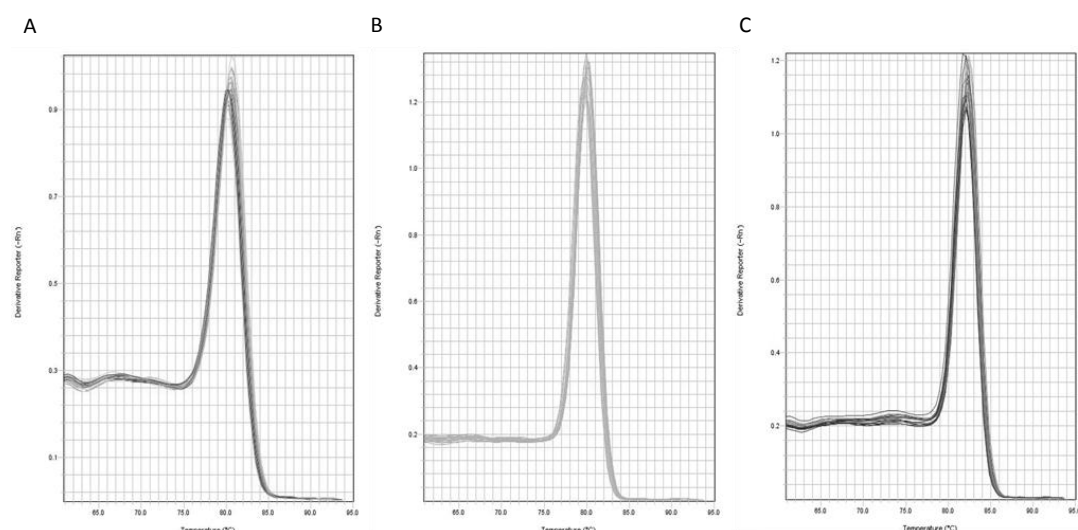


**Figure 9.14. Validation of specificity of real time PCR amplification for A) HO-1 B) UBE2D2 and C) PRDM4.** Melt curve analysis of RT-qPCR product following 50 cycles denaturation/data collection. Real time PCR was conducted using 25 ng cDNA generated from basal (unstimulated) HUVEC, and cells incubated with 10  $\mu$ M quercetin, 4-hydroxybenzoic acid, or protocatechuic acid-4-sulfate for 6 h.

### 9.5.2. Example melt curves for Chapter 4

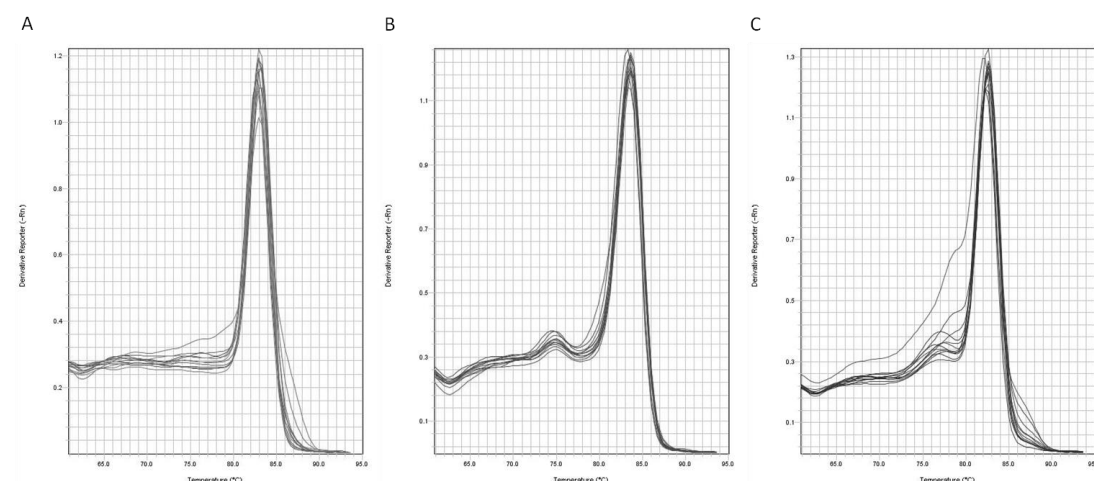


**Figure 9.15. Validation of specificity of real time PCR amplification for A) Hmox-1 B) Zgpat and C) Stau1.** Melt curve analysis of RT-qPCR product following 50 cycles denaturation/data collection. Real time PCR was conducted using 25 ng cDNA generated from basal (unstimulated) HUVEC, and cells incubated with 10  $\mu$ M quercetin, peonidin-3-glucoside, or protocatechuic acid for 6 h.

### 9.5.3. Example melt curves for Chapter 5

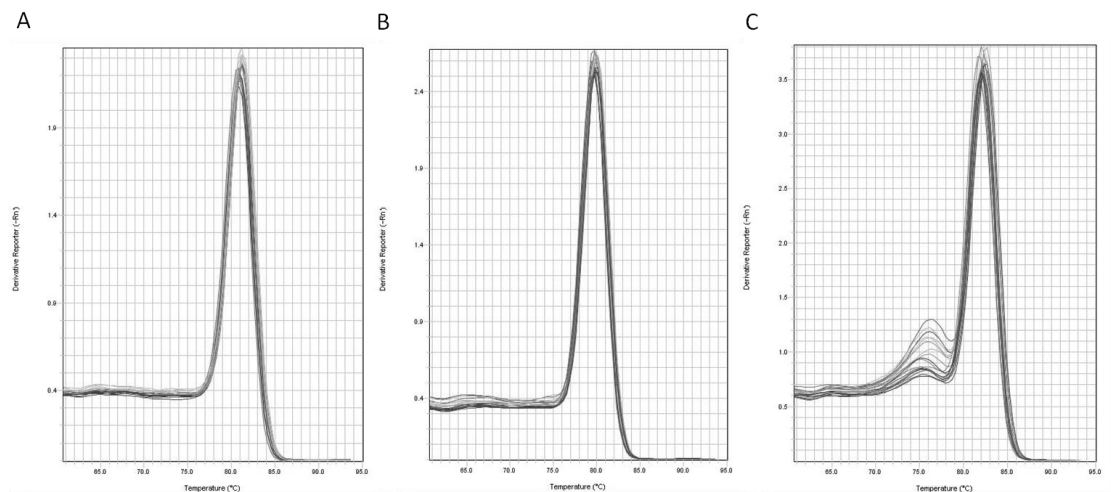


**Figure 9.16. Example of validation of specificity of real time PCR amplification for A) VCAM-1 B) UBE2D2 and C) PRDM4.** Melt curve analysis of RT-qPCR product following 50 cycles denaturation/data collection. Real time PCR was conducted using 25 ng cDNA generated from basal (unstimulated) HUVEC, and cells incubated with 0.01-100  $\mu$ M protocatechuic acid or 0.01-100  $\mu$ M protocatechuic acid-4-sulfate for 4 h.

#### 9.5.4. Example melt curves for Chapter 6

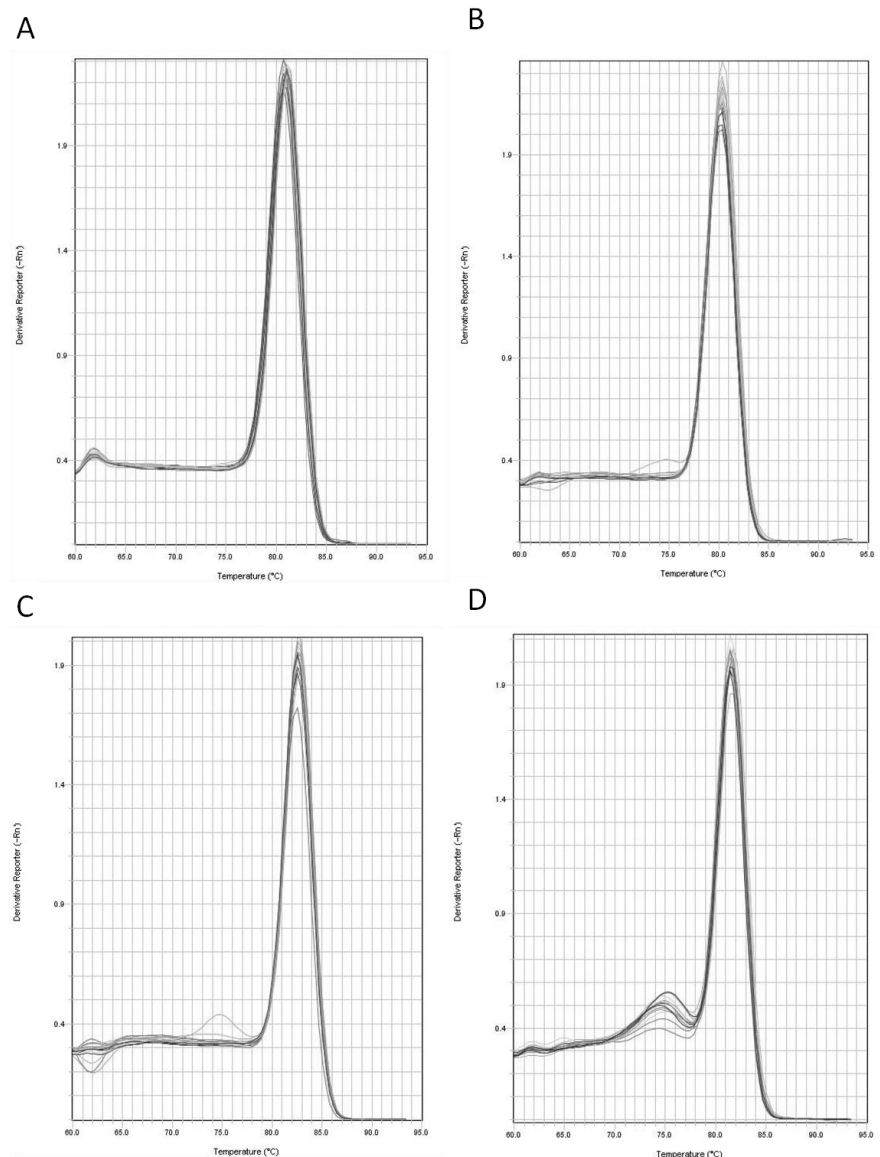


**Figure 9.17. Validation of specificity of real time PCR amplification for A) VCAM-1 B) IL-6 C) VIPA39 and D) PRDM4.** Melt curve analysis of RT-qPCR product following 50 cycles denaturation/data collection. Real time PCR was conducted using 25 ng cDNA generated from basal (unstimulated) HUVEC, and cells incubated with peak serum mixtures for 4 h.